2017

The Eastern Oyster Microbiome and its Implications in the Marine Nitrogen Cycle

Ann Arfken
College of William and Mary - Virginia Institute of Marine Science, annma31415@aol.com

The Eastern Oyster Microbiome and Its Implications in the Marine Nitrogen Cycle

---

A Dissertation

Presented to

The Faculty of the School of Marine Science

The College of William and Mary in Virginia

In Partial Fulfillment

of the Requirements for the Degree of

Doctor of Philosophy

---

by

Ann M. Arfken

January 2018

APPROVAL SHEET

This dissertation is submitted in partial fulfillment of

the requirements for the degree of

Doctor of Philosophy

Ann M. Arfken

Approved by the Committee, December 2017

Bongkeun Song, Ph.D.
Committee Chair / Advisor

Iris C. Anderson, Ph.D.

Ryan B. Carnegie, Ph.D.

Lisa M. Kellogg, Ph.D.

Michael F. Piehler, Ph.D.
University of North Carolina at Chapel Hill
Morehead City, North Carolina

TABLE OF CONTENTS

ACKNOWLEDGEMENTS

I am grateful for the many people who have supported me along the way in the pursuit of my PhD. First and foremost, I must thank my advisor, Bongkeun Song for keeping me on track and providing me an endless supply of optimism and encouragement. I am truly appreciative for his guidance. I also thank my committee members Iris Anderson, Ryan Carnegie, Lisa Kellogg, and Mike Piehler for their contributions, much needed second opinions, and helpful feedback.

Many thanks to the members of the Song lab past and present who have helped me tremendously with everything from locating missing samples to lugging dozens of 5lb carboys full of seawater back to VIMS. To Jess Lisa, for always offering support and being a true friend as we transitioned from UNCW to VIMS, to Miguel Semedo for his enthusiasm and keeping me sane, to Ken Czapla for his humor and dedication to field work despite eye injuries, Hunter Walker for his help piloting the boat and navigating the Anderson lab, to Ashley Smyth for keeping the MIMS happy, and to lab Raegan Bostic, Sam Fortin, Stephanie Wilson, Tavis Sparrer, Anjali Bhatnagar for their assistance with lab and field work.

Thanks are also in order to VIMS community and all many friendships that have been made. A special thanks to Terry Mayo for always looking out for me, to Tony Nalovic for always getting me to see a different side of things, to Quang Huynand Fei Ye for our dinners at Peter Chang's, and to Zoemma Warshafsky for being an awesome office mate. I am also thankful for my "special interest" group at VIMS, which has been a great escape from the rigors of academia. To Sarah Pease for being a great friend and a great support, to Lydia Bienlien for her encouragement and advice, to Seth West for helping with my computer issues and seemingly vast knowledge of everything, to Skyler West for his creativity and game mastery, to Robin Rennie for taking charge and making sure everyone was fed, and to Kelsey Knobloch for bringing a lot of laughs to the party.

A special thank you to the Shepherd family, who have been amazing. To Jim for his love and support through everything, to Lynn for her cooking and thoughtfulness that

has meant so much to me, and to Jack for all his help when I needed it and always offering to lend a hand.

And of course, I am especially grateful for the love and support of my family. To mom and dad, for always encouraging me to follow my passion, even if that meant switching my career from law to science. I am forever grateful for all you have done and continue to do for me. Thank you everyone!

LIST OF TABLES

LIST OF FIGURES

CHAPTER 1

CHAPTER 2

CHAPTER 2 – Supplementary Figures

CHAPTER 3

ABSTRACT

Microbial communities associated with a particular space or habitat, or microbiomes, play significant roles in host health and the regulation of biogeochemical cycles. In oysters these microbiomes may be important contributors in the removal of biologically available nitrogen (N) from the coastal and marine environment through the process of denitrification. Denitrification is the microbially mediated step-wise reduction of nitrate (NO_3^-) or nitrite (NO_2^-) to N_2 gas. Excess nitrogen in the Chesapeake Bay has been implicated in the increase of eutrophication and other detrimental effects including harmful algal blooms, hypoxia, and loss of benthic communities. Oyster reefs have been shown to enhance the rates of denitrification in nearby sediments, but little is known about the oyster microbiomes or associated microbes responsible for denitrification (denitrifiers). Furthermore, the identification of the oyster core microbiome, or set of resident microbes continually present in the oyster, is relatively unknown. Assessing the stable underlying core is necessary to evaluate and predict the effect of varying environmental conditions on the oyster microbiome and oyster denitrification. A combined 16S targeted metagenomic and metabolic inference approach was used in this study to investigate the gill, gut and shell microbiomes of the eastern oyster (*Crassostrea virginica*) and their associated denitrifiers in response to spatial and temporal changes. Denitrification activity was linked to community structure using methods such as quantitative PCR of nitrous oxide reductase genes (*nos*Z) and ^{15}N isotope pairing technique with experimental flow-through design. The oyster gill, gut, and shell microbiomes all showed distinct and unique core microbiomes, suggesting an importance of the core to oyster function or health. Denitrifier abundance and activities were most consistent in the shell microbiomes indicating a stable, pool of potential denitrifiers for oyster denitrification. In comparison, oyster gill and gut denitrifier abundances and activities were highly variable and likely related to transient denitrifiers ingested with food particles. Additionally, denitrifiers demonstrated niche differentiation between the different oyster microbiomes, indicating different groups of denitrifiers are responsible for performing denitrification in the oyster. Assessing the stability and variability of the oyster microbiome and associated denitrifiers provides a greater understanding of the oyster's role in denitrification and the mitigation of excess N in marine and coastal environments.

The Eastern Oyster Microbiome and Its Implications in the Marine Nitrogen Cycle

Chapter 1

Introduction to Dissertation

Nitrogen and Eutrophication

Nitrogen (N) is an essential element to life and is necessary for growth and production in both terrestrial and aquatic environments. In temperate coastal and marine ecosystems, N is often in relatively short supply compared to other nutrients, making it a limiting nutrient to primary production (Zehr and Kudela 2011) and a key component in controlling estuarine dynamics (Vitousek et al. 1997). Over the last century, global N inputs to aquatic systems have increased several-fold as a result of anthropogenic activity (Galloway et al. 2003), leading to alterations in estuarine and coastal environments (Burgin and Hamilton 2007). Most notably, human-altered N cycling has been implicated in increased coastal and estuarine eutrophication (Nixon 1995, Vitousek et al. 1997).

Eutrophication is defined as an increased rate of supply of organic matter to a system, often as a result of excess N's stimulating effect on biological production (Nixon 1995). Increased abundances of algal blooms, which may include harmful algae and nuisance macroalgae, are a common response to eutrophication (Rabalais et al. 2002, Paerl et al. 2011) leading to such effects as reduced light penetration, loss of biotic diversity, and alterations to marine food webs (Vitousek et al. 1997, Rabalais et al. 2002, Galloway et al. 2003). As these blooms begin to die off and sink, the increase in organic matter to bottom waters fuels aerobic microbial respiration resulting in zones of hypoxia or anoxia and disruption to the benthic community, including loss of sea grass beds and benthic fauna (Holmer and Bondgaard 200, Diaz and Rosenburg 2008).

Denitrification and N-removal

To mitigate the effects of N loading to the coastal and estuarine environments, significant focus has been placed on enhancing N removal. One form of N removal from aquatic systems involves the microbially-mediated process of denitrification (Newell et al. 2002). Denitrification is the step-wise reduction of biologically available nitrate (NO_3^-) to nitrite (NO_2^-) to nitric oxide (NO) to nitrous oxide (N_2O) and finally to dinitrogen (N_2) gas (Zumft 1997). Enzymes encoded by different genes mediate each transformation step in denitrification. In the initial step of denitrification, NO_3^- is converted to NO_2^- by nitrate reductase (*nar*), followed by the reduction of NO_2^- to nitric oxide (NO) by nitrite reductase (*nir*). NO is then reduced to nitrous oxide (N_2O) by nitrous oxide reductase (nirS/nirK). The final step of denitrification is the reduction of N_2O to dinitrogen gas (N_2) by nitrous oxide reductase (*nos*Z). In some cases, such as incomplete denitrification and other N-transformation pathways, the unfavorable byproduct N_2O may be released (Zumft 1997, Galloway et al. 2003, Burgin et al. 2013). N_2O is a potent greenhouse and ozone-depleting gas with a 100-year global warming potential approximately 310 times higher than that of CO_2 (Jones et al. 2013). Thus, *nos*Z is an ecologically critical gene in reducing harmful N_2O emissions from the environment. While this gene has been traditionally associated with complete microbial denitrifiers, increased microbial genome sequencing has revealed a much greater range of bacteria carrying the *nos*Z gene, indicating a much greater potential for N_2O reduction than has previously been known or investigated (Sanford et al. 2012, Jones et al. 2013, Hallin et al. 2017).

Oysters and Sedimentary N Processes

Chesapeake Bay, the largest estuary in the United States, is one of many systems that has experienced the detrimental effects of excess N and cultural eutrophication, including bottom water hypoxia, reduced fisheries harvests, and loss of submerged aquatic vegetation (Cerco and Noel 2007, Glibert et al. 2014). Over the last several years, restoration of the eastern oyster (*Crassostrea virginica*) to the Bay has gained momentum as a potential means to enhance N removal and mitigate eutrophication (Beck et al. 2011, Kellogg et al. 2014). Oysters are a keystone species and serve as natural ecosystem engineers in estuaries, providing important services such as enhancing water quality and habitat biodiversity (Grabowski et al. 2007, Hoellein and Zarnoch 2014), as well as ecological functions, such as altering the biogeochemical N cycle and enhancing denitrification (Newell et al. 2002, Smyth et al. 2013).

Oysters are able to influence N processes in the environment (Fig. 1) by filtering organic rich phytoplankton out of the water column (Grizzle et al. 2008) and assimilating N into biomass (Higgins et al. 2005, Carmichael et al. 2012), or excreting N in the form of ammonium or biodeposits, a combination of feces and pseudofeces (Newell and Jordan 1983, Dame et al. 1984). These biodeposits may subsequently be buried, consumed by deposit-feeding organisms, or remineralized to ammonium (NH_4^+; Newell et al. 2005, Giles et al. 2006, Kellogg et al. 2014). Depending on environmental conditions, NH_4^+ can be further nitrified to NO_2^- and NO_3^- or diffuse back into the water column (Kellogg et al. 2014). NH_4^+ remineralized from oyster biodeposits and excretions may increase the coupling of nitrification-denitrification in the sediments and enhances N removal via denitrification (Newell et al. 2005, Smyth et al. 2013). Studies have

demonstrated that oyster reefs and reef sediments have higher rates of denitrification than bare sediments without oysters (Piehler and Smyth 2011, Kellogg et al. 2013, Smyth et al. 2013). Ideally, NH_4^+ from the remineralized oyster biodeposits and excretions provides substrate for nitrifying communities, which oxidize NH_4^+ to NO_3^- via nitrification. This increase in NO_3^- along with electrons from the organic biodeposits stimulates denitrification, consumes NO_3^- and removes N from the system through the generation of the relatively inert N_2 gas (Newell et al. 2002).

Oyster Microbiomes and the N-Cycle

While N processes are relatively well studied in oyster reefs and reef sediments (Kellogg et al. 2013, Hoellein et al. 2015, Humprhies et al. 2016, Smyth et al. 2016), microbial N cycling within and on oysters themselves has not been well examined. A few recent studies have shown that live oysters (Smyth et al. 2013) and oyster shells (Arfken et al. 2017) have significantly higher rates of denitrification than sediments. Microbial communities associated with oysters may play an important role in NO_3^- removal and N_2O reduction in estuarine ecosystems. While microbes are present throughout the oyster, there are diverse physical and chemical 'microhabitats' within and on the oyster, such as those relating to specific tissues or organs, which likely select for various microbes. Microbial communities favored by these distinct environments comprise a microbiome, defined as the "characteristic microbial community occupying a reasonably well defined habitat which has distinct physico-chemical properties (Whipps et al. 1988)".

Among the various oyster microhabitats, the microbiomes associated with the gut, gill, and shell biofilm are most likely to influence the N cycle. The gut organs in animals provide conditions favorable to NO_3^- reduction including anoxia, high moisture content, large amounts of NO_3^- and NO_2^-, and high quality organic compounds (Depkat-Jakob et al. 2010). Recent studies have linked N_2O production and denitrification to the gut of earthworms, insects, and bivalves (Stief et al. 2009, Wüst et al. 2009, Gaulke et al. 2010, Ngugi and Brune 2012, Svenningsen et a. 2012) making the oyster gut, defined here as the digestive gland and intestine, a likely and important source of N_2 and N_2O in the marine environment. In contrast to the oyster gut, the gills are key sites for respiration, providing an aerobic environment for microbial colonization and nitrification to occur, and the potential to increase coupled nitrification-denitrification in oysters. In a study examining nitrification rates in marine macrobenthic invertebrates, dissected gill tissues of the bivalves *Tapes philippinarium* and *Mytilus galloprovicialis* had the highest rates of nitrification, suggesting that gill microbiomes play a significant role in nitrification in the marine environment (Welsh and Castadelli 2004). Furthermore, the complex structure of the oyster shell may also provide a microhabitat for N transforming microbes. A recent study by Heisterkamp et al. (2013) found that nitrification and denitrification co-occurring in marine mollusc shell biofilms contributed up to 94% of animal-associated N_2O emissions. Overall, oysters provide several distinct microhabitats for N transforming microbes to colonize, and therefore may be potential hotspots for denitrification and other N cycling transformations in the estuarine ecosystem.

Oyster Microbiome Structure and Function

To understand how oyster gut, gill, and shell biofilm microbiomes contribute to N cycling in estuaries, the diversity and composition of microbial members that comprise these various oyster microbiomes must be identified. Identifying the stable, resident core members as well as the normal fluctuations and variation that occur within a host microbiome are necessary to understand and predict the impact of disturbances on the microbiome and microbiome function (Shade and Handelsman 2012, Stenuit and Agathos 2015) including those related to a host's health (Turnbaugh et al. 2007, Costello et al. 2012) and ecosystem processes (Schimel et al. 2007, Chaparro et al. 2012, Jousset et al. 2017). Disruptions to a microbiome may alter its ecological function in the environment (Allison and Martiny 2008, Blaser et al. 2016).

A core microbiome is defined as an assemblage of microorganisms that is shared by all organisms of a species, or set of microorganisms that are consistently present in a defined habitat (Hamady et al. 2009, Turnbaugh et al. 2007). In general, a core microbiome is defined in relation to a 'healthy' organism, as the core is likely to be closely linked to important functions of the host such as homeostasis, development, biological function, and defense against disease (McFall-Ngai et al. 2013). Furthermore, the core microbiome may be defined in relation to an entire ecosystem. The core microbiome is likely to play a critical role in the environment, such as regulating biogeochemical cycles (Shade and Handelsman 2012). Once identified, a stable, consistent core may be compared across complex microbial assemblages in response to factors such as diet, physiological and pathological states, or environmental conditions in

order to identify their effects on microbiome structure (Turnbaugh et al. 2007, Shade and Handelsman 2012, Schmitt et al. 2012).

Ultimately, the structure of a microbiome may depend on the selective pressures that shape it. If the microbiome is shaped by the composition of the microbial community present in a local environment, there is unlikely to be a core. In comparison, if the selective pressures within the host favor certain microbes, this is likely to result in a core community (Roeselers et al. 2011). Inside the oyster, internal tissues of are exposed to a more stable, uniform set of conditions compared to the exterior environment and thus likely more likely to exhibit a core microbiome structure. For example, oysters are able to regulate internal oxygen concentrations by opening shell valves and increasing water flow (Galtsoff 1964, Shumway and Koehn 1982) or avoid exposure to toxic algal species and other harmful substances by closing their shells and reducing filtration (Manfrin et al. 2012). In comparison, the shell microbiome is less likely to present a core microbiome, due to greater exposure to the fluctuating external environment and less influence from the selective pressures of the oyster host.

Furthermore, determination of the oyster microbiome and its core is a necessary in unraveling the role of microbiomes in oyster health, which ultimately impacts the function of oyster denitrification in the marine environment and its ability to mitigate eutrophication. Host microbiomes are critical for maintaining homeostasis and survival, with imbalances in the microbiome linked to disease (McFall-Ngai et al. 2013) reduced lifespan (Brummel et al. 2004, Rawls et al. 2004) and higher mortality (Sison-Mangus et al. 2015). Additionally, oyster microbiomes may offer protection against pathogens by creating competition for nutrients, reducing space for settlement, or producing

antimicrobials (Harris 1993, Gomez-Gil et al. 2000, Castro et al. 2002, Schulze et al. 2006, Prado et al. 2010, Kesarcodi-Watson et al. 2012).

Overall, oyster microbiomes are likely to play both an important role in oyster health and N-transformations in the environment, including denitrification. Currently, the core structures of oyster microbiomes have not been identified, and the overall diversity of the oyster microbiomes remains relatively unknown, particularly regarding the eastern oyster. Only a handful of studies have examined the structure of oyster microbiomes using in depth characterization methods (King et al. 2012, Wegner et al. 2013, Trabal Fernández et al. 2014, Lokmer and Wegner 2015, Lokmer et al. 2016a, Lokmer et al. 2016b, Vezzulli et al. 2017) and none to date have linked oyster microbiome structure to ecological function. Thus, in order to understand the contribution of oyster microbiomes to the estuarine N cycle and predict an oyster's potential to remove N and from the Chesapeake Bay, it is important to determine the variability, composition and identity of oyster microbiomes and associated N cycling microbes and their responses to varying environmental conditions.

Study Objectives

The overall objectives of this dissertation are to examine the spatiotemporal variation in the composition and diversity of *Crassostrea virginica* microbiomes, identify the core microbiomes of the different oyster tissues, and link oyster microbiome function to denitrification in the marine environment. This dissertation is divided into four main chapters that investigate different factors that may affect the composition and function of the oyster microbiomes. In Chapter 2, the microbiomes of the oyster digestive gland,

shell, and reef sediment were examined and a customized gene database, in conjunction with a metabolic inference bioinformatic program, to identify oyster denitrifiers was developed. In Chapter 3, the effects of seasonality on the oyster microbiomes and associated denitrifiers were explored and the presence of core microbiomes was investigated. In Chapter 4, temporal and spatial environmental changes on oyster microbiomes and associated denitrifiers in addition to the existence of a core microbiome were examined by conducting oyster deployment experiments. And finally, in Chapter 5, the effects of developmental stages and hatchery operation on oyster larval microbiomes were investigated for the presence of a core larval microbiome.

REFERENCES

Allison, SD, and Martiny, JBH (2008) Colloquium paper: resistance, resilience, and redundancy in microbial communities. *Proc Natl Acad Sci* **105**(Supplement 1): 11512–19. doi: 10.1073/pnas.0801925105.

Arfken, A, Bongkeun, S, Bowman, JS, and Piehler, M (2017) Denitrification potential of the eastern oyster microbiome using a 16S rRNA gene based metabolic inference approach. *PLoS ONE* **12**(9): 1–21. doi: 10.1371/journal.pone.0185071.

Asmani, K, Petton, B, Le Grand, J, Mounier, J, et al. (2016) Establishment of microbiota in larval culture of Pacific Oyster, *Crassostrea Gigas*. *Aquaculture* **464**: 434–44. doi: 10.1016/j.aquaculture.2016.07.020.

Beck, MW, Brumbaugh, RD, Airoldi, L, Carranza, A, Coen, LD, Crawford, C, Defeo, O, Edgar, GJ, Hancock, B, Kay, MC, Lenihan, HS, Luckenbach, MW, Toropova, CL, Zhang, G, and Guo, X (2011) Oyster reefs at risk and recommendations for conservation, restoration, and management. *BioScience* **61**(2): 107–16. doi: 10.1525/bio.2011.61.2.5.

Blaser, MJ, Cardon, ZG, Cho, MK, Dangi, JL, Donohue, TJ, Green, JL, Knight, R, Maxon, ME, Northern, TR, Pollard, KS, and Brodie, EL (2016) Toward a predictive understanding of earth's microbiomes to address 21st century challenges. *MBIO* **7**(3): 1–16. doi: 10.1128/mBio.00714-16.

Brummel, T, Ching, A, Seroude, L, Simon, AF, and Benzer, S (2004) *Drosophila* lifespan enhancement by exogenous bacteria. *Proc Natl Acad Sci* **101**(35): 12974–79. doi: 10.1073/pnas.0405207101.

Burgin, AJ, and Hamilton, SK (2007) Have we overemphasized the role of denitrification

in aquatic systems? A review of nitrate removal pathways. *Front Ecol Environ* **5**(2): 89–96.

Burgin, AJ, Lazar, JG, Groffman, PM, Gold, AJ et al. (2013). Balancing nitrogen retention ecosystem services and greenhouse gas disservices at the landscape scale. *Ecol Eng* **56**: 26–35. doi: 10.1016/j.ecoleng.2012.05.003.

Carmichael, RH, Walton, W, Clark, H, and Ramcharan, C (2012) Bivalve-enhanced nitrogen removal from coastal estuaries. *Can J Fish Aquat Sci* **69**(7): 1131–49. doi: 10.1139/f2012-057.

Castro, D, Pujalte, MJ, Garay, E, and Borrego, JJ (2002) Vibrios isolated from the cultured manila clam (*Ruditapes Phillippinarum*): numerical taxonomy and antibacterial activities. J Appl Microbiol **93**: 438-447.

Cerco, CF, and Noel, MR (2007) Can oyster restoration reverse cultural eutrophication in Chesapeake Bay? *Estuaries Coasts* **30**(2): 331–43. doi: 10.1007/BF02700175.

Chaparro, JM, Sheflin, AM, Manter, DK, and Vivanco, JM (2012) Manipulating the soil microbiome to increase soil health and plant fertility. *Biol Fert Soils* **48**(5): 489–99. doi: 10.1007/s00374-012-0691-4.

Costello, EK, Stagaman, K, Dethlefsen, L, Bohannan, BJM, and Relman, DA (2012) The application of ccological theory. *Science* **336**(June): 1255–62. doi: 10.1126/science.1224203.

Dame, RF, Zingmark, RG, and Haskin, E (1984) Oyster reefs as processors of estuarine materials. *J Exp Mar Bio Ecol* **83**: 239–247. doi: 10.1016/S0022-0981(84)80003-9.

Depkat-Jakob, PS, Hilgarth, M, Horn, MA, and Drake, HL (2010) Effect of earthworm feeding guilds on ingested dissimilatory nitrate reducers and denitrifiers in the

alimentary canal of the earthworm. *Appl Environ Microbiol* **76**: 6205–6214. doi: 10.1128/AEM.01373-10.

Diaz, RJ and Rosenberg, R. (2008) Spreading dead zones and consequences for marine ecosystems. *Science* **321**: 926–929. doi: 10.1126/science.1156401.

Galloway, JN, Aber, JD, Erisman, JW, Seitzinger, SP, et al. (2003) The nitrogen cascade. Bioscience **53**: 341–356.

Galstoff, PS (1964) The American oyster, *Crassostrea virginica* Gmelin. *US Fish Wildl Serv Fish Bull* **64**: 1-457. doi: 10.4319/lo.1966.11.2.

Gaulke, AK, Wetz, MS, and Paerl, HW (2010) Picophytoplankton: A major contributor to planktonic biomass and primary production in a eutrophic, river-dominated estuary. *Estuar Coast Shelf Sci* **90**: 45–54. doi: 10.1016/j.ecss.2010.08.006.

Giles, H, Pilditch, CA, and Bell, DG (2006) Sedimentation from mussel (*Perna canaliculus*) culture in the Firth of Thames, New Zealand: impacts on sediment oxygen and nutrient fluxes. *Aquaculture* **261**: 125–140. doi: 10.1016/j.aquaculture.2006.06.048.

Glibert, PM, Hinkle, DC, Sturgis, B, and Jesien, RV (2014) Eutrophication of a Maryland/Virginia coastal lagoon: a tipping point, ecosystem changes, and potential causes. *Estuaries and Coasts* **37**: 128–146. doi: 10.1007/s12237-013-9630-3.

Gomez-Gil, B, Roque, A, and Turnball, JF (2000) The use and selection of probiotic bacteria for use in the culture of larval aquatic organisms. *Aquaculture* **191**: 259-270.

Grabowski, JH, Peterson, CH, Bishop, MJ, and Conrad, R (2007) The bioeconomic feasibility of culturing triploid *Crassostrea ariakensis* in North Carolina. *J Shellfish*

Res 26: 529–542. doi: 10.2983/0730-8000(2007)26[529:TBFOCT]2.0.CO;2.

Grizzle, RE, Greene, JK, and Coen, LD (2008) Seston removal by natural and constructed intertidal eastern oyster (*Crassostrea virginica*) reefs: A comparison with previous laboratory studies, and the value of in situ methods. *Estuaries and Coasts* **31**: 1208–1220. doi: 10.1007/s12237-008-9098-8.

Hallin, S, Philippot, L, Löffler, F, Sanford RA, Jones, CM (2017) Genomics and ecology of novel N_2O-Reducing microorganisms. *Trends Microbiol* **xx:** 1–13. doi: 10.1016/j.tim.2017.07.003.

Hamady, M, Knight, R, Stern, A, Mick, E, and Tirosh, I. (2009) Microbial community profiling for human microbiome projects: tools, techniques, and challenges. *Genome Res.* **19**: 1141–1152. doi: 10.1038/nature06244.

Harris, J (1993) The presence, nature, and role of gut microflora in aquatic invertebrates: a synthesis. *Microbiol Ecol* **25**(3): 195-231.

Higgins, CB, Stephenson, K, and Brown, BL (2005) Nutrient bioassimilation capacity of aquacultured oysters: quantification of an ecosystem service. *J Environ Qual* **40**: 271-77. doi: 10.2134/jeq2010.0203.

Hoellein, TJ, and Zarnoch, CB (2014) Effect of eastern oysters (*Crassostrea virginica*) on sediment carbon and nitrogen dynamics in an urban estuary. *Ecol Appl* **24**: 271–286. doi: 10.1890/12-1798.1.

Hoellein, TJ, Zarnoch, CB, and Grizzle, RE (2015) Eastern oyster (*Crassostrea virginica*) filtration, biodeposition, and sediment nitrogen cycling at two oyster reefs with contrasting water quality in Great Bay Estuary (New Hampshire, USA). *Biogeochemistry* **122**(1): 113–29. doi: 10.1007/s10533-014-0034-7.

Holmer, M and Bondgaard, EJ (2001) Photosynthetic and growth response of eelgrass to low oxygen and high sulfide concentrations during hypoxic events. *Aquat Bot* **70**: 29–38. doi: 10.1016/S0304-3770(00)00142-X.

Humphries, AT, Ayvazian, SG, Carey, JC, Hancock, BT, Grabbert, S, Cobb, D, Strobel, CJ, and Fulweiler, RW (2016) Directly measured denitrification reveals oyster aquaculture and restored oyster reefs remove nitrogen at comparable high rates. *Front Mar Sci* **3**(May): 74. doi: 10.3389/fmars.2016.00074.

Jones, CM, Graf, DRH, Bru, D, Philippot, L, and Hallin, S (2013) The unaccounted yet abundant nitrous oxide-reducing microbial community: a potential nitrous oxide sink. *ISME J* **7**: 417–26. doi: 10.1038/ismej.2012.125.

Jousset, Alexandre, Bienhold, C, Chatzinotas, A, Gallien, L, Gobet, A, Kurm, V, Küsel, K, et al. (2017) Where less may be more: how the rare biosphere pulls ecosystems strings. *ISME J* **11** (4): 853–62. doi: 10.1038/ismej.2016.174.

Kellogg, ML, Cornwell, JC, Owens, MS, and Paynter, KT (2013) Denitrification and nutrient assimilation on a restored oyster reef. *Mar Ecol Prog Ser* **480**: 1–19. doi: 10.3354/meps10331.

Kellogg, ML, Smyth, AR, Luckenbach, MW, Carmichael, RH, et al. (2014) Use of oysters to mitigate eutrophication in coastal waters. *Estuar Coast Shelf Sci* **151**: 156–168. doi: 10.1016/j.ecss.2014.09.025.

King, GM, Judd, C, Kuske, CR, and Smith, C (2012) Analysis of stomach and gut microbiomes of the eastern oyster (*Crassostrea virginica*) from coastal Louisiana, USA. *PLoS One* **7** (12): e51475. doi: 10.1371/journal.pone.0051475.

Lokmer, A, Goedknegt AM, Thieltges, DW, Fiorentino, D, Kuenzel, S, Baines, JF, and

Wegner, KM (2016a) Spatial and temporal dynamics of Pacific oyster hemolymph microbiota across multiple ccales. *Front Microbiol* **7** (August): 1–18. doi: 10.3389/fmicb.2016.01367.

Lokmer, A, Kuenzel, S, Baines, JF and Wegner, KM (2016b) The role of tissue-specific microbiota in initial establishment success of Pacific oysters. *Environ Microbiol* **18**(3): 970–87. doi: 10.1111/1462-2920.13163.

Lokmer, A and Wegner, KM (2015) Hemolymph microbiome of Pacific oysters in response to temperature, temperature stress and infection. *ISME J* **9**: 670–682. doi: 10.1038/ismej.2014.160.

Manfrin, C, De Moro, G, Torboli, V, Venier, P, Pallavicini, A, and Gerdol, M (2012) Physiological and molecular responses of bivalves to toxic dinoflagellates. *Idaho State J* **9**: 184–99.

McFall-Ngai, M, Hadfield, MG, Bosch, TCG, Carey, HV, Domazet-Lošo, T, Douglas, AE, Duilier, N, et al. (2013) Animals in a bacterial world, a new imperative for the life sciences. *Proc Natl Acad Sci* USA **110**: 3229–36. doi: 10.1073/pnas.1218525110.

Newell, RIE and Jordan, SJ (1983) Preferential ingestion of organic material by the American oyster *Crassostrea virginica*. *Mar Ecol Prog Ser* **13**: 47–53. doi: 10.3354/meps013047

Newell, RIE, Cornwell, JC, and Owens, MS (2002) Influence of simulated bivalve biodeposition and microphytobenthos on sediment nitrogen dynamics: a laboratory study. *Limnol Oceanogr* **47**: 1367–1379. doi: 10.4319/lo.2002.47.5.1367.

Newell, RIE, Fisher, TR, Holyoke, RR, and Cornwell, JC (2005) Influence of eastern

oysters on nitrogen and phosphorus regeneration in Chesapeake Bay, USA. In, Dame, R and Olenin, S (eds), The Comparative roles of suspension feeders in ecosystems. NATO Science Ser IV: Earth and Environmental Sciences. Springer, Dordrecht, pp. 93–120.

Ngugi, DK and Brune, A (2012) Nitrate reduction, nitrous oxide formation, and anaerobic ammonia oxidation to nitrite in the gut of soil-feeding termites (*Cubitermes* and *Ophiotermes spp.). Environ Microbiol* **14**: 860–871. doi: 10.1111/j.1462-2920.2011.02648.x.

Nixon, SW (1995) Coastal marine eutrophication: a definition, social causes, and future concerns *Ophelia* **41**: 199–219.

Paerl, HW, Hall, NS, and Calandrino, ES (2011) Controlling harmful cyanobacterial blooms in a world experiencing anthropogenic and climatic-induced change. *Sci Total Environ* **409**: 1739–1745.

Piehler, MF and Smyth, AR (2011) Habitat-specific distinctions in estuarine denitrification affect both ecosystem function and services. *Ecosphere* **2**: art12. doi: 10.1890/ES10-00082.1.

Prado, S, Romalde, JL, Barja, JL (2010) Review of probiotics for use in bivalve hatcheries. *Vet Microbiol* **145**(3-4): 187-97. doi: 10.1016/j.vetmic.2010.08.021.

Rabalais, NN, Turner, RE, and Wiseman, WJ (2002) Gulf of Mexico hypoxia, a.k.a. "the dead zone." *Annu Rev Ecol Syst* **33**: 235–63. doi: 10.1146/annurev.ecolsys.33.010802.150513.

Rawls, J. F., B. S. Samuel, and J. I. Gordon. 2004. From The Cover: Gnotobiotic Zebrafish Reveal Evolutionarily Conserved Responses to the Gut Microbiota. *Proc*

Natl Acad Sci USA **101**(13): 4596–4601. http://www.pnas.org/cgi/doi/10.1073/pnas.0400706101.

Roeselers, G, Mittge, EK, Stephens, WZ, Parichy, DM, Cavanaugh, CM, Guillemin, K, and Rawls, JF (2011) Evidence for a core gut microbiota in the zebrafish. *ISME J* **5**: 1595–1608. doi: 10.1038/ismej.2011.38.

Sanford, RA, Wagner, DD, Qingzhong, W, Chee-Sanford, JC, Thomas, SH, Cruz-García, C, Rodríguez, G, et al. (2012) Unexpected nondenitrifier nitrous oxide reductase gene diversity and abundance in soils. *Proc Natl Acad Sci USA* **109**: 19709-19714. doi: 10.1073/pnas.1211238109.

Schimel, J, Balser, TC and Wallenstein. M (2007) Microbial stress-response physiology and its implications for ecosystem function *Ecology* **88**(6): 1386–94.

Schmitt, S, Tsai, P, Bell, J, Fromont, J, Ilan, M, Lindquist, N, Perez, T, Rodrigo, A, Schupp, P, Vacelet, J, Webster, N, Hentschel, U, and Taylor, MW (2012) Assessing the complex sponge microbiota: core, variable and species-specific bacterial communities in marine sponges. *ISME J* **6**: 564–576. doi: 10.1038/ismej.2011.116.

Shade, A and Handelsman, J (2012) Beyond the venn diagram: the hunt for a core microbiome. *Environ Microbiol* **14**: 4–12. doi: 0.1111/j.1462-2920.2011.02585.x.

Shumway, SE and Koehn, RK (1982) Oxygen consumption in the American oyster *Crassostrea virginica. Mar Ecol Prog* **9**(1): 59-68.

Sisson, M, Kellogg, L, Luckenbach, M, Lipcius, R, Colden, A, Cornwell, J, and Owens, M (2011) Assessment of oyster reefs in Lynnhaven River as a Chesapeake Bay TMDL best management practice.

Smyth, AR, Geraldi, NR, and Piehler, MF (2013) Oyster-mediated benthic-pelagic

coupling modifies nitrogen pools and processes. *Mar Ecol Prog Ser* **493**: 23–30. doi: 10.3354/meps10062.

Smyth, AR, Thompson, SP, Siporin, KN, Gardner, WS, et al. (2013) Assessing nitrogen dynamics throughout the estuarine landscape. *Estuaries and Coasts* **36**: 44–55. doi: 10.1007/s12237-012-9554-3.

Stenuit, B and Agathos, SA (2015) Deciphering microbial community robustness through synthetic ecology and molecular systems synecology. *Curr Opin Biotech* **33**(1): 305–17. doi: 10.1016/j.copbio.2015.03.012.

Stief, P, Poulsen, M, Nielsen, LP, Brix, H, and Schramm, A (2009) Nitrous oxide emission by aquatic macrofauna. *Proc Natl Acad Sci USA* **106**: 4296–300. doi: 10.1073/pnas.0808228106.

Svenningsen, NB, Heisterkamp, IM, Sigby-Clausen, M, Larsen, LH, Nielsen, LP, Stief, P, and Schramm, A (2012) Shell biofilm nitrification and gut denitrification contribute to emission of nitrous oxide by the invasive freshwater mussel *Dreissena polymorpha* (Zebra mussel). *Appl Environ Microbiol* **78**: 4505–4509. doi: 10.1128/AEM.00401-12.

Trabal Fernández, N, Mazón-Suástegui, JM, Vázquez-Juárez, R, Ascencio-Valle, F, and Romero, J (2014) Changes in the composition and diversity of the bacterial microbiota associated with oysters (*Crassostrea corteziensis*, *Crassostrea gigas* and *Crassostrea sikamea*) during commercial production. *FEMS Microbiol Ecol* **88**: 69–83. doi: 10.1111/1574-6941.12270.

Turnbaugh, PJ, Ley, RE, Hamady, M, Fraser-Liggett, CM, Knight, R, and Gordon, JI (2007) The human microbiome project. *Nature* **449**: 804–810. doi:

10.1038/nature06244.

Vezzulli, L, Stagnaro, L, Grande, C, Tassistro, G. Canesi, L, and Pruzzo, C (2017) Comparative 16SrDNA gene-based microbiota profiles of the Pacific oyster (*Crassostrea gigas*) and the Mediterranean mussel (*Mytilus galloprovincialis*) from a shellfish farm (Ligurian Sea, Italy). *Microb Ecol*: 1–10. doi: 0.1007/s00248-017-1051-6.

Vitousek, PM, Aber, JD, Howarth, RW, Likens, GE, et al. (1997) Human alteration of the global nitrogen cycle: sources and consequences. *Ecol Appl* **7**(3): 737–50.

Wegner, KM, Volkenborn, N, Peter, H, and Eiler, A (2013) Disturbance induced decoupling between host genetics and composition of the associated microbiome. *BMC Microbiol* **13**(1) doi: 10.1186/1471-2180-13-252.

Welsh, DT, and Castadelli, G (2004) Bacterial nitrification activity directly associated with isolated benthic marine animals. *Mar Biol* **144**(5): 1029–37. doi: 10.1007/s00227-003-1252-z.

Whipps, JM, Karen, L, and Cooke, RC (1988) Mycoparasitism and plant disease control. In, Burge, NM (ed), *Fungi in Biological Control Systems*. Manchester University Press, Manchester, United Kingdom, pp. 161-187.

Wüst, PK, Horn, MA, Henderson, G, Janssen, PH, Rehm, BHA, and Drake, HL (2009) Gut-associated denitrification and in vivo emission of nitrous oxide by the earthworm families *Megascolecidae* and *Lumbricidae* in New Zealand. *Appl Environ Microbiol* **75**(11): 3430–36. doi: 10.1128/AEM.00304-09.

Zehr, JP, and Kudela, RM (2011) Nitrogen cycle of the open ocean: from genes to ecosystems. *Annu Rev Mar Sci* **3**: 197–225. doi: 10.1146/annurev-marine-120709-

142819

Zumft, WG (1997) Cell biology and molecular basis of denitrification *Microbiol Mol Biol R* **61** (4): 533-616.

FIGURES

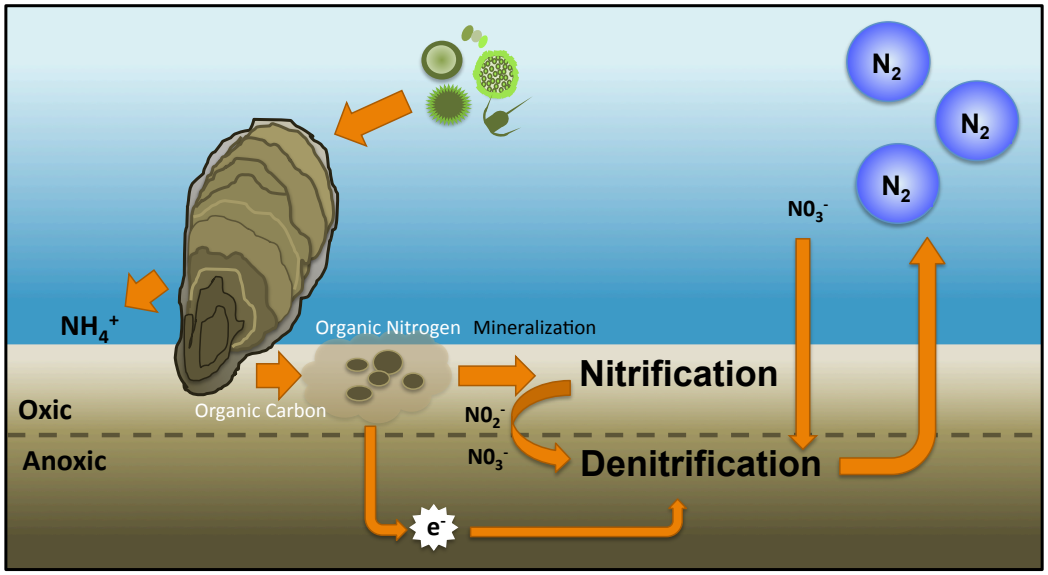

Fig. 1 Proposed mechanism of enhanced N removal in oyster reef sediments.

Oysters take up nutrient rich phytoplankton, which are excreted as NH_4^+ or repackaged to the sediments as biodeposits. Excreted NH_4^+ and organic nitrogen in biodeposits, that has undergone mineralization to NH_4^+, is utilized by nitrifiers in the oxic layers of the sediment. NH_4^+ is oxidized to NO_3^- via nitrification. Nitrified NO_3^- or NO_3^- present in the water column is used by denitrifiers in the anoxic layers of the sediment. Electrons donated from organic carbon in oyster biodeposits support enhanced denitrification.. Denitrification is the process in which fixed N is removed from the environment.

Chapter 2

Denitrification potential of the eastern oyster microbiome using a 16S rRNA gene based metabolic inference approach

Published: 2017 PLOS ONE 12(9): 1-21

ABSTRACT

The eastern oyster (*Crassostrea virginica*) is a foundation species providing significant ecosystem services. However, the roles of oyster microbiomes have not been integrated into any of the services, particularly nitrogen removal through denitrification. We investigated the composition and denitrification potential of oyster microbiomes with an approach that combined 16S rRNA gene analysis, metabolic inference, qPCR of the nitrous oxide reductase gene (*nosZ*), and N_2 flux measurements. Microbiomes of the oyster digestive gland, the oyster shell, and sediments adjacent to the oyster reef were examined based on next generation sequencing (NGS) of 16S rRNA gene amplicons. Denitrification potentials of the microbiomes were determined by metabolic inferences using a customized denitrification gene and genome database with the paprica (PAthway PRediction by phylogenetIC plAcement) bioinformatics pipeline. Denitrification genes examined included nitrite reductase (*nir*S and *nir*K) and nitrous oxide reductase (*nos*Z), which was further subdivided by genotype into clade I (*nos*ZI) or clade II (*nos*ZII). Continuous flow through experiments measuring N_2 fluxes were conducted with the oysters, shells, and sediments to compare denitrification activities. Paprica properly classified the composition of microbiomes, showing similar classification results from Silva, Greengenes and RDP databases. Microbiomes of the oyster digestive glands and shells were quite different from each other and from the sediments. The relative abundance of denitrifying bacteria inferred by paprica was higher in oysters and shells than in sediments suggesting that oysters act as hotspots for denitrification in the marine environment. Similarly, the inferred *nos*ZI gene abundances were also higher in the oyster and shell microbiomes than in the sediment microbiome. Gene abundances for

*nos*ZI were verified with qPCR of *nos*ZI genes, which showed a significant positive correlation ($F_{1,7}$ = 14.7, p=6.0x10^{-3}, R^2 = 0.68). N_2 flux rates were significantly higher in the oyster (364.4 ± 23.5 μmol N-N_2 m^{-2} h^{-1}) and oyster shell (355.3 ± 6.4 μmol N-N_2 m^{-2} h^{-1}) compared to the sediment (270.5 ± 20.1 μmol N-N_2 m^{-2} h^{-1}). Thus, bacteria carrying *nos*ZI genes were found to be an important denitrifier, facilitating nitrogen removal in oyster reefs. In addition, this is the first study to validate the use of 16S gene based metabolic inference as a method for determining microbiome function, such as denitrification, by comparing inference results with qPCR gene quantification and rate measurements.

INTRODUCTION

Chesapeake Bay, the largest estuary in the United States, is one of many systems that has experienced the detrimental effects of excess nitrogen (N) and cultural eutrophication, including bottom water hypoxia, reduced fisheries harvests, and loss of submerged aquatic vegetation (Cerco and Noel 2007, Glibert et al. 2014). Over the last several years, restoration of the eastern oyster (*Crassostrea virginica*) to the Bay has gained momentum as a potential means to enhance N removal and mitigate eutrophication by increasing rates of denitrification (Newell et al. 2002, Kellogg et al. 2014). Denitrification is the microbially-mediated stepwise reduction of nitrate (NO_3^-) and nitrite (NO_2^-) to gaseous nitric oxide (NO), nitrous oxide (N_2O) and dinitrogen (N_2) Zumft 1997.

The majority of studies addressing denitrification associated with oysters have primarily focused on whether oysters enhance denitrification in sediments within and adjacent to oyster reefs (Kellogg et al. 2013, Hoellein et al. 2015, Humphries et al. 2016, Smyth et al. 2016). Oysters may stimulate denitrification by supplying organic carbon (C) and N in the form of biodeposits to denitrifying communities in sediments (Newell et al. 2005, Giles et al. 2006, Kellogg et al. 2014). Ammonium (NH_4^+) remineralized from oyster biodeposits and excretions can be nitrified to NO_3^-, which supports denitrification (Jenkins and Kemp 1984, Newell et al. 2002). In addition, the oyster itself can provide a microbial habitat for denitrification (oyster denitrification). Live oysters have been shown to have significantly higher rates of denitrification than sediments (Smyth et al. 2013). Oyster gut organs in particular, may be hotspots for denitrification, as gut organs of several invertebrates including insects, earthworms, and mussels have shown to exhibit

denitrification activity (Stief et al. 2009, Wüst et al. 2009, Ngugi et al. 2012, Svenningsen et al. 2012). Denitrification in the invertebrate gut is thought to be a result of the anoxic conditions and availability of labile organic carbon provided within the gut environment (Stief et al. 2009, Depkat-Jakob et al. 2010). Oyster shells were also found to have denitrification activity even though the rates were much lower than those measured in live oysters (Caffrey et al. 2016). Shell denitrification may be influenced by factors similar to those impacting sedimentary denitrification. Like oyster reef sediments, the shell microbiome is exposed to increased C and N from biodeposits and excretions, which may enhance denitrification. Both the gut and shell microbiomes are likely important contributors to oyster denitrification, however, no previous studies have identified denitrifying taxa or genes in the oyster microbiome.

Studies investigating the composition of oyster microbiomes are also limited compared to those regarding sediment microbiomes. Previous examinations of oyster microbiomes by cloning and sequencing of 16S rRNA genes, DNA fingerprinting and fluorescent in situ hybridization (FISH) revealed *Proteobacteria* and *Firmicutes* as dominant taxa in different oyster species, but were restrictive in scale or resolution (Romero et al. 2002, Hernández-Zárate et al. 2006, Green and Barnes 2010, Zurel et al. 2011, Fernandez-Piquer et al. 2012, Trabal et al. 2012).. King et al. (2012) was one of the first studies using high-throughput next-generation sequencing (NGS) of 16S rRNA gene amplicons to characterize the intestine and stomach microbiome of the eastern oyster. This study showed a dominance of *Mollicutes* or *Planctomycetes* in the oyster stomach, while intestines were found to be more species rich and largely composed of the phyla *Chloroflexi*, *Proteobacteria, Verrucomicrobia* and *Planctomycetes* (King et al.

2012). Follow-up microbiome studies using 16S NGS included further examination of the oyster gut microbiome, as well as microbiomes of oyster gills, mantle and hemolymph (Wegner et al. 2013, Trabal Fernández et al. 2014, Lokmer et al. 2016a, Lokmer et al. 2016b). For example, in Lokmer et al. (2016b) higher abundances of *Gammaproteobacteria* were reported in the gut, gill, mantle, and hemolymph microbiomes compared to the surrounding seawater. However, none of the studies to date have attempted to connect the oyster microbiome structure to its function using NGS of 16S rRNA gene amplicons.

Exploring the linkage between the structure and function of microbiomes presents a financial and logistical challenge. Whole-genome shotgun metagenomics offer the ability to identify community structure and functional genes related to metabolic processes in an environment, such as those of microbiomes. Wide-scale, whole-genome metagenomic studies however, are often prohibitively costly and may not be sufficient for large sample sets or for samples where prokaryotic genetic contribution to the metagenome is low (Sharpton 2014). As a result, many microbiome studies rely on much less expensive and accessible 16S rRNA gene based amplicon sequencing, which traditionally has offered little insight into functionality. To address this shortcoming with 16S rRNA gene sequencing, bioinformatic programs, Phylogenetic Investigation of Communities by Reconstruction of Unobserved States (PICRUSt; Langille et al. 2013), and more recently PAthway PRediction by phylogenetIC plAcement (paprica; Bowman et al. 2015), have been developed to infer metabolic pathways from 16S rRNA gene sequences. Several recent studies have used metabolic inference programs to infer microbial metabolisms in marine microbiomes such as those of macrobiota biofilms

(Pfister et al. 2014), sponges (Cleary et al. 2015), and corals (Rothig et al. 2016). Some key differences in the programs are in the assignment of pathways and user flexibility. PICRUSt uses ancestral state reconstruction to infer the probable metabolism (according to the KEGG ontology; Kenehisa and Goto 2000) of extant Greengenes operational taxonomic units (OTUs) (DeSantis et al. 2006). In comparison, paprica describes community structure through phylogenetic placement with pplacer (Matsen et al. 2010) onto a reference tree created from all completed genome in Genbank (Clark et al. 2016). Paprica then uses a pre-computed database to assign genomic features (including genes and metabolic pathways via the MetaCyc ontology; Caspi et al. 2014). Paprica is designed to maximize user flexibility and has options for adding reference draft genomes and customizing the enzyme commission (EC) numbers associated with reference genomes.

We combined a customized database of genomes and denitrification genes with the paprica program to link the oyster digestive gland (gut), shell, and reef sediment microbiome structures to denitrification by characterizing the composition of microbiomes and identifying potential denitrifiers from 16S rRNA amplicon sequences. Our main objectives were to (1) compare the oyster microbiomes' taxonomic classifications determined by paprica and other taxonomic databases, (2) examine the structure and diversity of the oyster microbiomes using a taxonomically independent OTU analysis, and (3) connect the oyster microbiome to rates of denitrification by comparing the relative abundances and composition of denitrification genes in each microbiome to measured N_2 fluxes. A customized paprica database was constructed with dissimilatory nitrite reductase genes (*nir*S and *nir*K), and nitrous oxide reductase gene

(*nos*Z) identified from completed or draft genomes. *Nir*S and *nir*K encode enzymes responsible for the reduction of nitrite (NO_2^-) to nitric oxide (NO), while *nos*Z encodes for enzyme in the reduction of nitrous oxide (N_2O) to nitrogen gas (N_2) in the denitrification pathway. The *nos*Z gene classification was further divided into two separate clades; clades I (*nos*ZI) and II (*nos*ZII). Gene clades *nos*ZI and *nos*ZII differ based on variations in signaling peptides, phylogeny (Jones et al. 2013), and responses to environmental conditions (Graf et al. 2014, Domeignoz-Horta et al. 2015). Continuous flow experiments were performed with live oysters, empty shells, and reef sediments to measure the associated denitrification activity.

MATERIALS AND METHODS

Sample collection and flow-through experiment

Triplicate samples of live oysters, pairs of empty oyster shells, and intertidal surficial sediment cores taken within oyster reefs (Piehler et al. 2011) were collected on 7 July 2013 at low tide from Hoop Hole Creek (Latitude 34.706483, Longitude 76.751931), a tidal creek located in Atlantic Beach, NC, and immediately transported to the University of North Carolina Institute of Marine Sciences (UNC IMS). Oysters samples were acquired according to conditions detailed in UNC IMS's research collection permit from NC Division of Marine Fisheries. Temperature, salinity, dissolved oxygen (DO) were measured using a YSI water quality sonde (YSI, Inc.). Water was filtered through Whatman GF/F filters (25 mm diameter, 0.7 l m nominal pore size) and the filtrate was analyzed with a Lachat Quick-Chem 8000 automated ion analyzer for NO_3^-.

Sediment cores were left in a water bath overnight with continuous aeration with air stones. Oysters and shells were stored overnight in raceway flumes and then added to individual cores and capped the following morning. Continuous, flow-through core incubation experiments to measure N_2 fluxes were conducted under dark conditions in an environmental chamber held at constant site water temperatures using each of the collected samples. The treatments consisted of: (1) live oyster, (2) oyster shells only, and (3) sediment. Samples from the bypass line (flowed directly from reservoir to 5ml ground glass vial) and each core's outflow were collected following the acclimation period. Inflow water and outflow water leaving the cores were analyzed for dissolved N_2, O_2 and Ar using a Balzers Prisma QME 200 quadruple mass spectrometer (Kana et al. 1994). Concentrations of O_2 and N_2 were determined using the ratio with Ar (Kana et al.

1994, Ensign et al. 2008). Following the experiment, oysters, oyster shells, and 50 mL of sediment from the cores were frozen and shipped to the Virginia Institute of Marine Science, where they were stored at -80°C.

Whole oysters were partially thawed at room temperature for approximately 30 minutes before dissection. Dissections were carried out using sterile scalpel blades. Digestive glands were carefully excised, transferred to 2.0 mL microcentrifuge tubes, and frozen at -80°C. Following dissection, the remaining oyster tissue was removed from its shell, and the interior of the shell was scrubbed with 75% ethanol. Oyster shells from live oysters (shell (live)) and paired oyster shells collected from the reef (shell (only)) were crushed into roughly 0.5-5.0 mm sized pieces using sterilized hammers to homogenize the exterior shell biofilm. Shell fragments were then transferred to 50 mL falcon tubes, and frozen at -80°C.

DNA extraction and amplification

DNA was extracted from 0.25-0.30 grams of digestive gland using the Qiagen DNA stool mini kit (Qiagen, Hilden, Germany) following the pathogen detection protocol. Shell (0.40-0.60 grams) and sediment (0.50-0.75 grams) extractions were conducted using MoBIO Powersoil extraction kits (Mo-Bio Laboratories, Inc., Carlsbad, CA) following the manufacture's protocol. As a result of variation in the source material, different kits were used to extract DNA from the oyster digestive gland and the oyster shell or reef sediment in order to optimize DNA quality and DNA yield for PCR and sequencing efficiency. While this may introduce some bias, these biases tend to have a minimal impact on 16S NGS microbiome studies (Rubin et al. 2014). Overall, 12 DNA

samples were extracted: triplicate DNA samples from (1) oyster digestive gland, (2) shell from live oysters, (3) collected (empty) paired shells, and (4) oyster sediment.

Initial amplification of the targeted hypervariable V4 region of the 16S rRNA gene was performed on extracted DNA using forward primer 515F and modified, barcoded reverse primer 806R (Caporaso et al. 2010), adapted for use with the Ion Torrent Personal Genome Machine (PGM). The basic manufacturer's PCR protocol was used with Taq DNA Polymerase (Invitrogen, Carlsbad, CA) to create a PCR master mix with the following modification: 1 mM dNTP mixture was used in place of 10 mM for a final concentration of 0.02 mM dNTP. Thermal cycling conditions consisted of an initial denaturation step at 94°C for 3 min, followed by 30 cycles of 94°C for 1 min, 54°C for 1 min, 68°C for 2 min. A final elongation step of 68°C for 10 min was added to ensure complete amplification. The amplified products were gene cleaned using the UltraClean GelSpin DNA Purification Kit (Mo-Bio Bio Laboratories, Inc., Carlsbad, CA). The resulting amplicon libraries were then used as templates for sequencing with the Ion S5 platform following the manufacture's instruction (Thermo Fisher Scientific, Waltham, MA). Sequences generated in this study may be downloaded from the NCBI Sequence Read Archive, BioSample accession numbers SAMN06897488 – SAMN06897499.

Bioinformatic analyses

An overview of the bioinformatic pipeline used for the 16S rRNA based microbiome analyses is shown in supplementary materials (S1 Fig). Removal of barcodes and primers from raw sequences and trimming of sequence length were conducted using the Ribosomal Database Project (RDP) pipeline initial process (Cole et

al. 2014; http://rdp.cme.msu.edu) with a minimum quality score of 20, minimum length of 200 bases, and a maximum length of 500. Mothur v1.35.1 (Schloss et al. 2009) was used to further trim sequences against the SILVA v123 (Yilmaz et al. 2014) alignment template, precluster, and screen for chimeric sequences using the uchime *denovo* program (Edgar et al. 2011). Unknown taxa, mitochondria, chloroplast, archaea, and eukaryotic sequences were removed from analysis using SILVA v123 reference taxonomy and the Wang classification method (Wang et al. 2007) with an 80% minimum identity. Archaea were excluded from this analysis due to their low abundances; archaea comprised <1.0% of the total overall sequencing reads and made up <3.8% of the reads in any one sample. Further analyses focused on high quality bacterial sequences only.

Phylotype analyses using Mothur were conducted on high quality, trimmed bacterial sequences to determine the taxonomical composition of oyster digestive gland, oyster shell, and oyster reef sediment microbiomes. Sequences were classified with SILVA v123, Greengenes v13_5, or RDP v14 reference taxonomy databases using the Wang classification method described previously. For all phylotype analyses, resulting taxonomic relative abundances from triplicate microbiome samples were averaged together, with oyster shells from live oysters (shell (live)) and collected paired shells (shell (only)) combined together to form the oyster shell microbiome. In addition, an operational taxonomic (OTU) analysis was conducted on the microbiome sequences to assess microbiome diversity. Sequences were clustered into OTUs based on a 97% identity using the average neighbor clustering algorithm. To remove sampling intensity error and normalize samples, individual sample reads were randomly subsampled to the lowest number of reads found in the sample data set (n = 66,687). All diversity metrics

are based on microbiome averages. For diversity metrics, both shell (live) and shell (only) treatments described previously were combined to form the shell microbiome; for principle coordinate analysis (PCoA), shell (live) and shell (only) microbiomes were analyzed separately to determine shell microbiome structure similarity.

To conduct phylotype and denitrification gene inference analyses using paprica, a customized paprica database was constructed with 5,445 complete and 222 draft bacterial genomes (S1 and S2 Tables). High quality draft genomes, where available, were selected for inclusion in the database based on their relevance to oyster microbiome taxonomical structures determined by the Silva, Greengenes, and RDP phylotype analyses. All draft genomes were downloaded from GenBank (https://www.ncbi.nlm.nih.gov/genbank/). Each individual genome was curated for the presence of *nir*S, *nir*K, and *nos*Z genes using either the KEGG database for completed genomes or gene annotations for draft genomes. Construction of the paprica reference database and inclusion of the gene-specific inferences were conducted following the instructions found on the developer's website (http://www.polarmicrobes.org/building-the-paprica-database/). Phylotype and gene inference analyses were performed by first aligning the quality controlled query reads to the reference alignment with Infernal, then placing them on the phylogenetic reference tree with pplacer (Matsen et al. 2010). Taxonomical classification and gene inferences were based on edge placement and consensus identity with either internal or terminal nodes as described in Bowman and Ducklow (2015). Resulting abundances from paprica were given as either values normalized to 16S rRNA gene copy number or as uncorrected values. Normalized values were calculated as the measured abundance divided by the number of 16S rRNA gene copies predicted for each taxon. Uncorrected values were

used for the phylotype analysis to perform an equivalent comparison with the Mothur phylotype analyses, while normalized values were used with gene abundances to better capture potential denitrifiers. Distinctions between *nos*ZI and *nos*ZII gene abundances and taxonomic classification were based on edge taxonomies only.

Quantitative PCR

Quantitative PCR (qPCR) assays were performed on oyster and sediment samples to determine the relative abundance of *nos*ZI genes. Relative abundances of *nos*ZI genes in each sample were calculated using the ratio of *nos*ZI abundance to the abundance of 16S rRNA genes. Gene abundances for *nos*ZI and 16S rRNA were determined using the 6 Flex Real-Time PCR system (Thermo Fisher Scientific, Waltham, MA). 16S rRNA gene qPCR assays were carried out in a volume of 20 µL consisting of 10 µL of 2X SYBR green based GoTaq qPCR Master Mix, 0.05 µL CXR reference dye (Promega Corporation, Madison, WI), 0.01 mg/mL BSA (Promega Corporation, Madison, WI), 0.5 µM each of 16S rRNA specific primers EU341F and 685R targeting hypervariable regions V3, and 1 uL of template DNA. Thermal cycling conditions consisted of an initial denaturing step at 95°C for 10 min, followed by 30 cycles of 95°C for 15 s, 55°C for 30 s, and 72 °C for 30 s with fluorescence detection. Quantification of *nos*ZI was performed using the same reaction volumes and components described for 16S, with *nos*ZI specific primers nosZ1F and nosZ1R (Henry et al. 2006). Thermal cycling conditions for *nos*ZI qPCR were the same as 16S with the exception that total cycle number was increased to 50 cycles, elongation step at 55°C was increased to 45 s, and additional step at 80°C with fluorescence detection was added. All reactions were

performed on 96-well plates with duplicate negative controls and standards. Standards were prepared by serially diluting plasmids carrying either the 16S or *nos*ZI gene and quantified with the Agilent 220 TapeStation System (Agilent Technologies, Santa Clara, CA). Standard curves and gel electrophoresis were used to confirm reaction specificity.

Statistical Analyses

For all results, variation within each microbiome is reported as the standard deviation. Diversity statistics including coverage, Chao I, and Shannon were conducted using the summary.single command in Mothur. A principle coordinate analysis (PCoA) and the Adonis function for Permanova (non-parametric permutational multivariate analysis of variance; Anderson; Anderson et al. 2001) using Bray-Curtis dissimilarity were performed on OTU distributions with the Phyloseq package (McMurdie et al. 2013) in R (version 3.1, https://wwww.R-project.org). Flux data was assessed for normality using the qqplot function and Shapiro-Wilk normality test ($p < 0.05$). One-way analysis of variance (ANOVA) and a post-hoc Tukey honest significant difference (HSD) tests were performed on flux measurements to test for significant differences. A one-tailed, paired t-test was used to determine differences between *nos*ZI and *nos*ZII within the shell and sediment microbiomes, and a one-tailed, Welch's t-test was used to compare gene abundances between the shell and sediment microbiomes. For comparisons between the oyster, shell, and sediment microbiomes, relative abundances of the digestive gland microbiome and shell (live) microbiome were combined to form the oyster microbiome. A simple linear regression analysis was conducted to compare the relative abundances of *nos*ZI measured by qPCR and the uncorrected *nos*ZI gene abundances predicted by

paprica; uncorrected paprica values were used so that equivalent comparisons between gene abundances and qPCR relative abundances could be made. Unless otherwise stated all statistics were conducted in R and significance was based on $p < 0.05$.

RESULTS

Phylotype comparison of microbiomes

A total of 982,504 trimmed, high quality 16S rRNA gene sequences were obtained from the oyster and sediment microbiome samples. Sequencing depth averages for each microbiome were 85,640 ± $1.5x10^4$ for oyster digestive gland, 86,745 ± $1.6x10^4$ for shell, and 68,378 ± $1.5x10^3$ for sediment. Among the 4 databases, paprica classified the greatest number of sequences at the family level (85.4 ± 9.8%), followed by Silva (76.5 ± 18.9%), Greengenes (75.8 ± 18.5%), and RDP (57.2 ± 18.7%). All four databases showed an overall similar pattern at the family classification level for the average relative abundance of sequences ≥1% (Fig 1). With the exception of one shell in the shell (only) treatment having a slightly different profile (S2 Fig), phylotype comparisons between the shell (live) and shell (only) microbiomes were similar in taxonomy and relative abundance, and were thus combined together to form the shell microbiome. Of the oyster-related microbiomes, the sediment microbiome showed the greatest number of families (n=12.5 ± 1.7) and the lowest percent of sequences identified (47.7 ± 6.7%), the oyster digestive gland microbiome showed the lowest number of families (n=1.3 ± 0.5) and the highest number of sequences identified (73.1 ± 24.5%), and the oyster shell microbiome fell somewhere in the middle (n=8.8 ± 2.5; 59.7 ± 7.7%) (Fig 1). Each of the four databases consistently identified family *Mycoplasmataceae* from phylum *Tenericutes* as the dominant family in the digestive gland microbiome. Paprica was the only method to also include the classification of *Odoribacteraceae* as another dominant family member in the digestive gland microbiome. Within the oyster shell microbiome, all four databases showed a dominance of families

Sphingomonadaceae, Erythrobacteraceae, and *Rhodobacteraceae* from phylum *Proteobacteria*, and *Flammeovirgaceae, Flavobacteriaceae*, and *Saprospiraceae* from phylum *Bacteroidetes*. *Desulfobacteraceae* and *Rhodobacteraceae* from phylum *Proteobacteria*, and *Flavobacteriaceae* and *Saprospiraceae* from phylum *Bacteroidetes*, were the dominant families consistently identified in the sediment microbiomes across all four databases. The greatest variation among the databases in the classification of families occurred in paprica's identification of sequences from phylum *Bacteroidetes* and Greengenes's identification of sequences from phylum *Proteobacteria*. However, at the phylum level, identification of sequences for each phylum was relatively consistent among the four databases.

Diversity comparison of microbiomes using OTU analysis

All 12 microbiome samples were subsampled to 66,687 sequences to conduct an OTU diversity analysis (Table 1 and Fig 2). Average coverage of sequences ranged from 89.1 ± 0.9% in the sediment microbiome to 99.6 ± 0.0% in the oyster digestive gland. Significant differences among the microbiomes were detected with Permanova ($F_{2,11}$ = 8.19, p = 0.001) and demonstrated using PCoA (Fig 2), which explained 65.8% of the variation found. The oyster digestive gland, shell, and sediment samples, formed distinct microbiomes, clustering separately based on sample type. The greatest dissimilarity occurred between the oyster digestive gland and the sediment microbiome. There were no differences between the shell microbiomes, whether the shell came from a live oyster or a discarded, empty shell. Similar trends were found among the microbiomes regarding Chao I richness, Shannon diversity, and OTU abundances (Table 1). Sediment

microbiomes had the highest level of diversity and richness than all other microbiomes (Chao 1 = 32,035 ± $1.8x10^3$, Shannon = 6.8 ± 0.2), and an average OTU abundance of 10,489 ± $9.3x10^2$. Shell microbiome had moderate diversity and richness (Chao 1 = 18,025 ± $3.2x10^3$, Shannon = 5.7 ± 0.5) with an average OTU abundance of 6,264 ± $1.5x10^3$, and the oyster digestive glands had the lowest levels of diversity and richness (Chao 1 = 1,234 ± $1.7x10^2$, Shannon = 1.2 ± 0.1) with an average OTU abundance of 525 ± $4.1x10^1$.

Microbiome denitrification gene inferences with the paprica database

The sediment and shell microbiomes had an inferred average relative abundance of 23.8 ± 2.8% and 26.1 ± 3.0 %, respectively, of denitrification genes (Fig 3). The digestive gland microbiome was comprised of a ≤ 0.1% relative abundance of denitrification genes. The greatest differences among the microbiomes were found in the relative abundances of the *nir*K, *nir*S, or *nos*Z genes only. Combined, organisms carrying one of these genes were more dominant than organisms carrying both *nir*S and *nos*Z or *nir*K and *nos*Z genes. Between the shell and sediment microbiomes, the shell microbiome had a significantly higher relative abundance of bacteria carrying the *nir*K only gene (unpaired t-test t_5=6.48, p=$2.6x10^{-5}$), while the sediment had a significantly higher abundance of the *nir*S only (unpaired t-test t_7=8.75, p=$2.6x10^{-5}$) and a higher, but not significant, abundance of *nosZ* only (unpaired t-test t_7=2.74, p>0.05) genes. Among the microbiomes, the average relative abundance of organisms carrying *nos*ZII gene was overall higher than those carrying the *nos*ZI gene (Fig. 4). In the sediment microbiome, this difference was significant (paired t-test t=7.14, p=$9.5x10^{-3}$), but it was not significant

in the shell or digestive gland microbiomes. Taxonomically, *nosZ*I bacteria were primarily from class *Alphaproteobacteria*, while *nosZ*II bacteria were from classes *Cytophygia* and *Flavobacteriia* in the shell, and *Gammaproteobacteria*, *Cytophygia*, and *Flavobacteriia* in the sediments (S3 Fig).

N_2 flux experiments

Site water physical and chemical parameters used in the flux experiments were as follows: 30°C temperature, 30 ppt salinity, 6.8 mg/L dissolved oxygen (DO), and 0.51 μmol N/L NO_3^-. Live oyster cores had the highest average flux of N_2 at 364.4 ± 23.5 μmol N-N_2 m^{-2} h^{-1}, followed by the shell only cores at 355.3 ± 6.4 μmol N-N_2 m^{-2} h^{-1}, and sediment cores with the lowest at 270.5 ± 20.1 μmol N-N_2 m^{-2} h^{-1} (Fig. 5). There were no significant differences in the N_2 fluxes between the live oyster and shell, but both were significantly higher than the sediment cores (ANOVA, $F_{2,6}$=23.7, p=1.4x10^{-3}; Tukey HSD, $p < 0.05$).

Microbiome nosZI gene inference comparison to flux measurements and qPCR

The rates of N_2 fluxes followed a similar trend to the average relative abundance of *nosZ*I genes inferred in oyster, shell, and sediment microbiomes (Fig 5 and 6B). Oysters and shells had similarly high N_2 flux rates and *nosZ*I genes, while sediment samples had lower rates of N_2 flux and lower abundances of *nosZ*I genes. This trend was not found in the average relative abundance of the *nosZ*II genes or in overall *nosZ* gene abundance (Fig 5 and 6A,C). A significant, positive linear correlation was determined

between the copy number of *nos*ZI genes quantified in the shell and sediment microbiomes by qPCR and the relative abundance of *nos*ZI genes inferred from paprica ($F_{1,7}$ = 14.7, p=6.0x10^{-3}, R^2 = 0.68) (Fig 7). Predicted values were on average 3.5 ± 1.7% x higher than those determined by qPCR. Copy numbers of *nos*ZI genes from oyster digestive gland microbiome samples were below detection level, and thus were excluded from the regression analysis.

DISCUSSION

Paprica's taxonomical classification of the oyster digestive gland, oyster shell and sediment microbiomes was comparable to other reference databases regarding the pattern of dominant families found within each microbiome (Fig 1). All four phylotype analyses in this study showed *Mycoplasmataceae,* from phylum *Tenericutes*, to clearly be dominant in the oyster digestive gland. While studies on oyster gut-related microbiomes are relatively small in number, several studies including Green and Barnes (2010), Lokmer et al (2016b), and King et al. (2012) found *Mycoplasma* to be highly abundant in digestive glands of Sydney rock oysters (*Saccostrea glomerata*), gut tissues of pacific oysters (*Crassostrea gigas*), and stomachs of eastern oysters, respectively. Even less is known about the oyster shell microbiome. While no known studies to date have examined the structure of the oyster shell microbiome, a related study conducted on mussel (*Mytilus californianus*) shell surface communities found in the Pacific Northwest showed *Gammaproteobacteria* to be the dominant class (Pfister et al. 2014). In comparison, our study found *Alphaproteobacteria* to be the dominant class in the oyster shell microbiome, while *Gammaproteobacteria* (and *Deltaproteobacteria*) were more dominant in the sediment microbiome. *Alphaproteobacteria*, in particular *Roseobacter* from family *Rhodobacteraceae*, have been shown to rapidly colonize surfaces in Atlantic temperate waters and may produce antibacterial components, preventing other bacteria from growing (Dang et al. 2008). This may explain our findings in the shell microbiomes, which were dominated by family *Rhodobacteraceae*. In the sediment, *Gamma-* and *Deltaproteobacteria* have been shown to be highly abundant in surface sediments (Polmenakou et al. 2005, Feng et al. 2009, Sun et al. 2013), which is consistent

with our findings. In addition to *Proteobacteria*, *Bacteroidetes* was another dominant phylum in both shell and sediment microbiomes. *Bacteroidetes* are common in the marine environment (Hehemann et al. 2011), and thus likely to be present in marine samples exposed to the environment.

Diversity of the microbiome determined by the paprica phylotype analyses was compared with a taxonomically independent OTU analysis performed by the Mothur program. The PCoA analyses (Fig 2) verified that the oyster digestive gland, shell, and sediment microbiomes were structurally different from each other, but also that the variation within each microbiome was relatively low. Interestingly, the microbiome structure between shells from live oysters vs. those from shells only was highly similar. Shells used in the shell only treatment grew and were collected on the same oyster reef from which the whole oysters were collected. Further studies would need to be conducted to see if mere proximity to an oyster or oyster reef influences the shell microbiome, or if once an oyster's shell microbiome is established, the microbiome remains after the animal has expired. The high similarity between samples within each microbiome provided a realistic ability to measure differences between the microbiomes despite the small number of samples analyzed, and a sufficient justification to assess microbiome structure based on pooled averages. Similarly, the diversity and richness patterns (Table 1) determined by the OTU analysis followed the same pattern as the taxonomical diversity demonstrated in the phylotype analyses (Fig 1). In the sediments, for example, high diversity and richness corresponded to a greater number of taxonomical families and a more even distribution of those families. Additionally, coverage of the microbiomes was determined to be $\geq$ 89% in the most OTU rich samples

(Table 1), indicating that the microbiome structure was adequately sampled, and inferences drawn from the microbiomes were representative of the community structure. All of these factors combined demonstrated that the taxonomical classifications determined by the paprica database accurately and thoroughly described the microbiome structures. This allowed for reasonable confidence in using the modified paprica database to infer the abundance and distribution of denitrification related genes in the oyster digestive gland, shell, and sediment microbiomes.

Despite having different taxonomical profiles (Fig 1) and distinct microbiome structures (Fig 2), The average relative % abundances of bacteria carrying *nir*S, *nir*K, *nos*Z, or a combination of those genes, were similar in the shell and sediments, making up between ~ 23-26% of the overall community (Fig 3). This suggests the abundance and distribution of denitrifying bacteria carrying these genes may be conserved between microbiomes. However, this pattern changed with respect to individual gene abundances. Both shell and sediment microbiomes had relatively similar overall abundances of *nir* only genes, yet *nir*K only was significantly more abundant in the shell microbiome, while *nir*S only was significantly more abundant in the sediment microbiome. In estuarine systems, *nir*S has been generally shown to be more abundant than *nir*K (Mosier et al. 2010, Smith et al. 2015). However, *nir*K has been shown to be dominant in environments associated with animal hosts (Graf et al. 2014) and in zones of high oxygen and pH fluctuation, like those found in microbial mats (Desnues et al. 2007). The higher abundance of *nir*K carrying bacteria versus *nir*S in oyster shells may be evidence of the shell microbiome's (current or past) connection to an oyster host, or a result of the potentially more oxic environment provided by the shell surface, compared to the marine

sediment. Also interesting, is that in both microbiomes the predicted relative abundances of complete denitrifiers, those carrying the *nir* and *nos* genes together, were less than those carrying either the *nir* or *nos* genes separately. This indicates that the complete transformation of NO_2^- to N_2 in of these microbiomes may be highly modular and dependent on community interaction and not individual denitrifiers.

Regarding *nos*Z gene abundances, all oyster-related microbiomes, showed the predicted relative abundance of *nos*ZII bacteria were higher than *nos*ZI carriers (Fig 4). This is consistent with other studies that have shown *nos*ZII denitrifiers to be dominant over *nos*ZI denitrifiers in a variety of different environments (Jones et al. 2013, Orellana et al. 2014). Microbes with the *nos*ZII gene have been shown to be more taxonomically and ecophysiologically diverse than those with *nos*ZI genes (Sanford et al. 2012). This was evident in the shell and sediment microbiomes in our study. Among the shell and sediment microbiomes, the primary driver of *nosZ*I abundances belonged to bacteria from a single class, *Alphaproteobacteria*, while *nosZ*II abundances were mainly driven by bacteria belonging to classes *Cytophygia*, and *Flavobacteriia* in the shell and *Gammaproteobacteria*, *Cytophygia*, and *Flavobacteriia* in the sediments (S3 Fig). Additionally, among all three microbiomes, as diversity increases in the microbiome, the differences between *nosZ*I and *nosZ*II abundances became much greater. This may suggest that *nos*ZII abundances may be positively linked to microbiome diversity.

Net N_2 production measured by flux experiments in this study determined that oysters and oyster shells had a significantly higher net production of N_2 compared to sediments (Fig 5). Comparisons between oyster nitrogen cycling studies are complicated by the unit at which studies are conducted (whole reef, sediments, oysters, shells), the

type of incubation (flow through vs. batch), and the setting of the oysters (natural reef, constructed reef, aquaculture). Despite all of these distinctions in oyster nitrogen cycling studies, we found the results from this study to be largely similar to previous research. Sediment N_2 production in this study was in line with summer values for oyster reef sediments in nearby reefs (Piehler and Smyth 2011, Smyth et al. 2013). N_2 production by oysters alone were in agreement with the results in Smyth et al. (2013), which also found live oysters to have higher net N_2 fluxes than tidal flat sediments. Shell only rates were lower than those in Caffrey et al. (2016).

Predicted relative abundances of *nos*Z (combined *nos*ZI and *nos*ZII), the gene responsible for transforming N_2O to N_2 (Fig 6A) and thus expected to be highest in microbiomes with the greatest denitrification, showed the opposite trend. The highest relative abundances of *nos*Z genes were found in the reef sediments with the lowest N_2 fluxes, while the lowest relative abundances of *nos*Z genes were found in the oyster shell (only) and in the oyster (combination of shell (live) and oyster digestive gland) with the highest N_2 fluxes. This may be a result of DNA-based gene abundances failing to correlate with gene expression. However, when *nos*ZI and II are analyzed separately, a pattern similar to the flux rates emerges with *nos*ZI abundance (Fig 6B and 6C). A significant positive correlation between *nos*ZI abundance measured by qPCR and the predicted relative abundances of *nos*ZI verified that as denitrification flux rates increased, so did the abundances of *nos*ZI (Fig 7). This pattern was not seen in the more dominant *nos*ZII gene abundances, suggesting that *nos*ZI carriers may be more important to denitrification in oyster microbiomes than *nos*ZII carriers. As mentioned previously, many organisms may carry the *nos*Z gene, but do not necessarily express the *nos*Z gene.

Organisms carrying the *nos*ZII gene are more likely than those with *nos*ZI to also carry genes relating to dissimilatory nitrate reduction to ammonium (DNRA), a competing reduction pathway to denitrification (Sanford et al. 2012). Thus, the predicted abundance of *nos*ZI genes may be a better indicator of denitrification potential in oyster and sediment microbiomes than overall *nos*Z gene abundance.

Similar to other gene-based metabolic inference analyses, limitations exist regarding the quality and scope of the reference database being used as well as the understanding of the gene and metabolic pathways themselves. Our reference database was constructed with 5,445 complete and 222 draft bacterial genomes and curated for denitrification genes using KEGG or draft genome annotations. While the combination of these genomes covers a wide taxonomic range of bacteria, a great number of bacteria in many environments still remain unclassified or have identified genomes that are either incomplete or of low quality. Furthermore, caution must be used in inferring metabolic processes from gene presence in a bacterial genome. Often metabolic processes are extremely complex and require the coordinated expression of several different genes. While results from our study indicated that the relative abundance of the *nos*ZI gene is linked to denitrification potential of the oyster microbiomes, our study was small in scale and from only one season and location. Additional studies combining 16S rRNA gene studies and metabolic data are necessary to further validate the use of gene-based metabolic inferences as a reliable method for assessing the metabolic potential of microbiomes.

CONCLUSIONS

By using a customized genome and denitrification gene database with the paprica program and 16S NGS data, we were able to characterize oyster microbiome structures and infer potential denitrifiers in the oyster digestive gland, shell, and sediment microbiomes. Phylotype comparisons of paprica with other taxonomic databases resulted in similar classifications of oyster microbiomes, providing reasonable confidence in gene inferences determined by paprica's phylogenetic placement approach. Furthermore, qPCR of *nos*ZI genes were significantly and positively correlated with the *nos*ZI abundances inferred by paprica, providing additional evidence of reliability for gene inference. Overall, comparison of N_2 fluxes with inferred denitrification genes from oyster digestive gland, shell, and sediment microbiomes suggest that increased denitrification activity in oyster reefs is driven by the increase of *nos*ZI gene-carrying bacteria, which may be important denitrifiers responsible for nitrogen removal in oyster reefs. Finally, this is the first study combining qPCR and N_2 flux measurements to validate the use of 16S rRNA gene based metabolic inference as an alternative to whole genome sequencing in an effort to assess microbiome structure and connect microbiome function to the environment.

ACKNOWLEDGMENTS

Suzanne Thompson, Caitlin Magel, and Luke Dodd provided excellent field and laboratory support. This work was performed in part using computing facilities at the College of William and Mary, which were provided by contributions from the National Science Foundation, the Commonwealth of Virginia Equipment Trust Fund and the Office of Naval Research.

REFERENCES

Anderson, MJ (2001) A new method for non-parametric multivariate analysis of variance. *Austral Ecol* **26**(2001):32-46. doiL 10.1111/j.1442-9993.2001.01070.pp.x.

Bowman JS, and Ducklow HW (2015) Microbial communities can be described by metabolic structure: A general framework and application to a seasonally variable, depth-stratified microbial community from the coastal West Antarctic Peninsula. *PLoS One* **10**(8):1–18. doi: 10.1371/journal.pone.0135868.

Caffrey, JM, Hollibaugh, JT and Mortazavi, B (2016) Living oysters and their shells as sites of nitrification and denitrification. *Mar Pollut Bull* **112**: 86–90. doi:10.1016/j.marpolbul.2016.08.038.

Caporaso JG, Lauber CL, Walters WA, Berg-lyons D, Lozupone CA, Turnbaugh PJ, et al. (2010) Global patterns of 16S rRNA diversity at a depth of millions of sequences per sample. *Proc Natl Acad Sci* **108**:4516–22. doi: 10.1073/pnas.1000080107.

Caspi R, Billington R, Ferrer L, Foerster H, Fulcher CA, Keseler IM, et al (2014) The MetaCyc database of metabolic pathways and enzymes and the BioCyc collection of pathway/genome databases. *Nucleic Acids Res* **44**(D1):D471–80. doi: 10.1093/nar/gkt1103.

Cerco, CF, and Noel, MR (2007) Can oyster restoration reverse cultural eutrophication in Chesapeake Bay? *Estuaries Coasts* **30**(2): 331–43. doi: 10.1007/BF02700175.

Clark K, Karsch-Mizrachi I, Lipman DJ, Ostell J, and Sayers EW (2016) GenBank.

Nucleic Acids Res **44**(D1):D67–72. doi: 10.1093/nar/gkv1276.

Cleary DFR, de Voogd NJ, Polonia ARM, Freitas R, and Gomes NCM (2015) Composition and predictive functional analysis of bacterial bommunities in seawater, sediment and sponges in the Spermonde Archipelago, Indonesia. *Microb Ecol* **70**(4):889–903. doi: 10.1007/s00248-015-0632-52015;70(4):889–903.

Cole JR, Wang Q, Fish JA, Chai B, McGarrell DM, Sun Y, et al. (2014) Ribosomal Database Project: Data and tools for high throughput rRNA analysis. *Nucleic Acids Res* **42**(D1):633–42.

Dang H, Li T, Chen M, and Huang G (2008) Cross-ocean distribution of *Rhodobacterales* bacteria as primary surface colonizers in temperate coastal marine waters. *Appl Environ Microb* **74**(1):52–60. doi: 10.1128/AEM.01400-07.

Depkat-Jakob, PS, Hilgarth, M, Horn, MA, and Drake, HL (2010) Effect of earthworm feeding guilds on ingested dissimilatory nitrate reducers and denitrifiers in the alimentary canal of the earthworm. *Appl Environ Microbiol* **76**: 6205–6214. doi: 10.1128/AEM.01373-10.

DeSantis TZ, Hugenholtz P, Larsen N, Rojas M, Brodie EL, Keller K, et al. (2006) Greengenes, a chimera-checked 16S rRNA gene database and workbench compatible with ARB. Appl *Environ Microbiol* **72**(7):5069–72. doi: 1128/AEM.03006-05.

Desnues C, Michotey D, Wieland A, Zhizang C, Fourcans A, Duran R, et al (2007) Seasonal and diel distributions of denitrifying and bacterial communities in a hypersaline microbial mat (Camargue, France). *Water Res* **41**:3407–19. doi:

10.1016/j.watres.2007.04.018.

Domeignoz-Horta LA, Spor A, Bru D, Breuil MC, Bizouard F, Léonard J, et al. (2015) The diversity of the N_2O reducers matters for the N_2O:N_2 denitrification end-product ratio across an annual and a perennial cropping system. *Front Microbiol* **6**(SEP). doi: 10.3389/fmicb.2015.00971.

Edgar RC, Haas BJ, Clemente JC, Quince C, and Knight R (2011) UCHIME improves sensitivity and speed of chimera detection. *Bioinformatics* **27**(16):2194–200. doi: 10.1093/bioinformatics/btr381.

Ensign SH, Piehler MF, and Doyle MW (2008) Riparian zone denitrification affects nitrogen flux through a tidal freshwater river. *Biogeochemistry* **91**(2–3):133–50. doi: 10.1007/s10533-008-9265-9.

Feng BW, Li XR, Wang JH, Hu ZY, Meng H, Xiang LY, et al. (2009) Bacterial diversity of water and sediment in the Changjiang estuary and coastal area of the East China Sea. *FEMS Microbiol Ecol* **70**(2):236–48. doi: 10.1111/j.1574-6941.2009.00772.x.

Fernandez-Piquer, J, Bowman, JP, Ross, T, and Tamplin, ML (2012) Molecular analysis of the bacterial communities in the live Pacific oyster (*Crassostrea gigas*) and the influence of postharvest temperature on its structure. *J Appl Microbiol* **112**(6): 1134–43. doi: 0.1111/j.1365-2672.2012.05287.x.

Giles, H, Pilditch, CA, and Bell, DG (2006) Sedimentation from mussel (*Perna canaliculus*) culture in the Firth of Thames, New Zealand: impacts on sediment oxygen and nutrient fluxes. *Aquaculture* **261**: 125–140. doi: 10.1016/j.aquaculture.2006.06.048.

Glibert, PM, Hinkle, DC, Sturgis, B, and Jesien, RV (2014) Eutrophication of a

Maryland/Virginia coastal lagoon: a tipping point, ecosystem changes, and potential causes. *Estuaries and Coasts* **37**: 128–146. doi: 10.1007/s12237-013-9630-3.

Graf DRH, Jones CM, and Hallin S (2014) Intergenomic comparisons highlight modularity of the denitrification pathway and underpin the importance of community structure for N_2O emissions. PLoS One **9**(12):1–20. doi: 1371/journal.pone.0114118

Green, TJ, and Barnes, AC (2010) Bacterial diversity of the digestive gland of Sydney rock oysters, *Saccostrea glomerata* infected with the paramyxean parasite, *Marteilia sydneyi*. *J Appl Microbiol* **109**(2): 613–22. doi:10.1111/j.1365-2672.2010.04687.x.

Henry S, Bru D, Stres B, Hallet S, and Philippot L (2006) Quantitative detection of the *nos*Z gene, encoding nitrous oxide reductase, and comparison of the abundances of 16S rRNA, *nar*G, *nir*K, and *nos*Z genes in soils. *Appl Environ Microb* **72**(8):5181–9. doi: 10.1128/AEM.00231-06.

Hernández-Zárate, G, and Olmos-Soto, J (2006) Identification of bacterial diversity in the oyster *Crassostrea gigas* by fluorescent in situ hybridization and polymerase chain reaction. *J Appl Microbiol* **100**(4): 664–72. doi:10.1111/j.1365-2672.2005.02800.x.

Hoellein, TJ, Zarnoch, CB, and Grizzle, RE (2015) Eastern oyster (*Crassostrea virginica*) filtration, biodeposition, and sediment nitrogen cycling at two oyster reefs with contrasting water quality in Great Bay Estuary (New Hampshire, USA). *Biogeochemistry* **122**(1): 113–29. doi: 10.1007/s10533-014-0034-7.

Humphries, AT, Ayvazian, SG, Carey, JC, Hancock, BT, Grabbert, S, Cobb, D, Strobel, CJ, and Fulweiler, RW (2016) Directly measured denitrification reveals oyster aquaculture and restored oyster reefs remove nitrogen at comparable high rates.

Front Mar Sci **3**(May): 74. doi: 10.3389/fmars.2016.00074.

Jenkins, MC, and Kemp, WM (1984) The coupling of nitrification and denitrification in two estuarine sediments. *Limnol Oceanogr* **29**(3): 609-19.

Jones, CM, Graf, DRH, Bru, D, Philippot, L, and Hallin, S (2013) The unaccounted yet abundant nitrous oxide-reducing microbial community: a potential nitrous oxide sink. *ISME J* **7**: 417–26. doi: 10.1038/ismej.2012.125.

Kana TM, Darkangelo C, Hunt MD, Oldham JB, Bennett GE, and Cornwell JC (1994) Membrane inlet mass spectrometer for rapid high-precision determination of N_2, O_2, and Ar in environmental water samples. *Anal Chem* **66**(23):4166–70. doi: 10.1021/ac000951009.

Kanehisa M, Goto S. KEGG: Kyoto encyclopedia of genes and genomes (2000) *Nucleic Acids Res* **27**(1):29–34. doi: 10.1093/nar/27.1.29.

Kellogg, ML, Cornwell, JC, Owens, MS, and Paynter, KT (2013) Denitrification and nutrient assimilation on a restored oyster reef. *Mar Ecol Prog Ser* **480**: 1–19. doi: 10.3354/meps10331.

Kellogg, ML, Smyth, AR, Luckenbach, MW, Carmichael, RH, et al. (2014) Use of oysters to mitigate eutrophication in coastal waters. *Estuar Coast Shelf Sci* **151**: 156–168. doi: 10.1016/j.ecss.2014.09.025.

King, GM, Judd, C, Kuske, CR, and Smith, C (2012) Analysis of stomach and gut microbiomes of the eastern oyster (*Crassostrea virginica*) from coastal Louisiana, USA. *PLoS One* **7** (12): e51475. doi: 10.1371/journal.pone.0051475.

Langille MGI, Zaneveld J, Caporaso JG, McDonald D, Knights D, Reyes JA, et al (2013) Predictive functional profiling of microbial communities using 16S rRNA marker

gene sequences. *Nat Biotechnol* **31**(9):814–21. doi: 10.1038/nbt.2676.

Lokmer, A, Goedknegt AM, Thieltges, DW, Fiorentino, D, Kuenzel, S, Baines, JF, and Wegner, KM (2016a) Spatial and temporal dynamics of Pacific oyster hemolymph microbiota across multiple ccales. *Front Microbiol* **7** (August): 1–18. doi: 10.3389/fmicb.2016.01367.

Lokmer, A, Kuenzel, S, Baines, JF and Wegner, KM (2016b) The role of tissue-specific microbiota in initial establishment success of Pacific oysters. *Environ Microbiol* **18**(3): 970–87. doi: 10.1111/1462-2920.13163.

Matsen FA, Kodner RB, and Armbrust EV (2010) pplacer: linear time maximum-likelihood and Bayesian phylogenetic placement of sequences onto a fixed reference tree. *BMC Bioinformatics* **11**(1):538.

McMurdie PJ, and Holmes S (2013) Phyloseq: an R package for reproducible interactive analysis and graphics of microbiome census data. *PLoS One* **8**(4). doi: 10.1371/journal.pone.0061217.

Mosier AC, and Francis CA (2010) Denitrifier abundance and activity across the San Francisco Bay estuary. *Environ Microbiol Rep* **2**:667–76. doi: 10.1111/j.1758-2229.2010.00156.x.

Newell, RIE, Cornwell, JC, and Owens, MS (2002) Influence of simulated bivalve biodeposition and microphytobenthos on sediment nitrogen dynamics: a laboratory study. *Limnol Oceanogr* **47**: 1367–1379. doi: 10.4319/lo.2002.47.5.1367.

Newell, RIE, Fisher, TR, Holyoke, RR, and Cornwell, JC (2005) Influence of eastern oysters on nitrogen and phosphorus regeneration in Chesapeake Bay, USA. In, Dame, R and Olenin, S (eds), The Comparative roles of suspension feeders in

ecosystems. NATO Science Ser IV: Earth and Environmental Sciences. Springer, Dordrecht, pp. 93–120.

Ngugi, DK and Brune, A (2012) Nitrate reduction, nitrous oxide formation, and anaerobic ammonia oxidation to nitrite in the gut of soil-feeding termites (*Cubitermes* and *Ophiotermes spp.). Environ Microbiol* **14**: 860–871. doi: 10.1111/j.1462-2920.2011.02648.x.

Orellana LH, Rodriguez-R LM, Higgins S, Chee-Sanford JC, Sanford RA, Ritalahti KM, et al. (2014) Detecting nitrous oxide reductase (nosZ) genes in soil metagenomes: method development and implications for the nitrogen cycle. *MBio* **5**(3):e01193-14.

Pfister CA, Gilbert JA, and Gibbons SM (2014) The role of macrobiota in structuring microbial communities along rocky shores. *PeerJ* **2**:e631. doi: 10.7717/peerj.631.

Piehler, MF and Smyth, AR (2011) Habitat-specific distinctions in estuarine denitrification affect both ecosystem function and services. *Ecosphere* **2**: art12. doi: 10.1890/ES10-00082.1.

Polymenakou PN, Bertilsson S, Tselepides A, Stephanou EG (2005) Links between geographic location, environmental factors, and microbial community composition in sediments of the Eastern Mediterranean Sea. *Microb Ecol* **49**(3):367–78. doi: 10.1007/s00248-004-0274-5.

Romero, J, García-Varela M, Laclette JP, and Espejo RT (2002) Bacterial 16S rRNA gene analysis revealed that bacteria related to Arcobacter spp. constitute an abundant and common component of the oyster microbiota (*Tiostrea chilensis*). *Microb Ecol* **44**(4):365–71. doi: 10.1007/s00248-002-1063-7.

Rothig T, Ochsenkuhn MA, Roik A, Van Der Merwe R, and Voolstra CR (2016) Long-term salinity tolerance is accompanied by major restructuring of the coral bacterial microbiome. *Mol Ecol* **25**(6):1308–23. doi: 10.1111/mec.13567.

Rubin BE, Sanders JG, Hampton-Marcell J, Owens SM, Gilbert JA, and Moreau CS (2014) DNA extraction protocols cause differences in 16S rRNA amplicon sequencing efficiency but not in community profile composition or structure. *MicrobiologyOpen* **3**(6):910-921. doi: 10.1002/mbo3.216.

Sanford, RA, Wagner, DD, Qingzhong, W, Chee-Sanford, JC, Thomas, SH, Cruz-García, C, Rodríguez, G, et al. (2012) Unexpected nondenitrifier nitrous oxide reductase gene diversity and abundance in soils. *Proc Natl Acad Sci USA* **109**: 19709-19714. doi: 10.1073/pnas.1211238109.

Schloss PD, Westcott SL, Ryabin T, Hall JR, Hartmann M, Hollister EB, et al. (2009) Introducing mothur: Open-source, platform-independent, community-supported software for describing and comparing microbial communities. *Appl Environ Microb* **75**(23):7537–41. doi: 10.1128/AEM.01541-09.

Sharpton TJ (2014) An introduction to the analysis of shotgun metagenomic data. *Front Plant Sci* **5**(June):209. doi: 10.3389/fpls.2014.00209.

Smith CJ, Dong LF, Wilson J, Stott A, Osborn AM, and Nedwell DB (2015) Seasonal variation in denitrification and dissimilatory nitrate reduction to ammonia process rates and corresponding key functional genes along an estuarine nitrate gradient. *Front Microbiol* **6**(JUN):1-11. doi: 10.3389/fmicb.2015.00542.

Smyth, AR, Geraldi, NR, and Piehler, MF (2013) Oyster-mediated benthic-pelagic

coupling modifies nitrogen pools and processes. *Mar Ecol Prog Ser* **493**: 23–30. doi: 10.3354/meps10062.

Smyth, AR, Geraldi, NR, Thompson, SP, and Piehler, MF (2016) Biological activity exceeds biogenic structure in influencing sediment nitrogen cycling in esxperimental oyster reefs. *Mar Ecol Prog Ser* **560**: 173-83. doi: 10.3354/meps1922.

Stief, P, Poulsen, M, Nielsen, LP, Brix, H, and Schramm, A (2009) Nitrous oxide emission by aquatic macrofauna. *Proc Natl Acad Sci USA* **106**: 4296–300. doi: 10.1073/pnas.0808228106.

Sun MY, Dafforn KA, Johnston EL, and Brown, MV (2013) Core sediment bacteria drive community response to anthropogenic contamination over multiple environmental gradients. *Environ Microbiol* **15**(9):2517–31. doi: 10.1111/1462-2920.12133.

Svenningsen, NB, Heisterkamp, IM, Sigby-Clausen, M, Larsen, LH, Nielsen, LP, Stief, P, and Schramm, A (2012) Shell biofilm nitrification and gut denitrification contribute to emission of nitrous oxide by the invasive freshwater mussel *Dreissena polymorpha* (Zebra mussel). *Appl Environ Microbiol* **78**: 4505–4509. doi: 10.1128/AEM.00401-12.

Thomas F, Hehemann JH, Rebuffet E, Czjzek M, and Michel G (2011) Environmental and gut *Bacteroidetes*: The food connection. *Front Microbiol* **2**(MAY):1–16. doi: 10.3389/fmicb.2011.00093.

Trabal, N, Mazón-Suástegui, JM, Vázquez-Juárez, R, Ascencio-Valle, F, Morales-Bojórquez, E, and Romero, J (2012) Molecular analysis of bacterial microbiota associated with oysters (*Crassostrea gigas* and *Crassostrea cortieziensis*) in

different growth phases at two cultivation sites. *Microb Ecol* **64**: 555-69. doi: 10.1007/s00248-012-0039-5.

Trabal Fernández, N, Mazón-Suástegui, JM, Vázquez-Juárez, R, Ascencio-Valle, F, and Romero, J (2014) Changes in the composition and diversity of the bacterial microbiota associated with oysters (*Crassostrea corteziensis*, *Crassostrea gigas* and *Crassostrea sikamea*) during commercial production. *FEMS Microbiol Ecol* **88**: 69–83. doi: 10.1111/1574-6941.12270.

Wang Q, Garrity GM, Tiedje JM, and Cole JR (2007) Naive Bayesian classifier for rapid assignment of rRNA sequences into the new bacterial taxonomy. *Appl Environ Microb* **73**(16):5261–7. doi: 10.1128/AEM.00062-07.

Wegner, KM, Volkenborn, N, Peter, H, and Eiler, A (2013) Disturbance induced decoupling between host genetics and composition of the associated microbiome. *BMC Microbiol* **13**(1) doi: 10.1186/1471-2180-13-252.

Wüst, PK, Horn, MA, Henderson, G, Janssen, PH, Rehm, BHA, and Drake, HL (2009) Gut-associated denitrification and in vivo emission of nitrous oxide by the earthworm families *Megascolecidae* and *Lumbricidae* in New Zealand. *Appl Environ Microbiol* **75**(11): 3430–36. doi: 10.1128/AEM.00304-09.

Yilmaz P, Parfrey LW, Yarza P, Gerken J, Ludwig W, Pruesse E, et al. (2014) The SILVA and "All-species Living Tree Project (LTP)" taxonomic frameworks. Nucleic Acids Res **42**(November 2013):D643–8. doi: 10.1093/nar/gkt1209.

Zumft, WG (1997) Cell biology and molecular basis of denitrification *Microbiol Mol Biol R* **61** (4): 533-616.

Zurel, D, Benayahu, Y, Or, A, Kovacs, A, and Gophna, U (2011) Composition and

dynamics of the gill microbiota of an invasive Indo-Pacific oyster in the Eastern Mediterranean Sea. *Environ Microbiol* **13**(6): 1467–76. doi:10.1111/j.1462-2920.2011.02448.x.

TABLES

Table 1. Summary statistics of 16S rRNA gene amplicon sequencing for oyster-related microbiomes.

Sample	No. of OTUs[a]	Coverage (%)	Chao Index	Shannon Diversity
Digestive Gland 1	477	1.00	1038.17	1.06
Digestive Gland 2	545	1.00	1292.67	1.10
Digestive Gland 2	552	1.00	1372.33	1.33
Shell (Live) 1	6,508	0.93	18777.19	5.46
Shell (Live) 2	7,491	0.93	22004.59	6.31
Shell (Live) 3	6,387	0.94	19435.59	5.90
Shell (Only) 1	7,027	0.93	18966.56	6.24
Shell (Only) 2	5,616	0.94	16288.26	5.37
Shell (Only) 3	4,555	0.96	12681.37	5.19
Sediment 1	10,946	0.89	33237.59	6.88
Sediment 2	9,417	0.90	29882.63	6.57
Sediment 3	11,106	0.89	32986.13	7.00

All metrics are based on subsamples of n=66,687.

[a] OTUs are based on 97% sequence identity using Mothur's average neighbor clustering algorithm

FIGURES

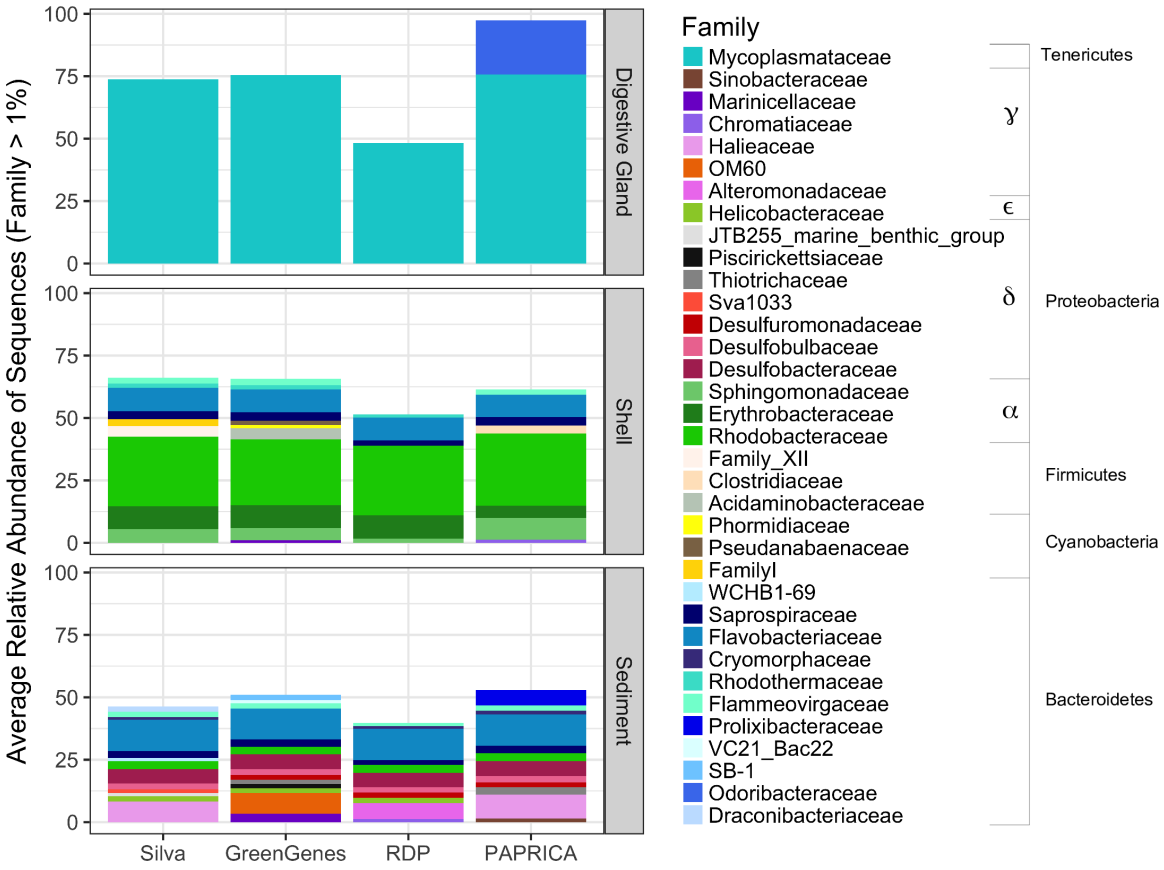

Fig 1. Average relative abundances of bacterial families in the oyster-related microbiomes, classified by different reference databases. Families with ≥ 1% relative abundance in samples are shown. Shell microbiome consists of shell (live) and shell (only) treatments.

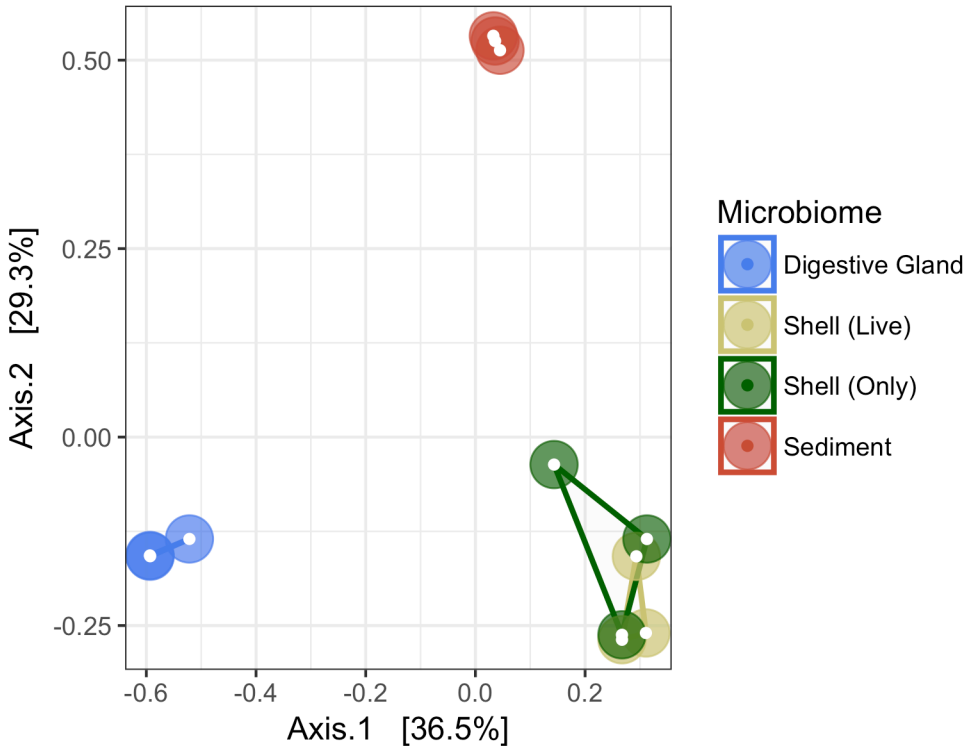

Fig 2. Principal coordinate analysis (PCoA) of oyster-related microbiomes. PCoA based on 16S rRNA gene sequences using Bray-Curtis similarity matrix.

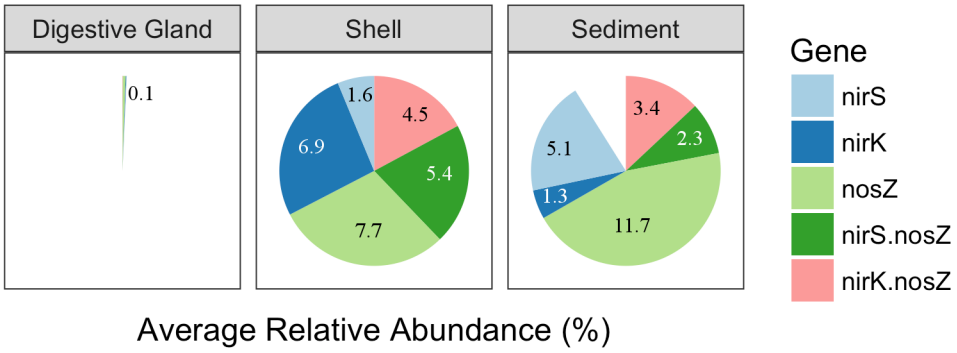

Fig 3. Predicted average relative abundances of denitrification genes by paprica for oyster-related microbiomes. Shell microbiome includes shell (live) and shell (only) treatments. Each full circle represents a relative abundance of 26.1%.

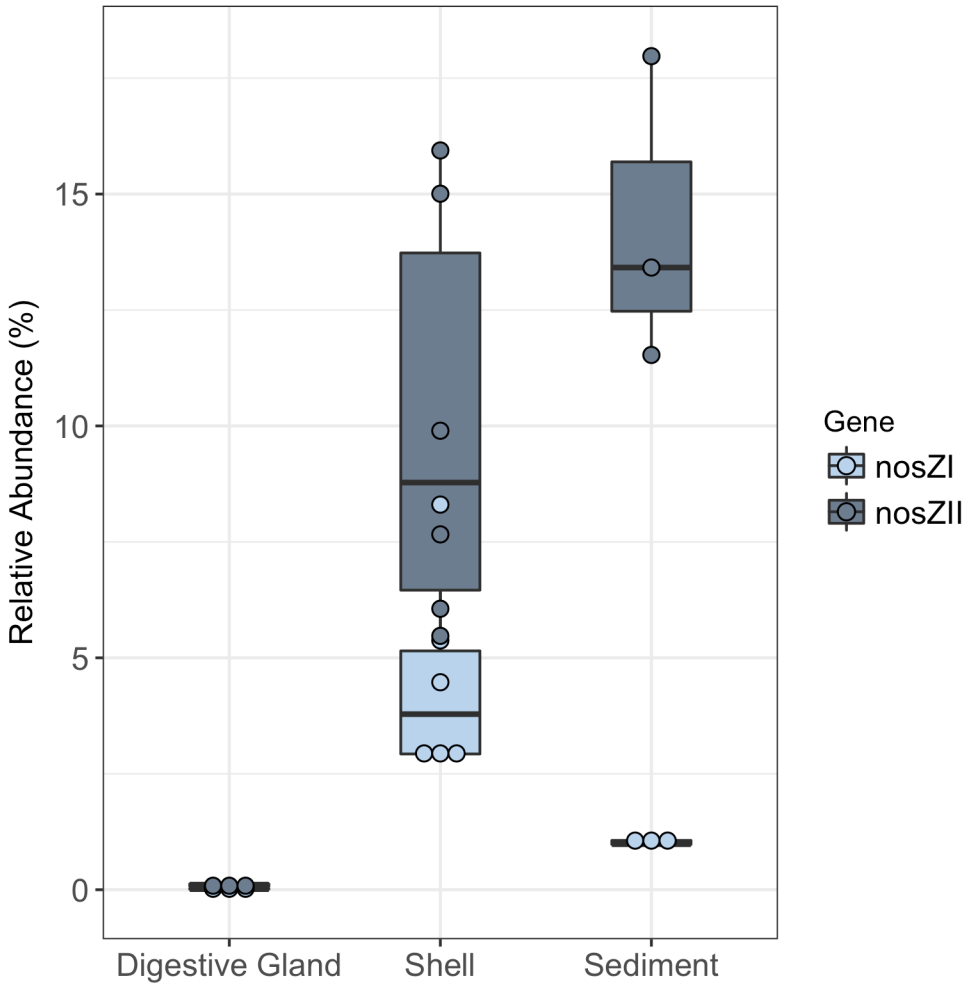

Fig 4. Predicted relative abundances of genes *nos*ZI and *nos*ZII by paprica in oyster-related microbiomes. Shell microbiome includes both shell (live) and shell (only) treatments.

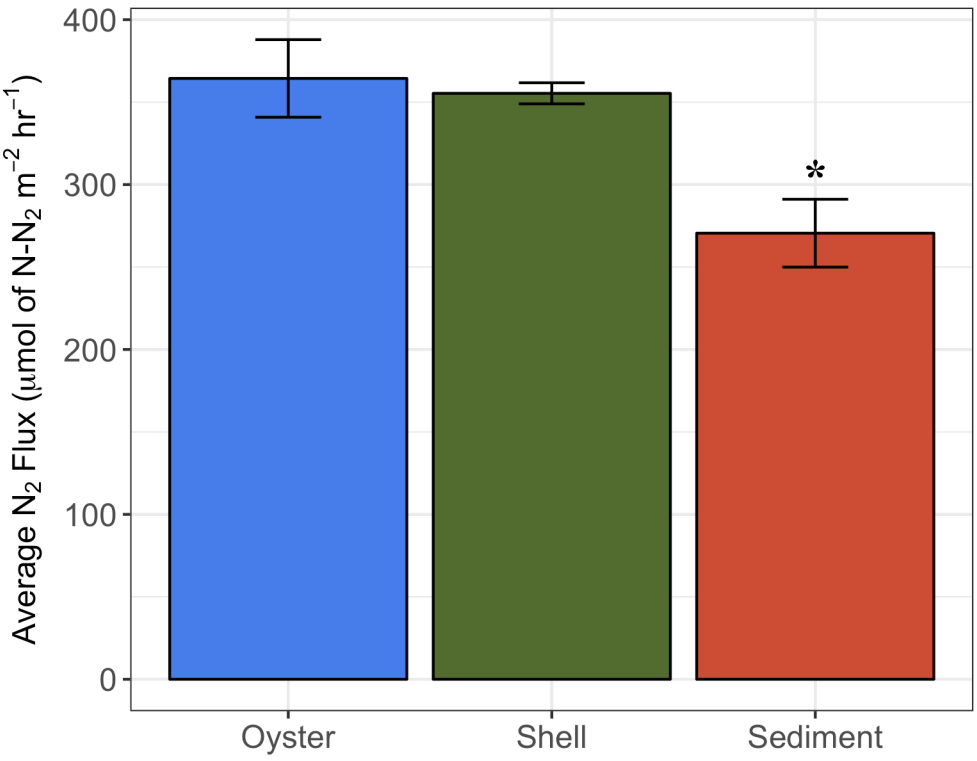

Fig 5. N_2 flux measurements from oysters, shell only, and sediment treatments using a continuous flow through design. For each treatment n=3 and error bars represent ± s.d. (*) significance $p < 0.05$

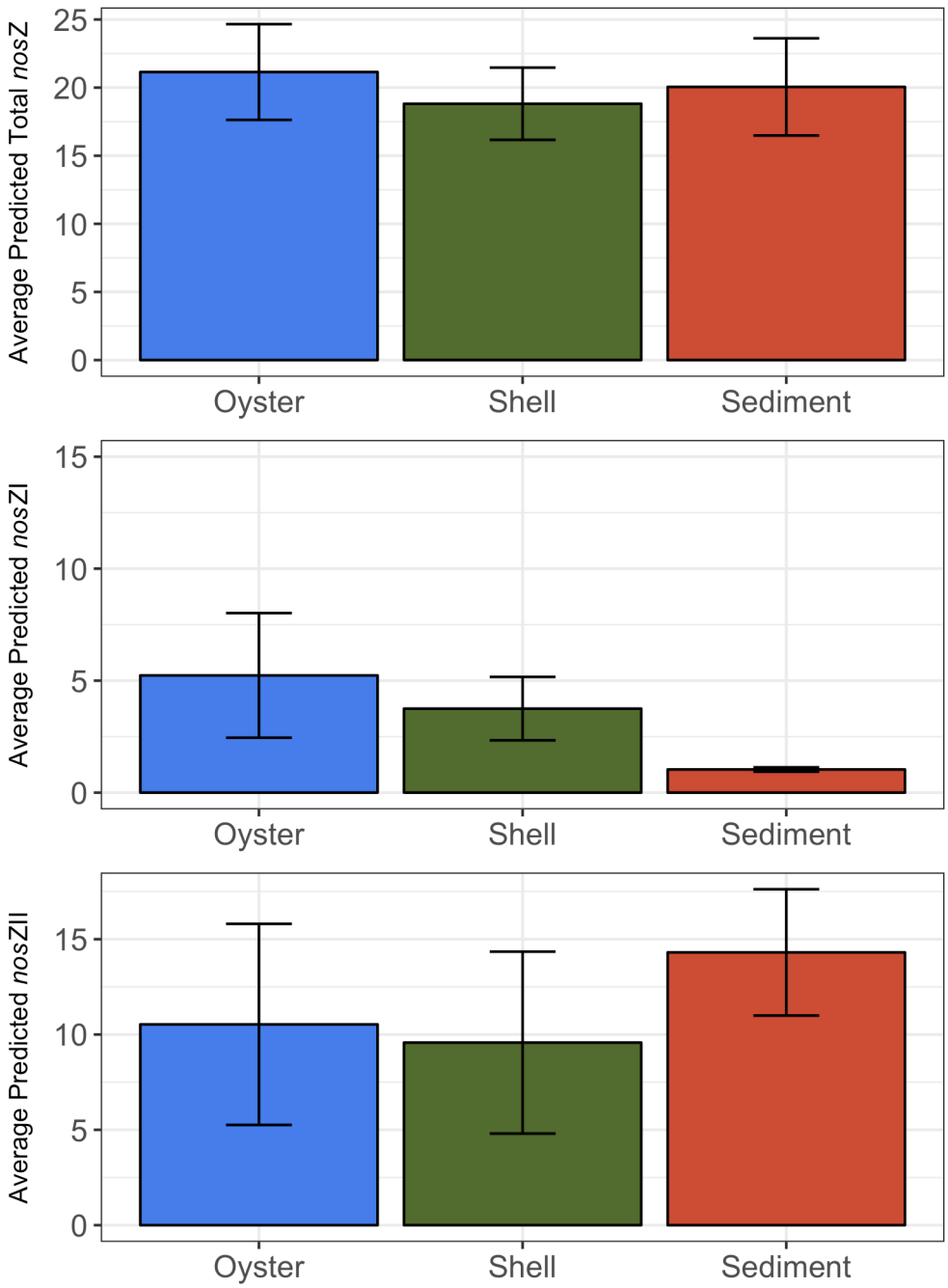

Fig 6. Average predicted relative abundances of total (A) *nos*Z, (B) *nos*ZI, and (C) *nos*ZII by paprica for oyster-related microbiomes. Digestive gland combined with shell (live) to form oyster microbiome. Shell (only) forms shell microbiome. For each treatment n=3 and error bars represent ± s.d.

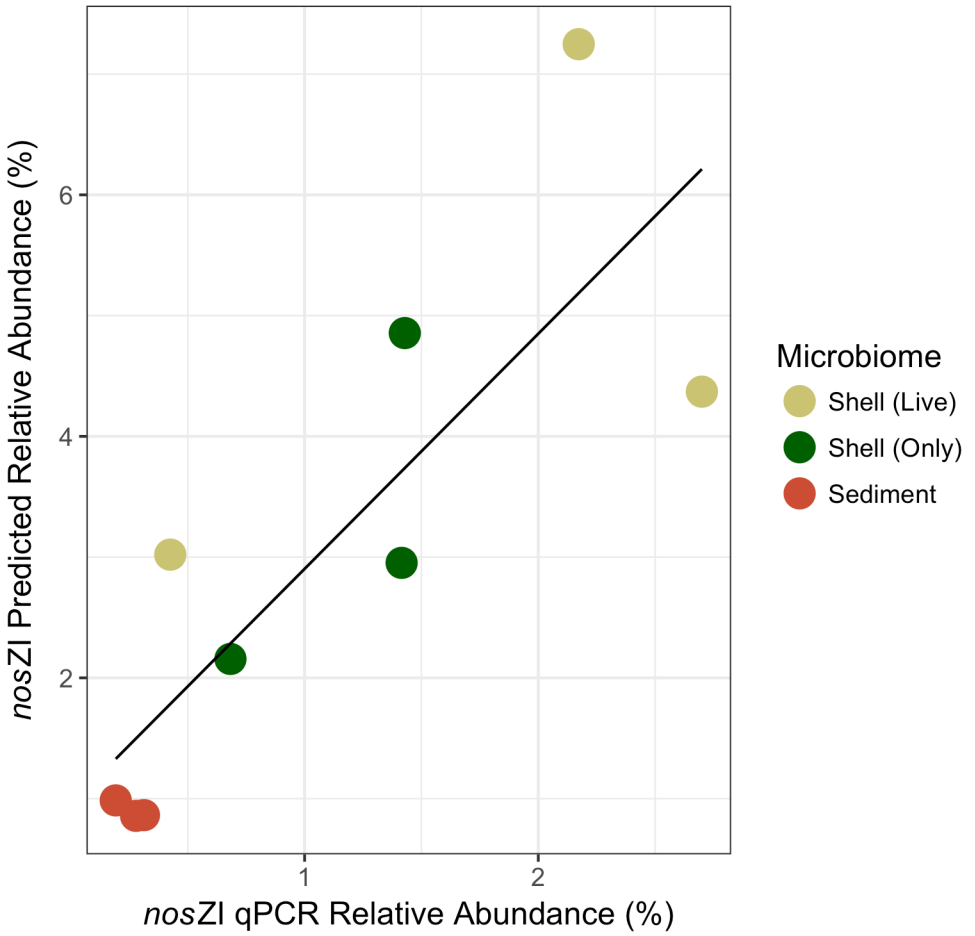

Fig 7. Linear regression comparing predicted and quantified relative abundances of *nosZI* genes for shell (live), shell (only) and sediment microbiomes. Predicted relative abundances based on paprica inferred *nosZI* gene abundances relative to 16S gene abundances. Quantified relative abundances based on qPCR of *nosZI* gene copy numbers relative to 16S gene copy numbers.

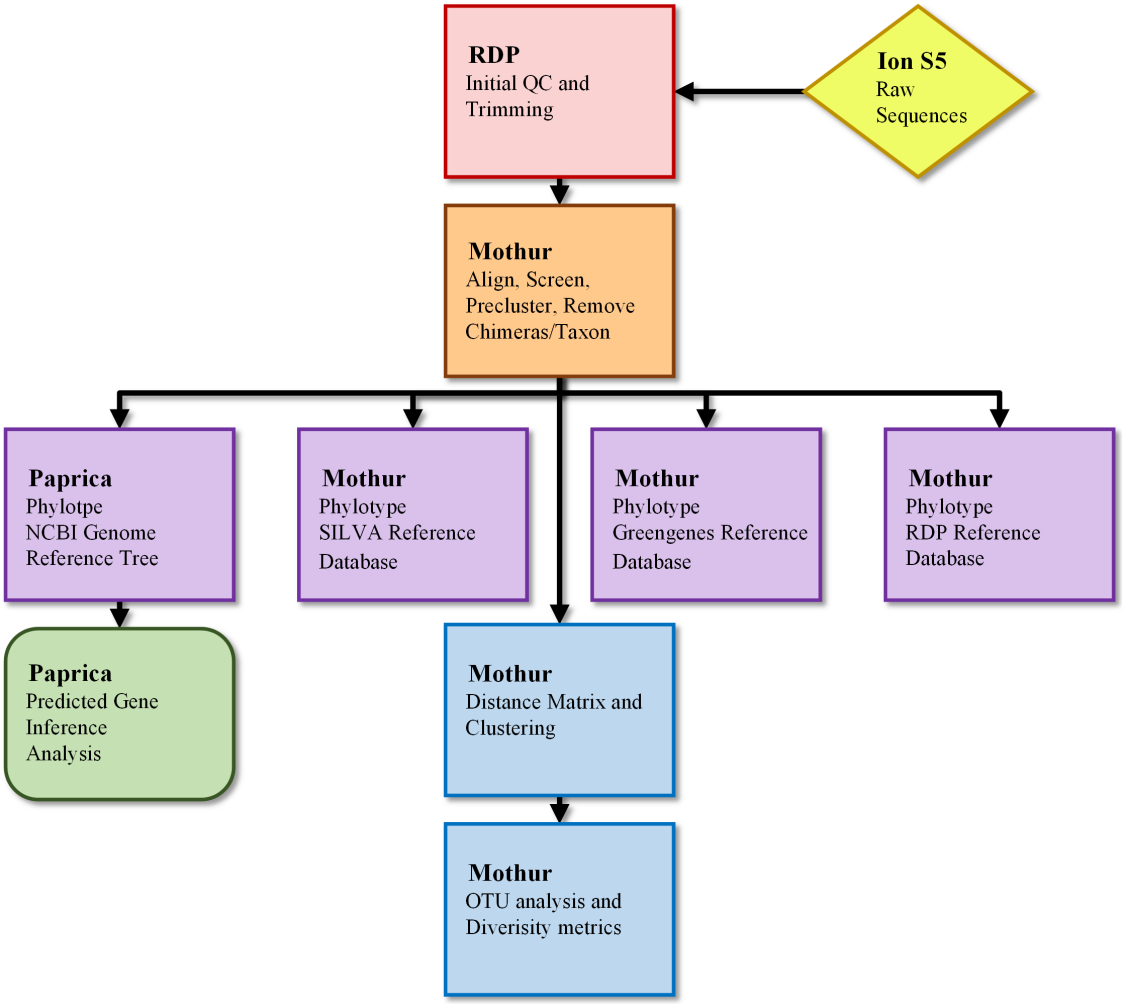

Figure S1. Flowchart of bioinformatic pipeline.

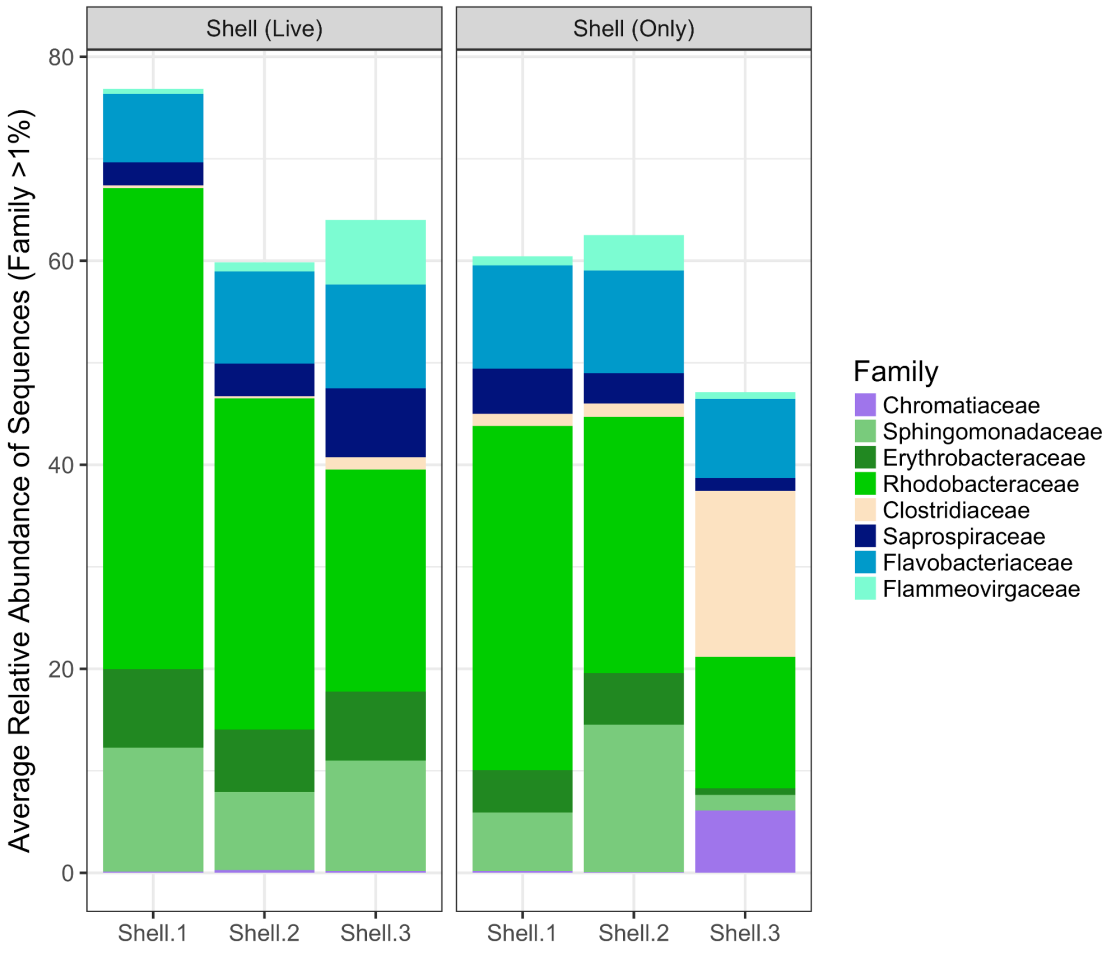

Figure S2. Relative abundances of bacterial families in shell (live) and shell (only) treatments

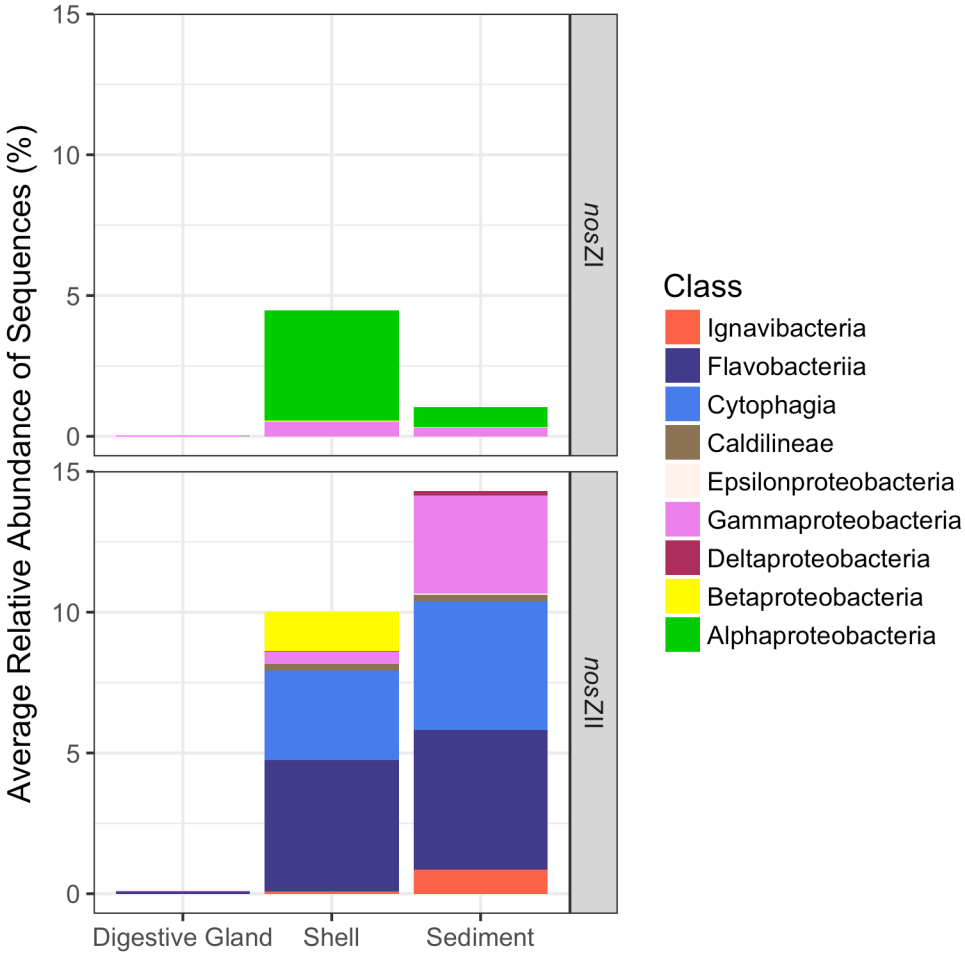

Figure S3. Relative abundances of *nos*ZI and *nos*ZII by taxonomical class.

Chapter 3

Seasonal effects on the eastern oyster (*Crassostrea virginica*) microbiome and associated denitrification activity in the Lynnhaven River, Virginia

ABSTRACT

Seasonal factors such as changes in temperature and salinity affect marine microbial communities. Annual variations that occur in the Chesapeake Bay are also likely to impact oyster microbiomes. Very few studies have examined the natural fluctuation of oyster microbiomes in response to seasonal changes or alterations to oyster microbiome function in the environment. An important ecosystem function provided by oyster microbiomes in marine environments is the removal of fixed nitrogen from the system through denitrification. In this study, we investigated the composition and diversity of the oyster gill, gut, shell, and reef sediment microbiomes as well as the presence of a stable core microbiome and associated denitrifiers for June (early summer), August (late summer) and October (fall) using a combined 16S rRNA amplicon-based metagenomic and metabolic inference approach. Denitrification rates of whole, live oysters, oysters with shell biofilms removed, empty shells, and reef sediments were measured using a ^{15}N isotope pairing method with a flow-through experimental design. All oyster and oyster-related microbiomes were found to be distinct from each other and were significantly affected by season, with exception of the reef sediment microbiome. Among each microbiome, there also existed a stable community present throughout all seasons defined in this study as the core microbiome, indicating a potential link to oyster health or function in the environment. In each microbiome, the core represented between 45 to 73% of the microbiome composition reflecting a high degree of stability in response to seasonal changes. The highest relative abundances of denitrifiers, identified as bacteria carrying the nitrous oxide reductase gene (*nos*Z), were found in the shell (18.3 ± 1.0%) and reef sediments (23 ± 0.8%), with much lower relative abundances in the gill

(7.7± 1.0%) and gut (2.5 ± 0.8%) microbiomes. Similarly, higher relative abundances of denitrifiers made up the shell (12.6%) and sediment (28.7%) core microbiomes, than in the gill (2.52%) and gut (<1%) microbiomes. Seasonally, the shell and sediment denitrifiers showed the least variability in denitrifier abundance and denitrification rates with overall denitrification rates (35.3 ± 8.4 μM N_2-N m^{-2} hr^{-1} and 46.8 ± 12.7 μM N_2-N m^{-2} hr^{-1}, respectively) significantly lower than live oysters (197.2 ± 36.2 μM N_2-N m^{-2} hr^{-1}) or oysters with biofilms removed (70.7 ± 20.8 μM N_2-N m^{-2} hr^{-1}), reflecting a potentially stable and constant pool of denitrifiers. In comparison, the high variability observed in the gill and gut microbiomes and oyster denitrification rates, coupled with low relative abundances of core denitrifiers indicates that an important contribution of denitrification by oysters may be seasonally linked to transient denitrifiers, such as those associated with food particles. Furthermore, niche differentiation of denitrifiers was observed between the different microbiomes, demonstrating separate and distinct denitrifiers are responsible for denitrification in different parts of the oyster.

INTRODUCTION

A variety of environmental factors affect the dynamics of microbial communities in the marine environment, including highly influential drivers such as temperature, salinity and nutrient availability associated with seasonality (Fuhrman et al. 2006, Gilbert et al. 2009, Herlemann et al. 2016). Eastern oysters (*Crassostrea virginica*) living in the Chesapeake Bay experience these annual temporal effects, potentially resulting in seasonal changes to the composition and function of the oyster and oyster-related microbiomes. Identifying the stable, resident core members as well as the normal fluctuations and variation that occur within a microbiome are necessary to understand and predict the impact of disturbances on the microbiome and microbiome function (Shade and Handelsman 2012, Stenuit and Agathos 2015) including those related to a host's health (Turnbaugh et al. 2007, Costello et al. 2012) and ecosystem processes (Schimel et al. 2007, Chaparro et al. 2012, Jousset et al. 2017).

Seasonal effects on oysters have been linked to increased occurrences of mortality during the warmer, summer months (Bricelji et al. 1992, Ford and Borrero 2001, Malham et al. 2009). Many factors have been attributed to seasonal mortalities including temperature and salinity (Hartwick 1988, Soletchnik et al. 2007, Southworth et al. 2017) as well as increased incidences of parasites such as *Perkinsus marinus* and *Haplosporidum nelsoni* (Calvo et al. 2003, Levinton et al. 2013) and bacterial pathogens (Friedman et al. 1991) such as *Roseobacter sp.* and *Vibrio splendidus* (Lacoste et al. 2001, Garnier et al. 2007). Many *Vibrio* species have been demonstrated to exhibit seasonality (Preheim et al. 2011) with factors such as high water temperature, high concentrations of chlorophyll *a*, and low salinity influencing greater vibrio abundances

(Oberbeckmann et al. 2012). While a great deal of research has focused on seasonal responses of oyster pathogens themselves, seasonal effects studies on the overall oyster microbiomes are relatively scarce. Host microbiomes are critical for maintaining homeostasis and survival, with imbalances in the microbiome linked to disease (McFall-Ngai et al. 2013). Additionally, oyster microbiomes may offer protection against pathogens by creating competition for nutrients, reducing space for settlement, or producing antimicrobials (Harris 1993, Gomez-Gil et al. 2000, Castro et al. 2002, Schulze et al. 2006, Prado et al. 2010, Kescardi-Watson et al. 2012).

Of the seasonal studies conducted on oyster microbiomes, Zurel et al. (2011) found that gill species richness significantly increased in warmer months in Indo-Pacific oysters (*Chama sp.*), while Pierce et al. (2016) showed strong correlations between community structure and season in both hemolymph and gut microbiomes of *C. virginica*. Both of these studies, however, used low-resolution techniques or relied on small clone libraries to determine microbial communities, limiting the characterization of diversity and identification of the microbiomes. Other studies have measured temperature effects on oyster microbiome communities in relation to stress. Wegner et al. (2013) found that heat shock to oyster gill microbiomes greatly reduced overall diversity, while Lokmer et al. (2015) found high resolution changes to the gill microbiome composition, but overall stability of dominant taxa in response to temperature stress. However, the temperature challenges tested in both studies were used to demonstrate induced stress on the oyster, and do not reflect gradual seasonal temperature changes or other seasonal fluctuations experienced in the Chesapeake Bay. Determining the natural seasonal variation and the stable, resident members of the oyster microbiome will lead to

a better understanding of the microbiome's response to seasonality and a critical first step in identifying possible predictors of oyster fitness and response to oyster pathogens.

In addition to the oyster microbiomes' role in oyster health, an important ecosystem function of the oyster-associated microbiomes that may be altered by seasonality is denitrification. Denitrification is the microbially mediated process by which biologically active nitrogen (N) is removed from the environment via the step-wise reduction of nitrate (NO_3^-) or nitrite (NO_2^-) to gaseous nitric oxide (NO), nitrous oxide (N_2O) and dinitrogen (N_2) (Zumft 1997). Excess N and cultural eutrophication in marine systems has been linked to several changes to the ecosystem including increased harmful algal blooms (Rabalais et al. 2002, Paerl et al. 2011) and loss of benthic habitat (Holmer and Bondgaard 2001, Diaz and Rosenberg 2008). Several studies have shown that oysters and oyster reefs enhance rates of denitrification (Piehler and Smyth 2011, Hoellein et al. 2015, Caffrey et al. 2016, Humphries et al. 2016, Arfken et al. 2017) with higher rates of denitrification occurring in the summer months (Kellogg et al. 2013, Smyth et al. 2013). While many of these studies have examined the denitrification rates and biogeochemical factors associated with oysters, very few have investigated the microbial communities and genes associated with oyster denitrification. Addition of microbial community analyses to environmental data has been demonstrated to improve model accuracy and prediction of ecosystem process rates (Graham et al. 2014).

An important enzyme involved in the denitrification pathway is nitrous oxide reductase, encoded by the *nosZ* gene, which reduces N_2O to N_2. Bacteria that carry the *nosZ* gene have traditionally been identified as complete denitrifiers, or bacteria that possess all the genes necessary to reduce NO_3^- or NO_2^- to N_2 (Zumft 1997). However,

increased genomic sequencing has revealed a diverse, and high abundance of non-denitrifying bacteria that also posses the *nos*Z gene and may contribute to the reduction of N_2O to N_2 in the environment (Sanford et al. 2012). Additionally, the *nos*Z gene itself may be further broken down into two clades, clades I and II (*nos*ZI and *nos*ZII, respectively) based on protein physiology (Sanford et al. 2012; Jones et al. 2013). Because the reduction of N_2O to N_2 is an ecologically important step in reducing greenhouse gas emissions from the system and is characteristic of complete denitrifiers, all bacteria carrying the *nos*Z gene are hereafter considered "denitrifiers" for the purposes of this study.

Very few studies to date have examined the functional genes associated with oyster denitrification and little is known about the diversity or abundance of the *nos*Z gene in oyster microbiomes. Lindemann et al. (2016) investigated the abundances of genes encoding for nitrite reductase (*nir*S/*nir*K), which reduce NO_2^- to NO, in sediments associated with deployed oysters. Oysters were not found to significantly impact the abundances of *nir*S or *nir*K and no relationship between the abundances of *nir*S or *nir*K genes in the sediments and denitrification potential was determined (Lindemann et al. 2016). However, many bacteria carry *nir* genes but do not possess the *nos*Z genes necessary to complete denitrification and produce N_2 (Zumft 1997, Wallenstein et al. 2016). A study by Arfken et al. (2017) reported the composition of the denitrifying communities present in the oyster shell, oyster digestive gland, and reef sediment microbiomes based on the *nos*Z gene. In Arfken et al. (2017), increased denitrification rates were associated with increased relative abundances of denitrifiers belonging to *Alphaproteobacteria* carrying *nos*ZI in the shell and sediments. However, only a small

sample set was examined for one time point, limiting the scope of the findings. Seasonality is known to affect denitrification rates (Kellogg et al. 2013, Smyth et al. 2013) and thus further exploration of the seasonal patterns of abundances of *nos*Z in the oyster microbiome will aid in establishing the link between oyster and oyster-related microbiomes and denitrification potential.

Characterization of the oyster microbiome and associated denitrifiers in response to season and identification of the stable, resident core microbiome will provide an overall greater understanding of microbial regulation in oyster denitrification. In our study, we examined the oyster gill, gut, shell, and reef sediment microbiomes during three different seasons to determine the (1) the seasonal variation found within each microbiome, (2) the existence of a core microbiome, and (3) the denitrification function of the core and total microbiome. Denitrification function was determined based on both the abundance of inferred *nos*Z genes in the oyster microbiomes using 16S rRNA gene-based metabolic approach and on the denitrification activities measured in oysters, shells, and reef sediments using isotope pairing technique.

MATERIALS AND METHODS

Sample site and collection

Live oysters, paired oyster shells (empty), water and reef sediments were collected in June (early summer), August (late summer), and October (fall) 2014 from a reconstructed oyster reef near Humes Marsh, located in the Lynnaven River, VA. Humes Marsh is a muddy, intertidal sand flat composed of shell mounds, which support oyster abundances ranging from tens to hundreds per m^2. Bare sediment and oysters clumped on bare sediment fill in the areas between the marsh. Water is polyhaline and tidal, with depths remaining relatively shallow at around 2.5 meters and a tidal range of approximately 0.5 meters. Temperature, salinity, and dissolved oxygen (DO) measurements were taken on the day of each sample collection with a Yellow Springs Instrument water quality sonde (YSI, Inc). Dissolved inorganic nitrogen including nitrate (NO_3) and ammonium (NH_4^+) was measured from site water for each month by filtering 25 mL of site water through Whatman GF/F filters (25 mm diameter, 0.7 μm nominal pore size). Filtrate was then analyzed for nutrients using a Lachat Quick-Chem 8000 automated ion analyzer (Lachat Instruments, Milwaukee, WI, USA).

Triplicate 10 x 4.75 cm sediment cores (n=3) and a single water sample (n=1) were taken for all months at low tide. Sample numbers of live oysters and paired oyster shells (empty) varied and were collected as follows: June, live oysters (n=3), shells (n=3;) August, live oysters (n=6), shells (n=4); October, live oysters (n=8), shells (n=4). An attempt was made to collect live oysters and empty shells of the same size was made with an average shell length of 8.5 ± 0.4 cm and shell width of 5.4 ± 0.3. All samples were transported in seawater from the Lynnhaven River to the Virginia Institute of Marine

Science immediately after collection. Live oysters collected from August and October sampling were divided evenly into two groups (1) live oyster and (2) live oysters with scrubbed shells. The live oyster group received no treatment to the oyster shells. In the scrubbed shell oyster group, the exteriors of the oysters' shells were carefully scrubbed with a 3.0% bleach solution to remove biofilms and thoroughly rinsed with DI water, followed by 3x seawater rinses. All samples were stored overnight in aerated tubs filled with site water maintained at field site temperature prior to conducting continuous flow-through experiments.

Continuous flow-through experiment: denitrification rate measurement

Denitrification activities were measured at each sampling season using a continuous flow-through design with individual sample cores, which allowed for incubations to occur under steady-state conditions (Groffman et al. 2006) and minimized oxygen depletion effects (Miller-Way and Twilley 1996). Fluxes of N_2 from individual cores were determined using the isotope pairing technique (IPT), which relies on an isotope tracer and isotopic ratios of the resulting $^{29}N_2$ and $^{30}N_2$ (Nielsen and Glud 1996). The IPT method provides measurements of both the actual (D_{14}) and potential (D_{15}) rates of N_2 production (Nielsen and Glud 1996). All measurements were analyzed using a Membrane Inlet Mass Spectrometer (MIMS) and fluxes were calculated as described in Smyth et al. (2013). Total denitrification fluxes were calculated as the sum of D_{14} and D_{15}.

To conduct the flow-through experiment, core tubes containing an individual oyster, a scrubbed oyster, a pair of empty oyster shells, or a 10 cm deep x 4.75 cm wide

sediment core from each sampling season were capped and checked for bubbles that would affect gas concentrations (Reeburgh 1969). Aerated seawater (60L) from each sampling site was held in reservoirs and fed through separate tubing lines at a rate of 3 mL min^{-1} to each core tube in addition to two bypass lines, serving as controls. All incubations were conducted under dark conditions in an environmental chamber held constant at site water temperatures. An initial 24-hour incubation period was allowed (approximately 2 turnover times) before reservoir tanks were spiked with 3 mL of 2M $K^{15}NO_3^-$ for final reservoir concentration of 100 μM. A second 24-incubation period elapsed prior to flux sampling. Seawater from each core was collected in 12 mL exetainer tubes from outflow lines to conduct flux sampling. Triplicates were taken of each sample at time intervals of approximately 1 hour (T_0, T_1, T_F). Exetainers were immediately spiked with 7M ZnCl to prevent further microbial activity from occurring, capped, and stored upside down at 4°C. Samples were stored for less than 4 weeks prior to analysis on the MIMS. DIN concentrations were measured in seawater collected from the bypass and outflow lines described above.

Oyster dissections and sample preservation

Immediately upon completing each seasonal flow-through experiment, whole live oysters were removed from individual oyster treatment cores. Dissections were performed using sterile scalpel blades. A small 2-5 mm crosswise section of posterior tissue containing the intestinal tract (hereafter referred to as 'gut') was excised from the oyster gut, carefully avoiding the digestive gland, stomach, and style sac and transferred to a 2.0 mL microcentrifuge tube. A 10 mm section of gill tissue was also excised from

the oyster and placed in a 2.0 mL microcentrifuge tube. Empty paired shells were removed from shell treatment cores and crushed into roughly 0.5-5.0 mm sized pieces using sterilized hammers. Paired shell fragments for each core were combined and transferred to 50 mL falcon tubes. The top 5 cm of sediment was removed from the sediment cores, slurried, and placed in 50 mL falcon tubes. 375 mL of water from the Lynnhaven site was filtered using 0.2 μm Supor PES membrane filters (Pall Corporation, New York, USA) immediately following field collections and prior to conducting flux experiments. All samples were stored at -80°C prior to extractions.

DNA extraction and amplification

DNA extractions for both oyster gill (0.25-0.30 g) and gut tissues (0.05-0.2 g) were carried out using Qiagen DNA stool mini kit (Qiagen, Hilden, Germany) following the pathogen detection protocol. Shell (0.4-0.5 g), sediment (0.5-0.7 g), and water (1/2 filter) extractions were performed using MoBIO Powersoil extraction kits (Mo-Bio Laboratories, Inc., Carlsbad, CA) following the manufacture's protocol. Two different extraction kits were necessary to optimize DNA yields based on sample type. Initial amplification of targeted hypervariable V4 region of the 16S rRNA gene was performed on extracted DNA using forward primer 515F and modified, barcoded reverse primer 806R (Caporaso et al. 2010), adapted for use with the Ion Torrent Personal Genome Machine (PGM). The basic manufacturer's PCR protocol was used with Taq DNA Polymerase (Invitrogen, Carlsbad, CA) to make a PCR master mix with 1 mM dNTP mixture. Thermal cycling conditions consisted of an initial denaturation step at 94°C for 3 min, followed by 30 cycles of 94°C for 1 min, 54°C for 1 min, 68°C for 2 min. A final

elongation step of 68°C for 10 min was added to ensure complete amplification. The amplified products were gene cleaned using the UltraClean GelSpin DNA Purification Kit (Mo-Bio Bio Laboratories, Inc., Carlsbad, CA). The resulting amplicon libraries were then used as templates for sequencing with the Ion S5 platform following the manufacture's instruction (Thermo Fisher Scientific, Waltham, MA

Sequence processing and OTU assignment

Removal of barcodes and primers from raw sequences and trimming of sequence length were conducted using the Ribosomal Database Project (RDP) pipeline initial process (Cole et al. 2014; http://rdp.cme.msu.edu) with a minimum quality score of 20, minimum length of 200 bases, and a maximum length of 500. Following initial trimming, sequences were denoised with Acacia (Bragg et al. 2012) using a minimum quality score of 25. Mothur v1.35.1 (Schloss et al. 2009) was used to further trim sequences against the SILVA v123 (Yilmaz et al. 2014) alignment template, precluster (diffs=1), and screen for chimeric sequences using the chimera.vsearch command (Rognes et al. 2016). Unknown taxon, mitochondria, chloroplast, archaea, and eukaryotic sequences were removed from analysis using SILVA v123 reference taxonomy and the Wang classification method (Wang et al. 2007) with an 80% minimum identity. Archaea made up < 1.0% of total sequences, and were therefore excluded from further analysis. Sequences were clustered into operational taxonomic units (OTUs) based on a 97% identity using the vsearch abundance-based greedy clustering (AGC) algorithm in Mothur

Oyster-related microbiome and core microbiome

Taxonomic classifications of microbiomes were based on the mean relative abundance of OTUs for each microbiome type and for each month. Taxonomic classifications were assigned using the SILVA v123 database. For the core microbiome analyses, OTUs obtained from Mothur were analyzed using InteractiveVenn (Heberle et al. 2015) and the R packages Phyloseq (McMurdie and Holmes 2013) and VennDiagram (Chen and Boutros 2011). Sequencing reads prior to subsampling were used to prevent reduction in coverage of samples. Core microbiomes for each sample type were defined as the collection of OTUs present in 100% of samples for all months examined. Due to the limited number of samples (n=1 per month), water samples were excluded from taxonomic and core microbiome analyses.

Metabolic potential and gene inference

Gene inference analyses to assess denitrification potential of the oyster gill, gut, shell, and reef sediment microbiomes were performed on clean, trimmed bacteria sequences using the bioinformatic tool paprica (Bowman and Ducklow 2015) and a customized gene database as described in chapter in Arfken et al. (2017). Each sample library (n=54) was analyzed separately for the presence of the denitrification gene, nitrous oxide reductase (*nos*Z), for both clades I and II (*nos*ZI and *nos*ZII). To identify the core denitrifiers in each microbiome, sequences associated with each core OTU generated by Mothur in the core microbiome analysis were analyzed with the paprica database for the presence of *nos*ZI and *nos*ZII genes.

Statistical analyses

Diversity metrics on OTUs including coverage, OTU numbers, Chao1, and Shannon diversity were conducted with subsampled sequencing reads (n=11,142) in Mothur using the summary.single command. Non-metric multidimensional scaling (nMDS) performed on log (x+1) transformed OTU counts was conducted on Bray-Curtis resemblance matrices in PRIMER v7 (Clarke et al. 2014). Due to the low number of sequencing reads, the August water microbiome sample was excluded from diversity and nMDS analysis. Tests for the effects of overall microbiome type and seasonality and the homogeneity of dispersions among the microbiome types were conducted on Bray-Curtis resemblance matrices using PERMANOVA and PERMDISP, respectively in PRIMER. Comparisons between sample types and the interaction between samples and month were made using the PAIRTEST function in PRIMER. Due to the low number of permutations possible between months for each sample type, Monte Carlo simulations were used to determine p-values. Pairwise tests were not corrected for multiple comparisons. Differences between Chao richness and Shannon diversity indices among the microbiome types and differences between the actual (D_{14}) and potential (D_{15}) rates of denitrification among the various treatments were both tested using one factor ANOVAs with post-hoc Tukey's HSD test in R. Actual and potential denitrification rate comparisons were based on October flux data only, due to incomplete treatment sets for June and August. Variance was calculated as the sum of the squared differences between data values and the mean, divided by the count minus 1. Paired t-tests were used to evaluate differences between actual and potential rates of denitrification among the different treatments. Spearman rank correlations were used to compare the relative

abundances of inferred *nos*Z genes for the scrubbed oyster, shell, and sediment microbiomes to the total denitrification rates. Microbiomes comprising each treatment were analyzed as follows: (1) the scrubbed oyster treatment consisted of the combined averages of the gill + gut *nos*Z relative abundances, (2) the empty shell treatment consisted of the shell *nos*Z relative abundances, and (3) the sediment treatment consisted of the sediment *nos*Z relative abundance. Unless stated, all tests are based on a significance of $p < 0.05$ and error bars represent ± standard error.

RESULTS

Coverage, richness, and diversity

A combined total of 2,110,353 clean, trimmed bacterial reads were sequenced from seasonal gill, intestine, shell, sediment, and water microbiome samples. Average sequencing read number was 39,081 ± 7,901 with an average coverage of > 0.99 among the gill and gut samples, > 0.96 in the water samples, > 0.96 in the shell samples, and > 0.86 in the sediment samples. (Table 1). Using subsampled reads (n=11,142), the oyster gut microbiome had the lowest number of OTUs (146 ± 16), Chao1 richness index (190.1 ± 20.9), and Shannon diversity index (2.12 ± 0.23). The oyster gill microbiome had the second lowest number of OTUs (181 ± 21) and the second lowest Chao1 richness (201.7 ± 26.1) and diversity (2.96 ± 0.18) indices, followed by the water microbiome with the numbers of OTUs ranging from 684 in June to 785 in October, a Chao1 richness index ranging from 1,642.0-1,698.8, and Shannon diversity index ranging from 3.65-4.38. In comparison the oyster shell microbiome had a significantly higher number OTUs (1,224 ± 87) ($F_{3,47}$ = 452.3, p = 1.1x10^{-16}, Tukey's HSD, p < 0.05), Chao1 richness index (2,358.3 ± 181.3) ($F_{3,47}$ = 432.5, p = 1.1x10^{-16}, Tukey's HSD, p < 0.05), and Shannon diversity index (5.07 ± 0.14) ($F_{3,47}$ = 87.5, p = 1.1x10^{-16}, Tukey's HSD, p < 0.05) than the gill or gut microbiomes, but significantly lower than the sediment microbiome, which had the highest overall number of OTUs (2,471 ± 85), Chao1 richness index (5,831.7 ± 266.3), and Shannon diversity index (6.26 ± 0.07). Seasonally, there was no consistent trend among the microbiomes regarding richness or diversity. The only significant seasonal change identified in microbiome diversity was regarding the average gut microbiome

richness, which was significantly higher in October (248 ± 26.8) than in August (113 ± 11.29) ($F_{3,47} = 5.2$, p = 0.02, Tukey's HSD, $p < 0.05$).

Microbiome composition

Comparisons among the various oyster-related and water microbiomes were visualized using an nMDS plot (Fig 1) and effects tested using PERMANOVA and PERMDISP tests. PERMANOVA showed that the interaction between the different microbiomes and month had a significant effect among the microbiomes, indicating the effect of season or microbiome type was not consistent among the samples (Table 2). Pairwise tests regarding microbiome type showed significant differences between all the microbiomes for all three months (Table 3A). Among the microbiomes, the highest similarity was found between the gill and gut, while the lowest similarity was found between the gut and sediment. Pairwise tests of the interaction between month and type determined significant seasonal effects between June and October in the gill and shell microbiomes, and between August and October in the shell microbiome (Table 3B). No significant seasonal effects were found in the sediment microbiome. PERMDISP tests showed the dispersion effect was not significant among the different months, however, it was found to be significant among the different microbiomes types (Table 4). While differences in dispersion may sometimes confound the interpretation of the effect of sample type on microbiome structure, the nMDS plot clearly identified distinct clusters among the oyster gill, gut, shell, reef sediments, and water microbiomes. Among the sample types, there also appeared to be some separation between the exterior (shell, reef sediments, and water) and interior (oyster gill and gut) microbiomes.

All four oyster-related microbiomes showed unique taxonomic patterns based on the average relative abundance of sequences > 1% at the order classification level (Fig 2). Within each microbiome, some seasonality was evident based on the variation in abundances of taxonomic orders by month. However, in general, the overall taxonomic composition of each of the microbiomes remained relatively consistent across seasons. The three most abundant orders across all seasons for the gill microbiome consisted of *Alteromonadales, Oceanospirillales, and Vibrionales* from class *Gammaproteobacteria* and comprised on average 37.7 ± 2.8% of the gill microbiome reads. A few of the larger seasonal changes in the gill microbiome occurred among orders *Campylobacterales*, which was highest in June, and *Mycoplasmatales*, which peaked in August. In the gut microbiome, only order *Mycoplasmatales* was found to be dominant across all seasons with an average relative abundance of 72.2 ± 7.6%. There were no major seasonal changes to the overall taxonomic orders, although October showed a decrease in the relative abundance of *Mycoplasmatales* and an increase in orders *Vibrionales*, *Fusobacteriales*, and *Alteromonadales*. In the shell microbiome, *Flavobacteriales, Rhodobacterales,* and *Sphingomonadales* were the three most abundant orders and made up 39.4 ± 5.3% of shell sequences. Seasonally, *Rhodobacterales* showed a reduction in relative abundance from June to August, while the combined orders from class Cyanobacteria (Subsection II, III, and IV) correspondingly increased. *Cellvibrionales, Desulfobacteriales, and Flavobacteriales* were the three most abundant orders in the sediment microbiome and made up 24 ± 1.5% of sequences. Of the four microbiomes, the sediment microbiome appeared to show the most consistency throughout the seasons.

While several orders within the sediment microbiome fluctuated in relative abundance, no orders varied by more than 5.0% in relative abundance among the seasons.

Core oyster microbiome composition

The consistent presence of OTUs in each of the microbiomes across all seasons was deemed the 'core microbiome'. The relative abundance of sequences comprising each of the microbiome cores remained relatively constant across the seasons, with the exception the gut microbiome core, which dropped from 84.2 ± 10.8 in June to 51.7 ± 9.7% in October (Fig 3 and Table 5). This change was primarily driven by the reduction in the relative abundance of core Otu00001 identified as *Mycoplasma* from 61.1 ± 12.1% in June to 14.9 ± 8.3% in October. On average, 45.2 ± 3.7% of sequences made up the gill core microbiome, 64.5 ± 6.2% of sequences made up the gut core microbiome, 49.4 ± 1.6% sequences made up the shell core microbiome, and 73.2 ± 1.1% of sequences made up the sediment core microbiome.

In the gill microbiome, four OTUs from genera *Vibrio* (Otu00004), *Neptunibacter* (Otu00006), *Alteromonas* (Otu00012), and *Pseudoalteromonas* (Otu00015), and one unclassified OTU made up the gill core microbiome (Table 6). The gut core microbiome was composed of three OTUs from genus *Mycoplasma* (Otu00001, Otu00003, and Otu00005), one OTU from genus *Vibrio* (Otu00004), and one from an unclassified *Rhodobacteraceae* genus (Otu00011). The shell core microbiome was primarily composed of OTUs from orders Subsection II (*Cyanobacteria*), *Sphingomonadales*, and *Rhodobacterales* (Fig 3), which is reflected in the top five OTUs from genera *Erythrobacter* (Otu00016), *Pleurocapsa* (Otu00024 and Otu00026), and unclassified

Rhodobacteraceae genus (Otu00018 and Otu00011) (Table 6). In the sediment core microbiome, the top five core OTUs were from orders *Flavobacteriales*, (Otu00030), *Desulfuromonadales* (Otu00046), *Cellvibrionales* (Otu00028), *Gammaproteobacteria Incertae sedis* (Otu00048), and an unclassified *Gammaproteobacteria* order (Otu00041).

Among the microbiomes, the gill and gut core microbiomes shared the lowest number of OTUs with 5 each, but also had the lowest average number of OTUs per sample at 181 ± 21 and 146 ± 16, respectively (Fig. 4A and B). 131 core OTUs made up the core shell microbiome, 507 core OTUs made up the sediment core microbiome, and 209 core OTUs made up the water core microbiome (Figs 4C and D). Only 1 OTU, Otu00004 from order *Vibrionales*, was present in all of the core microbiomes (Fig 5) with the highest relative abundances in the internal oyster gill (9.5 ± 1.8%) and gut core (5.6 ± 2.4%) microbiomes, and lowest in the exterior shell (0.21 ± 0.1%), and sediment (0.45 ± 0.0%). A total of 36 core OTUs was shared between the sediment and shell microbiomes making up 23.3 ± 1.6% and 25.6 ± 3.8% of the core microbiomes, respectively.

Core denitrifiers

Within each core microbiome, reads associated with core OTUs were analyzed for the presence of 'core denitrifiers', defined as *nos*ZI or *nos*ZII gene carrying bacteria, using the metabolic inference database paprica (Table 7 and Fig 6). Core denitrifiers comprised 2.52% and 0.09% of the gill and gut core microbiomes, respectively. All core denitrifiers in the gill carried the *nos*ZII gene and belonged to order *Vibrionales*. The same core denitrifiers from *Vibrionales* in the gill were also found in the gut core microbiome and made up 0.05% of the gut core denitrifiers. The remaining core

denitrifiers (0.04%) in the gut carried the *nos*ZI gene and belonged to order *Rhodobacterales*. In the oyster shell microbiome, core denitrifiers made up 12.6% of the core. Of these shell core denitrifiers, 6.6% were *nos*ZI gene carrying bacteria primarily from order *Rhodobacterales* and 6.0% were *nos*ZII, with the majority belonging to orders *Chitinophagales* (1.4%) and *Flavobacteriales* (2.9%). Core denitrifiers made up 28.7% of the sediment core microbiome, with the majority of reads (24.3%) identified as *nos*ZII gene carrying bacteria and 4.4% identified as *nos*ZI. Orders *Nevskiales* (3.2%) and *Rhodobacterales* (0.6%) were the dominant orders among the nosZI gene carrying bacteria in the sediment core microbiome, while an unclassified *Gammaproteobacteria* (14.6%) order identified as genus *Thiolapillus* was the dominant order among the *nos*ZII gene carrying bacteria.

Microbiome denitrifiers

In addition to core denitrifiers, the total relative abundances of *nos*ZI and *nos*ZII gene carrying bacteria in each of the microbiomes were also examined using the paprica database (Table 8). Out of the oyster gut, gill, shell, and reef sediment the highest relative abundance of total *nos*Z carrying bacteria was found in the sediment (23 ± 0.8%), followed by the oyster shell (18.3 ± 0.8%). The oyster gill and gut microbiomes had the lowest relative abundance of total *nos*Z with 7.7 ± 1.0% and 2.5 7 ± 0.8 %, respectively. This trend was the same for *nos*ZII relative abundances. However, separating out *nos*ZI carrying bacteria only, the gill microbiome had the highest relative abundance (5.3 ± 0.9%), followed by the oyster shell (4.5 ± 0.5%), and gut (1.7 ± 0.7). The sediment microbiome had the lowest relative abundance of nosZI with 1.4 ± 0.1%. On average,

the interior gill and gut microbiomes had higher relative abundances of *nos*ZI (5.3 ± 0.9% and 1.7 ± 0.7%, respectively) than *nos*ZII (2.4 ± 0.4 and 0.9 ± 0.3%), while the exterior shell and sediment microbiomes had higher relative abundances of *nos*ZII (13.7 ± 1.2% and 21.6 ± 0.9%, respectively) than *nos*ZI (4.5 ± 0.5% and 1.4 ± 0.1%, respectively). Seasonally, the gut and gill microbiome had the lowest relative abundances of total *nos*Z in August (6.2 ± 2.11% and 0.8 ± 0.3%, respectively), while in the sediment microbiome they were the highest (25.7 ± 1.0%). In the oyster shell microbiome, total *nos*Z relative abundances increased from June to August (15.9 ± 1.3% to 18.3 ± 1.9% and 7.1% to 11.1%, respectively).

Water Chemistry

Water temperature followed a seasonal trend with an increase from 25.1 °C in early summer (June 2014) to 28.0 °C in late summer (August 2014), and a decrease to 19.2 °C in October (fall 2014) (Table 9). Salinity fluctuated at the site from 18.8 ppt in June 2014 to 26 ppt in August 2014. DO levels ranged between 6.3-7.9 mg/L with highest DO occurring in October 2014. NO_3^- remained below 1.03 μM for all seasons, with the highest measurement taken during October 2014. NH_4^+ varied between months with June 2014 having the highest concentration (3.53 μM) and October 2014 having the lowest (1.68 μM). PO_4^{3-} concentrations ranged from 0.10 in June 2014 to 0.21 in October 2014.

Denitrification rates of oyster, shell and sediments

Seasonal denitrification rates were determined for live oysters, empty oyster shells, and reef sediments using IPT (Table 10). June sediment samples 2 and 3, June shell sample 3, and August scrubbed oyster sample 1 were removed from the N_2 flux analysis for the following reasons: (1) both June sediment samples contained large clams that were discovered at the end of the experiment, (2) June shell sample 3 core leaked and formed an air bubble during the course of the experiment, and (3) August scrubbed oyster sample 1S died before the experiment concluded. For all treatments, potential rates (D_{15}) of denitrification were significantly higher than actual rates (D_{14}) ($t_{32} = 4.94$, $p = 1.3x10^{-5}$). Among the different treatments, oysters and scrubbed oysters showed the highest amounts variation for both actual (variation =120.0 and 59.0, respectively) and potential rates (variation = 11083.2 and 2159.1, respectively) of denitrification. The shell had the least amount of variation in D_{14} and D_{15} among the samples (variation = 3.4 and 552.7, respectively) followed by the sediments (variation = 4.2 and 1001.3, respectively). Seasonally among the oyster samples, June had the highest total denitrification rates out of all months sampled, with an average actual rate of 32.4 ± 7.4 μM N_2-N m^{-2} hr^{-1} and potential rate of 284.9 ± 63.0 μM N_2-N m^{-2} hr^{-1}, while August had the lowest rates with an average active rate of 16.2 ± 23.3 μM N_2-N m^{-2} hr^{-1} and potential rate of 96.9 ± 20.3 μM N_2-N m^{-2} hr. Active denitrification rates were not found to be significantly different among the oysters for the different seasons (D_{14}: $F_{2,7} = 2.39$, $p > 0.05$). However, potential denitrification rates among the oysters were found to be significantly higher in June than in August (D_{15}: $F_{2,7} = 5.0$, $p = 0.04$, Tukey's HSD $p < 0.05$). Due to the low number of samples and/or missing samples, no seasonal patterns could be determined for the remaining treatments including scrubbed oysters, shell, and reef sediment.

Comparisons among different treatments were based on the complete October sampling set. The highest average actual and potential denitrification rates (28.6 ± 4.5 and 141.9 ± 35.0 μM N_2-N m^{-2} hr^{-1}, respectively) were found in the live oyster treatment (Fig. 7). The lowest average actual denitrification rates were measured in the reef sediments (4.0 ± 0.1 μM N_2-N m^{-2} hr^{-1}) and the lowest average potential denitrification rates were measured in the empty shells (15.9 ± 3.5 μM N_2-N m^{-2} hr^{-1}). Of these treatments, only the live oysters were found to have significantly higher actual ($F_{3,14}$ = 10.6, p = 0.0014, Tukey's HSD $p < 0.05$) and potential ($F_{3,14}$ = 9.7, p = 0.0020, Tukey's HSD $p < 0.05$) denitrification rates than the other treatments.

Microbiome denitrifiers and Correlations to N_2 production

Using spearman rank correlations, comparisons were made between the total relative abundances of *nos*ZI and *nos*ZII genes inferred from the oyster gill, gut, shell and sediment microbiomes to the total denitrification rates ($D_{14} + D_{15}$) measured from scrubbed oysters, empty shells, and sediments (Table 11). Microbiomes comprising each treatment are described in the methods section under statistical analysis section. Among the treatments, only one significant correlations was found between the relative abundances of *nos*Z genes, and total denitrification rates. Relative abundances of *nos*ZII were significantly and negatively correlated with shell total denitrification rates (ρ = -0.72, $p < 0.05$). Due to the low number of samples within each treatment ($n \leq 10$), increased sample sizes may detect additional significant correlations. Overall trends observed between the relative abundances of *nos*Z and total denitrification rates were an increase in *nos*ZI and a decrease in *nos*ZII relative abundances corresponding to an

increase in total denitrification rates in the shell and sediment treatments. The reverse trend was found in the scrubbed oyster treatment, with an increase in *nos*ZII and a decrease in *nos*ZI abundances corresponding to an increase in total denitrification rates.

DISCUSSION

Oyster-Related Microbiomes

Diversity, Richness, and Composition

All four oyster-related microbiomes were unique in composition and distinct from the surrounding environment as evidenced by the nMDS plots and taxonomical bar graphs (Figs 1 and 2). Not surprisingly, the gill and gut microbiomes were more similar to each other than the surrounding environment, while the shell and sediment were more similar to each other than the interior of the oyster (Fig 1 and Table 2A). This is likely due to the different pressures exerted on the microbiome communities from either the internal or external environment. Additionally, OTU diversities in the internal gill and gut microbiomes were significantly lower than the external shell and sediment microbiomes. Both gut and gill microbiome diversities in this study were within ranges found in previous studies examining different oyster species and locations (Zurel et al. 2011, Wegner et al. 2013, Trabal Fernández et al. 2014), suggesting that low diversity in the oyster microbiome is uniform. According to the intermediate disturbance theory, low species diversity may occur when disturbances to the community are rare or too frequent (Connell 1978). Inside the oyster, internal tissues of are exposed to a more stable, uniform set of conditions compared to the exterior environment. For example, oysters are able to regulate internal oxygen concentrations by opening shell valves and increasing water flow (Galtsoff 1964; Shumway and Koehn 1982) or avoid exposure to toxic algal species and other harmful substances by shell closure and filtration reduction (Manfrin et al. 2012). In comparison, the shell and sediment microbiomes are likely exposed to

greater disturbances than the internal environment of the oyster, which may favor higher diversity.

In addition to diversity, species richness was also significantly lower in the oyster gill and gut microbiomes compared to the shell and sediment microbiomes (Table 1). The lowest species richness was found in the gut microbiome, which was dominated by order *Mycoplasmatales* from phylum *Tenericutes* (Fig 2). Other studies investigating the oyster tissues have also found a high abundance of *Tenericutes* bacteria in the gut microbiomes (Green and Barnes 2010, Lokmer et al. 2016b, Arfken et al. 2017). However, one study by King et al. (2012) found oyster stomach microbiomes to be heavily dominated by *Tenericutes* or *Planctomycetes*, while gut microbiomes were found to be more species rich and abundant in phyla such as *Chloroflexi*, *Proteobacteria, Verrucomicrobia* and *Planctomycetes* (King et al. 2012). The term 'gut' may encompass several different possible organs in the oyster explaining some of these differences. In the King et al. 2012 study, gut referred to hindgut material taken from the anus (King et al. 2012), while in our study gut samples were taken from intestinal tissue located between the stomach and anus. It is unclear as to why the hindgut section of the oyster is more species rich than other organs in the gut region, but the hindgut may include more fecal matter/biodeposits, which in turn, may encourage more species richness. The gill microbiome had the second lowest species richness of the oyster-related microbiomes, with high abundances of *Alteromonadales, Oceanospirillales, and Vibrionales* from class *Gammaproteobacteria*. These findings are consistent with previous studies have found *Gammaproteobacteria* to be highly abundant in oyster gills (Hernández-Zárate and Olmos-Soto 2006) particularly those from order *Oceanospirillales* (Zurel et al. 2011,

Wegner et al. 2013). Compared to the gut and gill microbiomes, the shell and sediment microbiomes had relatively high OTU richness and large numbers of different taxonomical orders making up their respective microbiomes. In the shell microbiome the taxonomical order with the highest relative abundance was order *Rhodobacterales* from class *Alphaproteobacteria*. While shell microbiome composition is relatively unknown, Arfken et al. (2017) also found to have a high abundance of *Rhodobacterales.* *Rhodobacterales* have been suggested as important in early biofilm formation and initial colonizers of surfaces in the marine environment (Dang et al. 2008, Celikkol-Aydin et al. 2016). The high abundance of *Rhodobacterales* on empty oyster shells that are at least a year or more in age (based on size and date of reef construction) indicate *Rhodobacterales* remain part of the shell microbiome well past early colonization. The sediment microbiome by far showed the greatest amount of species richness and taxonomic orders, with *Desulfobacterales* as the most abundant order averaging only around 10% of the microbiome in relative abundance. *Desulfobacterales* are anaerobic sulfate-reducers commonly identified from sulfate rich environments (Andreote et al. 2012, Ruff et al. 2015), and capable of degrading organic matter in marine sediments (Leloup et al. 2009). Based on the presence of *Desulfobacterales* the sediment microbiome, the reef sediments in this study are likely high in organic matter and sulfate.

Seasonal Effects on the Oyster Microbiomes

Seasonally, significant differences at the OTU level were detected in the gill, gut, and shell, but not in the sediment microbiome (Figs 1 and 3). The consistency of the sediment microbiome across the different seasons is reflected in the relatively stable

taxonomic composition of the microbiome (Fig 2). The lack of significant seasonal effect in the sediments is unexpected as temporal changes such as temperature and salinity have been shown to affect microbial composition (Zhou et al. 2011, Zhang et al. 2014). Additional sampling in the winter months would be useful for determining whether the microbiome composition in the sediment remains consistent throughout the course of a year. Of the remaining microbiomes, however, significant differences in microbiome composition were detected between June and October in the gill and shell microbiomes, and between August and October in the gut microbiome. Taxonomically, differences in the gill microbiome between June and October included a decrease in the relative abundance of *Campylobacterales* and the disappearance of orders SAR11 clade and *Pseudomonadales*. Both SAR11 clade and *Pseudomonadales* are both known to exhibit strong temporal trends in the marine environment (Gilbert et al. 2012, Meziti et al. 2015, Salter et al. 2015), which may explain their absence in the October gill microbiome. In the shell microbiome, the greatest seasonal differences between June and October were the increased relative abundance of *Cyanobacteria* and decreased relative abundance of *Rhodobacterales* from June to October. Temporally, *Cyanobacteria* found in southeastern US estuaries are generally most abundant in the summer months when temperatures are warmer, but also when water residences times are longer, water flow is reduced, or nutrients are elevated (Valdes-Weaver et al. 2006). In our study, relative abundances of *Cyanobacteria* were highest in October, when temperatures were at their lowest among our sample seasons. This suggests that factors other than temperature, such as water flow, retention times or nutrients, are influencing the temporal changes to the shell microbiome. In the gut microbiome, the month of October showed the greatest

amount of seasonal change with a decrease in the relative abundance of *Mycoplasmatales*, and an increase in other taxonomical orders. *Mycoplasma* has been postulated to preferentially proliferate in oyster tissues at higher temperatures (Wegner et al. 2013), and thus may explain the higher abundances of *Mycoplasmatales* and lower species richness during the months of June and August in the gut microbiome

Core Microbiomes

While seasonality was considered to significantly affect several of the oyster-related microbiomes to some degree, there still remained a set of resident bacteria or a 'core' microbiome that persisted throughout the different seasons from late spring to late fall in all of the samples (Figs 3-5). Numbers of OTUs comprising each core was relative to species richness and diversity of the respective microbiome. In the gill and gut microbiomes, low diversity and richness corresponded to core microbiomes of only 5 OTUs each. In the shell and sediment microbiomes, high diversity and richness resulted in core microbiomes of 131 and 507 OTUs, respectively. Despite the difference in core OTU numbers among microbiomes, these cores nevertheless represented a large percentage of total sequences for each microbiome ranging from 45% in the gill microbiome to 73% in the sediment microbiome and remained fairly consistent in relative abundance throughout the sampling period (Table 5). Together, the continuous and stable high relative abundance of the core microbiomes suggest that these core microbes are well adapted to filling some role in the oyster or oyster reef environment. The only exception to stability in the cores was a relatively large decrease in the relative abundance of the gut core microbiome, which fell from 84.2% in June to 51.7% in October primarily

as a result of a dramatic decrease in Otu0001 (*Mycoplasma*) from 61.1% to 14.9% (Table 6). As mentioned previously, a dominance of *Mycoplasma* in oyster tissue may be temperature related. However, the remaining core *Mycoplasma* OTUs did not follow a similar trend, suggesting that some unknown factor other than temperature may be influencing *Mycoplasma* in the oyster, or that certain species of *Mycoplasma* may be more responsive to temperature changes. Additionally, within the gut and gill core microbiomes, there was more variation in the relative abundance of different core OTUs among the seasons compared to the shell and sediment microbiomes, which fluctuated very little. This is not entirely surprising because the internal microbiomes of oysters face many individual factors such as oyster health, age, genetics, or feeding preferences in addition to seasonality. In contrast, the shell and sediment for the most part are influenced by environmental parameters tied directly to seasonality and temperature.

Gill Core Microbiome

In the gill core microbiome, 4 of the 5 OTUs belonged to class *Gammaproteobacteria* (Fig 3 and Table 6). As described earlier, *Gammaproteobacteria* are commonly found in the oyster gill microbiome (Zurel et al. 2011, Lokmer et al. 2016b). Within class *Gammaproteobacteria*, genus *Endozoicomonas* from order *Oceanospirillales* has been shown to form symbiotic relationships in sponges, corals, and worms (Verna et al. 2010, Neave et al. 2016) has also been found to exist intracellularly in gills of deep water bivalves (Jensen et al. 2010). While *Endozoicomonas* was not found in the gill core microbiome, core OTU (Otu00006) belonging to the closely related Oceanospirillales genus Neptuniibacter, may play a similar symbiotic role in oysters.

Two marine species of *Neptuniibacter* have been previously identified and isolated from great scallop hatchery seawater and larvae (*Pecten maximus*) (Diéguez et al. 2017).

Other core OTUs from class Gammaproteobacteria were from genera *Vibrio* (Otu00004), *Alteromonas* (Otu00012), and *Pseudoalteromonas* (Otu00015). *Vibrios* are common in the marine environment and routinely identified in oyster and oyster tissues (Pujalte et al. 1999, Green and Barnes 2010, Trabal Fernández et al. 2014, Asmani et al. 2016). While several *Vibrio* species are associated with disease (Schulze et al. 2006, Dubert et al. 2017), many are nonpathogenic and some may even be beneficial. Kapareiko et al. (2011) showed enhanced oyster larval survival against a pathogenic *Vibrio* when larvae were supplemented with a naturally-occurring *Vibrio* spp. isolated from the digestive glands of bay scallops (Lim et al. 2011). Interestingly, core *Vibrio* (Otu00004) was found in not only the gill core microbiome, but also in the gut (Table 6), shell, and sediment cores (data not shown). Due to its ubiquitous nature in the oyster-related environment, it is possible that the presence of the core *Vibrio* OTU is unrelated to the function or health of the oyster. However, the relative abundance of Otu00004 is much higher in the oyster gut and gill microbiomes (9.5 ± 1.8% and 5.6 ± 2.4%, respectively) than in the shell or sediment microbiomes (0.2 ± 0.1% and 0.5 ± 0.0%, respectively). This suggests that *Vibrio* may be selectively concentrated in the oyster microbiome through feeding or through proliferation of *Vibrio* inside the oyster tissues. Like some *Vibrio*, core OTUs from genera *Alteromonas* and *Pseudoalteromonas* may provide a benefit to the oyster. A variety of strains assigned to *Alteromonas* and *Pseudoalteromonas* have been isolated and used as probiotics in oyster larvae rearing and have shown to exhibit antimicrobial activity and protection against disease Holmström

and Kjelleberg 1999, Isnansetyo and Kamei 2003, Kescardi-Watson et al. 2012, Defer et al. 2013). The combination of core OTUs belonging to genera *Vibrio*, *Alteromonas* and *Pseudoalteromonas* in the gill core microbiome may collectively offer or confer some disease protection to the oysters in our study, although a much more comprehensive investigation is warranted to examine such a link.

The remaining core OTU (Otu00002) had the highest relative abundance of OTUs found in the gill core microbiome and belonged to an unidentified phylum of bacteria. Closest matches to the unidentified OTUs using a phylogenetic placement method with the paprica database identified the unidentified OTUs as belonging to phylum *Spirochaetes*. Lokmer et al. (2016a) found a similar abundant and unidentified bacterium related to *Spirochaetes* in the oyster hemolymph microbiome. In that study, the unidentified bacterium was shown to be abundant in field samples and rare in the lab. The authors suggested the discrepancy in field and lab abundances as a possible result from starvation during lab pretreatment periods decreasing the bacteria in lab samples (Lokmer et al. 2016a). Bacteria from phylum *Spirochaetes* have been previously connected to digestion in oyster digestive glands (Green and Barnes 2010), and thus may play a role in oyster feeding in the gill core microbiome.

Gut Core Microbiome

The gut core microbiome was primarily composed of OTUs belonging to the genus *Mycoplasma* from class *Mollicutes,* phylum *Tenericutes* (Fig 3 and Table 6). It is unclear as to the role of *Mycoplasma* in oyster gut tissues, but the high abundance of *Mycoplasma* in the gut microbiome in this study and other oyster gut-related

microbiomes (Green and Barnes 2010, King et al. 2012, Lokmer et al. 2016b, Arfken et al. 2017) suggest it may have an impact on oyster digestion or health. Class *Mollicutes* contains several endosymbiotic bacteria that have been hypothesized to affect an organism's survival on low-quality food (Fraune and Zimmer 2008) and aid in amino acid synthesis for its host (Tanaka et al. 2004). In contrast, other studies have suggested that *Mycoplasma* is negatively linked to oyster disease (Paillard et al. 2004, Wegner et al. 2013).

In addition to the *Vibrio* OTU also found in the gill core microbiome (Otu00004) and core OTUs belonging to genus *Mycoplasma*, an OTU (Otu00011) from an unidentified genus in family *Rhodobacteraceae* was present in the gut core microbiome. Genera from *Rhodobacteraceae* are prevalent in the marine environment and are often associated with bacterioplankton and algae in the marine environment (Zubkov et al. 2001, Nicolas et al. 2004, Simon et al. 2017). In the oyster gut core microbiome, the relative abundance of Otu000011 from *Rhodobacteraceae*, remained low at 0.3 ± 0.1%, but was consistent across all three seasons. Interestingly, core Otu00011 was also found in the shell core microbiome, but at a higher relative abundance 2.1-6.6% that fluctuated seasonally. It is unclear as to what potential role (if any) core Otu00011 plays in the oyster gut core microbiome. However, the continuous presence and consistency of Otu00011 in the gut core microbiome may reflect a *Rhodobacteraceae* associated with a food source that does not fluctuate with season or it may indicate a more complex, unknown relationship with the bacterium.

Shell and Sediment Core Microbiomes

The shell and sediment core microbiomes were comprised of over a hundred different core OTUs, with no single core OTU making up more than 5% of the microbiome (Fig 3 and Table 6). In the shell core microbiome, the top 5 core OTUs belonged to classes *Alphaproteobacteria* and *Cyanobacteria*. Of the *Cyanobacteria* class, both OTUs were identified as genus *Pleurocapsa*. Abundance of several species of *Pleurocapsa* have been associated with epilithic biofilms in intertidal zones due to their presumed tolerance to thermal stress and desiccation (Ortega-Morales et al. 2005). The shells collected in this study were located within the intertidal zone during low tide and regularly experienced periods of heat stress, wave action, and possible desiccation, favoring *Pleurocapsa* biofilm growth. In the sediment core microbiome, the top 5 OTUs belonged to classes *Flavobacteriia*, *Deltaproteobacteria*, and *Gammaproteobacteria* with many of the genera unclassified. Of those genera identified, *Marinicella* and *Haliea* have previously been found in intertidal and tidal flat sediments (Spring et al. 2013, Zheng et al. 2014). While the shell and sediment microbiomes were distinct in overall composition from each other, several of the core OTUs (n=36) identified in the shell and sediment core microbiomes were shared (Fig 5). These shared core OTUs represented roughly a quarter of the total sediment and shell microbiomes (23.3 ± 1.6% and 25.6 ± 3.8%, respectively), and may represent a ubiquitous set of microbes present in the marine environment and/or a community of organisms with similar functionality in the shell and sediment microbiome.

Core Denitrifiers, Denitrification, and the Oyster Microbiome

Core Denitrifiers

In addition to examining the possible roles of several of the genera found in the oyster-related core microbiomes, each core microbiome was also analyzed using a metabolic inference approach to assess the presence of core denitrifiers (*nos*Z carrying bacteria) (Fig 6 and Table 7). Surprisingly, only a few core denitrifiers with low relative abundance were found in the gut or gill microbiome. This is unexpected in the gut core microbiome as the anoxic and carbon rich environment provided by the gut is thought to potentially favor a core group of denitrifiers. Instead, denitrifiers in the gill and gut microbiomes appear to be transient in nature and likely associated with food particles. For example, active *nos*Z transcripts and denitrification activity in the earthworm are linked to ingested soil microbes passing through the alimentary canal (Depkat-Jakob et al. 2010), with only marginal contributions coming from gut associated microbes (Wüst et al. 2009). In oysters, the source of food consumed by an oyster and the amount or frequency of feeding may have the greatest impact on denitrification.

Unlike the gill and gut microbiomes, several core denitrifiers were identified in the shell and sediment microbiomes. The highest abundance of denitrifiers was found in the sediments and primarily belonged to several taxa identified as *nos*Z clade II. Bacteria carrying the *nos*ZII gene are more taxonomically and ecophysiologically diverse than those with *nos*ZI genes (Sanford et al. 2012) and are often more abundant than *nos*ZI in environments such as salt marshes and wetlands (Jones et al. 2013, Graves et al. 2016). The reef sediment microbiomes examined in this study showed a higher degree of diversity compared to the other microbiomes, suggesting a more heterogeneous environment that may favor *nos*ZII gene denitrifiers. In comparison, the shell microbiome core denitrifiers were less abundant than the sediments and showed no

dominance of either *nos*ZI and *nos*ZII denitrifiers. Furthermore, the overall composition of the denitrifier taxa, particular among *nos*ZI gene carrying denitrifiers, differed between the shell and sediment microbiomes. In the sediment, the majority of *nos*ZI denitrifiers belonged to order *Nevskiales*, while in the shell the majority of *nos*ZI denitrifiers belonged to order *Rhodobacterales*, suggesting a strong niche selection for different denitrifiers between the microbiomes.

Total Microbiome Denitrifiers & Denitrification

While only a few core denitrifiers were detected in the gut and the gill microbiome, there were consistencies in the relative abundances of potential denitrifiers in the gut and gill total microbiomes (Table 2). Abundances of denitrifiers in the gill ranged from 6.2-8.7% of the gill microbiome seasonally, while the gut denitrifiers remained low at abundances between 0.8-3.7% in the gut microbiome. In the shell and the sediment microbiomes, there was also stability regarding the relative abundances of total denitrifiers across the seasons ranging from 15.9-19.8% in the shell microbiome, and 19.6-20.7% in the sediment microbiome. Interestingly, despite this consistency in total denitrifiers, the distribution of *nos*ZI carrying denitrifiers and *nos*ZII carrying denitrifiers showed some slight seasonal variation. Seasonality was most evident in the shell microbiome, which showed an increase in the relative abundance of *nos*ZII carrying bacteria from June-October and a corresponding decrease in *nos*ZI during the same time period. This relatively stable seasonal presence of total denitrifiers in the microbiomes despite the change in *nos*ZI or *nos*ZII carrying denitrifier composition suggests that denitrifiers in the oyster microbiomes might exhibit some type of functional redundancy.

In other words, the composition of denitrifiers may be changing but the relative abundance of denitrifiers is not. Functional redundancy of denitrification genes has been demonstrated in many different environments including stream biofilms, wetland sediments, and peat soils (Peralta et al. 2010, Andert et al. 2012, Dopheide et al. 2015).

To compare the denitrification activity of the different microbiomes, denitrification rates were measured with oysters (gill + gut + shell microbiomes), scrubbed oysters (gill + gut microbiomes), shell (shell microbiome), and reef sediment cores (sediment microbiome). Overall, oysters showed higher actual and potential denitrification rates than all other treatments (Fig 7 and Table 10), suggesting the combination of the shell biofilm and internal gill and gut microbiomes are both important for high denitrification rates. The lower denitrification rates found in the shell and in the scrubbed oyster (shell biofilm removed) treatments support this finding. Because the combined conditions of our study including the use of the IPT method, the selection of different seasons & locations, and the rate measurements of single oysters, shells, or sediments vary from other previous studies, comparison among rate measurements should be interpreted within the context of this study only. However, the overall trends found in this study are consistent with previous studies examining denitrification, which have found whole, live oysters to have higher N_2 fluxes than sediments (Smyth et al. 2013, Arfken et al. 2017) and shells (Caffrey et al. 2016).

Direct comparisons between potential denitrifiers by metabolic inference and total denitrification rates were performed on scrubbed oysters, shells, and sediments. Only one significant correlation, a negative correlation between the relative abundance of *nos*ZII denitrifiers and total denitrification rates in the shell microbiome, was determined among

the different treatments (Table 11). The lack of correlation between bacteria carrying *nos*Z genes and denitrification rates may be the result of DNA-based gene abundances failing to correspond with gene expression or the presence of *nos*Z genes in the microbiomes that were not identified by metabolic inference (i.e. unclassified bacterium). Overall trends in denitrification rates, however, were evident among the different microbiomes relating to *nos*ZI and *nos*ZII relative abundances. In both the shell and reef sediments, relative abundances of *nos*ZI increased with increasing total denitrification rates, while nosZII decreased. This same trend was determined by Arfken et al. (2017), who found that *nos*ZI relative abundances in oyster, shell, and sediment microbiomes mirrored patterns of denitrification rates and may indicate an importance of *nos*ZI denitrifiers in shell and sediment denitrification. In contrast, the scrubbed oyster showed the reverse trend, with increased *nos*ZII relative abundances corresponding to increased denitrification rates. This suggests that *nos*ZII denitrifiers may be more important to denitrification in the internal oyster microbiomes than *nos*ZI. While further investigation of these relationships needs to be explored, these preliminary data indicate that there exists a partitioning between *nos*ZI and *nos*ZII clades within the different niches of the oyster reef, impacting denitrification rates. Several studies have demonstrated separation of *nos*Z clades due to factors such as C:N ratios and oxygen availability (Domeignoz-Horta et al. 2015, Wittorf et al. 2016, Hallin et al. 2017), which may vary greatly within the oyster and among the different reef components.

CONCLUSIONS

All four oyster-related microbiomes were composed of a set of core OTUs that were present throughout the seasons from June-October. The interior oyster microbiomes, including the gill and gut, had the lowest diversity and species richness among the oyster-related microbiomes as well as the lowest number of core OTUs. Despite the small number of core OTUs, however, these OTUs made up a large portion of the total relative abundance for each microbiome suggesting an important role in oyster health or ecosystem services. The shell and sediment microbiomes, in contrast to the gill and gut, had high diversity and species richness, and several low abundance core OTUs that made up a large percent of the total microbiomes. The shell and sediment microbiomes' greater number of core OTUs likely signifies a more widespread and diverse role of the core microbiomes in the environment. In regard to the role of denitrification in the environment, shell and sediment microbiomes had a consistent set of core denitrifiers making up approximately 12-28% of their respective core microbiomes, indicating a possibly stable and constant contribution of shell and sediment microbiomes to denitrification. The overall stability of the shell and sediment microbiomes denitrification rates is reflected in the relatively low amount of variability among the different samples across the seasons. In contrast, the gill and gut microbiomes had only a few core denitrifiers of low relative abundance. The majority of potential denitrifiers identified in the gill and gut were transient members of the total microbiome, suggesting that denitrification in the oyster gut and gill may be linked individually or temporally to the type or amount of food consumed by an oyster. Individual/temporal effects on gill and gut denitrifiers were supported by the high amount of variability in denitrification

rates among oysters and scrubbed oysters. Furthermore, niche differentiation of denitrifiers carrying *nos*ZI and *nos*ZII genes among the oyster-related microbiomes, suggests that the denitrification in the oysters, shells, and reef sediments is performed by separate and distinct communities of bacterial denitrifiers.

ACKNOWLEDGEMENTS

I thank the Song and Anderson lab for their assistance in field and with lab experimentation, particularly Ashley Smyth for help with IPT and the MIMS machine, Hunter Walker for driving the boat and other general helpfulness, Jennifer Stanhope for assisting with the environmental chamber, and Miguel Semedo, Ken Czapla, Tavis Sparrer for helping out in the field collecting oysters and filling carboys. This study was funded by NSF Biological Oceanography program. This work was performed in part using computing facilities at the College of William and Mary, which were provided by contributions from the National Science Foundation, the Commonwealth of Virginia Equipment Trust Fund and the Office of Naval Research.

REFERENCES

Andert, J, Börjesson, G and Hallin, S (2012) Temporal changes in methane oxidizing and denitrifying communities and their activities in a drained peat soil. *Wetlands* **32**(6): 1047–55. doi:10.1007/s13157-012-0335-3.

Andreote, FD, Jiménez, DJ, Chaves, DJ, Cavalcante, A, Dias, F, Luvizotto, DM, Dini-Andreote, F, Fasanella, CC, Lopez, MV, Baena, S, Taketani, RG, and de Melo, IS (2012) The microbiome of Brazilian mangrove sediments as revealed by metagenomics. *PLoS ONE* **7**(6): e386000. doi:10.1371/journal.pone.0038600.

Arfken, A, Bongkeun, S, Bowman, JS, and Piehler, M (2017) Denitrification potential of the eastern oyster microbiome using a 16S rRNA gene based metabolic inference approach. *PLoS ONE* **12**(9): 1–21. doi: 10.1371/journal.pone.0185071.

Asmani, K, Petton, B, Le Grand, J, Mounier, J, Robert, R, and Nicolas, J-L (2016) Establishment of microbiota in larval culture of Pacific oyster, *Crassostrea Gigas*. *Aquaculture* **464**: 434–44. doi: 10.1016/j.aquaculture.2016.07.020.

Bowman JS, and Ducklow HW (2015) Microbial communities can be described by metabolic structure: A general framework and application to a seasonally variable, depth-stratified microbial community from the coastal West Antarctic Peninsula. *PLoS One* **10**(8):1–18. doi: 10.1371/journal.pone.0135868

Bricelji, VM, Ford, SE, Borrero, FJ, Perkins, FO, Rivara, Gm Hillman, RE, Elston, RA, and Chang, J (1992) Unexplained mortalities of hatchery-reared juvenile oysters, *Crassostrea virginica* (Gmelin). J Shellfish Res 19: 353-59.

Brown, JR, Hartwick, BE (1988) Influences of temperature, salinity and available food upon suspended cultre of the Pacific oyster. II. Condition index and survival.

Aquaculture **70**: 253–67.

Caffrey, JM, Hollibaugh, JT and Mortazavi, B (2016) Living oysters and their shells as sites of nitrification and denitrification. *Mar Pollut Bull* **112**: 86–90. doi:10.1016/j.marpolbul.2016.08.038.

Calvo, LM, Dungan, CF, Roberson, BS, and Burreson, EM (2003) Systematic evaluation of factors controlling *Perkinsus marinus* transmission dynamics in lower Chesapeake Bay. *Dis Aquat Org* **56**: 75-86. doi: 10.3354/dao056075.

Caporaso, JG, Lauber, CL, Walters, WA, Berg-lyons, D, Lozupone, CA, Turnbaugh, PJ, Fierer, N, and Knight, R (2010) Global patterns of 16S rRNA diversity at a depth of millions of sequences per sample. *Proc Natl Acad Sci USA* **108**: 4516–22. doi:10.1073/pnas.1000080107.

Castro, D, Pujalte, MJ, Garay, E, and Borrego, JJ (2002) Vibrios isolated from the cultured manila clam (*Ruditapes Phillippinarum*): numerical taxonomy and antibacterial activities. J *Appl Microbiol* **93**: 438-447.

Celikkol-Aydin, S, Gaylarde, CG, Lee, T, Melchers, RE, Witt, DL, and Beech, IB (2016) 16S rRNA gene profiling of planktonic and biofilm microbial populations in the Gulf of Guinea using Illumina NGS. *Mar Environ Res* **122**: 105–12. doi:10.1016/j.marenvres.2016.10.001.

Chaparro, JM, Sheflin, AM, Manter, DK, and Vivanco, JM (2012) Manipulating the soil microbiome to increase soil health and plant fertility. *Biol Fert Soils* **48**(5): 489–99. doi: 10.1007/s00374-012-0691-4.

Chen, H, and Boutros, PC (2011) VennDiagram: a package for the generation of highly-customizable venn and euler diagrams in R. *BMC Bioinformatics* **12**(1): 35.

doi:10.1186/1471-2105-12-35.

Clarke, KR, Gorley, RN, Somerfield, PJ and Warwick, RM (2014) Change in marine communities: an approach to statistical analysis and interpretation, 3rd edition. PRIMER-E, Plymouth, 260 pp.

Cole, JR, Wang, Q, Fish, JA, Chai, B, McGarrell, DM, Sun, Y, Brown, CT, Porras-Alfaro, A, Kuske, CR, and Tiedje, JT (2014) Ribosomal database project: data and tools for high throughput rRNA analysis. *Nucleic Acids Res* **42** : D633–42. doi:10.1093/nar/gkt1244.

Connell, JH (1978) Diversity in tropical rain forests and coral Reefs. *Science* **199**(4335): 1302–10.

Costello, EK, Stagaman, K, Dethlefsen, L, Bohannan, BJM, and Relman, DA (2012) The application of ccological theory. *Science* **336**(June): 1255–62. doi: 10.1126/science.1224203.

Dang, H, Li, T, Chen, M and Huang, G (2008) Cross-ocean distribution of *Rhodobacterales* bacteria as primary surface colonizers in temperate coastal marine waters. *Appl Environ Microb* **74**(1): 52–60. doi:10.1128/AEM.01400-07.

Defer, D, Desriac, F, Henry, J, Bourgougnon, N, Baudy-Floc'h, M, Brillet, B, Le Chevalier, P, and Fleury, Y (2013) Antimicrobial peptides in oyster hemolymph: the bacterial connection. *Fish Shellfish Immun* **34**(6): 1439–47. doi:10.1016/j.fsi.2013.03.357.

Depkat-Jakob, PS, Hilgarth, M, Horn, MA, and Drake, HL (2010) Effect of earthworm feeding guilds on ingested dissimilatory nitrate reducers and denitrifiers in the alimentary canal of the earthworm. *Appl Environ Microb* **76**: 6205–6214. doi:

10.1128/AEM.01373-10.

Diaz, RJ and Rosenberg, R. (2008) Spreading dead zones and consequences for marine ecosystems. *Science* **321**: 926–929. doi: 10.1126/science.1156401.

Diéguez, AL, Balboa, S, Magnesen, T, and Romalde, JL (2017) *Neptuniibacter pectenicola* sp. nov. and *Neptuniibacter marinus* sp. nov., two novel species isolated from a Great scallop (*Pecten maximus*) hatchery in Norway and emended description of the genus *Neptuniibacter*. *Syst Appl Microbiol* **40**(2): 80–85. doi:10.1016/j.syapm.2016.12.002.

Domeignoz-Horta, LA, Spor, A, Bru, D, Breuil, MC, Bizouard, F, Léonard, J, and Philippot, L (2015) The diversity of the N_2O reducers matters for the N_2O:N_2 denitrification end-product ratio across an annual and a perennial cropping system. *Front Microbiol* **6**(SEP): Article 971. doi:10.3389/fmicb.2015.00971.

Dopheide, A, Lear, G, He, Z, Zhou, J, and Lewis, GD (2015) Functional gene composition, diversity and redundancy in microbial stream biofilm communities. *PLoS ONE* **10**(4): 1–21. doi:10.1371/journal.pone.0123179.

Dubert, J, Barja, JL, and Romalde, JL (2017) New insights into pathogenic vibrios affecting bivalves in hatcheries: present and future prospects. *Front Microbiol* **8**(May): Article 762. doi:10.3389/fmicb.2017.00762.

Ford, SE and Borrero, FJ (2001) Epizootiology and pathology of juvenile oyster disease in the eastern oyster, *Crassostrea virginica*. *J Invertebr Pathol* **78**: 141-54.

Fraune, S, and Zimmer, M (2008) Host-specificity of environmentally transmitted *Mycoplasma*-like isopod symbionts. *Environ Microbiol* **10**(10): 2497–2504. doi:10.1111/j.1462-2920.2008.01672.x.

Fuhrman, JA, Hewson, I, Schwalbach, MS, Steele, JA, Brown, MV, and Naeem, S (2006) Annually reoccurring bacterial communities are predictable from ocean conditions. *Proc Natl Acad Sci USA* **103**(35): 13104–9. doi:10.1073/pnas.0602399103.

Galstoff, PS (1964) The American oyster, *Crassostrea virginica* Gmelin. *US Fish Wildl Serv Fish Bull* **64**: 1-457. doi: 10.4319/lo.1966.11.2.

Garnier, M, Labreuche, Y, Garcia, C, Robert, M, and Nicolas, JL (2007) Evidence for the involvement of pathogenic bacteria in summer mortalities of the Pacific oyster *Crassostrea Gigas*. *Microbiol Ecol* **53**(2): 187–96. doi:10.1007/s00248-006-9061-9.

Gilbert, JA, Field, D, Swift, P, Newbold, L, Oliver, A, Smyth, T, Somerfield, PJ, Huse, S, and Joint, I (2009) The seasonal structure of microbial communities in the Western English Channel. *Environ Microbiol* **11**(12): 3132–39. doi:10.1111/j.1462-2920.2009.02017.x.

Gilbert, JA, Steele, JA, Caporaso, JG, Steinbrück, L, Reeder, J, Temperton, B, Huse, S, et al. (2012) Defining seasonal marine microbial community dynamics. *ISME J* **6**(2): 298–308. doi:10.1038/ismej.2011.107.

Gomez-Gil, B, Roque, A, and Turnball, JF (2000) The use and selection of probiotic bacteria for use in the culture of larval aquatic organisms. *Aquaculture* **191**: 259-270.

Graham, EB, Wieder, WR, Leff, JW, Weintraub, SR, Townsend, AR, Cleveland, CC, Philippot, L, and Nemergut, DR (2014) Do we need to understand microbial communities to predict ecosystem function? A comparison of statistical models of nitrogen cycling processes. *Soil Biol Biochem* **68**:279–82. doi:10.1016/j.soilbio.2013.08.023.

Graves, CJ, Makrides, EJ, Schmidt, VT, Giblin, AE, Cardon, ZG, and Rand, DM (2016) Functional responses of salt marsh microbial communities to long-term nutrient enrichment. *Appl Environ Microb* **82**(9): 2862–71. doi:10.1128/AEM.03990-15.

Green, TJ, and Barnes, AC (2010) Bacterial diversity of the digestive gland of Sydney rock oysters, *Saccostrea glomerata* infected with the paramyxean parasite, *Marteilia sydneyi*. *J Appl Microbiol* **109**(2): 613–22. doi:10.1111/j.1365-2672.2010.04687.x.

Groffman, PM, Altabet, MA, Bohlke, JK, Butterbach-Bahl, K, David, MB, Firestone, MK, Giblin, AE, et al. (2006) Methods for measuring denitrification: diverse approaches to a difficult problem. *Ecol Appl* **16**(6): 2091–2122. doi:10.1890/1051-0761(2006)016[2091:MFMDDA]2.0.CO;2.

Hallin, S, Philippot, L, Löffler, F, Sanford RA, Jones, CM (2017) Genomics and ecology of novel N_2O-Reducing microorganisms. *Trends Microbiol* **xx:** 1–13. doi: 10.1016/j.tim.2017.07.003.

Harris, J (1993) The presence, nature, and role of gut microflora in aquatic invertebrates: a synthesis. *Microbiol Ecol* **25**(3): 195-231.

Heberle, H, Meirelles, GV, da Silva, FR, Telles, GP, and Minghim, R (2015) InteractiVenn: a web-based tool for the analysis of sets through venn diagrams. *BMC Bioinformatics* **16**(1): 169. doi:10.1186/s12859-015-0611-3.

Herlemann, DPR, Lundin, D, Andersson, AF, Labrenz, M, and Jürgens, K (2016) Phylogenetic signals of salinity and season in bacterial community composition across the salinity gradient of the Baltic Sea. *Front Microbiol* **7**(NOV): 1–13. doi:10.3389/fmicb.2016.01883.

Hernández-Zárate, G, and Olmos-Soto, J (2006) Identification of bacterial diversity in the

oyster *Crassostrea gigas* by fluorescent in situ hybridization and polymerase chain reaction. *J Appl Microbiol* **100**(4): 664–72. doi:10.1111/j.1365-2672.2005.02800.x.

Hoellein, TJ, Zarnoch, CB, and Grizzle, RE (2015) Eastern oyster (*Crassostrea virginica*) filtration, biodeposition, and sediment nitrogen cycling at two oyster reefs with contrasting water quality in Great Bay Estuary (New Hampshire, USA). *Biogeochemistry* **122**(1): 113–29. doi: 10.1007/s10533-014-0034-7.

Holmer, M and Bondgaard, EJ (2001) Photosynthetic and growth response of eelgrass to low oxygen and high sulfide concentrations during hypoxic events. *Aquat Bot* **70**: 29–38. doi: 10.1016/S0304-3770(00)00142-X.

Holmström, C, and Kjelleberg, S (1999) Marine *Pseudoalteromonas* species are associated with higher organisms and produce biologically zctive cxtracellular agents. *FEMS Microbiol Ecol* **30**: 285–93. doi:10.1111/j.1574-6941.1999.tb00656.x.

Humphries, AT, Ayvazian, SG, Carey, JC, Hancock, BT, Grabbert, S, Cobb, D, Strobel, CJ, and Fulweiler, RW (2016) Directly measured denitrification reveals oyster aquaculture and restored oyster reefs remove nitrogen at comparable high rates. *Front Mar Sci* **3**(May): 74. doi: 10.3389/fmars.2016.00074.

Isnansetyo, A, and Kamei, Y (2003) MC21-A , a bactericidal antibiotic produced by a new marine against methicillin-resistant *Staphylococcus Aureus*. *Antimicrob Agents Ch* **170**(2): 481–90. doi:10.1128/AAC.47.2.480.

Jensen, S, Duperron, S, Birkeland, NK, and Hovland, M (2010) Intracellular *Oceanospirillales* bacteria inhabit gills of Acesta bivalves. *FEMS Microbiol Ecol* **74**(3): 523–33. doi:10.1111/j.1574-6941.2010.00981.x.

Jones, CM, Graf, DRH, Bru, D, Philippot, L, and Hallin, S (2013) The unaccounted yet

abundant nitrous oxide-reducing microbial community: a potential nitrous oxide sink. *ISME J* **7**: 417–26. doi: 10.1038/ismej.2012.125.

Jousset, Alexandre, Bienhold, C, Chatzinotas, A, Gallien, L, Gobet, A, Kurm, V, Küsel, K, et al. (2017) Where less may be more: how the rare biosphere pulls ecosystems strings. *The ISME J* **11** (4): 853–62. doi: 10.1038/ismej.2016.174.

Kellogg, ML, Cornwell, JC, Owens, MS, and Paynter, KT (2013) Denitrification and nutrient assimilation on a restored oyster reef. *Mar Ecol Prog Ser* **480**: 1–19. doi: 10.3354/meps10331.

Kesarcodi-Watson, A, Miner, P, Nicolas, J-L, and Robert, R (2012) Protective effect of four potential probiotics against pathogen-challenge of the larvae of three bivalves: Pacific oyster (*Crassostrea gigas*), flat oyster (*Ostrea edulis*) and scallop (*Pecten maximus*). *Aquaculture* **344–349**: 29–34. doi:10.1016/j.aquaculture.2012.02.029.

King, GM, Judd, C, Kuske, CR, and Smith, C (2012) Analysis of stomach and gut microbiomes of the eastern oyster (*Crassostrea virginica*) from coastal Louisiana, USA. *PLoS One* **7**(12): e51475. doi: 10.1371/journal.pone.0051475.

Lacoste, A, Jalabert, F, Malham, S, Cueff, A, Gélébart, F, Cordevant, C, Lange, M, and Poulet, SA (2001) A *Vibrio splendidus* strain is associated with summer mortality of juvenile oysters *Crassostrea gigas* in the Bay of Morlaix (North Brittany, France). *Dis Aquat Organ* **46**(2): 139–45. doi:10.3354/dao046139.

Leloup, J, Fossing, H, Kohls, K, Holmkvist, L, Borowski, C, and Jørgensen, BB (2009) Sulfate-reducing bacteria in marine sediment (Aarhus Bay, Denmark): abundance and diversity related to geochemical zonation. *Environ Microbiol* **11**(5): 1278–91. doi:10.1111/j.1462-2920.2008.01855.x.

Levinton, J, Doall, M, and Allam, B (2013) Growth and mortality patterns of the eastern oyster *Crassostrea virginica* in impacted waters in coastal waters in New York, USA. *J Shellfish Res* **32**(2): 417-27. doi: 10.2983/035.032.0222.

Lim, HJ, Kapareiko, D, Schott, EJ, Hanif, A, and Wikfors, GH (2011) Isolation and evaluation of new probiotic bacteria for use in shellfish hatcheries: I. Isolation and screening for bioactivity. *J Shellfish Res* **30**(3): 609–15. doi:10.2983/035.030.0303.

Lindemann, S, Zarnoch, CB, Castignetti, D, and Hoellein, TJ (2016) Effect of eastern oysters (*Crassostrea virginica*) and seasonality on nitrite reductase gene abundance (*nir*S, *nir*K, *nrf*A) in an urban estuary. *Estuaries Coasts* **39**: 218–32. doi:10.1007/s12237-015-9989-4.

Lokmer, A, Goedknegt AM, Thieltges, DW, Fiorentino, D, Kuenzel, S, Baines, JF, and Wegner, KM (2016a) Spatial and temporal dynamics of Pacific oyster hemolymph microbiota across multiple scales. *Front Microbiol* **7**(August): 1–18. doi: 10.3389/fmicb.2016.01367.

Lokmer, A, Kuenzel, S, Baines, JF and Wegner, KM (2016b) The role of tissue-specific microbiota in initial establishment success of Pacific oysters. *Environ Microbiol* **18**(3): 970–87. doi: 10.1111/1462-2920.13163.

Malham, SK, Cotter, E, O'Keeffe, S, Lynch, S, Culloty, SC, King, JW, Latchford, JW and Beaumont, AR (2009) Summer mortality of the Pacific oyster, *Crassostrea gigas*, in the Irish Sea: the influence of temperature and nutrients on health and survival. *Aquaculture* **287**(1–2): 128–38. doi:10.1016/j.aquaculture.2008.10.006.

Manfrin, C, De Moro, G, Torboli, V, Venier, P, Pallavicini, A, and Gerdol, M (2012) Physiological and molecular responses of bivalves to toxic dinoflagellates. *Idaho*

State J **9**: 184–99.

McFall-Ngai, M, Hadfield, MG, Bosch, TCG, Carey, HV, Domazet-Lošo, T, Douglas, AE, Duilier, N, et al. (2013) Animals in a bacterial world, a new imperative for the life sciences. *Proc Natl Acad Sci* USA **110**: 3229–36. doi: 10.1073/pnas.1218525110.

McMurdie, PJ, and Holmes, S (2013) Phyloseq: an R package for reproducible interactive analysis and graphics of microbiome census data. *PLoS ONE* **8**(4): e61217. doi:10.1371/journal.pone.0061217.

Meziti, A, Kormas, KA, Moustaka-Gouni, M, and Karayanni, H (2015) Spatially uniform but temporally variable bacterioplankton in a semi-enclosed coastal area. *Syst Appl Microbiol* **38**(5): 358–67. doi:10.1016/j.syapm.2015.04.003.

Miller-Way, T, and Twilley, RR (1996) Theory and operation of continuous flow systems for the study of benthic-pelagic coupling. *Mar Ecol Prog Ser* **140**: 257–69. doi:10.3354/meps140257.

Neave, MJ, Apprill, A, Ferrier-Pagès, C, and Voolstra, CR (2016) Diversity and function of prevalent symbiotic marine bacteria in the genus *Endozoicomonas*. *Appl Microbiol Biot* **100**(19): 8315– 24. doi:10.1007/s00253-016-7777-0.

Nicolas, JL, Corre, S and Cochard, JC (2004) Bacterial population association with phytoplankton cultured in a bivalve hatchery. *Microbiol Ecol* **48**(3): 400–13. doi:10.1007/s00248-003-2031-6.

Nielsen, LP, and Glud, RN (1996) Denitrification in a coastal sediment measured *in situ* by the nitrogen isotope pairing technique applied to a benthic flux chamber. *Mar Ecol Prog Ser* **137**(1–3): 181–86. doi:10.3354/meps137181.

Oberbeckmann, S, Fuchs, BM, Meiners, M, Wichels, A, Wiltshire, KH, and Gerdts, G (2012) Seasonal dynamics and modeling of a *Vibrio* community in coastal waters of the North Sea. *Microbiol Ecol* **63**(3): 543–51. doi:10.1007/s00248-011-9990-9.

Ortega-Morales, BO, Santiago-Garcia, JL, and López-Cortés, A (2005) Biomass and taxonomic richness of epilithic cyanobacteria in a tropical intertidal rocky habitat. *Botanica Marina* **48**(2): 116–21. doi:10.1515/BOT.2005.020.

Paerl, HW, Hall, NS, and Calandrino, ES (2011) Controlling harmful cyanobacterial blooms in a world experiencing anthropogenic and climatic-induced change. *Sci Total Environ* **409**: 1739–1745.

Paillard, C, Le Roux, F, and Borrego, JJ (2004) Bacterial disease in marine bivalves, a review of recent studies: trends and evolution. *Aquat Living Resour* **17**(4): 477–98. doi:10.1051/alr:2004054.

Peralta, AL, Matthews, JW, and Kent, AD (2010) Microbial community structure and denitrifikation in a wetland mitigation bank. *Appl Environl Microb* **76**(13): 4207–15. doi:10.1128/AEM.02977-09.

Piehler, MF and Smyth, AR (2011) Habitat-specific distinctions in estuarine denitrification affect both ecosystem function and services. *Ecosphere* **2**: art12. doi: 10.1890/ES10-00082.1.

Pierce, ML, Ward, JE, Holohan, BA, Zhao, X, and Hicks, RE (2016) The influence of site and season on the gut and pallial fluid microbial communities of the eastern oyster, *Crassostrea virginica* (Bivalvia , Ostreidae): community-level physiological profiling and genetic structure. *Hydrobiologia* **765**(1): 97–113. doi:10.1007/s10750-015-2405-z.

Prado, S, Romalde, JL, Barja, JL (2010) Review of probiotics for use in bivalve hatcheries. *Vet Microbiol* **145**(3-4): 187-97. doi: 10.1016/j.vetmic.2010.08.021.

Preheim, SP, Boucher, Y, Wildschutte, H, David, LA, Veneziano, D, Alm, EJ, and Polz, MF (2011) Metapopulation structure of *Vibrionaceae* among coastal marine invertebrates. *Environ Microbiol* **13** (1): 265–75. doi:10.1111/j.1462-2920.2010.02328.x.

Pujalte, MJ, Ortigosa, M, Macián, MC, and Garay, E (1999) Aerobic and facultative anaerobic heterotrophic bacteria associated to Mediterranean oysters and seawater. *Int Microb* **2**(4): 259–66.

Rabalais, NN, Turner, RE, and Wiseman, WJ (2002) Gulf of Mexico hypoxia, a.k.a. "the dead zone." *Annu Rev Ecol Syst* **33**: 235–263. doi: 10.1146/annurev.ecolsys.33.010802.150513.

Reeburgh, WS (1969) Observations of gases in Chesapeake Bay sediments. *Limnol Oceanogr* **14**(3): 368–75. doi:10.4319/lo.1969.14.3.0368.

Rognes, T, Flouri, T, Nichols, B, Quince, C, and Mahé, F (2016) VSEARCH: a versatile open source tool for metagenomics. *PeerJ* **4**: e2584. doi:10.7717/peerj.2584.

Ruff, SE, Biddle, JF, Teske, AP, Knittel, K, Boetius, A, and Ramette, A (2015) Global dispersion and local diversification of the methane seep microbiome. *Proc Natl Acad Sci USA* **112**(13): 4015–20. doi:10.1073/pnas.1421865112.

Salter, I, Galand, PE, Fagervold, SK, Lebaron, P, Obernosterer, I, Oliver, MJ, Suzuki, MT, and Tricoire, C (2015) Seasonal dynamics of active SAR11 ecotypes in the oligotrophic Northwest Mediterranean Sea. *ISME J* **9**(2): 347–60. doi:10.1038/ismej.2014.129.

Sanford, RA, Wagner, DD, Qingzhong, W, Chee-Sanford, JC, Thomas, SH, Cruz-García, C, Rodríguez, G, et al. (2012) Unexpected nondenitrifier nitrous oxide reductase gene diversity and abundance in soils. *Proc Natl Acad Sci USA* **109**: 19709-19714. doi: 10.1073/pnas.1211238109.

Schimel, J, Balser, TC and Wallenstein. M (2007) Microbial stress-response physiology and its implications for ecosystem function *Ecology* **88**(6): 1386–94.

Schloss, PD, Westcott, SL, Ryabin, T, Hall, JR, Hartmann, M, Hollister, EB, Lesniewski, RA, et al. (2009) Introducing Mothur: open-source, platform-independent, community-supported software for describing and comparing microbial communities. *Appl Environ Microb* **75**(23): 7537–41. doi:10.1128/AEM.01541-09.

Schulze, AD, Alabi, AO, Tattersall-Sheldrake, AR, and Miller, KM (2006) Bacterial diversity in a marine hatchery: balance between pathogenic and potentially probiotic bacterial strains.

Aquaculture **256**(1–4): 50–73. doi:10.1016/j.aquaculture.2006.02.008.

Shade, A and Handelsman, J (2012) Beyond the venn diagram: the hunt for a core microbiome. *Environ Microbiol* **14**: 4–12. doi: 0.1111/j.1462-2920.2011.02585.x

Shumway, SE and Koehn, RK (1982) Oxygen consumption in the American oyster *Crassostrea virginica. Mar Ecol Prog* **9**(1): 59-68.

Simon, M, Scheuner, C, Meier-Kolthoff, JP, Brinkhoff, T, Wagner-Döbler, I, Ulbrich, M, Klenk, H-P, Schomburg, D, Petersen, J, and Göker, M (2017) Phylogenomics of *Rhodobacteraceae* reveals evolutionary adaptation to marine and non-marine habitats. *ISME J* **11**(6): 1483–99. doi:10.1038/ismej.2016.198.

Smyth, AR, Geraldi, NR, and Piehler, MF (2013) Oyster-mediated benthic-pelagic

coupling modifies nitrogen pools and processes. *Mar Ecol Prog Ser* **493**: 23–30. doi: 10.3354/meps10062.

Soletchnik, P, Ropert, M, Mazurié, J, Fleury, PG, and Le Coz, F (2007) Relationships between oyster mortality patterns and environmental data from monitoring databases along the coasts of France. *Aquaculture* **271**(1–4): 384–400. doi:10.1016/j.aquaculture.2007.02.049.

Southworth, M, Long, CM, and Mann, R (2017) Oyster (Crassostrea virginica [GMELIN, 1791]) mortality at prolonged exposures to high temperature and low salinity. *J Shellfish Res* **36**(2): 335-340. doi: 10.283/035.036.0305.

Spring, S, Riedel, T, Spröer, C, Yan, S, Harder, J, and Fuchs, BM (2013) Taxonomy and evolution of bacteriochlorophyll *a*-containing members of the OM60/NOR5 clade of marine gammaproteobacteria: description of *Luminiphilus syltensis* gen. nov., sp. nov., reclassification of *Haliea rubra* as *Pseudohaliea rubra* gen. nov., comb. nov. and emendation of *Chromatocurvus halotolerans*. *BMC Microbiol* **13**(1): 118. doi:10.1186/1471-2180-13-118.

Stenuit, B and Agathos, SA (2015) Deciphering microbial community robustness through synthetic ecology and molecular systems synecology. *Curr Opin Biotech* **33**(1): 305–17. doi: 10.1016/j.copbio.2015.03.012.

Tanaka, R, Ootsubo, M, Sawabe, T, Ezura, Y, and Tajima, K (2004) Biodiversity and in situ abundance of gut microflora of abalone (*Haliotis discus hannai*) determined by culture-independent techniques. *Aquaculture* **241**(1–4): 453–63. doi:10.1016/j.aquaculture.2004.08.032.

Trabal Fernández, N, Mazón-Suástegui, JM, Vázquez-Juárez, R, Ascencio-Valle, F, and

Romero, J (2014) Changes in the composition and diversity of the bacterial microbiota associated with oysters (*Crassostrea corteziensis*, *Crassostrea gigas* and *Crassostrea sikamea*) during commercial production. *FEMS Microbiol Ecol* **88**: 69–83. doi: 10.1111/1574-6941.12270

Turnbaugh, PJ, Ley, RE, Hamady, M, Fraser-Liggett, CM, Knight, R, and Gordon, JI (2007) The human microbiome project. *Nature* **449**: 804–810. doi: 10.1038/nature06244

Valdes-Weaver, LM, Piehler, MF, Pinckney, JL, Howe, KE, Rossignol, K, and Paerl, HW (2006) Long-term temporal and spatial trends in phytoplankton biomass and class-level taxonomic composition in the hydrologically variable Neuse-Pamlico estuarine continuum, North Carolina, U.S.A. *Limnol Oceanogr* **51**(3): 1410–20. doi:10.4319/lo.2006.51.3.1410.

Verna, C, Ramette, A, Wiklund, H, Dahlgren, TG, Glover, AG, Gaill, F, and Dubilier, N (2010) High symbiont diversity in the bone-eating worm *Osedax mucofloris* from shallow whale-falls in the North Atlantic. *Environ Microbiol* **12**(8): 2355–70. doi:10.1111/j.1462-2920.2010.02299.x.

Wallenstein, MD, Myrold, DD, Firestone, M, and Voytek, M (2016) Environmental controls on denitrifying communities and denitrification rates: insights from molecular methods. *Ecol Appl* **16**(6): 2143–52.

Wang, Qi, Garrity, GM, Tiedje, JM, and Cole, JR (2007) Naive bayesian classifier for rapid assignment of rRNA sequences into the new bacterial taxonomy. *Appl Environ Microb* **73** (16): 5261–67. doi:10.1128/AEM.00062-07.

Wegner, KM, Volkenborn, N, Peter, H, and Eiler, A (2013) Disturbance induced

decoupling between host genetics and composition of the associated microbiome. *BMC Microbiol* **13**(1) doi: 10.1186/1471-2180-13-252.

Wittorf, L, Bonilla-Rosso, G, Jones, CM, Bäckman, O, Hulth, S, and Hallin, S (2016) Habitat partitioning of marine benthic denitrifier communities in response to oxygen availability. *Environ Microbiol Rep* **8**(4): 486–92. doi:10.1111/1758-2229.12393.

Wüst, PK, Horn, MA, Henderson, G, Janssen, PH, Rehm, BHA, and Drake, HL (2009) Gut-associated denitrification and in vivo emission of nitrous oxide by the earthworm families *Megascolecidae* and *Lumbricidae* in New Zealand. *Appl Environ Microb* **75**(11): 3430–36. doi: 10.1128/AEM.00304-09.

Yilmaz, P, Parfrey, LW, Yarza, P, Gerken, J, Ludwig, W, Pruesse, E, Quast, C, Schweer, T, and Glo, FO (2014) The SILVA and "all-species living tree project (LTP)" taxonomic frameworks. *Nucleic Acids Res* **42**(November 2013): D643–48. doi:10.1093/nar/gkt1209.

Zhang, L, Gao, G, Tang, X, and Shao, K (2014) Can the freshwater bacterial communities shift to the "marine-like" taxa? *J Basic Microbiol* **54**: 1264–72. doi:10.1002/jobm.201300818.

Zheng, B, Wang, L, and Liu, L (2014) Bacterial community structure and its regulating factors in the intertidal sediment along the Liaodong Bay of Bohai Sea, China. *Microbiol Res* **169** : 585–92. doi:10.1016/j.micres.2013.09.019.

Zhou, W, Long, A, Jiang, Tao, Chen, S, Huang, L, Huang, H, Cai, C, and Yan, Y (2011) Bacterioplankton dynamics along the gradient from highly eutrophic Pearl River Estuary to oligotrophic Northern South China Sea in wet season: implication for anthropogenic inputs. *Mar Pollut Bull* **62**(4): 726–33.

doi:10.1016/j.marpolbul.2011.01.018.

Zubkov, MV, Fuchs, BM, Archer, SD, Kiene, RP, Amann, R, and Burkill, PH (2001) Linking the composition of bacterioplankton to rapid turnover of dissolved dimethylsulphoniopropionate in an algal bloom in the North Sea. *Environ Microbiol* **3**(5): 304–11. doi:10.1046/j.1462-2920.2001.00196.x.

Zumft, WG (1997) Cell biology and molecular basis of denitrification *Microbiol Mol Biol R* **61**(4): 533-616.

Zurel, D, Benayahu, Y, Or, A, Kovacs, A, and Gophna, U (2011) Composition and dynamics of the gill microbiota of an invasive Indo-Pacific oyster in the Eastern Mediterranean Sea. *Environ Microbiol* **13**(6): 1467–76. doi:10.1111/j.1462-2920.2011.02448.x.

TABLES

Table 1. Summary statistics of 16S rRNA gene amplicon sequencing for oyster gill, gut, shell, reef sediment (sed), and water microbiomes for sampling months June, August, and October.

Sample	Month	Sequence Total	coverage	coverage*	OTUs*	Chao1*	Shannon*
Gill.1	June	117,737	1.0	1.00	141	142.31	2.93
Gill.2	June	87,713	1.0	1.00	232	261.25	3.15
Gill.3	June	11,142	1.0	0.99	303	439.50	3.67
Gill.1	August	31,235	1.0	1.00	47	47.00	1.88
Gill.2	August	68,273	1.0	1.00	124	157.00	2.61
Gill.3	August	60,697	1.0	1.00	129	129.50	2.42
Gill.2s	August	52,492	1.0	1.00	211	214.00	3.75
Gill.3s	August	47,539	1.0	1.00	225	231.00	4.19
Gill.1	October	49,571	1.0	1.00	153	162.75	3.14
Gill.2	October	60,635	1.0	1.00	89	128.67	1.27
Gill.3	October	36,284	1.0	1.00	299	307.40	3.28
Gill.4	October	15,083	1.0	1.00	360	387.77	3.77
Gill.1s	October	34,923	1.0	1.00	109	112.75	2.59
Gill.2s	October	18,361	1.0	1.00	146	152.43	3.16
Gill.3s	October	37,116	1.0	1.00	200	216.67	2.63
Gill.4s	October	116,527	1.0	1.00	133	137.00	2.89
Gut.1	June	21,925	1.0	1.00	118	121.00	2.91
Gut.2	June	423,589	1.0	1.00	110	177.50	0.88
Gut.3	June	21,556	1.0	0.99	113	189.00	1.22
Gut.1	August	36,362	1.0	1.00	114	132.33	2.20
Gut.2	August	18,420	1.0	1.00	111	141.88	1.77
Gut.3	August	31,684	1.0	1.00	74	77.33	1.89
Gut.2s	August	38,158	1.0	1.00	99	106.86	1.66
Gut.3s	August	35,691	1.0	1.00	100	107.50	2.90
Gut.1	October	14,786	1.0	1.00	110	178.06	0.87
Gut.2	October	16,370	1.0	0.99	123	293.40	1.93
Gut.3	October	34,017	1.0	1.00	172	175.50	3.43
Gut.4	October	33,213	1.0	0.99	223	341.83	1.59
Gut.1s	October	18,257	1.0	1.00	169	208.08	1.68
Gut.2s	October	36,751	1.0	1.00	175	201.46	1.75
Gut.3s	October	21,317	1.0	1.00	338	369.10	3.23
Gut.4s	October	22,830	1.0	1.00	182	220.25	3.95

Sample	Month	Sequence Total	coverage	coverage*	OTUs*	Chao1*	Shannon*
Shell.1	June	16,905	0.95	0.93	1,404	2613.48	5.44
Shell.2	June	26,321	0.96	0.93	1,420	3010.08	5.33
Shell.3	June	23,526	0.95	0.92	1,559	2927.75	5.54
Shell.1	August	19,752	0.96	0.95	1,046	2120.47	4.75
Shell.2	August	27,395	0.95	0.92	1,695	3342.74	5.64
Shell.3	August	17,045	0.96	0.95	988	2056.48	4.83
Shell.1	October	32,017	0.97	0.95	1,156	1906.68	5.15
Shell.2	October	15,396	0.96	0.95	1,128	2056.46	5.11
Shell.3	October	19,669	0.97	0.96	908	1616.91	4.49
Shell.4	October	17,346	0.97	0.96	938	1932.08	4.40
Sed.1	June	20,569	0.92	0.89	1,990	4233.54	5.90
Sed.2	June	12,625	0.88	0.88	2,208	5430.34	6.02
Sed.3	June	16,239	0.89	0.87	2,427	5307.59	6.23
Sed.1	August	28,191	0.91	0.85	2,718	6496.29	6.52
Sed.2	August	16,826	0.88	0.85	2,588	6397.29	6.37
Sed.3	August	14,400	0.87	0.85	2,598	6329.27	6.42
Sed.1	October	16,567	0.88	0.86	2,500	5711.20	6.26
Sed.2	October	18,235	0.87	0.83	2,819	6870.08	6.46
Sed.3	October	38,252	0.93	0.87	2,395	5709.82	6.20
Water	June	15,236	0.97	0.96	684	1641.95	3.65
Water	August	8,891	0.96	*NA*	*NA*	*NA*	*NA*
Water	October	18,696	0.97	0.96	785	1698.78	4.38

* Based on subsampled sequences (n=11,142)

Table 2. PERMANOVA results showing the effect of microbiome (type) and season (month) on oyster microbiomes. PERMANOVA was conducted using Bray-Curtis resemblance matrices. Significance is indicated in bold ($p<0.05$).

PERMANOVA Type x Month

Source	Degrees of Freedom	Mean Squares	Pseudo-F	Estimate Variation (Sq. root)	p-value
Type	4	23693.0	15.356	10.575	**0.001**
Month	2	3062.4	1.8017	49.218	**0.001**
Type x Month	7	2779.8	1.9848	18.636	**0.001**

Table 3. Permutational pair-wise comparisons between (A) different microbiomes (type) and (B) different seasons (months). Pairwise tests were based on the interaction term type x month using PERMANOVA and Bray-Curtis resemblance matrices**.** Significance is indicated in bold ($p<0.05$).

A

Type	Month	t	Similarity	p-value (MC)
Gill				
	June, August	1.556	32.624	0.061
	June, October	1.747	31.785	**0.011**
	August, October	1.166	38.179	0.230
Gut				
	June, August	1.949	41.877	0.226
	June, October	1.319	31.860	0.107
	August, October	1.444	31.229	**0.046**
Shell				
	June, August	1.9165	32.163	0.056
	June, October	2.8481	27.040	**0.004**
	August, October	1.1813	44.048	0.273
Sediment				
	June, August	1.6054	58.598	0.092
	June, October	1.5913	58.768	0.094
	August, October	1.4898	58.032	0.104

B

Month	Type	t	Similarity	p-value (MC)
June				
	Gill, Gut	2.473	13.947	**0.015**
	Gill, Shell	3.321	9.665	**0.006**
	Gill, Sediment	3.610	5.694	**0.004**
	Gut, Shell	3.352	4.326	**0.011**
	Gut, Sediment	3.473	3.864	**0.010**
	Shell, Sediment	3.915	7.242	**0.004**
August				
	Gill, Gut	2.146	22.226	**0.009**
	Gill, Shell	2.446	5.510	**0.005**
	Gill, Sediment	2.980	4.742	**0.004**
	Gut, Shell	2.710	3.271	**0.004**
	Gut, Sediment	3.312	2.954	**0.001**
	Shell, Sediment	2.762	10.523	**0.014**
October				
	Gill, Gut	2.322	20.810	**0.001**
	Gill, Shell	3.224	8.741	**0.001**
	Gill, Sediment	3.115	7.158	**0.001**
	Gut, Shell	2.908	4.930	**0.001**
	Gut, Sediment	2.739	4.086	**0.001**
	Shell, Sediment	3.715	8.655	**0.003**

Table 4. Dispersion effect on microbiome (type) and season (month). Dispersion effects were determined using the PERMDISP test and are based on Bray-Curtis resemblance matrices**.** Significance is indicated in bold ($p<0.05$).

PERMDISP

Source	Degrees of Freedom	F	p-value
Type	4	21.8690	**0.001**
Month	2	0.026184	0.978

Table 5. Relative abundance of core OTUs in the oyster gill, gut, shell, and reef sediment microbiomes for each season. Errors are ± SE.

Microbiome	June (%)	August (%)	October (%)	Total Average (%)
Gill	45.2 ± 8.7	39.1 ± 6.2	48.9 ± 5.6	45.2 ± 3.7
Gut	84.2 ± 10.8	73.2 ± 4.6	51.7 ± 9.7	64.5 ± 6.2
Shell	53.5 ± 1.0	49.8 ± 2.4	46.1 ± 3.5	49.4 ± 1.6
Sediment	77.1 ± 1.6	71.3 ± 0.7	71.1 ± 1.1	73.2 ± 1.1

Table 6. Relative abundances of the top five most abundant core OTUs in the oyster gill, gut, shell, and reef sediment microbiomes for each season. Errors are ± SE.

Microbiome	OTU	Phylum	Class	Order	Family	Genus	June (%)	August (%)	October (%)	Total Average (%)
Gill	Otu00002	Unclassified	Unclassified	Unclassified	Unclassified	Unclassified	11.1 ± 9.0	25.9 ± 8.7	32.6 ± 5.8	26.5 ± 4.5
	Otu00004	*Proteobacteria*	*Gammaproteobacteria*	*Vibrionales*	*Vibrionaceae*	*Vibrio*	12.9 ± 3.6	4.8 ± 1.9	11.1 ± 2.8	9.5 ± 1.8
	Otu00006	*Proteobacteria*	*Gammaproteobacteria*	*Oceanospirillales*	*Oceanospirillaceae*	*Neptuniibacter*	12.4 ± 4.3	5.3 ± 2.4	2.0 ± 0.8	5.0 ± 1.4
	Otu00012	*Proteobacteria*	*Gammaproteobacteria*	*Alteromonadales*	*Alteromonadaceae*	*Alteromonas*	5.8 ± 1.4	1.8 ± 0.8	1.0 ± 0.4	2.2 ± 0.6
	Otu00015	*Proteobacteria*	*Gammaproteobacteria*	*Alteromonadales*	*Pseudoalteromonadaceae*	*Pseudoalteromonas*	3.0 ± 0.9	1.3 ± 0.3	2.3 ± 0.6	2.1 ± 0.4
Gut	Otu00001	*Tenericutes*	*Mollicutes*	*Mycoplasmatales*	*Mycoplasmataceae*	*Mycoplasma*	61.1 ± 12.1	29.7 ± 7.5	14.9 ± 8.3	28.2 ± 6.6
	Otu00003	*Tenericutes*	*Mollicutes*	*Mycoplasmatales*	*Mycoplasmataceae*	*Mycoplasma*	14.4 ± 4.6	23.7 ± 7.7	18.7 ± 7.2	19.5 ± 4.3
	Otu00004	*Proteobacteria*	*Gammaproteobacteria*	*Vibrionales*	*Vibrionaceae*	*Vibrio*	1.0 ± 0.4	0.9 ± 0.3	10.3 ± 4.3	5.6 ± 2.4
	Otu00005	*Tenericutes*	*Mollicutes*	*Mycoplasmatales*	*Mycoplasmataceae*	*Mycoplasma*	7.4 ± 2.8	18.7 ± 6.6	7.5 ± 4.2	11.0 ± 3.1
	Otu00011	*Proteobacteria*	*Alphaproteobacteria*	*Rhodobacterales*	*Rhodobacteraceae*	Unclassified	0.4 ± 0.3	0.3 ± 0.1	0.3 ± 0.1	0.3 ± 0.1
Shell	Otu00016	*Proteobacteria*	*Alphaproteobacteria*	*Sphingomonadale*	*Erythrobacteraceae*	*Erythrobacter*	4.0 ± 0.8	6.2 ± 0.3	5.6 ± 0.4	5.3 ± 0.4
	Otu00018	*Proteobacteria*	*Alphaproteobacteria*	*Rhodobacterales*	*Rhodobacteraceae*	Unclassified	4.0 ± 0.2	6.1 ± 0.8	2.6 ± 0.1	4.1 ± 0.5
	Otu00024	*Cyanobacteria*	*Cyanobacteria*	SubsectionII	FamilyII	*Pleurocapsa*	0.1 ± 0.0	0.5 ± 0.3	9.7 ± 5.3	4.0 ± 2.5
	Otu00011	*Proteobacteria*	*Alphaproteobacteria*	*Rhodobacterales*	*Rhodobacteraceae*	Unclassified	6.6 ± 1.0	2.9 ± 1.4	2.1 ± 0.7	3.7 ± 0.8
	Otu00026	*Cyanobacteria*	*Cyanobacteria*	SubsectionII	FamilyII	*Pleurocapsa*	2.3 ± 0.7	6.6 ± 3.8	1.4 ± 0.3	3.2 ± 1.3
Sediment	Otu00041	*Proteobacteria*	*Gammaproteobacteria*	Unclassified	Unclassified	Unclassified	1.9 ± 0.2	2.5 ± 0.2	2.4 ± 0.2	2.3 ± 0.1
	Otu00030	*Bacteroidetes*	*Flavobacteriia*	*Flavobacteriales*	*Flavobacteriaceae*	Unclassified	2.1 ± 0.2	1.5 ± 0.1	3.0 ± 0.1	2.2 ± 0.2
	Otu00046	*Proteobacteria*	*Deltaproteobacteria*	*Desulfuromonadal*	*Sva1033*	Unclassified	3.9 ± 0.4	1.0 ± 0.2	1.6 ± 0.1	2.2 ± 0.4
	Otu00028	*Proteobacteria*	*Gammaproteobacteria*	*Cellvibrionales*	*Halieaceae*	*Haliea*	3.5 ± 0.3	0.9 ± 0.2	2.0 ± 0.2	2.1 ± 0.4
	Otu00048	*Proteobacteria*	*Gammaproteobacteria*	*Order_Incertae_S*	*Family_Incertae_Sedis*	*Marinicella*	2.6 ± 0.2	1.7 ± 0.0	1.9 ± 0.1	2.1 ± 0.2

Table 7. Mean relative abundances of core *nosZ* gene comprising the gill, gut, shell, and reef sediment core microbiomes. The *nosZ*.combined gene is the combination of gene clades *nosZ*I and *nosZ*II.

Microbiome	Gene	Relative Abundance (%)
Gill		
	nosZ.combined	2.52
	*nosZ*I	0.00
	*nosZ*II	2.52
Gut		
	nosZ.combined	0.09
	*nosZ*I	0.04
	*nosZ*II	0.05
Shell		
	nosZ.combined	12.60
	*nosZ*I	6.60
	*nosZ*II	6.00
Sediment		
	nosZ.combined	28.70
	*nosZ*I	24.30
	*nosZ*II	4.40

Table 8. Mean relative abundances of nosZ genes in the oyster gill, gut, shell, and reef sediment microbiomes for each season. The "*nos*Z.comb" gene is the combination of gene clades *nos*ZI and *nos*ZII. Errors are ± SE.

Gene	Microbiome	June (%)	August (%)	October (%)	Total (%)
*nos*Z.comb	Gill	7.7 ± 1.4	6.2 ± 2.1	8.7 ± 1.4	7.7 ± 1
	Gut	2.1 ± 1.9	0.8 ± 0.3	3.7 ± 1.3	2.5 ± 0.8
	Shell	15.9 ± 1.3	18.7 ± 0.8	19.8 ± 1.9	18.3 ± 1.0
	Sediment	22.0 ± 1.1	25.7 ± 1.0	21.2 ± 0.5	23.0 ± 0.8
*nos*ZI	Gill	3.0 ± 0.5	4.1 ± 1.4	6.9 ± 1.3	5.3 ± 0.9
	Gut	0.6 ± 0.5	0.5 ± 0.2	2.8 ± 1.2	1.7 ± 0.7
	Shell	6.7 ± 0.2	4.1 ± 0.4	3.3 ± 0.6	4.5 ± 0.5
	Sediment	1.3 ± 0.1	1.1 ± 0.1	1.7 ± 0.2	1.4 ± 0.1
*nos*ZII	Gill	4.7 ± 1.0	2.1 ± 0.1	1.8 ± 0.3	2.4 ± 0.4
	Gut	1.5 ± 1.4	0.4 ± 0.1	0.9 ± 0.4	0.9 ± 0.3
	Shell	9.2 ± 1.1	14.6 ± 0.4	16.5 ± 1.6	13.7 ± 1.2
	Sediment	20.7 ± 1.2	24.6 ± 1.0	19.6 ± 0.3	21.6 ± 0.9

Table 9. Environmental parameters of Lynnhaven surface water for each sampling season.

Sample Date	Temp (°C)	Salinity (ppt)	DO (mg/L)	NO_3^- (μM)	NH_4^+ (μM)	PO_4^{3-} (μM)
June.2014	25.1	18.8	6.3	0.64	3.53	0.10
August.2014	28.0	24.0	6.5	0.66	2.58	0.12
October.2014	19.2	26.0	7.9	1.03	1.68	0.21

Table 10. Actual (D_{14}), potential (D_{15}), and total denitrification (D_{Total}) rates measured in oysters using isotope-pairing technique (IPT) for each sampling season.

Total D is the combined sum of D_{14} and D_{15}.

Treatment	Sample	Month	D_{14}	D_{15}	D_{Total}
				$\mu M\ N_2\text{-}N\ m^{-2}\ hr^{-1}$	
Oyster					
	Oyster.1	June	17.5	166.0	183.5
	Oyster.2	June	40.0	308.1	348.0
	Oyster.3	June	39.7	380.6	420.3
	Oyster.1	August	11.4	80.8	92.2
	Oyster.2	August	14.6	72.7	87.2
	Oyster.3	August	22.5	137.1	159.6
	Oyster.1	October	29.3	90.7	120.0
	Oyster.2	October	41.0	244.3	285.3
	Oyster.3	October	23.4	105.9	129.3
	Oyster.4	October	20.6	126.4	147.0
Scrubbed Oyster					
	Oyster.S2	August	19.4	112.8	132.2
	Oyster.S3	August	14.1	118.3	132.4
	Oyster.S1	October	4.3	16.3	20.7
	Oyster.S2	October	24.7	46.1	70.8
	Oyster.S3	October	10.2	33.3	43.5
	Oyster.S4	October	7.2	17.2	24.4
Shell					
	Shell.1	June	7.7	45.2	52.8
	Shell.2	June	10.1	84.8	94.9
	Shell.1	August	5.3	31.2	36.5
	Shell.2	August	5.4	19.2	24.6
	Shell.3	August	3.8	18.3	22.1
	Shell.1	October	6.0	16.6	22.6
	Shell.2	October	5.4	6.1	11.5
	Shell.3	October	5.0	18.7	23.7
	Shell.4	October	6.8	22.1	28.9
Sediment					
	Sediment.1	June	2.7	41.3	44.1
	Sediment.1	August	3.8	23.8	27.6
	Sediment.2	August	9.0	112.7	121.8
	Sediment.3	August	4.5	26.0	30.5
	Sediment.1	October	3.9	34.3	38.1
	Sediment.2	October	4.2	27.1	31.4
	Sediment.3	October	3.8	30.3	34.1

Table 11. Spearman rank correlation results between relative abundances of *nosZ* genes and total denitrification (D_{Total}) rates. The total denitrification rate is the sum of actual (D_{14}) and potential denitrification (D_{15}) rates. The *nos*Z.combined gene is the combination of gene clades *nos*ZI and *nos*ZII. Significance is indicated in bold ($p<0.05$).

			D_{Total}	
Treatment	n	Gene	ρ	p-value
Scrubbed Oyster	5			
		Total.*nos*Z	0.09	0.87
		*nos*ZI	-0.03	0.96
		*nos*ZII	0.71	0.11
Shell	9			
		Total.*nos*Z	-0.23	0.55
		*nos*ZI	0.40	0.28
		*nos*ZII	-0.72	**0.03**
Sediment	7			
		Total.*nos*Z	0.11	0.82
		*nos*ZI	0.40	0.38
		*nos*ZII	-0.07	0.88

FIGURES

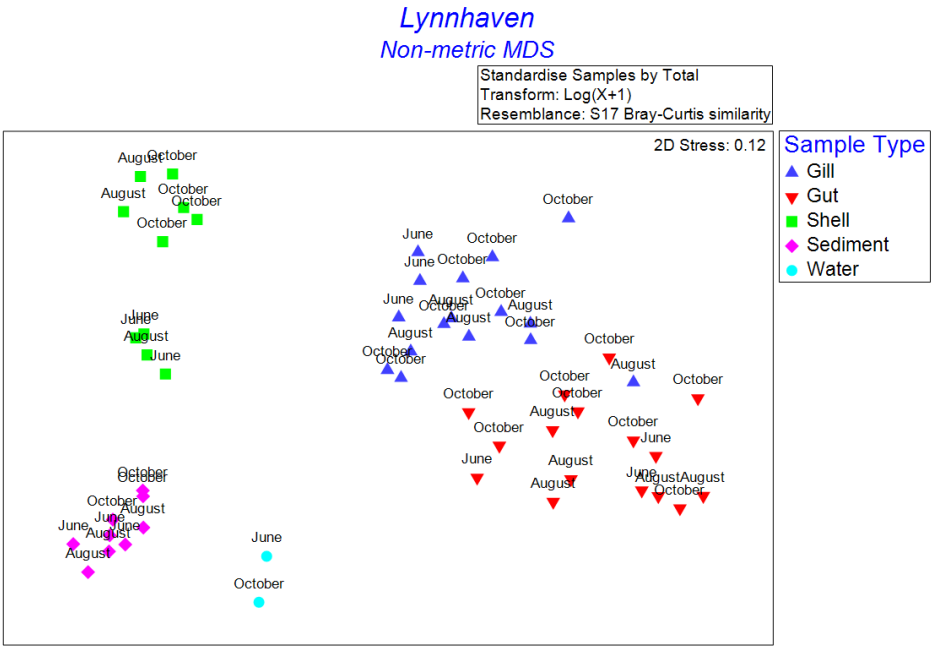

Figure 1. Non-metric multidimensional scaling (nMDS) plot based on Bray-Curtis dissimilarity matrices depicting β-diversity between microbiomes and season.

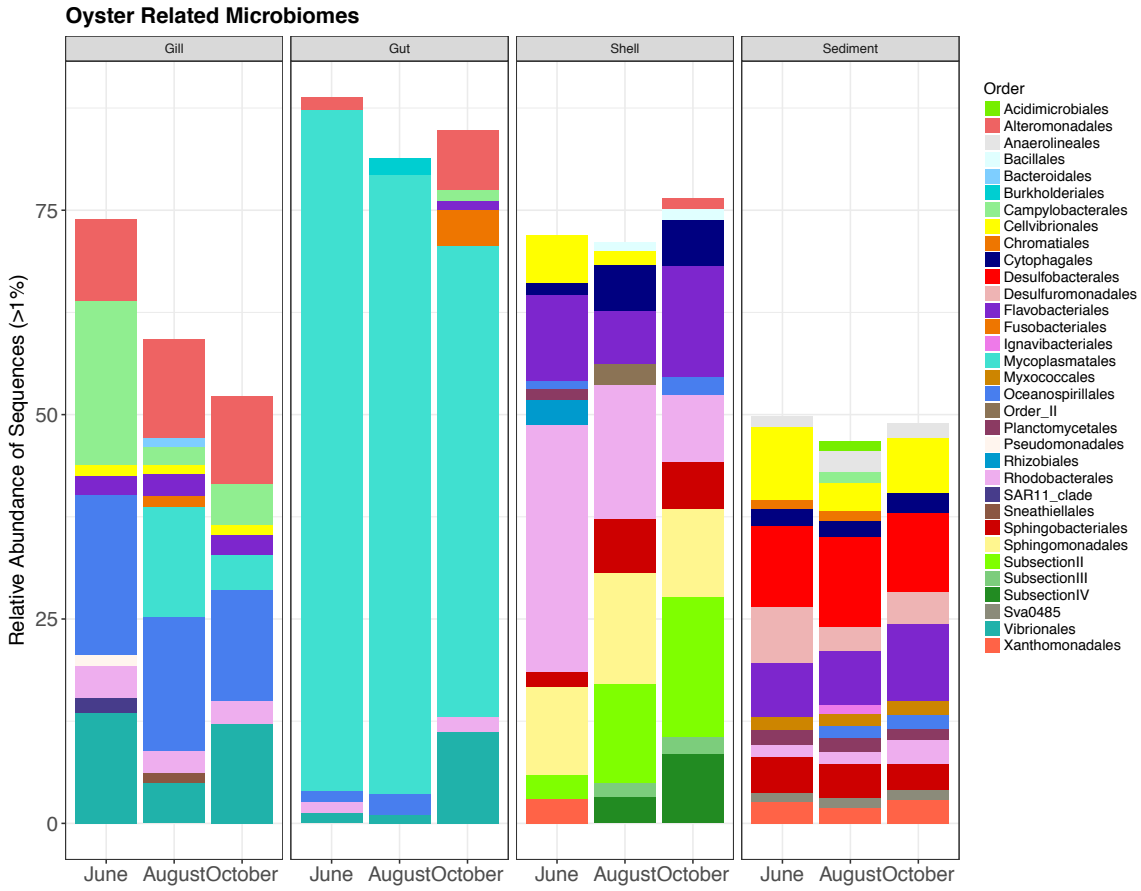

Figure 2. Average relative abundance of bacterial orders found in the oyster gill, gut, shell, and reef sediment microbiomes grouped by month.

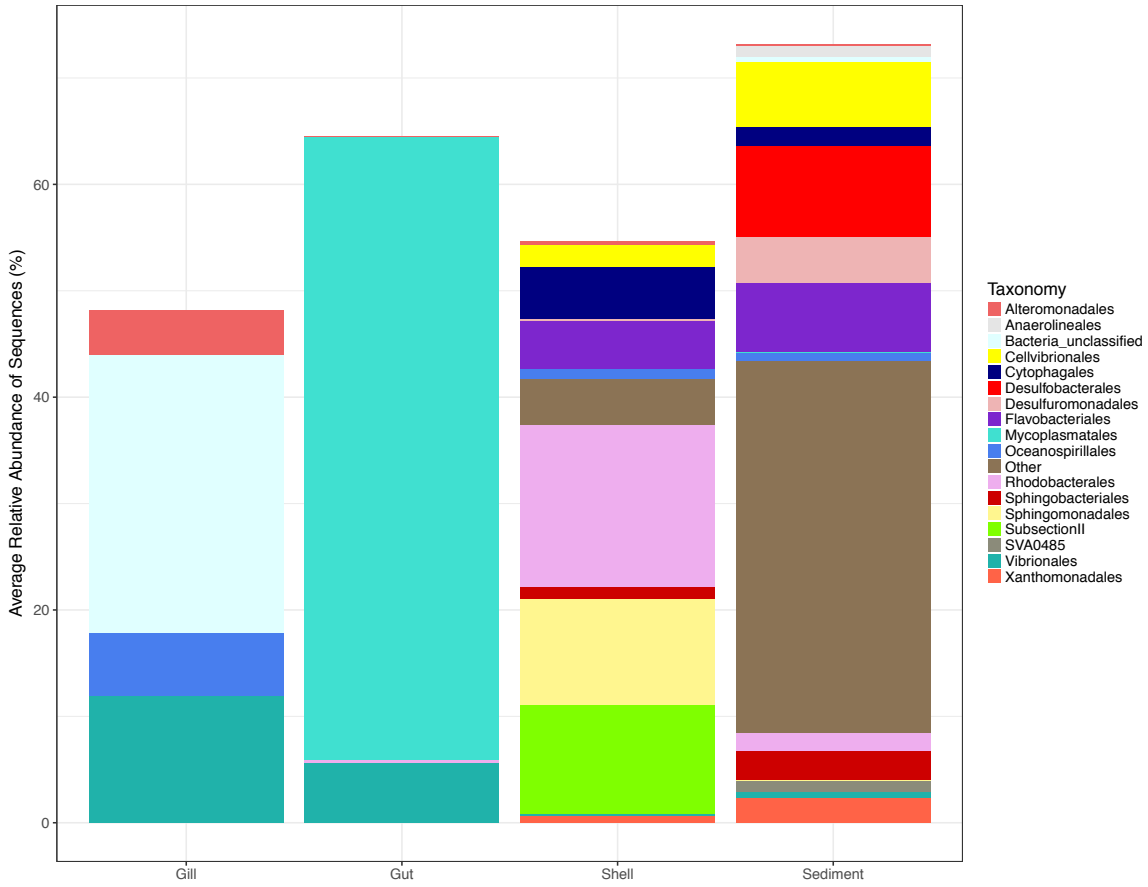

Figure 3. Average relative abundance of bacterial orders found in the core microbiomes of the oyster gill, gut, shell, and reef sediment.

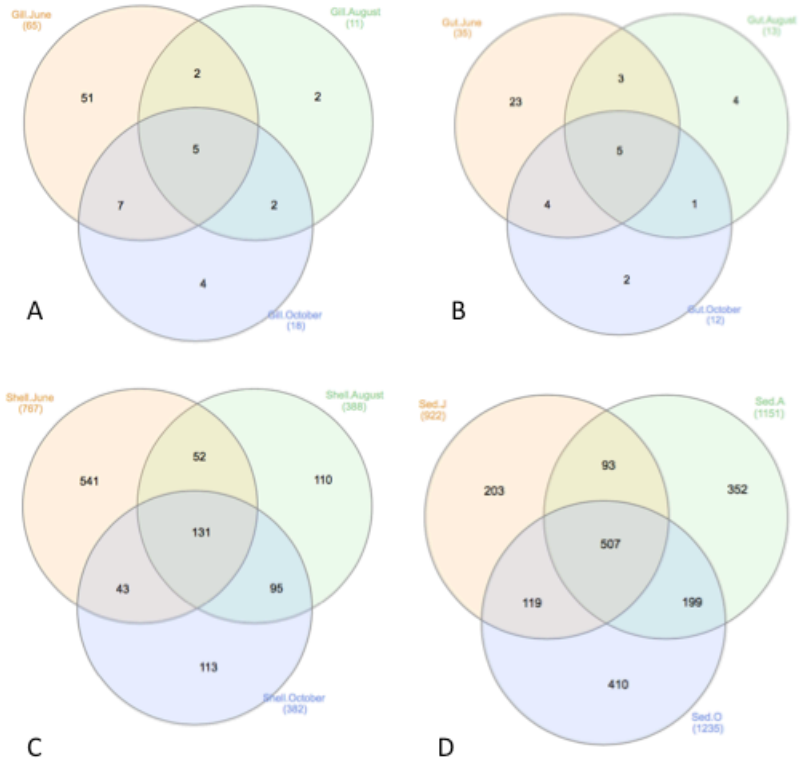

Figure 4. Venn diagrams showing the number of shared OTUs for each month among the oyster gill (A), gut (B), shell (C), and reef sediment (D) microbiomes. The center of the venn diagram indicates the number of core OTUs.

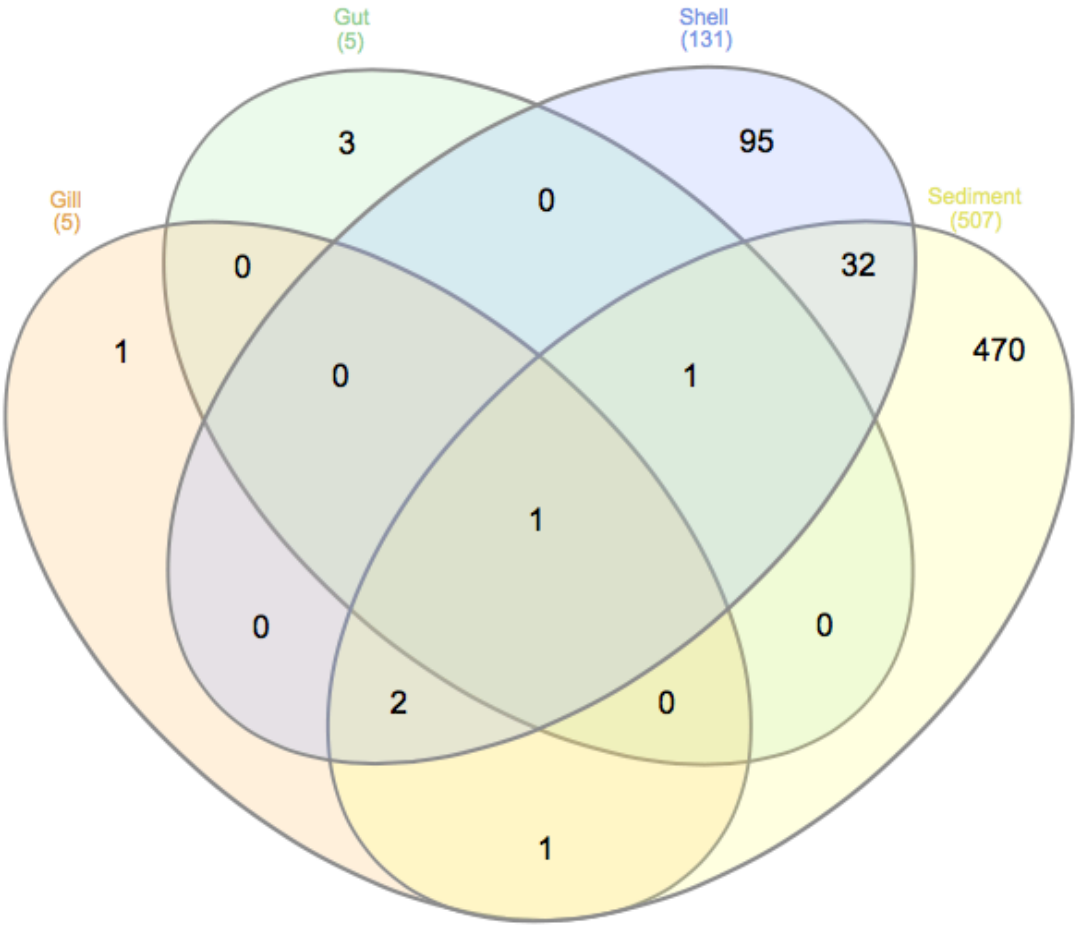

Figure 5. Venn diagram showing the shared OTUs among the oyster gill, gut, shell and reef sediment microbiomes.

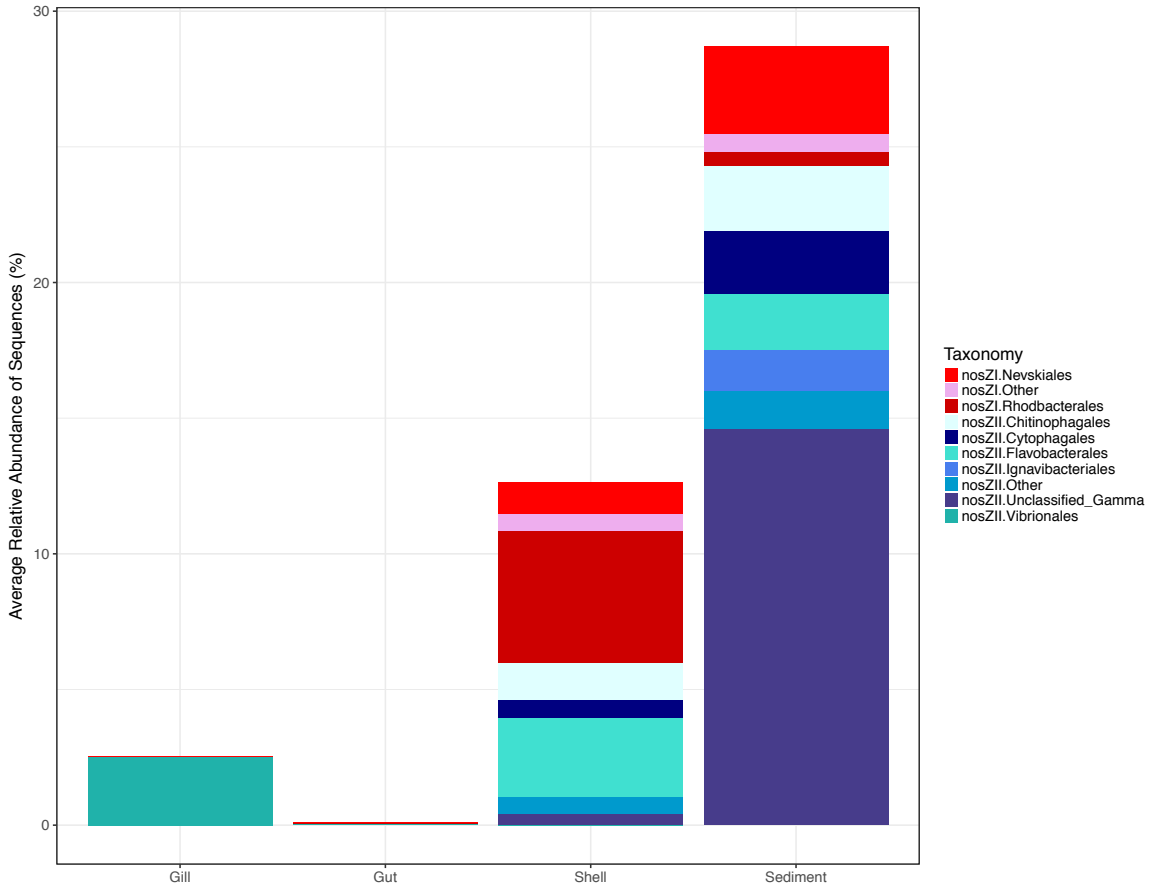

Figure 6. Average relative abundance and taxonomic classification of bacteria carrying *nos*ZI and *nos*ZII genes in the oyster core gill, gut, shell, and reef sediment microbiomes.

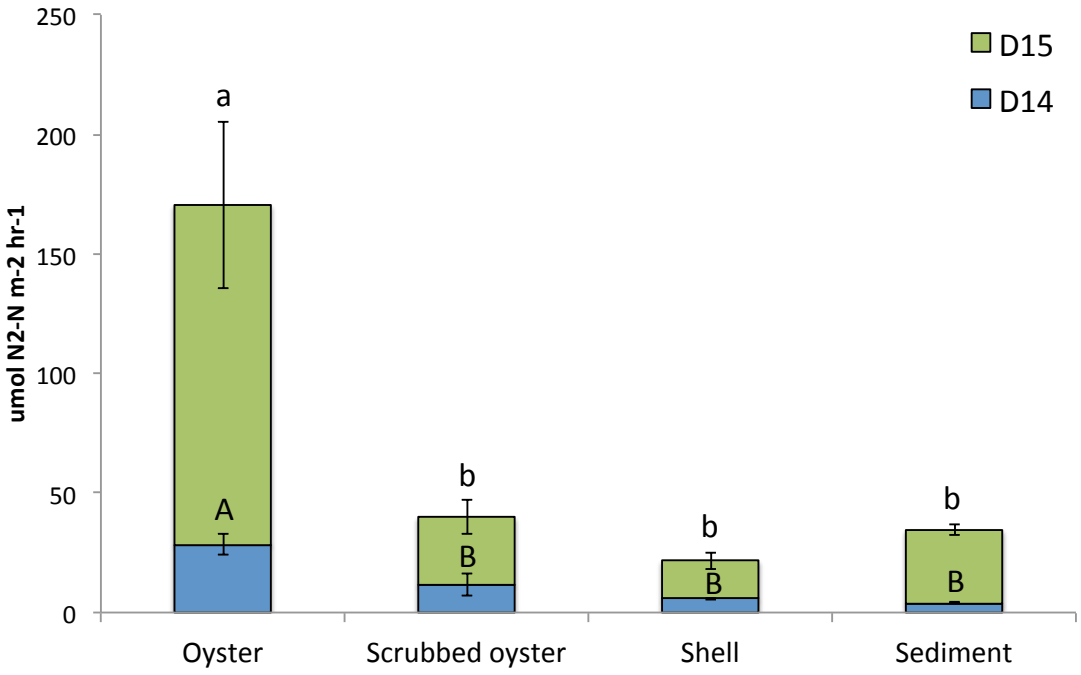

Figure 7. Average actual (D_{14}) and potential (D_{15}) denitrification rates of oyster, scrubbed oyster, shell, and reef sediment for October. Scrubbed oysters are live oysters with their shell biofilms removed. Error bars represent ± SE. Significance is denoted in upper case letters for actual denitrification rates (D_{14}) and in lower case letters for potential denitrification rates (D_{15}) ($p<0.05$).

Chapter 4

Composition and diversity of the eastern oyster (*Crassostrea virginica*) microbiome and associated denitrifiers in response to spatial and temporal changes in the Chesapeake Bay, Virginia

ABSTRACT

Environmental changes to a host microbiome may be linked to reduced health and function and may contribute to disease progression. In oysters, changes to microbiomes may also have an impact on the ecological process of denitrification, the reduction of bioavailable nitrate or nitrite to nitrogen gas. Understanding these dynamics in microbiomes is important for predicting and assessing the denitrification potential of oysters in a fluctuating environment. To assess the effects of different environmental conditions on oyster microbiomes, we deployed cages of oysters to three different subtidal locations in the Elizabeth and Lafayette Rivers and sampled the oysters three times over a time period of three months (T_0, T_1, and T_2). Prior to deployment, oyster shell biofilms were removed and oysters were held in tanks filled with filtered seawater for two weeks (T_0). Both total and active microbiomes were analyzed using 16S rRNA genes and transcripts with a metabolic inference approach to identify changes to the deployed oyster gill, gut, and shell microbiomes and associated denitrifiers, defined in this study as bacteria carrying the *nosZ* gene. Furthermore, native oysters at each of the sites for each sampling time point (T_1 and T_2) were similarly analyzed. Significant changes were detected to all three oyster microbiomes, with greater variation in the gut microbiome due to spatial effects, while temporal effects had a greater effect on the gill and shell microbiomes. In each of the microbiomes, a distinct set of resident, core microbes (core microbiome) making up between 35-60% of the total (16S rDNA) and 14-48% of the active (16S rRNA) microbiomes was determined despite spatial and temporal changes, suggesting an importance of the core in oyster health or function. Of these core microbiomes, denitrifiers in the shell core microbiome made up the highest percent of the

total and active core (20.5 and 25.1%, respectively), suggesting an important, conserved role of the shell in oyster potential denitrification. Furthermore, denitrifiers in the whole shell total and active microbiomes were relatively constant in response to site, oyster type, and time point indicating stability and rapid recovery of the shell denitrifiers following shell biofilm removal. In comparison, gut and gill denitrifiers of both the deployed and native oysters were much more variable in relative abundances with respect to their total and active microbiomes, showing some evidence of abundance tied to site. This, coupled with the lower abundance of denitrifiers in the core microbiomes, suggests that denitrifiers in the gill may be more transient in nature and may be connected with ingestion of denitrifiers associated with food particles. Assessing the changes to the oyster microbiomes in response to different environmental conditions offer valuable insight into the dynamics and complexity of the oyster microbiomes and provides a greater understanding of the effects of spatial and temporal effects on potential denitrification in oyster microbiomes.

INTRODUCTION

The composition and activity of animal-associated microbiomes play a key role in maintaining host health including digestion, nutrition, and host immunity (Harris 1993, Erasmus et al. 1997, Austin 2006) and may also mediate important biogeochemical processes in the environment such as nitrogen cycling (Weigel and Erwin 2017). Disruptions to an organism's microbiome are linked to disease (McFall-Ngai et al. 2013), reduced lifespan (Brummel et al. 2004, Rawls et al. 2004), and higher mortality (Sison-Mangus et al. 2015). Similarly, disturbance to a microbiome may alter its ecological function in the environment (Allison and Martiny 2008, Blaser et al. 2016). Most microbiomes are sensitive to environmental changes (Shade et al. 2012) and highly reactive due to short generation times and high diversity (Needham et al. 2013, Hunt and Ward 2015). To understand the effects of environmental changes on a microbiome and its function, the underlying stability and dynamics of the community must be assessed (Shade et al. 2012, Hunt and Ward 2015).

Relocation of oysters to new environments creates substantially different living conditions for the host and its associated microbiome. Transplanting of oysters to different cultivation sites is a common practice in the aquaculture industry to increase yields (Leard et al. 1999, Powell 2004, Muehlbauer et al. 2014). Unlike many host organisms, the filter-feeding lifestyle of the oyster allows for continual exposure of internal tissues to bacteria in the surrounding seawater (Prieur et al. 1990) intimately linking the oyster microbiome to the dynamic external environment. In marine sedentary aquatic animals site has been demonstrated to have an important influence on microbiome composition (Burgsdorf et al. 2014, Luter et al. 2015), however very little is

known as to the stability or response of the oyster microbiomes to different environmental conditions or its effect on microbiome function. Recent translocation studies of oysters have demonstrated a strong connection between the environment and the oyster hemolymph immediate response to translocation as well as the presence of a relatively stable hemolymph microbiome among the dominant taxa (Lokmer et al. 2016a, Lokmer et al. 2016b). Compared to the hemolymph, oyster gill microbiomes have shown a greater persistence of microbiota after translocation suggesting microbiome stability (Lokmer et al. 2016b). Site has also been shown to influence the gut microbiome composition among post-larvae and adult *Crassostrea gigas* and *Crassostrea corteziensis* oysters at different grow-out sites (Trabal et al. 2012, Trabal Fernández et al. 2014) but season was shown to have a greater effect on the oyster gut and pallial microbiomes of adult oysters (Pierce et al. 2016). In both studies, however, some microbiota persisted despite location differences, hinting at the presence of a core microbiome. While these studies provide a foundation for investigating oyster microbiomes and response to changing environmental conditions, the high amount of variability and complexity in the oyster microbiomes in relation to a variety of factors including species and genetic differences (Zurel et al. 2011, Trabal et al. 2012, Wegner et al. 2013, Trabal Fernández et al. 2014), tissue type (King et al. 2012, Arfken et al. 2017), season (Pierce et al. 2016), development stage (Asmani et al. 2016), and health (Green and Barnes 2010) require much greater exploration to disentangle the complex dynamics of the oyster microbiome. Furthermore, there is a gap in knowledge regarding the activity of the oyster microbiome as well as links between the oyster microbiome and function in the environment.

Enhanced removal of biologically available nitrogen from the water column through oyster-facilitated denitrification (Beck et al. 2011) may be affected by disturbance to the oyster microbiomes. Denitrification is the microbially-mediated step-wise reduction of NO_3^- or NO_2^- to gaseous nitric oxide (NO), nitrous oxide (N_2O) and dinitrogen (N_2) (Zumft 1997). Several studies demonstrated enhanced denitrification rates by oysters and oyster reefs (Piehler and Smyth 2011, Hoellein et al. 2015, Caffrey et al. 2016, Humphries et al. 2016, Arfken et al. 2017). In the Chesapeake Bay, effort is being made to restore *Crassostrea virginica* and *C. virginica* reefs from historical losses in order to recover ecosystem services such as denitrification provided by oysters (Luckenbach et al. 1999, Brumbaugh and Coen 2009, Ermgassen et al. 2013). One method of reef restoration involves the transplantation of adult eastern oysters (*Crassostrea virginica*) to various sites within the Bay to enhance reef development and increase settlement of oyster larvae (Fit and Coon 1992, Turner et al. 1994, Kennedy and Sanford 1999, Brumbaugh et al. 2000). However, it is unknown how environmental changes or dynamic shifts in the oyster microbiomes may affect denitrification. While studies on the functional composition of oyster microbiomes are rare, in Arfken et al. (2017) denitrifiers were found to vary by oyster tissues. However, no investigation into the effect of environmental changes on the microbiome was investigated, limiting the scope and predictive possibilities of these findings.

Assessing the variability among oyster microbiomes and identifying the stable, resident core shared by oysters in response to environmental changes will provide greater insights into the physiology and functionality of oyster microbiomes and their role in denitrification. In this study, we aim to (1) evaluate the variability and stability of the

oyster gill, gut, and shell total microbiomes in response to different environmental conditions (2) identify the activity and composition of the core members and core denitrifiers of the microbiomes, and (3) assess the spatial and temporal composition and activity changes to the denitrifiers in the microbiomes. To investigate the activity and composition of the microbiomes, we utilized 16S rRNA gene transcripts (active) in conjunction with 16S rDNA (total). Denitrifiers were identified from 16S rRNA/rDNA sequences with the metabolic inference bioinformatic program paprica, using a phylogenetic placement method to infer the presence of the nitrous oxide reductase (*nos*Z) gene. The *nos*Z gene reduces N_2O to N_2 and was further categorized by clades I and II (*nos*ZI and *nos*ZII, respectively) based on protein physiology (Sanford et al. 2012, Jones et al. 2013). While the *nos*Z gene is characteristic of complete denitrifiers, some non-denitrifying bacteria may also carry *nos*Z. However the reduction and removal of the greenhouse gas N_2O to N_2 is an ecologically important step, and we therefore consider all bacteria carrying *nos*Z "denitrifiers" for the purposes of this study. We expect that translocation will have a significant effect on the oyster microbiomes and denitrifiers, but the microbiomes will retain a resident, core microbiome through the course of the experiment. We also hypothesize that translocated oyster microbiomes will more closely resemble native oyster microbiomes at the final time point than at the initial time point, representing adaptation. Furthermore, we predict that denitrifiers will vary in activity and abundance based on where the oysters are translocated to, and that denitrifiers will be present in the oyster core microbiomes. This is the first study of its kind to examine the effects of environmental changes on the activity and composition of denitrifiers in the oyster gill, gut, and shell microbiomes.

MATERIALS AND METHODS

Site Descriptions

The 10 km long Lafayette River forms the northernmost branch of the Elizabeth River tidal estuary. Each deployment site within the river system was selected based on average nutrient concentrations, the surrounding environment, and proximity to a natural oyster reef. The Lafayette Downstream site (N 36.9083333 W -76.31463889) was located near the mouth of the Lafayette River closest to the main branch of the Elizabeth River. This site was selected based on its relatively low average nutrient concentrations compared to the other three sites (Table 1). The Lafayette Midstream site (N 36.88936111 W -76.28144444) was located in the midstream portion of the Lafayette River and had the highest average nutrient concentrations and fecal coliform counts of all three sites, likely related to septic tank leakage and storm water runoff from the surrounding residential developments along the river. The Elizabeth site (N 36.86558333 W -76.32897222) was located along a highly industrial and commercial section of the main branch of the Elizabeth River next to several ship building docks and an active marina. Average nutrient concentrations at this site were intermediate to the low nutrient concentrations at the Lafayette Downstream and the high nutrient concentrations at the Lafayette Midstream sites.

Deployment

125 3-year-old adult oysters from the same genetic lineage with an average approximate shell size of 13 cm L x 7 cm W were collected from an aquaculture site on the Lynnhaven River in May 2015 and transported in mesh oyster bags to the

Aquaculture Genetics and Breeding Technology Center(ABC) located at the Virginia Institute of Marine Science. Upon arrival at the facility, oyster shell surfaces were carefully scrubbed with a 0.2% bleach solution to remove algae and biofilm material and then rinsed with filtered seawater. After scrubbing the exterior shells, the oysters were placed in baskets located in large tubs filled with filtered and aerated seawater. Oysters were fed a commercially prepared algal paste daily and water changes with filtered seawater were conducted every other day for a period of 2 weeks. After two weeks, randomly selected (n=5; T_0) oysters were collected for tissue dissection. The remaining oysters were divided into three groups and placed into one of three 2'x3', 1"x 16" wire mesh single stack bottom cages (n=30/cage). Cages filled with oysters were then deployed subtidally at one of three natural reef sites: (1) Lafayette Downstream (2) Lafayette Midstream and (3) Elizabeth. Cages containing deployed oysters were sampled at two time points roughly one month apart: (1) T_1 = late June 2015 and (2) T_2= early August 2015. For each sampling event randomly selected deployed caged oysters (n=5), native reef oysters (n=5), and a 1-L water sample (n=1) were collected from each site. Water parameters including temperature, salinity, pH, turbidity, chlorophyll *a* (Chl*a*) and dissolved oxygen (DO) were also measured at each sampling site using a Yellow Springs Instrument water quality sonde (YSI, Inc.). Following collection, oysters were immediately transferred from site locations in buckets to the Virginia Institute of Marine Science. Oysters designated for dissections were stored overnight in a 5°C refrigerator.

Dissections and Sample Preparations

Seawater collected at each sampling site in the field was filtered immediately upon returning to VIMS. Approximately 300 mL of site water was filtered through a 0.22 μm pore size Millipore Sterivex filter. Collected oysters stored overnight at 5°C were retrieved the following morning and prepped for dissections. Oysters were carefully shucked with sterilized oyster knives and internal organs were lightly rinsed with DI water prior to dissections. Dissections were performed using sterile scalpel blades. A small 2-5 mm crosswise section of posterior tissue containing the intestinal tract (hereafter referred to as 'gut') was excised from the oyster gut, carefully avoiding the digestive gland, stomach, and style sac and transferred to a 2.0 mL microcentrifuge tube. A 5-10 mm section of gill tissue excluding the mantle was also excised from the oyster with a sterile scalpel blade and placed in a 2.0 mL microcentrifuge tube. After removing the internal organs, the interior of the shell was scrubbed with a 70% ethanol solution to remove any remaining oyster tissue and bacteria. Each pair of oyster shells was then crushed into roughly 0.5-5.0 mm sized pieces using sterilized hammers and transferred to a 50 mL falcon tubes. Water filters and oyster tissue samples were stored at -80°C until processing.

RNA/DNA extraction and amplification

Combined RNA and DNA extractions for both oyster gill (0.25-0.30 g) and gut tissues (0.05-0.2 g) were carried out using the MoBio Power Microbiome RNA Isolation kit (Qiagen, Hilden, Germany) following the manufacturer's protocol for simultaneous DNA and RNA extractions. RNA extractions for oyster shell (0.4-0.5 g) were performed using the MoBio PowerSoil Total RNA Isolation Kit (Qiagen, Hilden, Germany),

followed by DNA extractions using the MoBio PowerSoil DNA Elution Accessory Kit (Qiagen, Hilden, Germany) following the manufacturer's protocols. RNA and DNA extractions for water filter samples were conducted with the AllPrep Bacterial DNA/RNA Mini Kit (Qiagen, Hilden, Germany) using the manufacturer's protocol with the following modifications to the initial step: (1) 600 μL of RLT buffer was added to the Sterivex filter, vortexed for 2 minutes, sonicated for 15 min in ice bath, and placed in a rotating oven at 65°C for 30 min (2) after 30 min, the solution was removed from the filter and placed in a 2 mL collection tube (3) 14 μL of β-Mercaptoethanol was added to the sample and (4) two more rinses of 600 μL and 200 μL RLT buffer followed by vortexing and oven incubation described above were performed on the filter and combined with the original sample. Different extraction kits were used with different sample sources to optimize RNA and DNA yields. All RNA samples were cleaned with the TURBO DNA-free Kit (Thermo Fisher Scientific, Waltham, MA) to remove DNA contamination following the manufacturer's protocol. RNA samples were checked for residual DNA by conducting PCR with 1 μL RNA template, 0.5 μM each of primers 341F and 685R targeting the hypervariable V3 region of the 16S rRNA gene, and 2X GoTaq Master mix (Promega Corporation, Madison, WI). PCR thermal cycling conditions consisted of an initial denaturation step at 94°C for 3 min, followed by 30 cycles of 94°C for 1 min, 54°C for 1 min, 68°C for 2 min, and elongation step of 68°C for 10 min. For each clean RNA sample, cDNA libraries were constructed using iScript cDNA Synthesis kit (Bio-Rad, Hercules, CA) following the manufacturer's protocol. Initial amplification of targeted hypervariable V4 region of the 16S rRNA gene (rDNA) and transcripts (rRNA) was conducted on DNA and cDNA samples, respectively, using

forward primer 515F and modified, barcoded reverse primer 806R (Caporaso et al. 2010), adapted for use with the Ion Torrent S5. The basic manufacturer's PCR protocol was used with Taq DNA Polymerase (Invitrogen, Carlsbad, CA) to create a PCR master mix with the following modification: 1 mM dNTP mixture was used in place of 10 mM for a final concentration of 0.02 mM dNTP. Thermal cycling conditions were identical to the PCR used to detect DNA contamination in RNA samples. The amplified products were gene cleaned using the UltraClean GelSpin DNA Purification Kit (Mo-Bio Bio Laboratories, Inc., Carlsbad, CA). The resulting amplicon libraries were then used as templates with the Ion S5 platform following the manufacture's instruction (Thermo Fisher Scientific, Waltham, MA).

Sequence processing and OTU assignment

Removal of barcodes and primers from raw sequences and trimming of sequence length were conducted using the Ribosomal Database Project (RDP) pipeline initial process (Cole et al. 2014; http://rdp.cme.msu.edu) with a minimum quality score of 20, minimum length of 200 bases, and a maximum length of 500. Due to processing limitations of the software, sequences were then divided into separate rRNA gene (n=4) and transcript (n=4) libraries based on the microbiome categories of (1) gill, (2) gut, (3) shell, and (4) water. For each library, mothur v1.35.1 (Schloss et al. 2009) was used to further trim sequences against the SILVA v123 (Yilmaz et al. 2014) alignment template, precluster (diffs=2), and screen for chimeric sequences using the chimera.vsearch command (Rognes et al. 2016). Unknown taxon, mitochondria, chloroplast, archaea, and eukaryotic sequences were removed from analysis using SILVA v123 reference

taxonomy and the Wang classification method (Wang et al. 2007) with an 80% minimum identity. Sequences were clustered into operational taxonomic units (OTUs) based on a 97% identity using the vsearch abundance-based greedy clustering (AGC) algorithm in Mothur.

Oyster-related microbiome and core microbiome

Mean relative abundances of OTUs were used to conduct taxonomic classifications of 16S rDNA and rRNA sequences. Oyster microbiome sequences from Lafayette Midstream at T_1 were excluded from further analysis due to the partial burial of the deployed oyster cage in site sediment and suffocation of several of the oysters at that site and time point. Taxonomic classifications were assigned using the SILVA v123 database. For the core microbiome analyses, OTUs obtained from Mothur were analyzed using InteractiveVenn (Heberle et al. 2015) and the R packages Phyloseq (McMurdie and Holmes 2013) and VennDiagram (Chen and Boutros 2011). Sequences prior to subsampling were used to prevent reduction in coverage of samples. Core microbiomes were defined as the collection of OTUs present in 80% of the replicate oyster samples (n=5) for each site, time point, and oyster type. Classifications among sites and time points are based on 16S rDNA sequences, while the overall taxonomic comparisons among the different microbiomes and core microbiomes include both 16S rDNA (total microbiome) and rRNA (active microbiome). As a result of the limited number of samples (n=1 per month per site), water samples were only included in the overall taxonomic comparison of the different microbiomes.

Metabolic potential and gene inference

Gene inference analyses to assess denitrification potential of the oyster gill, gut, and shell microbiomes were performed with bacterial 16S rDNA and rRNA sequences using the bioinformatic program paprica (Bowman and Ducklow 2015) and a customized gene database described in Arfken et al. (2017). Briefly, each 16S rDNA and rRNA microbiome sequencing library (n=65) was analyzed separately for the presence of the genes encoding nitrous oxide reductase (*nos*ZI and *nos*ZII) based on phylogenetic placement with 16S rDNA sequences extracted from complete and draft genomes downloaded from the National Center for Biotechnology Information (NCBI) repository. Core denitrifiers were determined from each core microbiome using the paprica database with sequences associated with core OTUs identified in Mothur.

Statistical analyses

To capture all changes to the microbiome structure and composition, 16S rDNA sequences were used for diversity and spatial/temporal taxonomic comparisons among the microbiomes. 16S rRNA sequences were used to identify overall activity of the oyster microbiomes, core microbiomes, and predicted *nos*Z gene relative abundances. Metrics measuring the alpha diversity of the total microbiomes including coverage, OTU numbers, Chao1 richness, and Shannon diversity were conducted with subsampled 16S rDNA sequences (n=8,075) in Mothur using the summary.single command. Significant differences among the various metrics were determined using ANOVAs. Correlations between richness and diversity of total microbiomes were performed using Spearman Rank tests. Non-metric dimensional multidimensional scaling (nMDS) performed on

Bray-Curtis resemblance matrices with 4^{th}-root transformed OTU counts from 16S rDNA sequences were used to visualize the total microbiome data. PRIMER's PERMANOVA and PERMDISP tests were used to analyze for significant effects of factors and dispersion on the resemblance matrices for each microbiome. Models used for the PERMANOVA included site x time point for comparisons between deployed oysters at time points T_1 and T_2 at the Elizabeth and Lafayette Downstream sites and site x type comparisons between deployed and native oysters at each site for time point T_2. Due to a cage failure at the Lafayette Midstream site for T1, the Lafayette Midstream site was excluded from the site x time model. Likewise, only time point T_2 was examined in the site x type model to allow for comparisons among all sites. Individual pairwise comparisons of the total microbiomes were conducted between time points T_0, T_1, and T_2 for sites Elizabeth and Lafayette Downstream, and between all sites at T_2 using the pairwise test function in PRIMER (Clarke et al. 2014). Pairwise comparisons were not corrected for multiple testing. One-tailed paired t-tests were used to determine significance between the relative abundances of *nos*ZI and *nos*ZII in each of the oyster microbiomes. The coefficient of variation calculated as the standard deviation relative to the mean was used to compare variation among the different microbiomes. Unless otherwise stated, all tests are based on a significance of $p < 0.05$ and error bars represent ± standard error.

RESULTS

Site water parameters

Surface temperatures showed a steady increase from T_0 (June; 23.5 ± 0.51°C) to T_2 (August; 29.9 ± 0.74°C), with a slight variation between sites for each sampling time point (Table 2). Average salinity was highest during T_2 (20.7 ± 0.69 ppt) and lowest during T_1 (July; 17.3 ± 1.09 ppt). Among the sites, Lafayette Midstream had the lowest average salinity (17.2 ± 1.22 ppt) and Elizabeth had the highest (20.6 ± 0.93). The highest overall measurement of Chl*a* (52.1 mg/mL) was taken at T_2 from the Lafayette Midstream site, followed by Lafayette Downstream at T_1 with a Chl*a* measurement of 27. Both high Chl*a* concentrations at each site corresponded with relatively high levels of DO for T_1 at Lafayette Downstream (11.6 mg/L) and T_2 at Lafayette Midstream (10.4 mg/L).

Sequencing results of 16S rDNA and rRNA

A total of 7,841,652 and 7,459,356 clean and trimmed bacterial 16S rDNA and rRNA sequences, respectively, were obtained from oyster gill, gut, shell, and water microbiome libraries. With the exception of the water microbiome, which contained 6 samples (n=1 replicate x 3 sites x 2 time points) each library consisted of 65 samples (n=5 replicates x 2 time points x 3 sites + initial T_0). Average numbers of sequences for each library ranged from 26,821 ± 4,633 in the shell 16S rRNA microbiome to 68,815 ± 6,224 in the water 16S rDNA microbiome (Table 3). Coverage of sequences for all libraries was greater than 93.4 ± 03%, with the lowest coverage found in the shell 16S rDNA microbiome.

Richness and diversity of total microbiomes based on 16S rDNA sequences

Using subsampled 16S rDNA sequences (n=8,075), the oyster gut total microbiome had the lowest number of OTUs (273 ± 21), Chao richness index (447.19 ± 37.15), and Shannon diversity index (2.53 ± 0.10). Both water and gill total microbiomes were similar in regard to Chao richness index (water: 1219.06 ± 91.10, gill: 1196.34 ± 112.49). However, the gill total microbiome had a greater number of OTUs (715 ± 46) and a higher Shannon diversity index (3.83 ± 0.13) than the water total microbiome (OTUs: 471 ± 30, Shannon: 3.36 ± 0.09). The shell total microbiome had a significantly higher number of OTUs (1538 ± 40) (ANOVA: $F_{3,185} = 205.45$, $p = 1.1 \times 10^{-16}$; Tukey's HSD: $p < 0.01$), Chao richness index (3869.34 ± 130.35) (ANOVA: $F_{3,185} = 215.26$, $p = 1.1 \times 10^{-16}$; Tukey's HSD: $p < 0.01$), and Shannon diversity index (5.56 ± 0.07) (ANOVA: $F_{3,185} = 113.39$, $p = 1.1 \times 10^{-16}$; Tukey's HSD: $p < 0.01$) than the gut, gill, and water total microbiomes. Correlations between richness and diversity were significant, with the highest correlations found in the shell total microbiome ($\rho = 0.79$, $p=2 \times 10^{-16}$), followed by the gill ($\rho = 0.44$, $p=0.0005$), and least in the gut total microbiome ($\rho = 0.26$, $p =0.048$).

Among the deployed oysters at different locations and time points, the Lafayette Downstream site showed a general trend of high diversity of total microbiomes compared to other locations (Table 4). The Lafayette Downstream site had significantly higher diversity in the deployed gill total microbiome than the Elizabeth site (ANOVA: $F_{2,29} = 3.55$, $p = 0.046$; Tukey's HSD $p<0.05$) and a significantly higher diversity in the deployed shell total microbiome than the Lafayette Midstream site (ANOVA: $F_{2,29} = 11.04$, $p=0.0003$; Tukey's HSD: $p<0.01$). The general trend of high diversity at the

Lafayette Downstream site was also consistent in the native oysters at each location, with exception of the gut total microbiome, which showed higher diversity in the native oysters at the Elizabeth site. Overall richness in the deployed oysters was significantly higher at the Lafayette Downstream site than the Elizabeth site for the gill microbiome (ANOVA: $F_{2,29} = 4.48$, $p=0.02$; Tukey's HSD: $p<0.05$), and higher but not significant for the gut total microbiome. The richness of the shell total microbiome varied among the sites and time points with no distinct trend.

Structure and Variability of total microbiomes based on 16S rDNA sequences

In each total microbiome, there was a clear separation of the initial T_0 oysters from the other time points. A shift in microbiome structures was also observed between T_1 and T_2 deployed oysters at the Elizabeth and Lafayette Downstream site. Both site and time were found to have a significant effect on the total microbiomes, with site explaining a greater portion of the variation than time in the gill and shell total microbiomes (Table 5A) while time having a greater effect on variation than site in the gut total microbiome. Pairwise tests incorporating time point T_0 among the deployed oyster total microbiomes from the Elizabeth and Lafayette Downstream site, showed a significant difference between all time point comparison among the total microbiomes (Table 7A). In all total microbiomes at each of the sites, lower similarity was observed between time point T_0 and time points T_1 and T_2 than between T_1 and T_2. Of the total microbiomes at time point T_2, the highest similarity was found in the shell total microbiomes and the lowest was observed in the gut total microbiomes. Site differences

and clustering of the different oyster types at T_2 were visible in the nMDS plots, particular in the shell total microbiome at the Elizabeth site (Figs 1 A-C).

Comparisons among sites and between the different oyster types at each site at time point T_2, showed a significant effect of both site and type on all of the oyster total microbiomes (Table 5B). Significant differences based on pairwise comparisons of the sites were found between all sites in the gill and shell total microbiomes (Table 7B). Only the comparison between the Elizabeth site and the Lafayette Midstream site were found to be significant in the gut total microbiome. In the shell and gill total microbiome, similarity among the different sites was highest between the Lafayette Downstream and Lafayette Midstream site. In the gut microbiome, the Elizabeth and Lafayette Downstream site had the highest similarity. Among all of the microbiomes, similarity between the shell total microbiomes was highest for all sites, ranging from 34.4% to 40.1%. Gill total microbiomes had the second highest similarity between sites (27.2%-29.8%), and gut total microbiomes had the lowest (23.6%-25.8%). Dispersion effects testing the beta diversity among the total microbiomes were also examined in relation to site, oyster type, and time point. No significant dispersion effects on the total microbiomes were detected with the exception of the shell total microbiome (Table 6). In the shell total microbiome, dispersion was significant in relation to both site and oyster type. As a result, the significance of site and oyster type effects on the shell total microbiome may due to dispersion of the data alone, or a combination of dispersion and site/oyster type effects.

Taxonomic composition microbiomes in oysters

Taxonomic composition of total microbiomes

16S rDNA based OTUs were used to compare the taxonomic composition of the total bacterial communities among the different microbiomes (Fig 2). All four microbiomes showed distinct taxonomic differences amongst each other in classes with >1% mean relative abundance. Some major differences in the taxonomic classification of the total communities among the different microbiomes were the dominance of class *Gammaproteobacteria* (27.1 ± 2.3%) in the gill microbiome, class *Mollicutes* (44.6 ± 3.7%) in the gut microbiome and class *Alphaproteobacteria* (55.0 ± 3.3%) in the water microbiome. The shell microbiome was distinct from the other microbiomes with a shared dominance of both class *Alphaproteobacteria* (29.5 ± 1.5%) and *Gammaproteobacteria* (18.3 ± 0.7%), as well a high relative abundance of class *Deltaproteobacteria* (11.1 ± 0.9%) and presence of classes *Anaerolinea*, *Nitrospira*, *Cytophagia*, and *Sphingobacteriia*. Other differences included classes *Bacteroidia* and *Epsilonproteobacteria* that were unique to the gill microbiome, and classes *Fibrobacteria, Opitutate*, and *Actinobacteria* that were unique to the water microbiome.

Temporal taxonomic comparisons of total microbiomes

Differences in the taxonomic composition of total oyster microbiomes were compared both temporally and spatially from initial time point T_0 to final time point T_2 at the sites Elizabeth and Lafayette Downstream. In the gill total microbiome at both sites, class *Cyanobacteria* and *Planctomycetacia* appeared at time point T_1 and continued through time point T_2 (Fig 3). At the Elizabeth site, class *Bacteroidia* disappeared and the relative abundance of class *Epsilonproteobacteria* increased from T_0 to T_2. At site

Lafayette Downstream, the relative abundance of class *Bacteroidia* and *Fusobacteriia* increased and class *Mollicutes* decreased between time points T_0 and T_2. No major differences in the gut total microbiomes were evident between the two sites, with the exception of class *Fusobacteriia*, which retained a presence at the Elizabeth site and disappeared from the Lafayette Downstream site (Fig 4). With respect to time, changes to the total microbiomes occurred with the disappearance of class *Flavobacteriia* after T_0, the appearance of class *Clostridia* at time point T_1, and the appearance of *Cyanobacteria* at time point T_1 through time point T_2. Differences between the shell total microbiome were most distinct between time points T_0 and T_1, with time points T_1 and T_2 remaining somewhat similar within each site (Fig 5). Changes between T_0 and T_1 at both sites included the appearance of classes *Acidimicrobia*, *Cytophagia*, and *Sphingobacteriia*, and the increase in relative abundance of class *Deltaproteobacteria*.

Spatial and Oyster Type taxonomic comparisons of total microbiome

Comparisons of the differences in the taxonomic compositions of oyster total microbiomes were also evaluated among all sites and oyster types at time point T_2. Several differences were observed between the deployed and native oyster taxonomic composition in the gill microbiome, as well as between deployed oysters at the different sites (Fig 6). Only the native oyster gill total microbiomes at the Lafayette Downstream and Lafayette Midstream sites had similar relative abundances at class levels. The deployed oyster gill total microbiome at the Elizabeth Downstream site had a unique composition of highly abundant classes *Bacteroidia* and *Fusobacteriia* in comparison to all other gill total microbiomes. At the Lafayette Midstream site, the deployed gill total

microbiome was distinctly characterized by class *Flavobacteriia*, while the deployed Elizabeth site had a noticeably higher presence of *Epsilonproteobacteria* than the other total microbiomes. Among the gut total microbiomes, *Mollicutes* was the dominant class in all deployed and native oysters (Fig 7). There were not a lot of unique differences in class level composition between the gut total microbiomes, with the exception of deployed oysters at the Lafayette Downstream site and native oysters at the Elizabeth site. Both sites showed a higher abundance relative abundance of classes *Gammaproteobacteria*, *Cyanobacteria*, and *Planctomycetacia* than the other gut total microbiomes. All shell total microbiomes regardless of site or type were primarily composed of dominant classes *Alphaproteobacteria*, *Deltaproteobacteria*, and *Gammaproteobacteria* (Fig 8). Among the different oyster types, the deployed oysters had more similar relative abundances of classes than the native oysters. Native oyster shell total microbiomes at the Elizabeth site had a distinctly high abundance of class *Cyanobacteria* compared to all other shell total microbiomes. Additionally, at the Elizabeth site both native and deployed oyster shell microbiomes had the unique class of *Nitrospira*.

Taxonomic composition of active microbiomes and its comparison to total microbiome

16S rRNA based OTUs were used to compare the active bacterial communities among the different microbiomes and to compare the active microbiomes to the total microbiomes (Fig 2). Similar to the total microbiome, all four active microbiomes were distinct from each other. Major differences among the different microbiomes were the high abundances of *Flavobacteriaceae* (21.5 ± 2.6%) and *Betaproteobacteria* (9.2 ±

3.8%) in the water, Deltaproteobacteria (14.9 ± 1.1%) in the shell, *Spirochaetes* in the gut (9.5 ± 1.2%), and *Bacteroidia* (3.8 ± 0.9%) in the gill microbiome. Between the total and active microbiomes, differences were observed in the presence of class *Spirochaetes* and reduction of class *Mollicutes* in the active gill and gut microbiome (-5.8% and -33.3%, respectively), disappearance of class *Fusobacteriia* in the active gill microbiome but increased abundance in the active DNA gut microbiome (+ 1.5%), presence of classes *Ardenticatenia*, *Bacteroidia, and Fibrobacteria* and disappearance of classes *Anaerolinea* and *Cytophagi*a in the active shell microbiome, and decreased dominance of class *Alphaproteobacteria* (-36.4%), large increases in relative abundances in classes *Gammaproteobacteria* (+11.9%) and *Flavobacteriia* (+16.0%), and presence of classes *Deltaproteobacteria, Cytophagia*, and *Sphingobacteriia* in the active water microbiome.

Taxonomic composition of core microbiomes in total and active microbiomes

The total and active OTUs in each microbiome were examined for the presence of a continuous core among different time points, locations, and oyster types (Fig 9 and Table 8). The total core microbiomes represented on average 35.4 ± 2.6% of the gill microbiome, 37.7 ± 3.0% of the gut microbiome, and 60.6 ± 1.8% of the shell microbiome. In comparison, the average gill active core OTUs were higher than the total core OTUs making up an average of 42.6 ± 2.0% of the gill microbiome, while the gut active core and shell active core OTUs were both lower at 14.8 ± 1.7% and 46.6 ± 1.7%. 11 and 49 OTUs comprised the gill total and active core microbiome, respectively. In the gill total core microbiomes a large portion of the core OTUs was assigned to *Gammaproteobacteria* and a single OTU belonging to an unclassified bacterial class.

The same OTUs belonging to class *Gammaproteobacteria* remained dominant in the active core microbiomes, but the relative abundance of the unclassified bacterial class was reduced in the active microbiomes. Additional OTUs classified as *Cyanobacteria*, *Alpha-*, *Beta-*, *Gamma-*, *Delta-*, and *Epsilonproteobacteria* were found in the gill active core microbiomes, but not in the gill total core microbiomes. Among the top 5 most abundant OTUs present in the gill active core microbiomes, higher abundances of genera *Vibrio*, *Endozoicomonas*, *Synechococcus*, and *Rhodobacteraceae* were found. The gut core microbiome had the least number of OTUs shared, with only 5 OTUs making up the total core microbiomes, and 4 making up the active core microbiomes. The gut total core microbiome was predominately comprised of class *Mollicutes*, with some contribution from class *Gammaproteobacteria*, particularly genus *Vibrio*. *Mollicutes* was greatly reduced in the gut active core microbiomes, while *Vibrio* increased in relative abundance. The shell microbiome had the most number of shared OTUs making up the total and active core microbiomes (256 and 269 OTUs, respectively). Several classes made up the shell total core microbiomes, with the most dominant classes identified as *Alpha-*, *Gamma-*, and *Deltaproteobacteria*. The composition of the shell active core microbiomes remained similar to that of the total core microbiomes with the exception of a few lesser abundant classes. Classes *Sphingobacteriia*, *Planctomycetacia*, and *Flavobacteriia* were present in the total core microbiomes, but absent in the active core microbiomes. The top 3 most abundant OTUs in both the total and active shell core microbiome belonged to unidentified *Rhodobacteraceae* genera from class *Alphaproteobacteria*. The remaining 2 most abundant OTUs differed between the total and active core microbiomes, with unidentified *Halieaceae* and *Sphingobacteriales*

genera in the total core microbiomes and *Vibrio* and an unidentified *Rhodobacteraceae* genus in the active core microbiomes.

Microbiome Denitrifiers

Microbiome Total and Active Denitrifiers

Abundance of total and active denitrifiers in the oyster microbiomes was evaluated based on the relative abundance of the *nos*Z gene carrying OTUs found in 16S rDNA and rRNA sequences using the paprica (Fig 10). In total microbiomes, the shell microbiome had the highest relative abundance of *nos*Z (16.8 ± 0.4%), followed by the gill microbiome (8.1 ± 0.9%), and then by the gut microbiome with the lowest relative abundance (2.3 ± 0.5%). The relative abundances of *nos*Z carrying active OTUs followed a similar trend, but were slightly higher with relative abundances of 19.1 ± 0.7% in the shell active microbiome, 12.0 ± 1.3% in the gill active microbiome, and 5.1 ± 1.0% in the gut active microbiome. In both total and active microbiomes, the relative abundances of *nos*ZI and *nos*ZII were similar in the gill and gut microbiome, while *nos*ZII was approximately 15% greater than *nos*ZI in the shell microbiome.

Spatial and Temporal Comparisons of Total and Active Denitrifiers

For each microbiome, the coefficient of variation was calculated among all replicates to determine total variation. In both the total and active microbiomes, the shell microbiome showed the least amount of variation (total 0.20, active 0.28), followed by the gill microbiome (total 0.81, active 0.84) and then the gut microbiome with the highest amount of variation (total 1.32, active 1.56). The relative abundances of *nos*ZI, *nos*ZII

and combined *nosZ* in total and active microbiomes are listed in Table 8. With the exception of the native oysters at the Elizabeth site during time point T1, which had the lowest relative abundance of combined *nosZ* in the total (10. 53 ± 2.21%) and active (8.1 ± 2.8%) microbiomes, the relative abundances of combined *nosZ* in the shell microbiomes were consistently high and ranged from 15.49 to 20.2% in the total microbiome and from 15.70 to 23.60% in the active microbiome. There were no distinctive patterns among the different sites or time points in the total shell microbiome. However, in the active shell microbiome, combined *nosZ* relative abundances were higher at time point T_2 than T_1 for all sites and oysters, and the Lafayette Midstream had higher combined *nosZ* abundances in general. In comparison to the shell microbiome, the gut total and active microbiomes had the lowest relative abundances of combined *nosZ* ranging from <1% to 7.42% in the total microbiome and from 1.08 to 8.85% in the active microbiome. Time point T_0 showed the highest relative abundance of combined nosZ in both the active and total gut microbiome. There were generally no obvious patterns between sites, time points, or oyster types in either the total or active gut microbiomes. Relative abundances of combined *nosZ* in gill total and active microbiomes had the greatest variation and ranged from 5.12 to 14.82% in the total microbiome and from 6.95 to 17.05% in the active microbiome. Overall higher *nosZ* relative abundances were found at the Elizabeth site (10.58 ± 1.65) than at the Lafayette Midstream (8.45 ± 2.17%) and Downstream (5.44 ± 0.76%) sites for both time points and oyster types in the total microbiome. However, in the active gill microbiome, the Lafayette Midstream showed the overall highest relative abundances of combined *nosZ* (15.32 ± 3.56%) compared to the Lafayette Downstream (8.47 ± 1.50%) and Elizabeth

(12.60 ± 1.14%) site. In general, the relative abundances of *nosZ*II were greater than *nos*ZI in the total and active microbiomes with *nos*ZII relative abundances approximately 1.5 to 2.0x more abundant than *nos*ZI. In the total microbiome, the difference between the *nosZ* gene clades was significant in the gut (t_9=2.41, p = 0.02) and shell (t_9=2.79, p = 0.001), but not in the gill (t_9=1.51, p = 0.08). In the active microbiome, the difference between *nosZ* gene clades was significant in all microbiomes; gill (t_9=2.79, p = 0.009), gut (t_9=2.85, p = 0.008), and shell (t_9=3.28, p = 0.004).

Relative abundances of *nosZ* were compared in the total and active whole oyster microbiomes based on the combined average abundances of OTUs carrying *nos*ZI and *nos*ZII in the gill, gut, and shell microbiomes (Figs 11 & 12). Temporally among the deployed oysters at sites Elizabeth and Lafayette Downstream, overall *nosZ* relative abundances in total microbiomes were similar between the different time points with a slight decrease at the Lafayette Downstream site from 9.3% at T_0 to 8.3% at T_1 and 8.2% at T_2. During this time, the relative abundance of *nos*ZII decreased from 5.8 to 4.1%, but was also coupled with a small increase in *nos*ZI from 3.5 to 4.1%. A similar decrease in overall relative abundance from 11.8% at T0 to 10.4% at both T_1 and T_2 was found in the oyster active microbiome at the Lafayette Downstream site. However, unlike the total microbiome, relative abundances of *nos*ZI decreased from 5.8 to 4.1%, with an overall slight increase in *nos*ZII from 5.9% at T_0 to 6.3% at T_2.

Spatially among the oysters at T_2, relative abundances of combined *nosZ* were similar in both the total and active microbiomes, with deployed and native oysters at the Lafayette Downstream site showing only slightly lower relative abundance of *nosZ* in their total (8.2% and 7.6%, respectively) and active (10.4 and 11.6%, respectively)

microbiomes. The highest relative abundance of combined *nos*Z was found in the native oyster total microbiomes at the Elizabeth site (11.4%) and in the deployed oyster active microbiomes at the Lafayette Midstream site (13.9%). The higher relative abundance of combined *nos*Z in the native oyster total microbiome at the Elizabeth was due to greater relative abundances of *nos*ZI (7.0%), while in the deployed oyster active microbiome at the Lafayette midstream higher combined nosZ abundance was due to the combined greater relative abundance of *nos*ZI and *nos*ZII (6.1 and 7.8%, respectively). Overall, *nos*ZII relative abundances were higher than *nos*ZI in both active and total microbiomes and showed a greater increase (+ 20.3 ± 1.8%) in the active microbiome versus the total microbiome, than *nos*ZI (+ 9.6 ± 4.5%). The greatest change in the relative abundances between the total and active microbiome (+ 27.3%) occurred in the deployed oysters for *nos*ZII relative abundances at the Lafayette Midstream site.

Core Microbiome Total and Active Denitrifiers

The paprica program determined core denitrifiers by identifying the OTUs carrying *nos*Z genes within the core OTUs (Fig 13 & Table 10). Denitrifiers carrying *nos*ZI belonged to orders *Alteromonadales*, *Rhizobiales*, *Rhodobacterales*, and *Nevskiales*, while denitrifiers carrying *nos*ZII belonged to orders *Flavobacteriales, Chitinophagales*, *Vibrionales*, and genus *Thiolapillus* from an unclassified *Gammaproteobacteria* order. In all core microbiomes, active microbiomes had higher abundance of OTUs carrying *nos*Z than total microbiomes. The greatest difference between total and active denitrifiers was found in the gill core microbiome for *nos*ZI, which increased from a relative abundance of 5.3% in total microbiomes to 15.8% in

active microbiomes as a result of increased abundances of active OTUs assigned to *Rhodobacterales*. Corresponding relative abundances for *nos*ZII in the gill active microbiomes increased by <1%. However, within the active gill microbiomes the *nos*ZII carrying OTU composition shifted from *Vibrionales*-only to a mix of bacteria belonging to orders *Vibrionales*, an unclassified Gammaproteobacteria (genus *Thiolapillus*), and *Cytophagales*. The shell core microbiome had the highest relative abundance of core denitrifiers for both total (20.5%) and active (25.1%) microbiomes. Within the shell core microbiome, total denitrifier abundances carrying *nos*ZI were almost two times higher than *nos*ZII carrying denitrifiers, but the relative abundance difference of denitrifiers carrying either *nos*ZI or *nos*ZII was less pronounced in the active core microbiome. The gut core had the lowest relative abundance of denitrifiers in the total (0.3%) and active microbiome (2.3%) with all denitrifiers carrying *nos*ZII and belonging to order Vibrionales. In both total and active shell core microbiomes, *nos*ZI carrying denitrifiers included high abundances of orders *Rhizobiales*, *Nevskiales*, and *Rhodobacterales*, while *Flavobacteriales, Chitinophagales*, *Cytophagales*, and an unclassified *Gammaproteobacteria* (genus *Thiolapillus*) were the major orders for *nos*ZII carrying denitrifiers. Increases in *Rhodobacterales* and increases in an unclassified *Gammproteobateria* (genus *Thiolapillus*) explained the higher abundances of *nos*ZI and *nos*ZII, respectively, in the active versus total shell core microbiomes.

DISCUSSION

Oyster Microbiome Composition

Total Oyster Microbiome

Compositionally, the oyster and water microbiomes were highly distinct from each other, indicating tissue-specific microbiomes associated with the oyster (Fig 2). *Gammaproteobacteria* dominance in the gill microbiome (Hernández-Zárate and Olmos-Soto 2006, Zurel et al. 2011, Wegner et al. 2013), and *Mollicutes* dominance in the gut microbiome (Green and Barnes 2010, Lokmer et al. 2016b, Arfken et al. 2017) are consistent with previous studies investigating the composition of oyster microbiomes. Studies examining the shell microbiome are less known, however the high abundance of *Alphaproteobacteria* has been similarly found in oyster shell microbiomes in Arfken et al. (2017). Interestingly, however, the shell microbiomes in this study were comprised of a much greater range of taxonomic classes and species richness than Arfken et al. (2017). This probably reflects compositional variation due to environmental extremes experienced by sub-tidal oysters in this study versus intertidal oysters in Arfken et al. (2017). The exposure of intertidal oyster shell microbiomes to sunlight as well as intertidal gradients such as moisture, temperature, wave action, nutrients, and salinity (Menge and Branch 2001) create a strong selection pressure for microbes uniquely adapted to such environments (Arun et al. 2009). The water microbiome was distinct from the oyster microbiomes due to the presence of classes *Actinobacteria*, *Betaproteobacteria*, and *Opitutae*. The absence of these classes in the compositions of the oyster microbiome indicates these bacteria are environmental in nature and are not being ingested or utilized by the oyster.

Active Oyster Microbiomes

In most of the microbiomes, main differences between total (rDNA) microbiomes and active (rRNA) microbiomes were due changes to the relative abundances of dominant taxa (Fig 2). In the gut for example, *Mollicutes* was found to be less abundant and Gammaproteobacteria more abundant than was observed in the total microbiome. Interestingly, however, there were also some classes that were present in the active microbiome, but absent in the total microbiome. This suggests that several rare bacteria in the oyster microbiomes are disproportionately active. Several studies of marine environments have shown a similar trend of rare, but highly active microbes (Campbell et al. 2011, Campbell and Kirchman 2013, Wilhelm et al. 2014) that may support unique or complementary metabolic pathways to the community function or be important in host health (Jousset et al. 2017). Rare classes that were only observed in the active microbiomes included *Spirochaetes* in the gut and gill, *Ardenticatenia* and *Bacteroidia* in the shell, and *Cytophagia* and *Sphingobacteriia* in the water microbiome. Of these classes, class *Spirochaetes* has previously been identified in other oysters and marine bivalve gut and gill tissues (Green and Barnes 2010, Trabal Fernández et al. 2014, Lokmer et al 2016b), and are hypothesized to exploit the niche environments created by the oyster gut organs rather than exhibit endosymbiosis with the oyster host (Husmann et al. 2010). Interestingly, class *Ardenticatena* found only in the shell active microbiome includes novel species of bacteria capable of dissimilatory iron reduction (Kawaichi et al. 2013). The disproportionate activity of this class in the shell microbiome may indicate presence of iron in the environment. However, overall caution must be exercised when

interpreting results of rRNA relative abundance data as direct measurements of activity. The rRNA transcripts exhibit a much greater range of copy numbers per cell than rRNA gene numbers (Fegatella et al. 1998, Acinas et al. 2004), which may result in some instances of higher abundances of bacterial classes in the active microbiome that are not necessarily related to higher activity.

Oyster Microbiome Variability

Spatial, Temporal, and Oyster Type Effects on Total Microbiomes

Not surprisingly, in all of total microbiomes there was a significant effect of time among the deployed oysters (Table 5B). In this experiment, time points signify the transition and acclimation of oysters from a controlled hatchery environment (T_0) to different sites over a 1-month (T_1) and 2-month (T_2) time period. For the gill and gut total microbiomes, the introduction of the oysters to a different environment most likely constitutes a relatively minor disturbance to the community, while the removal of the shell biofilm prior to the initiation of this study would be considered a major disturbance. The time required for recovery of the microbiomes to a stable state, or if a stable state is even attainable in a fluctuating marine environment, is unknown (Galand et al. 2016, Lokmer et al. 2016a). Because we sampled oysters in a natural environment over a 2-moth time period, some effects of seasonality would also contribute to fluctuations in total microbiome composition and make assessment of recovery difficult. For example, abundances of *Vibrio* in oyster hemolymph have been shown to decrease from May through August, and increase again after spawning (Wendling et al. 2014). Despite these challenges, however, the increase in similarity between time points T_1 and T_2 versus T_0

(Table 7A) suggests that the microbiomes were responding quickly to the new environment with high turnover rates. Interestingly, despite distinct composition shifts shown in the nMDS plots (Figs 1 A-C), there were no major shifts in diversity or richness from T_0 to T_1 (Table 3). This may be indicative of oyster microbiome compositional resiliency or adaptability to substantial environmental changes as a result of translocation.

Between sampling time points and sites among the deployed oysters, the deployment site explained the highest amount of variation in the gill and shell microbiome, while the time point explained the most variation in the gut microbiome (Table 5B). The reduced effect of deployment site on the gut microbiome may be due to a more discriminatory nature of the gut microbiome. Of all the oyster microbiomes examined in this study, the gut organs have the least exposure to the external environment. Selective feeding, host immunity factors, unique internal variable to the gut environment such as nutrient supply and oxygen levels, and the functional role in nutrition in bivalves (Stief et al. 2009, Fernandez-Piquer et al. 2012, King et al. 2012, Svenningsen et al. 2012, Trabal Fernández et al. 2014) may be more important to the shaping of the gut microbiome than the surrounding environment. This selective nature may also correspond to the low levels of species richness and diversity that were observed in the gut total microbiome in this study (Tables 3 & 4) and in other studies examining oyster gut microbiomes (King et al. 2012, Trabal Fernández et al. 2014, Vezzulli et al. 2017). Among both native and deployed oyster microbiomes at time point T_2, only a significant difference was determined between the Elizabeth site and the Lafayette Midstream site (Table 7B). These two sites are geographically the most distinct sites, while the Elizabeth Downstream site is in contact with both river systems.

This suggests that the effects on the oyster microbiome may be due to food supply differences found in the water column, which are likely different between the two rivers. Overall taxonomical differences at the class level between the different sites were subtle. However, the Elizabeth site and Lafayette Downstream site generally had higher abundances of *Cyanobacteria* (Figs 3-8). Cyanobacteria have been shown to be associated with ingestion of food particles and ciliates in oyster stomach contents (Le Gall et al. 1997), further suggesting a link between food ingestion and the effect on oyster gut microbiomes. This hypothesis is strengthened by the observation that bacteria belonging to *Cyanobacteria* were absent from T_0 oyster gut microbiomes at the hatchery where oysters were fed a commercial algae paste and held in filtered seawater, but present at time points T_1 and T_2 following deployment to the natural environment.

In both the gill and shell total microbiomes, the effect of site was significant among the deployed oysters and among both native and deployed oysters at time point T_2 (Tables 5A & B). Between the sites at time point T_2, the Lafayette Midstream and Lafayette Downstream were more similar to each other than the Elizabeth site (Table 7B). As with the gut total microbiome, this indicates the microbial communities are likely different between the two rivers and influencing the microbiome composition of the oysters. Furthermore, this effect appears to be most pronounced in the shell microbiome and less so in the gut microbiome. In the both the native and deployed shell microbiome at time point T_2, slightly higher abundances or presence of classes *Nitrospira*, *Acidimicrobia*, and *Betaproteobacteria* were found at the Elizabeth site compared to the Lafayette sites (Fig 8). Genera associated with classes *Nitrospira* and *Betaproteobacteria* at these sites included genus *Nitrospira* and genus *Nitrosomonas*

(data not shown). Although, this was not explored in this study, the higher abundance of these genera suggests a greater potential for nitrification in the shell microbiomes at the Elizabeth site. In nitrification, ammonium (NH_4^+) is first oxidized to NO_{2-} by ammonia-oxidizing bacteria (e.g. *Nitrosomonas*), and then to NO_3^- by nitrite-oxidizing bacteria (e.g. *Nitrospira*) (Koch et al. 2015). In the gill total microbiome, a high amount of variation in the composition between sites was evident, with no discernible patterns consistent between both the native and deployed oysters at each site or between time points in the deployed oysters (Figs 3 and 6). Interestingly however, among the native oyster only, sites from Lafayette River were nearly identical in taxonomic composition and very different from the Elizabeth site. It is difficult to speculate as to why the gill microbiomes exhibit a greater amount of taxonomic variability than the gut or the shell, but it may indicate a combination of competing host-related and environmental factors. Whereas the gut microbiome primarily faces internal pressures and the shell primarily faces external pressures, the gill falls somewhere in between exposed to both the internal and external environment.

The effect of oyster type also had a significant effect on the composition of the oyster microbiomes (Table 5A). Deployed oysters were all from the same genetic line, while native oyster genotypes were unknown and variable. Between oyster type and site at time point T_2, oyster type explained more variation in the gut microbiome, while site explained more of the variation among the gill and shell microbiomes. In addition to factors influencing the gut microbiome described previously, genetic factors may also influence the assemblages of the gut microbiome. Host genotype has shown to have an effect on microbial composition, which is likely to be more pronounced in tissues that are

less exposed to the environment (Wegner et al. 2013, Lokmer et al. 2016b). This may explain the greater explanation power of oyster type in the variation in the gut microbiome over those in the gill or shell microbiome.

Dispersion Effect on Total Microbiomes

The shell total microbiome was the only microbiome that showed a significant dispersion effect among the sites and between the native and deployed oysters (Table 6). Among the oyster types, deployed oysters showed a greater homogeneity of variances than the native oysters. As described above, prior to deployment the oyster shell biofilms were removed before being placed in oyster tanks for two weeks. Following this major disturbance event to the shell microbiome, post-scrub colonization of shell microbiomes occurred under identical, controlled conditions (T_0 microbiomes). Rapid, initial colonizers in deployment oysters T_0 likely persisted during the course of the deployment experiment and may explain the greater homogeneity of variation displayed among the deployed oysters. Early, successful colonization of niches created by disturbance events may out-compete native community members by what is known as "Priority effects" (Shulman et al. 1983, Urban and De Meester 2009). For example, the deployed oysters at the Lafayette sites showed a greater abundance of *Alphaproteobacteria* than the native oysters at time point T_2 (Fig 8), which may demonstrate some persistence of *Alphaproteobacteria* colonizers from T_0 (Fig 5) in the deployed oyster shell total microbiomes. In comparison, native oysters were exposed to different environmental variables and seawater communities during shell development, likely increasing the range and distributions of variation shown in the shell microbiomes. Among the different

deployment sites, significant dispersion effect due to site was due to greater homogeneity of variances found at the Lafayette Midstream site. This may be due to the removal of deployed T_1 oysters from analysis and thus a reduction in heterogeneity among the remaining samples, or a result of environmental factors selecting for a more uniform assemblage of bacteria. The Lafayette Midstream site is located in a highly residential portion of the river and has shown to exhibit higher nutrient concentrations and fecal coliform counts than the other deployment sites, most likely due to septic leakage and runoff. Greater structure similarity among microbial communities due to eutrophication and nutrients may select for bacteria that are less sensitive to higher loads of pollutants or alternatively, provide a greater number of energy sources for similar species to co-exist (Ford 2000, Sawall et al. 2012).

Oyster Core Microbiomes

Core microbiomes

Despite the high amount of variability demonstrated to the gill, gut and shell microbiomes, all total microbiomes had a core set of members that were present in 80% of the replicates for each sampling time point, location, and oyster type (Fig 9 and Table 8). Members of the gill and gut core microbiomes likely indicate the stable residents of the total microbiomes to environmental changes and potential microbiota related to oyster health or digestion. In the shell total microbiome, however, members of the core microbiomes more likely represent the resilient or fast colonizing members due to the extreme nature of the disturbance to the shell biofilm. Among the core microbiomes, the gill and gut core microbiomes made up roughly one third of the sequences for their

corresponding total microbiomes and was comprised of 11 and 5 OTUs respectively. The low numbers of OTUs coupled with high abundance suggest these OTUs form some type of association with the oyster. This relationship may be beneficial to the host such as providing pathogen protection and aiding in digestion (McFall-Ngai et al. 2013) or commensal (Seong et al. 2008) with selective bacteria adapted to survive and thrive under the internal environment (Freter et al. 1983, Fabich et al. 2008) with no known advantages to the host. In the gill core microbiome, the total microbiome was composed of OTUs primarily belonging to class *Gammaproteobacteria* and an unidentified Bacteria class. Using a phylogenetic placement method with the paprica database, the closest match to the unidentified OTU belonged to phylum *Spirochaetes*. This OTU was identical to the one identified in chapter 2 and may be similar to the unidentified *Spirochaetes* found in the oyster hemolymph in Lokmer et al. (2016a). As discussed previously in the total and active microbiome, *Spirochaetes* have been linked to oysters (Green and Barnes 2010, Trabal Fernández et al. 2014) but not thought to be endosymbiotic (Husmann et al. 2010). However, the *Spirochaetes* genera investigated in Husmann et al. (2010) are presumably distinct from the unidentified genus associated with the gill core microbiome from this study. Symbiotic species of *Spirochaeta* have been identified in other marine organisms (Blazejak et al. 2005, Ruehland et al. 2008) suggesting further investigation of a *Spirochaetes* symbiotic relationship with the gill may be warranted. Another OTU found in the gill core microbiome that may be a potential endosymbiont belonged to class *Gammaproteobacteria*, genus *Endozoicomonas*. *Endozoicomonas* have been found to be associated with bivalve gills (Jensen et al. 2010) and have demonstrated to form symbiotic relationships in sponges,

worms, and corals (Verna et al. 2010, Neave et al. 2016). Interestingly, the gill core active microbiome was the only oyster microbiome that showed an increase in relative abundance and number of core members, primarily by OTUs belonging to *Proteobacteria* and *Cyanobacteria*. This suggests that a higher number of low abundance or rare bacteria may have a greater association with the gill microbiome than in the gut or shell microbiomes.

The gut core microbiome was comprised entirely of OTUs belonging to genus *Mycoplasma* from class *Mollicutes* and genus *Vibrio*, from class *Gammaproteobacteria*. While the relationship between *Mollicutes* and the oyster gut microbiome is unknown, it has been postulated that the proliferation of *Mollicutes* in the gut is a result of the microbes' ability to utilize substrates produced during digestion (King et al. 2012). Other studies have suggested a possible link between *Mollicutes* and stress events (Lokmer and Wegner 2015) or amino acid synthesis in host organisms (Tanaka et al. 2004). The occurrence of *Vibrio* in the core gut microbiome is unsurprising, based on previous studies which have found a high abundance of *Vibrio* associated with oyster tissues and hemolymph (Prieur et al. 1990, Olafsen et al. 1993, Faury et al. 2004, Lokmer et al. 2016b). Many *Vibrio* species associated with oysters are thought to be commensal (Hoffmann et al. 2010), but may be pathogenic during different life stages of the oyster or become virulent as a result of temperature or stress to the oyster host (Garnier et al. 2007, Eiston et al. 2008). Compared to the total core gut microbiome, the active core made up less than 15% of the total sequences for the gut microbiome. While *Vibrio* and *Mycoplasma* were still present in the active core microbiomes, the overall low abundance of the active gut core microbiome indicates that the majority of activity occurring in the

gut microbiome is not consistent among taxa and may be highly variable based on factors such as location, season, or genetic lineage of the oyster.

The largest numbers of OTUs, greatest variation in OTU taxa, and highest overall abundance of sequences were found in the shell core microbiome, suggesting a diverse role of the core shell microbiome in the marine environment. Shell surfaces provide a complex structure with strong oxygen gradients (Heisterkamp et al. 2013) providing unique microhabitats for biofilm colonization of diverse microorganisms (Pfister et al. 2014). The most abundant OTUs in both the total and active core microbiome belonged to genera from family *Rhodobacteraceae* of class Alphaproteobacteria. Members of *Rhodobacterales* have been suggested as important in early biofilm formation and initial colonizers of surfaces in the marine environment (Dang et al. 2008, Celikkol-Aydin et al. 2016). As a result of these OTUs being present in established native oysters as well as deployed oysters, this suggests these early colonizers are able to persist in shell microbiomes past initial biofilm formation.

Core Denitrifiers

Among each microbiome, core denitrifiers made up a larger percentage of the shell core microbiomes than the gill or the gut core total microbiomes (Fig 13 and Table 10), indicating a consistent strong presence of denitrifiers in the shell and a fast recovery from disruption to the shell microbiome. Surprisingly, the gut core denitrifiers made up a small percentage of the active and total core microbiomes despite providing a potentially favorable anoxic and carbon rich environment for denitrification to occur. This suggests that most denitrifiers in the gut are more likely transient in nature and likely associated

with food particles. Differences in % core denitrifiers between the shell and gill core total microbiomes were much less pronounced in the active core microbiomes. The increase in active denitrifier abundance of the gill microbiome was primarily due to the increase of bacteria carrying *Rhodobacterales nosZ*I in the gill core microbiomes. Arfken et al. (2017) showed that bacteria carrying *nos*ZI reflected patterns shown in denitrification rates suggesting an importance of *nos*ZI over *nos*ZII in oyster denitrification. This indicates the gill core may exhibit higher denitrification activity than would be suggested by the total core microbiomes, and may have similar denitrification activity as that found in the shell core microbiomes. Interestingly, the composition of denitrifier taxa was unique between the shell and gill core microbiomes for both *nos*ZI and *nos*ZII. Denitrifier classes *Rhizobiales* and *Nevskiales* carrying *nos*ZI and *Flavobacteriales* and *Chitinophagales* carrying nosZII were only found in shell core microbiomes, while Vibrionales carrying *nos*ZII was only found in the gill core microbiomes. These differences between the core microbiomes highlight the concept of niche differentiation among denitrifiers in the ecosystem, which can significantly affect denitrification and overall community functioning (Salles et al. 2017).

Oyster Microbiome Denitrifiers

Denitrifier abundances were also examined in the whole gill, gut, and shell total and active microbiomes (Figs 11 and 12, and Table 9). Total and active denitrifier relative abundances followed similar patterns among the oyster microbiomes, with active denitrifiers showing only slightly higher relative abundances than total denitrifiers (Fig 10). Overall, both active and total shell microbiomes consistently had the highest relative

abundance of denitrifiers among all locations, oyster types, and time points (Table 9). This suggests denitrifiers in the deployed shell microbiome quickly recovered from the disturbance and that denitrification potential and denitrifier activity at all sites in the Lafayette and Elizabeth Rivers are similar with respect to the shell microbiome. The only exception is the native oyster total and active shell microbiome at the Elizabeth site for time point T_2. It is unclear as to why only the native oyster shells at this site and time point had low abundances of *nos*Z and may be related to a variable not considered in this study. The presence of bacteria carrying the *nos*Z gene, however, is only one factor of many that contribute to denitrification in an environment. Factors such as oxygen levels, NO_3^- and carbon (C) substrate availability, temperature, and pH also influence denitrification (Wallenstein et al. 2016). Furthermore, bacteria carrying *nos*ZII genes are more likely to simultaneously carry genes for dissimilatory nitrate reduction to ammonium (DNRA), a competing reduction pathway to denitrification (Sanford et al. 2012), or lack *nir* genes necessary for reducing NO_2^- to NO in the denitrification pathway (Graf et al. 2014). Thus, the relative abundance of denitrifiers carrying *nos*Z genes must be interpreted carefully in relation to denitrification potential of a system. With these limitations in mind, characterizing the active and total *nos*Z communities is an important factor in determining the denitrification potential of a system.

In comparison to the shell, the gut and gill total and active microbiomes showed a greater amount of variation in denitrifier abundances among the sites, oyster types, and time points. This suggests that internal pressures of the oyster may be affecting the abundances of denitrifiers, and may indicate a relationship between food ingestion and denitrifiers. Bacteria able to survive digestion encounter different internal environmental

conditions than are found in the external environment, which may stimulate a shift in metabolic pathways (Poulsen et al. 2014). A reduction in O_2 and increased NO_3^- in the invertebrate gut, for example, may induce denitrification in ingested bacteria from the water column (Stief et al. 2009). In earthworms, active *nos*Z transcripts and denitrification activity has been linked to ingested soil microbes passing through the alimentary canal (Depkat-Jakob et al. 2010), with only minimal contribution from gut-associated microbes (Drake and Horn 2007). In addition to the oyster gut microbiome, the gill environment may also be conducive for denitrification. Reduced O_2 levels from the closing of the oyster valve and decreased water flow (Galtsoff 1964, Shumway and Koehn 1982) as well as increased nutrients found in the gill mucus, may all induce denitrification in bacteria filtered or ingested from the water column. Further evidence of a possible link between food ingestion and denitrifier abundance are the generally higher relative abundances of denitrifiers in the gill and gut microbiomes at the Elizabeth site compared to the Lafayette sites. With the exception of the deployed oyster gut microbiome at T_2, both native and deployed oyster gut and gill microbiomes during both time points had higher relative abundances of combined *nos*Z than the Lafayette sites. This same trend was not seen in the shell microbiomes, suggesting that oysters may be selectively ingesting similar denitrifiers from the water column at the Elizabeth site and increasing denitrifier abundances in their gill and gut microbiomes. Also interesting, is that combined *nos*Z abundances were always higher in the gill than the gut total and active microbiomes with gill denitrifiers ranging from around 5 to 17% and gut denitrifiers ranging from < 1 to 9%. This may indicate a lower percentage of denitrifiers are able to survive digestion or colonize the gut microbiome than the gill microbiome.

Combined average relative abundances of *nos*Z for the gill, gut, and shell of each oyster to form a whole oyster total and active microbiome did not show much variation between time points or among sites (Figs 11 and 12), with abundances ranging from 7.5 to 11.4% in the total microbiome and from 10.4 to 13.9% in the active microbiome. This may indicate similar abundances of denitrifiers in the whole oyster microbiome or it may be the result of giving equal weight to the gill, gut, and shell microbiome. In reality, the contribution of the gill, gut and shell microbiomes to the oyster is not the same due to differences in surface area or volume and concentrations of bacteria. In human tissue microbiomes, for example, total numbers of bacteria range from an estimate 10^7 in the stomach to 10^{14} in the colon (Sender et al. 2016). Further investigation of bacterial concentrations in different oyster tissues may reveal much greater differences between whole oyster denitrifiers. With these limitations in mind, however, the highest denitrifier relative abundances at time point T_2 found in native oysters at the Elizabeth site and in deployed oysters at the Lafayette Midstream site showed increased abundances of *nos*ZI in the total and active microbiomes. As stated previously, Arfken et al. (2017) showed that bacteria carrying *nos*ZI might be more important to denitrification in oysters than *nos*ZII, which suggests that the oysters at these sites may exhibit higher rates of denitrification than the other oysters or sites in this study.

CONCLUSIONS

Spatial and temporal changes to the oysters all had significant effects on the gill, gut, and shell microbiomes, with temporal differences affecting the gut more strongly and spatial differences having a greater impact on the gill and shell microbiomes. Among all of the variation resulting from these changes, however, each microbiome exhibited a consistent presence of a core set of microbiota that comprised the core microbiome. These core microbes indicate some level of stability despite substantial environmental changes to the microbiomes, signifying the core's potential importance to oyster function and health and demonstrating a pool of highly resistant and/or resilient microbes distinct to each microbiome. Within each core, there also existed a core group of denitrifiers, which was unique to the different microbiomes. The presence of core denitrifiers, particularly in the shell microbiome, suggests that denitrification potential in the shell is quickly recovered after a major disturbance. Furthermore, the high amount of variability of denitrifiers found in the gill and gut compared to the shell microbiome may indicate the importance of oyster diet in the denitrification potential of oysters. The findings of this study provide valuable insight into the effect of translocation on oyster microbiomes and denitrification potential, and may have future implications in the planning and placement of restored oyster reefs in the Chesapeake Bay to mitigate excess N.

ACKNOWLEDGEMENTS

I thank Jessica Small and the Virginia Institute of Marine Science Aquaculture Genetics and Breeding Technology Center for help in collecting oysters and providing facilities for this experiment, Joe Rieger with the Elizabeth River Project for providing guidance and assistance in deployment site selection, and Mike Unger for his help with initial planning and logistics of the deployment. I also thank Miguel Semedo, Tavis Sparrer, Ken Czapla, and Hunter Walker for their assistance in the field and with dissections, Anjali Bhatnagar and Lara Sierra for help with shell DNA and RNA extractions, and Seth West for assistance with computer coding. Funding for this study was provided by NSF Biological Oceanography program. This work was performed in part using computing facilities at the College of William and Mary, which were provided by contributions from the National Science Foundation, the Commonwealth of Virginia Equipment Trust Fund and the Office of Naval Research.

REFERENCES

Acinas, SG, Marcelino, LA, Klepac-Ceraj, V, and Polz, MF (2004) Divergence and redundancy of 16S rRNA sequences in genomes with multiple *rrn* operons." *Journal of Bacteriology* **186**(9): 2629–35. doi: 10.1128/JB.186.9.2629-2635.2004.

Allison, SD, and Martiny, JBH (2008) Colloquium paper: resistance, resilience, and redundancy in microbial communities. *Proc Natl Acad Sci* **105**(Supplement 1): 11512–19. doi: 10.1073/pnas.0801925105.

Arfken, A, Bongkeun, S, Bowman, JS, and Piehler, M (2017) Denitrification potential of the eastern oyster microbiome using a 16S rRNA gene based metabolic inference approach. *PLoS ONE* **12**(9): 1–21. doi: 10.1371/journal.pone.0185071.

Arun, AB, Chen, W-M, Lai, W-A, Choau, J-H, Rekha, PD, Shen, F-T, Singh, S, and Young, C-C (2009) *Parvularcula lutaonesis* sp. nov., a moderately thermotolerant marine bacterium isolated from a coastal hot spring." *Int J Syst Evol Micr* **59**: 998–1001. doi: 10.1099/ijs.0.004481-0.

Asmani, K, Petton, B, Le Grand, J, Mounier, J, Robert, R, and Nicolas, J-L (2016) Establishment of microbiota in larval culture of Pacific oyster, *Crassostrea Gigas*. *Aquaculture* **464**: 434–44. doi: 10.1016/j.aquaculture.2016.07.020.

Austin, B (2006) The bacterial microflora of fish. *Sci World J* **6**: 931–45. doi: 10.1100/tsw.2002.137.

Beck, MW, Brumbaugh, RD, Airoldi, L, Carranza, A, Coen, LD, Crawford, C, Defeo, O, Edgar, GJ, Hancock, B, Kay, MC, Lenihan, HS, Luckenbach, MW, Toropova, CL, Zhang, G, and Guo, X (2011) Oyster reefs at risk and recommendations for conservation, restoration, and management. *BioScience* **61**(2): 107–16. doi:

10.1525/bio.2011.61.2.5.

Blaser, MJ, Cardon, ZG, Cho, MK, Dangi, JL, Donohue, TJ, Green, JL, Knight, R, Maxon, ME, Northern, TR, Pollard, KS, and Brodie, EL (2016) Toward a predictive understanding of earth's microbiomes to address 21st century challenges. *MBIO* **7**(3): 1–16. doi: 10.1128/mBio.00714-16.

Blazejak, A, Erséus, C, Amann, R, and Dubilier, N (2005) Coexistence of bacterial sulfide oxidizers, sulfate reducers, and spirochetes in a gutless Worm (Oligochaeta) from the Peru Margin. *Appl Environ Microbiol* **71**(3): 1553–61. doi: 10.1128/AEM.71.3.1553-1561.2005.

Bowman JS, and Ducklow HW (2015) Microbial communities can be described by metabolic structure: A general framework and application to a seasonally variable, depth-stratified microbial community from the coastal West Antarctic Peninsula. *PLoS One* **10**(8):1–18. doi: 10.1371/journal.pone.0135868

Brumbaugh, RD, Sorabella, LA, Johnson, C, and Goldsborough, WJ (2000) Small scale aquaculture as a tool for oyster restoration in Chesapeake Bay. *Mar Technol Soc J* **34**(1): 79–86. doi: 10.4031/MTSJ.34.1.9.

Brumbaugh, RD, and Coen, LD (2009) Contemporary approaches for small-scale oyster reef restoration to address substrate *versus* recruitment limitation: a review and comments relevant for the Olympia Oyster, *Ostrea lurida* Carpenter 1864. *J Shellfish Res* **28**(1): 147–61. doi: 10.2983/035.028.0105.

Brummel, T, Ching, A, Seroude, L, Simon, AF, and Benzer, S (2004) *Drosophila* lifespan enhancement by exogenous bacteria. *Proc Natl Acad Sci* **101**(35): 12974–79. doi: 10.1073/pnas.0405207101.

Burgsdorf, I, Erwin, PM, López-Legentil, S, Cerrano, C, Haber, M, Frenk, S, and Steindler, L (2014) Biogeography rather than association with cyanobacteria structures symbiotic microbial communities in the marine sponge *Petrosia ficiformis*. *Front Microbiol* **5**(OCT): 1–11. doi: 0.3389/fmicb.2014.00529.

Caffrey, JM, Hollibaugh, JT and Mortazavi, B (2016) Living oysters and their shells as sites of nitrification and denitrification. *Mar Pollut Bull* **112**: 86–90. doi:10.1016/j.marpolbul.2016.08.038.

Campbell, BJ, Yu, L, Heidelberg, JF and Kirchman, DL (2011) Activity of abundant and rare bacteria in a coastal ocean." *Proc Natl Acad Sci USA* **108**(31): 12776–81. doi: 10.1073/pnas.1101405108.

Campbell, BJ, and Kirchman, DL (2013) Bacterial diversity, community structure and potential growth rates along an estuarine salinity gradient. *ISME J* **7**(1): 210–20. doi: 10.1038/ismej.2012.93.

Caporaso, JG, Lauber, CL, Walters, WA, Berg-lyons, D, Lozupone, CA, Turnbaugh, PJ, Fierer, N, and Knight, R (2010) Global patterns of 16S rRNA diversity at a depth of millions of sequences per sample. *Proc Natl Acad Sci USA* **108**: 4516–22. doi:10.1073/pnas.1000080107.

Celikkol-Aydin, S, Gaylarde, CG, Lee, T, Melchers, RE, Witt, DL, and Beech, IB (2016) 16S rRNA gene profiling of planktonic and biofilm microbial populations in the Gulf of Guinea using Illumina NGS. *Mar Environ Res* **122**: 105–12. doi:10.1016/j.marenvres.2016.10.001.

Chen, H, and Boutros, PC (2011) VennDiagram: a package for the generation of highly-customizable venn and euler diagrams in R. *BMC Bioinformatics* **12**(1): 35.

doi:10.1186/1471-2105-12-35.

Clarke, KR, Gorley, RN, Somerfield, PJ and Warwick, RM (2014) Change in marine communities: an approach to statistical analysis and interpretation, 3rd edition. PRIMER-E, Plymouth, 260 pp.

Dang, H, Li, T, Chen, M and Huang, G (2008) Cross-ocean distribution of *Rhodobacterales* bacteria as primary surface colonizers in temperate coastal marine waters. *Appl Environ Microbiol* **74**(1): 52–60. doi:10.1128/AEM.01400-07.

Defer, D, Desriac, F, Henry, J, Bourgougnon, N, Baudy-Floc'h, M, Brillet, B, Le Chevalier, P, and Fleury, Y (2013) Antimicrobial peptides in oyster hemolymph: the bacterial connection. *Fish Shellfish Immun* **34**(6): 1439–47. doi:10.1016/j.fsi.2013.03.357.

Depkat-Jakob, PS, Hilgarth, M, Horn, MA, and Drake, HL (2010) Effect of earthworm feeding guilds on ingested dissimilatory nitrate reducers and denitrifiers in the alimentary canal of the earthworm. *Appl Environ Microbiol* **76**: 6205–6214. doi: 10.1128/AEM.01373-10.

Drake, HL and Horn, MA (2007) As the worm turns: the earthworm gut as a transient habitat for soil microbial biomes." *Annu Rev Microbiol* **61**(1): 169–89. doi: 0.1146/annurev.micro.61.080706.093139.

Eiston, RA, Hasegawa, H, Humphrey, KL, Polyak, IK, and Häse, CC (2008) Re-emergence of *Vibrio tubiashii* in bivalve shellfish aquaculture: severity, environmental drivers, geographic extent and management. *Dis Aquat Organ* **82**(2): 119–34. doi: 10.3354/dao01982.

Erasmus, JH, Cook, PA and Coyne, VE (1997) The role of bacteria in the digestion of

seaweed by the abalone *Haliotis midae*. *Aquaculture* **155**(1–4): 377–86. doi: 10.1016/S0044-8486(97)00112-9.

Fabich, AJ, Jones, SA, Chowdhury, FZ, Cernose, A, Anderson, A, Smalley, D, McHargue, W, Hightower, GA, Smith, JT, Autieri, SM, Leatham, MP, Lins, JL, Allen, FL, Laux, DC, Cohen, PS, and Conway, T (2008) Comparison of carbon nutrition for pathogenic and commensal *Escherichia coli* strains in the mouse intestine. *Infect Immun* **76**(3): 1143–52. doi: 10.1128/IAI.01386-07.

Faury, N, Saulnier, D, Thompson, FL, Gay, M, Swings, J, and Le Roux, F (2004) *Vibrio crassostreae* sp. nov., isolated from the haemolymph of oysters (*Crassostrea gigas*). *Int J Syst Evol Micr* **54**(6): 2137–40. doi: 10.1099/ijs.0.63232-0.

Fegatella, F, Lim, J, Kjelleberg, S, and Cavicchioli, R (1998) Implications of rRNA operon copy number and ribosome content in the marine oligotrophic ultramicrobacterium *Sphingomonas* sp. strain RB2256. *Appl Environ Microbiol* **64**(11): 4433–38.

Fernandez-Piquer, J, Bowman, JP, Ross, T, and Tamplin, ML (2012) Molecular analysis of the bacterial communities in the live Pacific oyster (*Crassostrea gigas*) and the influence of postharvest temperature on its structure. *J Appl Microbiol* **112**(6): 1134–43. doi: 0.1111/j.1365-2672.2012.05287.x.

Fitt, WK, and Coon, SL (1992) Evidence for ammonia as a natural cue for recruitment of oyster larvae to oyster beds in a Georgia salt marsh. *Biol Bull* **182**(3): 401–8.

Ford, TE (2000) Response of marine microbial communities to anthropogenic stress. *J Aquat Ecosys Stress and Recovery* **7**(1): 75–89.

Freter, R, Brickner, H, Botney, M, Cleven, D, and Aranki, A (1983) Mechanisms that

control bacterial populations in continuous-flow culture models of mouse large intestinal flora. *Infect Immun* **39**(2): 676–85.

Galand, PE, Lucas, S, Fagervold, SK, Peru, E, Pruski, AM, Vétion, Dupuy, C, and Guizien, K (2016) Disturbance increases microbial community diversity and production in marine sediments. *Front Microbiol* **7**(DEC): 1–11. doi: 10.3389/fmicb.2016.01950.

Galstoff, PS (1964) The American oyster, *Crassostrea virginica* Gmelin. *US Fish Wildl Serv Fish Bull* **64**: 1-457. doi: 10.4319/lo.1966.11.2.

Garnier, M, Labreuche, Y, Garcia, C, Robert, M, and Nicolas, JL (2007) Evidence for the involvement of pathogenic bacteria in summer mortalities of the Pacific oyster *Crassostrea Gigas*. *Microb Ecol* **53**(2): 187–96. doi:10.1007/s00248-006-9061-9.

Graf, DRH, Jones, CM, and Hallin, S (2014) Intergenomic comparisons highlight modularity of the denitrification pathway and underpin the importance of community structure for N_2O emissions. *PLoS ONE* **9**(12): e114118. doi: 10.1371/journal.pone.0114118

Green, TJ, and Barnes, AC (2010) Bacterial diversity of the digestive gland of Sydney rock oysters, *Saccostrea glomerata* infected with the paramyxean parasite, *Marteilia sydneyi*. *J Appl Microbiol* **109**(2): 613–22. doi:10.1111/j.1365-2672.2010.04687.x.

Harris, J (1993) The presence, nature, and role of gut microflora in aquatic invertebrates: a synthesis. *Microbiol Ecol* **25**(3): 195-231.

Heberle, H, Meirelles, GV, da Silva, FR, Telles, GP, and Minghim, R (2015) InteractiVenn: a web-based tool for the analysis of sets through venn diagrams. *BMC Bioinformatics* **16**(1): 169. doi:10.1186/s12859-015-0611-3.

Heisterkamp, IM, Schramm, A, de Beer, D, and Stief, P (2013) Shell biofilm-associated nitrous oxide production in marine molluscs: processes, precursors and relative importance. *Environ Microbiol* **15**(7): 1943–55. doi: 10.3354/meps08727.

Hernández-Zárate, G, and Olmos-Soto, J (2006) Identification of bacterial diversity in the oyster *Crassostrea gigas* by fluorescent in situ hybridization and polymerase chain reaction. *J Appl Microbiol* **100**(4): 664–72. doi:10.1111/j.1365-2672.2005.02800.x.

Hoellein, TJ, Zarnoch, CB, and Grizzle, RE (2015) Eastern oyster (*Crassostrea virginica*) filtration, biodeposition, and sediment nitrogen cycling at two oyster reefs with contrasting water quality in Great Bay Estuary (New Hampshire, USA). *Biogeochemistry* **122**(1): 113–29. doi: 10.1007/s10533-014-0034-7.

Hoffmann, M, Fischer, M, Ottesen, A, McCarthy, PJ, Lopez, JV, Brown, EW, and Monday, SR (2010) Population dynamics of *Vibrio* spp. associated with marine sponge microcosms. *ISME J* **4**(12): 1608–12. doi: 10.1038/ismej.2010.85.

Humphries, AT, Ayvazian, SG, Carey, JC, Hancock, BT, Grabbert, S, Cobb, D, Strobel, CJ, and Fulweiler, RW (2016) Directly measured denitrification reveals oyster aquaculture and restored oyster reefs remove nitrogen at comparable high rates. *Front Mar Sci* **3**(May): 74. doi: 10.3389/fmars.2016.00074.

Hunt, DE, and Ward, CS (2015) A network-based approach to disturbance transmission through microbial interactions. *Front Microbiol* **6**(OCT): 1–8. doi: 10.3389/fmicb.2015.01182

Husmann, G, Gerdts, G, and Wichels, A (2010) Spirochetes in crystalline styles of marine bivalves: group-specific PCR detection and 16S rRNA sequence analysis. *J Shellfish Res* **29**(4): 1069–75. doi: 10.2983/035.029.0409

Jensen, S, Duperron, S, Birkeland, NK, and Hovland, M (2010) Intracellular *Oceanospirillales* bacteria inhabit gills of Acesta bivalves. *FEMS Microbiol Ecol* **74**(3): 523–33. doi:10.1111/j.1574-6941.2010.00981.x.

Jones, CM, Graf, DRH, Bru, D, Philippot, L, and Hallin, S (2013) The unaccounted yet abundant nitrous oxide-reducing microbial community: a potential nitrous oxide sink. *ISME J* **7**: 417–26. doi: 10.1038/ismej.2012.125.

Jousset, Alexandre, Bienhold, C, Chatzinotas, A, Gallien, L, Gobet, A, Kurm, V, Küsel, K, et al. (2017) Where less may be more: how the rare biosphere pulls ecosystems strings. *The ISME J* **11** (4): 853–62. doi: 10.1038/ismej.2016.174.

Kennedy, VS, and Sanford, LP (1999) Characteristics of relatively unexploited beds of the eastern oyster, *Crassostrea virginica*, and early restoration programs. In *Oyster Reef Habitat Restoration: A Synopsis of Approaches; Proceedings from the Symposium, Williamsburg, Virginia*, eds. Mark W Luckenbach, Roger Mann, and James A Wesson. Gloucester Point, Virginia: Virginia Institute of Marine Science Press, 25–46.

King, GM, Judd, C, Kuske, CR, and Smith, C (2012) Analysis of stomach and gut microbiomes of the eastern oyster (*Crassostrea virginica*) from coastal Louisiana, USA. *PLoS One* **7**(12): e51475. doi: 10.1371/journal.pone.0051475.

Koch, H, Lücker, S, Albertsen, M, Kitzinger, K, Herbold, C, Spieck, Nielsen, PH, Wagner, M, and Daims, H (2015) Expanded metabolic versatility of ubiquitous nitrite-oxidizing bacteria from the genus *nitrospira*. *Proc Natl Acad Sci* USA **112**(36): 11371–76. doi: 10.1073/pnas.1506533112.

Leard, RL, Dugas, R and Berrigan, M (1999) Resource management programs for the

eastern oyster, *Crassostrea virginica*, in the U.S. Gulf of Mexico... ...past, present, future. In *Oyster Reef Habitat Restoration: A Synopsis of Approaches; Proceedings from the Symposium, Williamsburg, Virginia*, eds. Mark W Luckenbach, Roger Mann, and James A Wesson. Gloucester Point, Virginia: Virginia Institute of Marine Science Press, 63–91.

Le Gall, S, Hassen, MB, and Le Gall, P (1997) "Ingestion of a bacterivorous ciliate by the oyster *Crassostrea gigas*: protozoa as a trophic link between picoplankton and benthic suspension-feeders. *Mar Ecol Prog Ser* **152**(1–3): 301–6. doi: 10.3354/meps152301

Lokmer, A, Goedknegt AM, Thieltges, DW, Fiorentino, D, Kuenzel, S, Baines, JF, and Wegner, KM (2016a) Spatial and temporal dynamics of Pacific oyster hemolymph microbiota across multiple scales." *Front Microbiol* **7**(August): 1–18. doi: 10.3389/fmicb.2016.01367.

Lokmer, A, Kuenzel, S, Baines, JF and Wegner, KM (2016b) The role of tissue-specific microbiota in initial establishment success of Pacific oysters." *Environ Microbiol* **18**(3): 970–87. doi: 10.1111/1462-2920.13163.

Lokmer, A and Wegner, KM (2015) Hemolymph microbiome of Pacific oysters in response to temperature, temperature stress and infection. *ISME J* **9**: 670–682. doi: 10.1038/ismej.2014.160.

Luckenbach, MW, Mann, R, and Wesson, JA (1999) *Oyster Reef Habitat Restoration : A Synopsis of Approaches; Proceedings from the Symposium, Williamsburg, Virginia,* eds. Mark W Luckenbach, Roger Mann, and James A Wesson. Gloucester Point, Virginia: Virginia Institute of Marine Science Press

Luter, HM, Widder, S, Botté, E, Wahab, MA, Whalan, S, Moitinho-Silva, Thomas, T, and Webster, NS (2015) Biogeographic variation in the microbiome of the ecologically important sponge, *Carteriospongia foliascens*. *PeerJ* **3**: e1435. doi: 10.7717/peerj.1435

McFall-Ngai, M, Hadfield, MG, Bosch, TCG, Carey, HV, Domazet-Lošo, T, Douglas, AE, Duilier, N, et al. (2013) Animals in a bacterial world, a new imperative for the life sciences. *Proc Natl Acad Sci* USA **110**: 3229–36. doi: 10.1073/pnas.1218525110.

McMurdie, PJ, and Holmes, S (2013) "Phyloseq: an R package for reproducible interactive analysis and graphics of microbiome census data." *PLoS ONE* **8**(4): e61217. doi:10.1371/journal.pone.0061217.

Menge, BA, and Branch, GM. 2001. Rocky Intertidal Communities. In *Marine Community Ecology*, eds. M D Bertness, S D Gaines, and M E Hay. Sinauer Associates, Sunderland, 221–51.

Muehlbauer, F, Fraser, D, Brenner, M, Nieuwenhoe, KV, Buck, BH, Strand, O, Mazurié, Thorarinsdottir, G, Dolmer, P, O'Beirn, Sanchez-Mata, A, Flimlin, G, and Kamermans, P. (2014) Bivalve aquaculture transfers in Atlantic Europe. Part A: transfer activities and legal framework." *Ocean and Coastal Management* **89**: 127–38. doi: 10.1016/j.ocecoaman.2013.12.003

Neave, MJ, Apprill, A, Ferrier-Pagès, C, and Voolstra, CR (2016) Diversity and function of prevalent symbiotic marine bacteria in the genus *Endozoicomonas*. *Appl Microb Biot* **100**(19): 8315– 24. doi:10.1007/s00253-016-7777-0.

Needham, DM, Chow, C-ET, Cram, JA, Sachdeva, R, Parada, A, and Fuhrman, JA (2013) Short-term observations of marine bacterial and viral communities: patterns, connections and resilience. *ISME J* **7**(7): 1274–85. doi: 10.1038/ismej.2013.19.

Olafsen, JA, Mikkelsen, HV, Glaever, HM, and Hansen, GH. (1993) Indigenous bacteria in hemolymph and tissues of marine bivalves at low temperatures. *Appl Environ Microb* **59**(6): 1848–54.

Pfister, CA, Gilbert, JA, and Gibbons, SM (2014) The role of macrobiota in structuring microbial communities along rocky shores. *PeerJ* **2**: e631. doi: 10.7717/peerj.631

Piehler, MF and Smyth, AR (2011) Habitat-specific distinctions in estuarine denitrification affect both ecosystem function and services. *Ecosphere* **2**: art12. doi: 10.1890/ES10-00082.1.

Pierce, ML, Ward, JE, Holohan, BA, Zhao, X, and Hicks, RE (2016) The influence of site and season on the gut and pallial fluid microbial communities of the eastern oyster, *Crassostrea virginica* (Bivalvia , Ostreidae): community-level physiological profiling and genetic structure. *Hydrobiologia* **765**(1): 97–113. doi:10.1007/s10750-015-2405-z.

Poulsen, M, Kofoed, MVW, Larsen, L, Schramm, A, and Stief, P (2014) *Chironomus plumosus* larvae increase fluxes of denitrification products and diversity of nitrate-reducing bacteria in freshwater sediment. *Syst Appl Microbiol* **37**(1): 51–59. doi: 10.1016/j.syapm.2013.07.006

Powell, E (2004) A comparison between a suction dredge and a traditional dredge in the transplantation of oysters in Delaware Bay. *J Shellfish Res* **23**(3): 803–23.

Prieur, D, Nicolas, JL, Plusquellec, A, and Vigneulle, M (1990) Interactions between

bivalve mollusks and bacteria in the marine-environment. *Oceanogr Mar Biol* **28**: 277–352.

Rawls, J. F., B. S. Samuel, and J. I. Gordon. 2004. From The Cover: Gnotobiotic Zebrafish Reveal Evolutionarily Conserved Responses to the Gut Microbiota. *Proc Natl Acad Sci USA* **101**(13): 4596–4601. http://www.pnas.org/cgi/doi/10.1073/pnas.0400706101.

Rognes, T, Flouri, T, Nichols, B, Quince, C, and Mahé, F (2016) VSEARCH: a versatile open source tool for metagenomics. *PeerJ* **4**: e2584. doi:10.7717/peerj.2584.

Roh, SW, Nam, Y-D, Chang, H-W, Kim, K-H, Kim, M-S, Ryu, J-H, Kim, S-H, Lee, W-J, and B, J-W (2008) Phylogenetic Characterization of two novel commensal bacteria involved in innate immune homeostasis in *Drosophila melanogaster*. *Appl Enivron Microb* **74**(20): 6171-77. doi: 10.1128/AEM.00301-08.

Ruehland, C, Blazejak, A, Loft, C, Loy, A, Erséus, Dubilier, N (2008) Multiple bacterial symbionts in two species of co-occurring gutless oligochaete worms from Mediterranean sea grass sediments. *Environ Microbiol* **10**(12): 3404–16. doi: 10.1111/j.1462-2920.2008.01728.x.

Salles, JF, Poly, F, Schmid, B, and Le Roux, X (2017) Community niche predicts the functioning of denitrifying bacterial assemblages. *Ecology* **90**(12): 3324–32.

Sanford, RA, Wagner, DD, Qingzhong, W, Chee-Sanford, JC, Thomas, SH, Cruz-García, C, Rodríguez, G, et al. (2012) Unexpected nondenitrifier nitrous oxide reductase gene diversity and abundance in soils. *Proc Natl Acad Sci USA* **109**: 19709-14. doi: 10.1073/pnas.1211238109.

Sawall, Y, Richter, C, and Ramette, A (2012) Effects of eutrophication, seasonality and

macrofouling on the diversity of bacterial biofilms in equatorial coral reefs." *PLoS ONE* **7**(7). doi: 10.1371/journal.pone.0039951.

Schloss, PD, Westcott, SL, Ryabin, T, Hall, JR, Hartmann, M, Hollister, EB, Lesniewski, RA, et al. (2009) Introducing Mothur: open-source, platform-independent, community-supported software for describing and comparing microbial communities. *Appl Environ Microb* **75**(23): 7537–41. doi:10.1128/AEM.01541-09.

Sender, R, Fuchs, S, and Milo, R (2016) Revised estimates for the number of human and bacteria cells in the body. *PLoS Biol* 14(8): 1-14. doi: 10.1371/journal.pbio.1002533.

Shade, A and Handelsman, J (2012) Beyond the venn diagram: the hunt for a core microbiome. *Environ Microbiol* **14**: 4–12. doi: 0.1111/j.1462-2920.2011.02585.x

Shulman, MJ, Ogden, JC, Ebersole, JP, McFarland, WN, Miller, SL, and Wolf, NG (1983) Priority effects in the recruitment of juvenile coral reef fishes. *Ecology* 64(6): 1508-13. doi: 10.2307/1937505

Shumway, SE and Koehn, RK (1982) Oxygen consumption in the American oyster *Crassostrea virginica. Mar Ecol Prog* **9**(1): 59-68.

Sison-Mangus, MP, Mushegian, AA, and Ebert, D (2015) Water fleas require microbiota for survival, growth, and reproduction. *ISME J* **9**: 59-67. doi: 0.1038/ismej.2014.116.

Stief, P, Poulsen, M, Nielsen, LP, Brix, H, and Schramm, A (2009) Nitrous oxide emission by aquatic macrofauna. *Proc Natl Acad Sci USA* **106**: 4296–300. doi: 10.1073/pnas.0808228106.

Svenningsen, NB, Heisterkamp, IM, Sigby-Clausen, M, Larsen, LH, Nielsen, LP, Stief,

P, and Schramm, A (2012) Shell biofilm nitrification and gut denitrification contribute to emission of nitrous oxide by the invasive freshwater mussel *Dreissena polymorpha* (Zebra mussel). *Appl Environ Microb* **78**: 4505–4509. doi: 10.1128/AEM.00401-12.

Tanaka, R, Ootsubo, M, Sawabe, T, Ezura, Y, and Tajima, K (2004) Biodiversity and in situ abundance of gut microflora of abalone (*Haliotis discus hannai*) determined by culture-independent techniques. *Aquaculture* **241**(1–4): 453–63. doi:10.1016/j.aquaculture.2004.08.032.

Trabal, N, Mazón-Suástegui, JM, Vázquez-Juárez, R, Ascencio-Valle, F, Morales-Bojórquez, E, and Romero, J (2012) Molecular analysis of bacterial microbiota associated with oysters (*Crassostrea gigas and Crassostrea corteziensis*) in different growth phases at two cultivation sites. *Microb Ecol* **64**: 555-69. doi: 10.1007/s00248-012-0039-5.

Trabal Fernández, N, Mazón-Suástegui, JM, Vázquez-Juárez, R, Ascencio-Valle, F, and Romero, J (2014) Changes in the composition and diversity of the bacterial microbiota associated with oysters (*Crassostrea corteziensis*, *Crassostrea gigas* and *Crassostrea sikamea*) during commercial production. *FEMS Microbiol Ecol* **88**: 69–83. doi: 10.1111/1574-6941.12270

Turnbaugh, PJ, Ley, RE, Hamady, M, Fraser-Liggett, CM, Knight, R, and Gordon, JI (2007) The human microbiome project. *Nature* **449**: 804–810. doi: 10.1038/nature06244

Turner, EJ, Zimmer-Faust, RK, Palmer, MA, Luckenbach, M, Pentcheff, ND (1994) Settlement of oyster (*Crassostrea virginica*) larvae: Effects of water flow and a

water-soluble chemical cue. Limnol Oceanogr 39(7): 1579-93. doi: 10.4319/lo.1994.39.7.1579.

Urban, MC, and De Meester, L (2009) Community monopolization: local adaptation enhances priority effects in an evolving metacommunity. *Proc R Soc B* 276: 4129-38. doi: 10.1098/rspb.2009.1382.

Verna, C, Ramette, A, Wiklund, H, Dahlgren, TG, Glover, AG, Gaill, F, and Dubilier, N (2010) High symbiont diversity in the bone-eating worm *Osedax mucofloris* from shallow whale-falls in the North Atlantic. *Environ Microbiol* **12**(8): 2355–70. doi:10.1111/j.1462-2920.2010.02299.x.

Vezzulli, L, Stagnaro, L, Grande, C, Tassistro, G. Canesi, L, and Pruzzo, C (2017) Comparative 16SrDNA gene-based microbiota profiles of the Pacific oyster (*Crassostrea gigas*) and the Mediterranean mussel (*Mytilus galloprovincialis*) from a shellfish farm (Ligurian Sea, Italy). *Microb Ecol*: 1–10. doi: 0.1007/s00248-017-1051-6.

Wallenstein, MD, Myrold, DD, Firestone, M, and Voytek, M (2016) Environmental controls on denitrifying communities and denitrification rates: insights from molecular methods. *Ecol Appl* **16**(6): 2143–52.

Wang, Qi, Garrity, GM, Tiedje, JM, and Cole, JR (2007) Naive bayesian classifier for rapid assignment of rRNA sequences into the new bacterial taxonomy. *Appl Environ Microb* **73**(16): 5261–67. doi:10.1128/AEM.00062-07.

Wegner, KM, Volkenborn, N, Peter, H, and Eiler, A (2013) Disturbance induced decoupling between host genetics and composition of the associated microbiome. *BMC Microbiol* **13**(1) doi: 10.1186/1471-2180-13-252.

Weigel, BL, and Erwin, PM (2017) Effects of reciprocal transplantation on the microbiome and putative nitrogen cycling functions of the intertidal sponge, *Hymeniacidon Heliophila*. *Sci Rep* **7**:43247. doi: 10.1038/srep43247.

Wendling, CC, Batista, FM, and Wegner, KM (2014) Persistence, seasonal dynamics and pathogenic potential of *Vibrio* communities from Pacific oyster hemolymph. *PLoS ONE* **9**(4): e94256. doi: 10.1371/journal.pone.0094256.

Wilhelm, L, Besemer, K, Fasching, C, Urich, T, Singer, GA, Quince, C, and Battin, TJ (2014) Rare but active taxa contribute to community dynamics of benthic biofilms in glacier fed streams. *Environ Microbiol* **16**(8): 2514-24. doi: 10.1111/1462-2920.12392.

Yilmaz, P, Parfrey, LW, Yarza, P, Gerken, J, Ludwig, W, Pruesse, E, Quast, C, Schweer, T, and Glo, FO (2014) The SILVA and "all-species living tree project (LTP)" taxonomic frameworks. *Nucleic Acids Res* **42**(November 2013): D643–48. doi:10.1093/nar/gkt1209.

Zu Ermgassen, PSE, Spalding, MD, Grizzle, RE, and Brumbaugh, RD (2013) Quantifying the loss of a marine ecosystem service: filtration by the eastern oyster in US estuaries. Estuar Coasts **36**: 36-43. doi: 10.1007/s12237-012-9559-y.

Zumft, WG (1997) Cell biology and molecular basis of denitrification *Microbiol Mol Biol R* **61**(4): 533-616.

Zurel, D, Benayahu, Y, Or, A, Kovacs, A, and Gophna, U (2011) Composition and dynamics of the gill microbiota of an invasive Indo-Pacific oyster in the Eastern Mediterranean Sea. *Environ Microbiol* **13**(6): 1467–76. doi:10.1111/j.1462-2920.2011.02448.x.

TABLES

Table 1. Average water parameters measured from surface water. Monitoring stations were located within 100 m of each sampling site. Errors are ± SE.

Station	Total Nitrogen (mg/L)	Total Phosphorus (mg/L)	Particulate Carbon (mg/L)	Fecal Coliform (cfu/100)
Elizabeth	0.59 ± 0.13	0.06 ± 0.02	0.90 ± 0.56	25 ± 0
Lafayette Downstream	0.45 ± 0.07	0.06 ± 0.02	0.78 ± 0.37	25 ± 0
Lafayette Midstream	0.69 ± 0.29	0.10 ± 0.04	1.68 ± 1.18	83 ± 150

Table 2. Environmental parameters measured in surface water at each deployment site and time point.

Timepoint	Site	Temp (C°)	Salinity (ppt)	pH	Turbidty (NTU)	Chl*a* (mg/mL)	DO (mg/L)
T0	Elizabeth	22.7	21.6	7.5	6.3	8.2	7.5
	Lafayette Downstream	23.6	19.4	7.9	17.2	5.0	7.5
	Lafayette Midstream	24.4	17.1	7.7	42.3	16.0	5.2
T1	Elizabeth	27.5	18.8	8.0	5.4	14.9	9.7
	Lafayette Downstream	29.1	18.0	8.1	10.3	27.0	11.6
	Lafayette Midstream	30.1	15.2	8.1	15.2	6.8	6.7
T2	Elizabeth	29.2	21.5	7.3	4.3	5.3	4.3
	Lafayette Downstream	29.1	21.4	7.5	14.9	7.7	5.5
	Lafayette Midstream	31.4	19.4	8.1	20.9	52.1	10.4

Table 3. Summary statistics of 16S rDNA (total) and 16S rRNA (active) amplicon sequencing for oyster and water microbiomes. Numbers of OTUs, percent coverage, Chao I richness, and Shannon diversity were given for subsampled 16S rDNA (total) sequences only. Errors are ± SE.

	Sequence Total		Coverage (%)		OTUs*	Coverage (%)*	Chao I*	Shannon*
	rDNA	rRNA	rDNA	rRNA		rDNA		
Gill	44799 ± 3568	39795 ± 5220	98.3 ± 0.3	96.3 ± 0.4	715 ± 46	95.9 ± 0.4	1196.34 ± 112.49	3.83 ± 0.13
Gut	42331 ± 3101	26387 ± 2163	99.4 ± 0.1	98.9 ± 0.1	273 ± 21	98.6 ± 0.1	447.19 ± 37.15	2.53 ± 0.10
Shell	36682 ± 2114	56398 ± 5214	93.4 ± 0.3	99.4 ± 0.1	1538 ± 40	88.1 ± 0.4	3869.34 ± 130.35	5.56 ± 0.07
Water	68815 ± 6224	26821 ± 4633	98.2 ± 0.2	97.7 ± 0.1	471 ± 30	96.5 ± 0.3	1219.06 ± 91.10	3.36 ± 0.09

*Based on subsamples of 8,075 rDNA sequences

Table 4. Summary statistics of 16S rDNA (total) amplicon sequencing for oyster microbiomes by site, time point, and oyster type. Errors are ± SE.

			Gill			Gut			Shell		
Location	Type	Timepoint	OTUs*	Chao*	Shannon*	OTUs*	Chao*	Shannon*	OTUs*	Chao*	Shannon*
	Deployed	T0	378 ± 94	486.75 ± 98.88	3.89 ± 0.42	130 ± 29	221.27 ± 45.17	2.49 ± 0.31	1602 ± 46	5035.00 ± 243.46	5.49 ± 0.07
Elizabeth	Deployed	T1	445 ± 59	733.90 ± 123.57	2.69 ± 0.07	208 ± 28	315.28 ± 52.67	3.05 ± 0.24	1978 ± 54	6014.33 ± 268.47	5.89 ± 0.06
	Native		590 ± 138	856.72 ± 226.40	3.33 ± 0.45	307 ± 44	446.88 ± 49.50	2.90 ± 0.18	1190 ± 102	3228.60 ± 480.22	4.18 ± 0.27
Lafayette Downstream	Deployed	T1	1098 ± 126	2265.04 ± 332.88	4.28 ± 0.45	400 ± 113	687.61 ± 208.3	2.77 ± 0.42	1853 ± 80	4772.08 ± 394.90	6.01 ± 0.10
	Native		1007 ± 297	2240.3 ± 908.37	3.52 ± 0.78	397 ± 98	649.02 ± 174.2	2.77 ± 0.33	2183 ± 118	6777.56 ± 537.64	5.96 ± 0.12
Lafayette Midstream	Deployed	T1	*NA*	*NA*	*NA*	*NA*	*NA*	*NA*	*NA*	*NA*	*NA*
	Native		949 ± 149	1520.27 ± 266.72	4.60 ± 0.23	389 ± 21	816.56 ± 69.58	2.71 ± 0.35	1724 ± 121	4546.52 ± 348.54	5.94 ± 0.17
Elizabeth	Deployed	T2	665 ± 195	1103.19 ± 353.15	3.52 ± 0.64	159 ± 33	274.97 ± 32.35	1.85 ± 0.34	1814 ± 91	4998.23 ± 269.59	5.60 ± 0.10
	Native		752 ± 102	1011.61 ± 195.16	3.70 ± 0.24	399 ± 72	583.90 ± 111.7	3.01 ± 0.33	1551 ± 84	4105.09 ± 313.77	5.21 ± 0.12
Lafayette Downstream	Deployed	T2	797 ± 110	1283.58 ± 204.59	4.42 ± 0.38	267 ± 67	374.34 ± 103.6	2.42 ± 0.48	1638 ± 68	3862.18 ± 254.43	5.94 ± 0.14
	Native		523 ± 71	679.62 ± 106.36	4.04 ± 0.27	156 ± 17	316.21 ± 39.08	1.68 ± 0.32	1925 ± 131	5346.91 ± 375.67	6.00 ± 0.21
Lafayette Midstream	Deployed	T2	678 ± 103	1183.61 ± 190.06	3.74 ± 0.22	229 ± 87	346.41 ± 156.2	2.41 ± 0.33	1653 ± 48	3688.25 ± 83.18	5.91 ± 0.15
	Native		696 ± 103	991.49 ± 147.97	3.79 ± 0.47	241 ± 78	333.78 ± 94.44	2.36 ± 0.42	1879 ± 81	4877.60 ± 348.07	5.98 ± 0.17

*Based on subsamples of 8,075 sequences

Table 5. PERMANOVA results showing the effect of (A) site and oyster type and (B) site and time point on oyster microbiomes. For model (A) comparisons were made between deployed and native oysters (oyster type) from sites Elizabeth, Lafayette Downstream, and Lafayette Midstream (site) at time point T_2 and for model (B) comparisons were made between deployed oysters from sites Elizabeth and Lafayette Midstream (site) at T_1 and T_2 (time points). PERMANOVAs were conducted using Bray-Curtis resemblance matrices. Significance is indicated in bold ($p<0.05$).

A

PERMANOVA Site x Type (Site)

	Source	Degrees of Freedom	Mean Squares	Pseudo-F	Estimate Variation (Sq. root)	p-value
Gill	Site	2	4533.4	1.9695	14.939	**0.001**
	Type (Site)	3	3024.8	1.3141	12.025	**0.002**
Gut	Site	2	4123	1.5832	12.324	**0.001**
	Type (Site)	3	3732.4	1.4332	15.021	**0.007**
Shell	Site	2	4853.6	3.0858	18.113	**0.001**
	Type (Site)	3	3165.4	2.0125	17.847	**0.001**

B

PERMANOVA Site x Time

	Source	Degrees of Freedom	Mean Squares	Pseudo-F	Estimate Variation (Sq. root)	p-value
Gill	Site	1	6174.5	2.6434	19.592	**0.001**
	Time	1	5203.8	2.2278	16.935	**0.001**
	Site x Time	1	3527.9	1.5103	15.440	**0.013**
Gut	Site	1	4118	1.5158	11.838	**0.047**
	Time	1	5408	1.9906	16.405	**0.002**
	Site x Time	1	3376.5	1.2429	11.487	0.122
Shell	Site	1	2991.6	1.9601	12.105	**0.001**
	Time	1	2515.5	1.6482	9.9463	**0.001**
	Site x Time	1	2494	1.6341	13.913	**0.001**

Table 6. Dispersion effect on oyster microbiomes by site, type, and time point. Sites include Elizabeth, Lafayette Midstream, and Lafayette Downstream, type includes deployed and native, and time includes T_0, T_1, and T_2. Dispersion effects were determined using the PERMDISP test and are based on Bray-Curtis resemblance matrices**.** Significance is indicated in bold ($p<0.05$).

PERMDISP

	Source	Degrees of Freedom	F	p-value
Gill	Site	2	4.6420	0.138
	Type	1	0.9363	0.354
	Time	2	0.4081	0.823
Gut	Site	2	2.1108	0.262
	Type	1	3.9262	0.066
	Time	2	0.9206	0.700
Shell	Site	2	8.1433	**0.006**
	Type	1	33.953	**0.001**
	Time	2	1.2357	0.352

Table 7. Permutational pair-wise comparisons between (A) time points at each site and (B) different sites for each oyster microbiome. Pairwise tests comparing (A) time points T_0, T_1, T_2 were separately run with sites Elizabeth and Lafayette Downstream using the one factor model time and (B) sites Elizabeth, Lafayette Midstream, and Lafayette Downstream were run using the model site x type for factor site and includes deployed and native oysters at time point T_2. All tests were run using PERMANOVAs and Bray-Curtis resemblance matrices. Significance is indicated by bold ($p<0.05$).

A

Microbiome	Site	Timepoints	t	Similarity	p-value
Gill					
	Elizabeth	T0, T1	1.6520	15.038	**0.021**
		T0, T2	1.6264	15.626	**0.022**
		T1,T2	1.2516	23.128	0.146
	Lafayette	T0, T1	1.9993	14.297	**0.005**
	Downstream	T0, T2	1.8197	16.225	**0.010**
		T1,T2	1.5072	29.158	**0.033**
Gut					
	Elizabeth	T0, T1	1.5883	16.063	**0.022**
		T0, T2	1.5293	16.827	**0.023**
		T1,T2	1.2489	22.280	0.129
	Lafayette	T0, T1	1.6872	13.842	**0.014**
	Downstream	T0, T2	1.5138	13.290	**0.038**
		T1,T2	1.2489	21.904	0.170
Shell					
	Elizabeth	T0, T1	1.6927	35.510	**0.020**
		T0, T2	1.9189	31.055	**0.010**
		T1,T2	1.3319	41.658	0.092
	Lafayette	T0, T1	1.7518	31.876	**0.012**
	Downstream	T0, T2	1.9348	31.387	**0.005**
		T1,T2	1.2316	41.059	0.160

B

Microbiome	Site	t	Similarity	p-value
Gill				
	Eliz, Laf.Down	1.3874	27.230	**0.028**
	Eliz, L.af.Mid	1.5152	27.172	**0.010**
	Laf.Down, Laf.Mid	1.2958	29.825	0.057
Gut				
	Eliz, Laf.Down	1.1291	25.832	0.210
	Eliz, L.af.Mid	1.4212	23.611	**0.029**
	Laf.Down, Laf.Mid	1.2059	24.287	0.133
Shell				
	Eliz, Laf.Down	1.6638	34.375	**0.002**
	Eliz, L.af.Mid	2.142	33.820	**0.001**
	Laf.Down, Laf.Mid	1.4038	40.079	**0.025**

Table 8. Relative abundances of the top five most abundant core OTUs in the total and active oyster microbiomes. Errors are ± SE.

Microbiome	OTU	Phylum	Class	Order	Family	Genus	Mean Rel. Abund (%)
Gill.Total							
	Gill.Otu01	Bacteria_unclassified	Bacteria_unclassified	Bacteria_unclassified	Bacteria_unclassified	*NA*	16.1 ± 2.0
	Gill.Otu02	*Proteobacteria*	*Gammaproteobacteria*	*Vibrionales*	*Vibrionaceae*	*Vibrio*	9.6 ± 1.7
	Gill.Otu04	*Proteobacteria*	*Gammaproteobacteria*	*Oceanospirillales*	*Hahellaceae*	*Endozoicomonas*	3.8 ± 1.0
	Gill.Otu12	*Proteobacteria*	*Gammaproteobacteria*	*Alteromonadales*	*Shewanellaceae*	*Shewanella*	2.4 ± 0.6
	Gill.Otu13	*Proteobacteria*	*Alphaproteobacteria*	*Rhodobacterales*	*Rhodobacteraceae*	*NA*	0.9 ± 0.2
Gill.Active							
	Gill.Otu02	*Proteobacteria*	*Gammaproteobacteria*	*Vibrionales*	*Vibrionaceae*	*Vibrio*	10.5 ± 1.7
	Gill.Otu01	Bacteria_unclassified	Bacteria_unclassified	Bacteria_unclassified	Bacteria_unclassified	*NA*	6.8 ± 1.0
	Gill.Otu04	*Proteobacteria*	*Gammaproteobacteria*	*Oceanospirillales*	*Hahellaceae*	*Endozoicomonas*	4.9 ± 1.2
	Gill.Otu05	*Cyanobacteria*	*Cyanobacteria*	*SubsectionI*	*FamilyI*	*Synechococcus*	4.3 ± 0.5
	Gill.Otu13	*Proteobacteria*	*Alphaproteobacteria*	*Rhodobacterales*	*Rhodobacteraceae*	*NA*	2.1 ± 0.8
Gut.Total							
	Gut.Otu01	*Tenericutes*	*Mollicutes*	*Mycoplasmatales*	*Mycoplasmataceae*	*Mycoplasma*	20.9 ± 2.3
	Gut.Otu03	*Tenericutes*	*Mollicutes*	*Mycoplasmatales*	*Mycoplasmataceae*	*Mycoplasma*	9.1 ± 1.5
	Gut.Otu07	*Tenericutes*	*Mollicutes*	*Mollicutes_unclassified*	*Mollicutes_unclassified*	*NA*	5.1 ± 0.8
	Gut.Otu08	*Tenericutes*	*Mollicutes*	*Mycoplasmatales*	*Mycoplasmataceae*	*Mycoplasma*	3.4 ± 1.6
	Gut.Otu14	*Proteobacteria*	*Gammaproteobacteria*	*Vibrionales*	*Vibrionaceae*	*Vibrio*	3.2 ± 0.8
Gut.Active							
	Gut.Otu07	*Proteobacteria*	*Gammaproteobacteria*	*Vibrionales*	*Vibrionaceae*	*Vibrio*	6.6 ± 0.8
	Gut.Otu01	*Tenericutes*	*Mollicutes*	*Mycoplasmatales*	*Mycoplasmataceae*	*Mycoplasma*	3.3 ± 0.4
	Gut.Otu03	*Tenericutes*	*Mollicutes*	*Mycoplasmatales*	*Mycoplasmataceae*	*Mycoplasma*	2.3 ± 0.3
	Gut.Otu08	*Tenericutes*	*Mollicutes*	*Mollicutes_unclassified*	*Mollicutes_unclassified*	*NA*	2.1 ± 0.3
Shell.Total							
	Sh.Otu01	*Proteobacteria*	*Alphaproteobacteria*	*Rhodobacterales*	*Rhodobacteraceae*	*NA*	7.4 ± 0.6
	Sh.Otu02	*Proteobacteria*	*Alphaproteobacteria*	*Rhodobacterales*	*Rhodobacteraceae*	*NA*	4.3 ± 0.3
	Sh.Otu03	*Proteobacteria*	*Alphaproteobacteria*	*Rhodobacterales*	*Rhodobacteraceae*	*NA*	3.3 ± 0.3
	Sh.Otu07	*Proteobacteria*	*Gammaproteobacteria*	*Cellvibrionales*	*Halieaceae*	*NA*	2.1 ± 0.1
	Sh.Otu14	*Bacteroidetes*	*Sphingobacteriia*	*Sphingobacteriales*	*Sphingobacteriales_unclassified*	*NA*	1.4 ± 0.2
Shell.Active							
	Sh.Otu01	*Proteobacteria*	*Alphaproteobacteria*	*Rhodobacterales*	*Rhodobacteraceae*	*NA*	4.8 ± 0.3
	Sh.Otu02	*Proteobacteria*	*Alphaproteobacteria*	*Rhodobacterales*	*Rhodobacteraceae*	*NA*	2.8 ± 0.2
	Sh.Otu03	*Proteobacteria*	*Alphaproteobacteria*	*Rhodobacterales*	*Rhodobacteraceae*	*NA*	2.7 ± 0.3
	Sh.Otu05	*Proteobacteria*	*Alphaproteobacteria*	*Rhodobacterales*	*Rhodobacteraceae*	*NA*	1.9 ± 0.1
	Sh.Otu15	*Proteobacteria*	*Gammaproteobacteria*	*Vibrionales*	*Vibrionaceae*	*Vibrio*	1.4 ± 0.3

Table 9. Relative abundances of total and active *nosZ* genes. *NosZ* genes are grouped by site, time point, and oyster type in the oyster gill, gut, and shell microbiomes. The *nosZ*.combined gene is the combination of gene clades *nosZI* and *nosZII*. Errors are ± SE.

				Total Microbiome			Active Microbiome		
Timepoint	Site	Oyster Type	Microbiome	*nosZI*	*nosZII*	*nosZ*.combined	*nosZI*	*nosZII*	*nosZ*.combined
T0		Deployed							
			Gill	1.88 ± 0.33	5.44 ± 1.71	7.26 ± 1.85	4.05 ± 0.61	5.08 ± 0.59	9.29 ± 0.96
			Gut	0.66 ± 0.27	1.30 ± 0.29	1.96 ± 0.54	4.80 ± 0.73	4.05 ± 1.94	8.85 ± 2.22
			Shell	7.93 ± 0.62	10.57 ± 0.73	18.43 ± 0.74	8.69 ± 0.38	8.81 ± 0.57	17.43 ± 0.71
T1	Elizabeth	Deployed							
			Gill	1.94 ± 0.54	7.15 ± 2.13	9.09 ± 2.58	3.29 ± 0.51	6.14 ± 1.67	9.41 ± 1.94
			Gut	1.06 ± 0.38	2.16 ± 0.69	3.22 ± 0.96	0.89 ± 0.15	2.82 ± 1.15	3.71 ± 1.30
			Shell	5.82 ± 0.49	14.41 ± 0.71	20.19 ± 0.60	7.21 ± 0.78	11.96 ± 0.54	19.13 ± 0.79
T2	Elizabeth	Deployed							
			Gill	5.80 ± 1.45	4.26 ± 1.57	9.92 ± 2.60	7.49 ± 1.40	6.30 ± 1.91	13.69 ± 2.68
			Gut	0.20 ± 0.15	0.16 ± 0.08	0.36 ± 0.23	0.88 ± 0.43	1.80 ± 1.40	2.67 ± 1.82
			Shell	7.18 ± 0.84	10.28 ± 0.50	17.43 ± 0.45	7.73 ± 0.78	15.22 ± 3.31	22.92 ± 2.58
T1	Elizabeth	Native							
			Gill	8.97 ± 4.44	5.86 ± 0.95	14.82 ± 5.26	4.39 ± 0.99	5.88 ± 0.93	10.26 ± 1.69
			Gut	1.49 ± 0.98	0.97 ± 0.35	2.46 ± 1.30	1.43 ± 0.44	3.76 ± 1.77	5.19 ± 2.06
			Shell	10.46 ± 1.19	6.45 ± 0.34	16.91 ± 1.04	3.52 ± 0.93	4.58 ± 1.85	8.10 ± 2.74
T2	Elizabeth	Native							
			Gill	9.29 ± 6.24	3.98 ± 0.42	13.26 ± 6.04	9.30 ± 0.47	7.76 ± 0.79	17.05 ± 1.25
			Gut	0.95 ± 0.77	1.40 ± 0.91	2.34 ± 1.67	3.54 ± 0.91	2.82 ± 0.68	6.34 ± 1.47
			Shell	9.20 ± 0.86	8.01 ± 0.92	17.21 ± 0.64	8.97 ± 1.56	7.08 ± 0.70	16.02 ± 1.58
T1	Lafayette Downstream	Deployed							
			Gill	1.32 ± 0.41	3.81 ± 1.81	5.12 ± 2.21	3.31 ± 0.20	3.82 ± 0.47	7.13 ± 0.61
			Gut	0.09 ± 0.04	0.16 ± 0.05	0.23 ± 0.08	1.99 ± 0.64	1.99 ± 0.92	3.94 ± 1.50
			Shell	6.07 ± 1.05	11.41 ± 2.03	17.43 ± 2.69	9.90 ± 0.95	10.35 ± 0.79	20.14 ± 0.35
T2	Lafayette Downstream	Deployed							
			Gill	3.19 ± 1.54	3.45 ± 0.63	6.60 ± 1.82	2.39 ± 0.30	4.61 ± 0.30	6.95 ± 0.30
			Gut	0.97 ± 0.72	1.05 ± 0.52	2.02 ± 0.91	1.85 ± 1.19	2.10 ± 1.00	3.94 ± 1.74
			Shell	8.24 ± 0.97	7.90 ± 0.56	16.11 ± 0.55	8.31 ± 1.10	12.18 ± 0.66	20.41 ± 0.51
T1	Lafayette Downstream	Native							
			Gill	1.32 0.41	3.81 1.81	5.12 2.21	1.75 ± 0.60	4.65 ± 2.52	6.39 ± 3.08
			Gut	0.33 0.08	1.28 0.24	1.61 0.32	0.88 ± 0.33	3.70 ± 2.18	4.58 ± 2.49
			Shell	5.23 1.06	10.26 1.26	15.49 1.74	6.43 ± 1.58	9.33 ± 1.35	15.70 ± 2.79
T2	Lafayette Downstream	Native							
			Gill	1.32 ± 0.41	3.81 ± 1.81	5.12 ± 2.21	2.73 ± 0.28	5.08 ± 0.50	7.77 ± 0.74
			Gut	0.09 ± 0.04	0.16 ± 0.05	0.23 ± 0.08	0.43 ± 0.25	0.67 ± 0.20	1.08 ± 0.43
			Shell	6.07 ± 1.05	11.41 ± 2.03	17.43 ± 2.69	10.66 ± 1.69	11.23 ± 0.81	21.78 ± 1.64
T2	Lafayette Midstream	Deployed							
			Gill	2.31 ± 0.65	4.46 ± 1.35	6.71 ± 1.62	6.58 ± 1.02	7.82 ± 0.97	14.37 ± 1.95
			Gut	0.49 ± 0.27	1.77 ± 0.58	2.26 ± 0.80	1.00 ± 0.58	1.56 ± 0.68	2.56 ± 1.26
			Shell	6.71 ± 1.00	11.37 ± 1.08	18.07 ± 0.22	9.90 ± 1.05	12.24 ± 0.95	22.10 ± 1.67
T1	Lafayette Midstream	Native							
			Gill	2.78 ± 0.36	3.26 ± 0.50	6.02 ± 0.81	3.54 ± 0.35	7.89 ± 1.51	11.35 ± 1.61
			Gut	0.74 ± 0.35	1.01 ± 0.40	1.75 ± 0.71	0.49 ± 0.27	1.77 ± 0.58	2.26 ± 0.80
			Shell	7.85 ± 0.67	9.42 ± 0.60	17.21 ± 0.34	7.09 ± 0.55	14.85 ± 0.64	21.90 ± 0.55
T2	Lafayette Midstream	Native							
			Gill	3.19 ± 1.54	3.45 ± 0.63	6.60 ± 1.82	4.28 ± 1.06	8.23 ± 2.04	12.43 ± 2.93
			Gut	0.97 ± 0.72	1.05 ± 0.52	2.02 ± 0.91	1.05 ± 0.54	2.74 ± 1.48	3.66 ± 1.90
			Shell	8.24 ± 0.97	7.90 ± 0.56	16.11 ± 0.55	9.75 ± 1.19	13.89 ± 1.31	23.60 ± 1.08

Table 10. **Mean relative abundances of the total and active core *nosZ* genes.** Relative abundances are the percentage of *nosZ* genes comprising the core microbiomes of the gill, gut, shell, and reef sediment. The *nosZ*.combined gene is the combination of gene clades *nosZ*I and *nosZ*II.

Microbiome	Gene	Total Relative Abundance (%)	Active Relative Abundance (%)
Gill			
	nosZ.combined	9.4	20.3
	*nosZ*I	5.3	15.8
	*nosZ*II	4.1	4.5
Gut			
	nosZ.combined	0.3	2.3
	*nosZ*I	0.0	0.0
	*nosZ*II	0.3	2.3
Shell			
	nosZ.combined	20.5	25.1
	*nosZ*I	13.3	14.6
	*nosZ*II	7.2	10.5

FIGURES

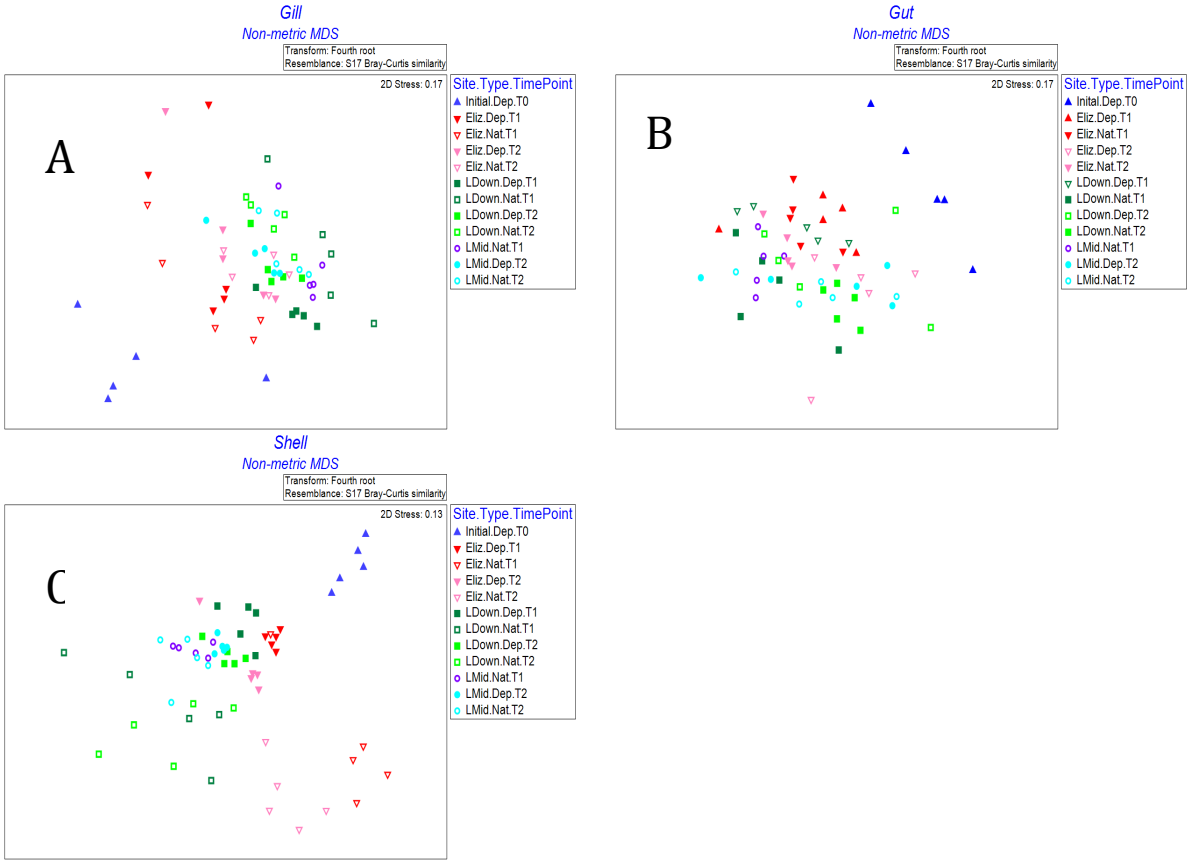

Figure 1. Non-metric multidimensional scaling (nMDS) plot based on a Bray-Curtis resemblance matrix depicting β-diversity among (A) gill, (B), gut, and (C) shell microbiomes in relation to site, time point, and oyster type.

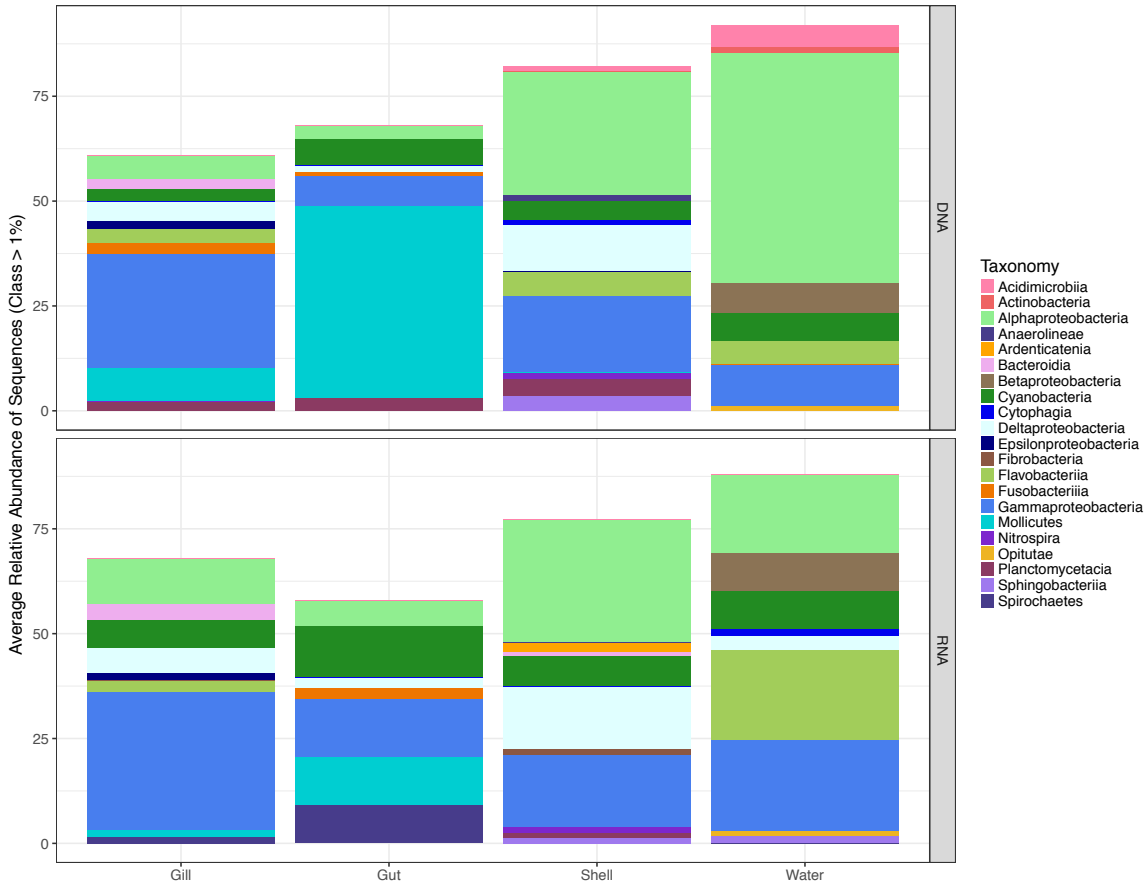

Figure 2. Average relative abundances of bacterial classes found in the total (rDNA) and active (rRNA) gill, gut, shell, and water microbiomes.

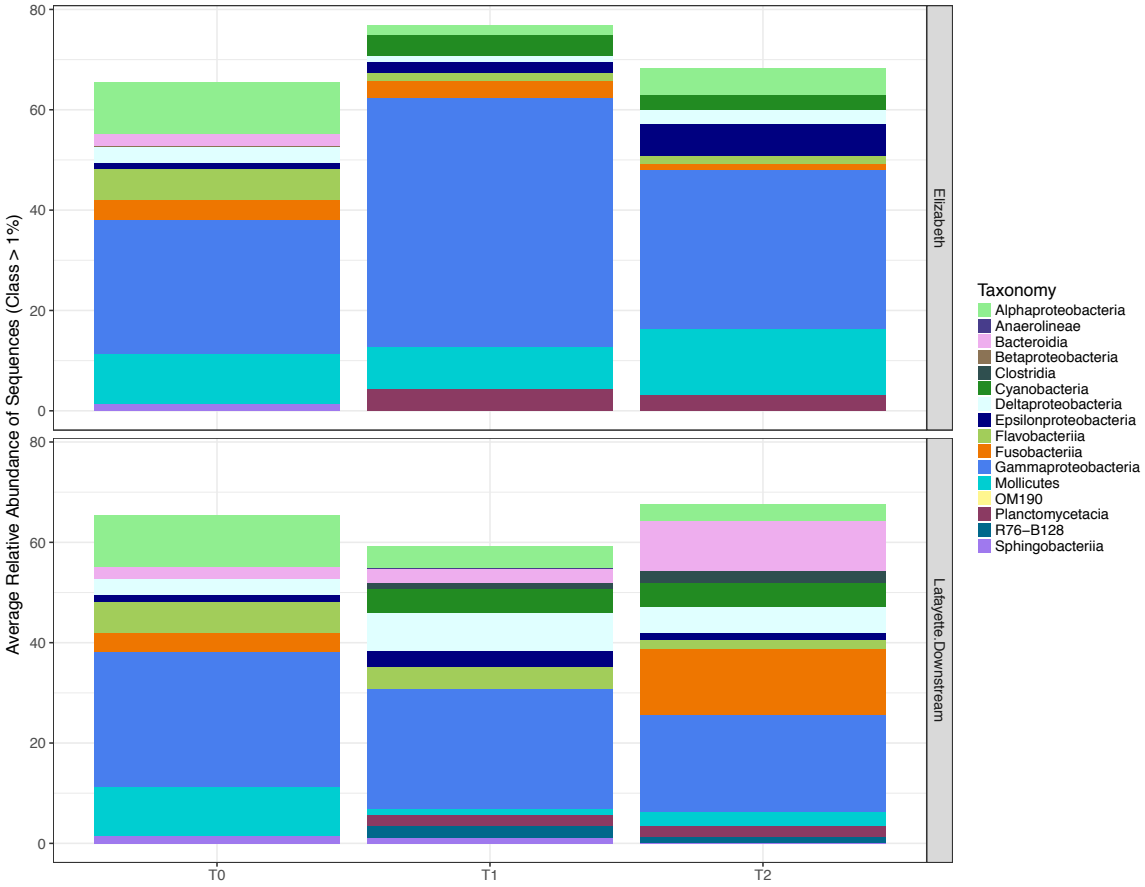

Figure 3. Average relative abundances of bacterial classes in deployed oyster total (rDNA) gill microbiome grouped by time point and site.

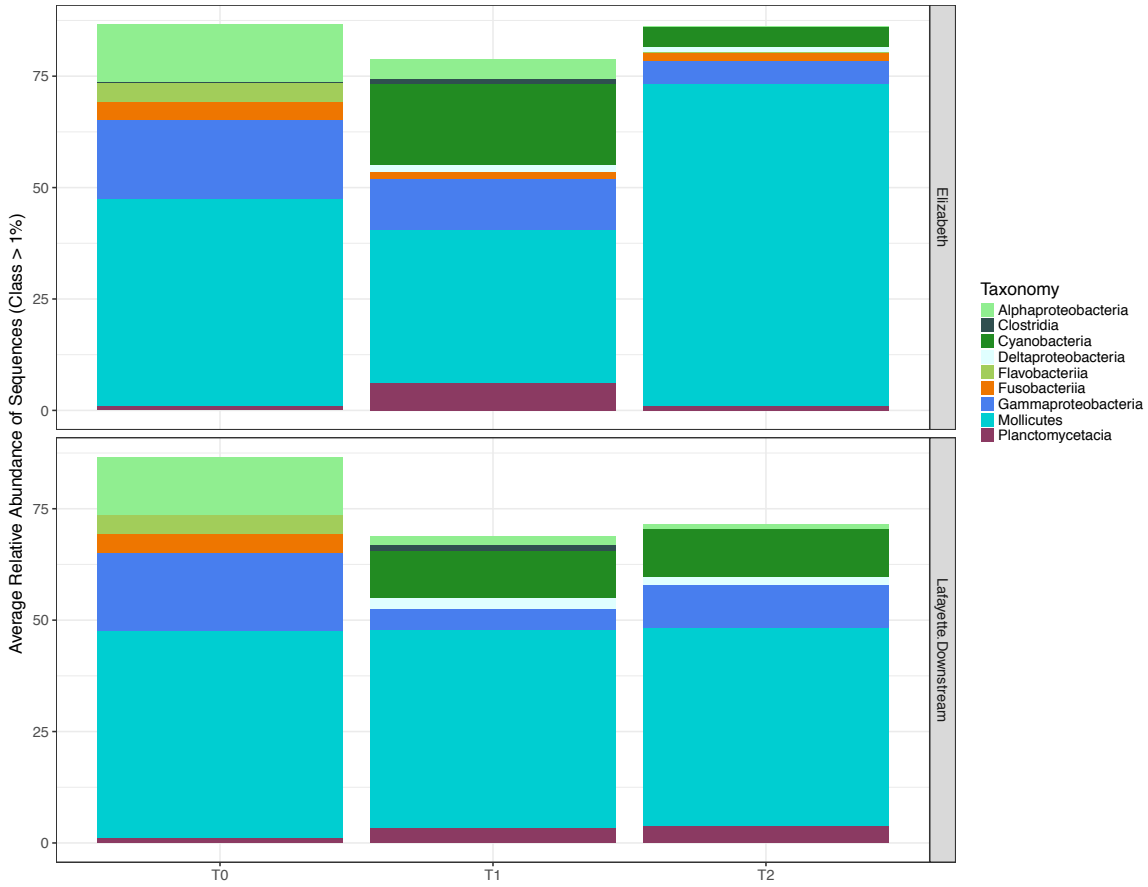

Figure 4. Average relative abundances of bacterial classes in deployed oyster total (rDNA) gut microbiome grouped by time point and site.

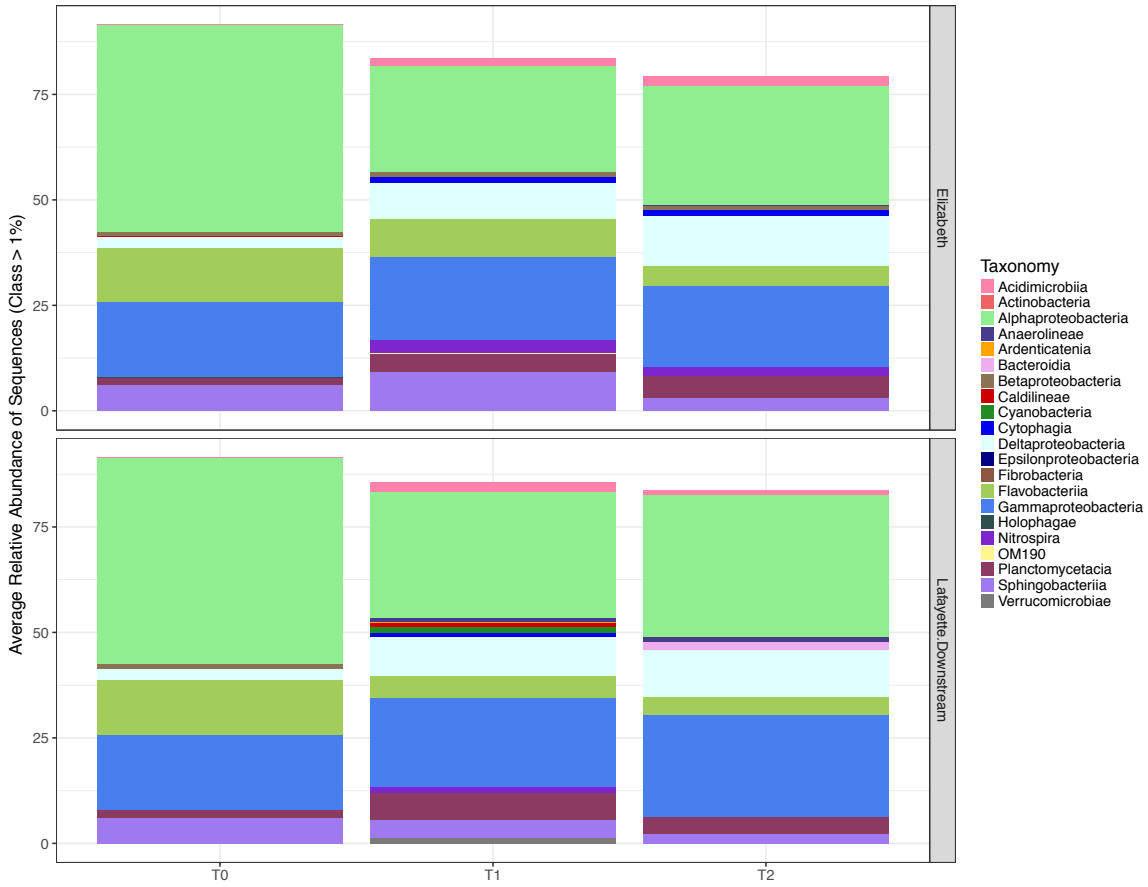

Figure 5. Average relative abundances of bacterial classes in deployed oyster total (rDNA) shell microbiome grouped by time point and site.

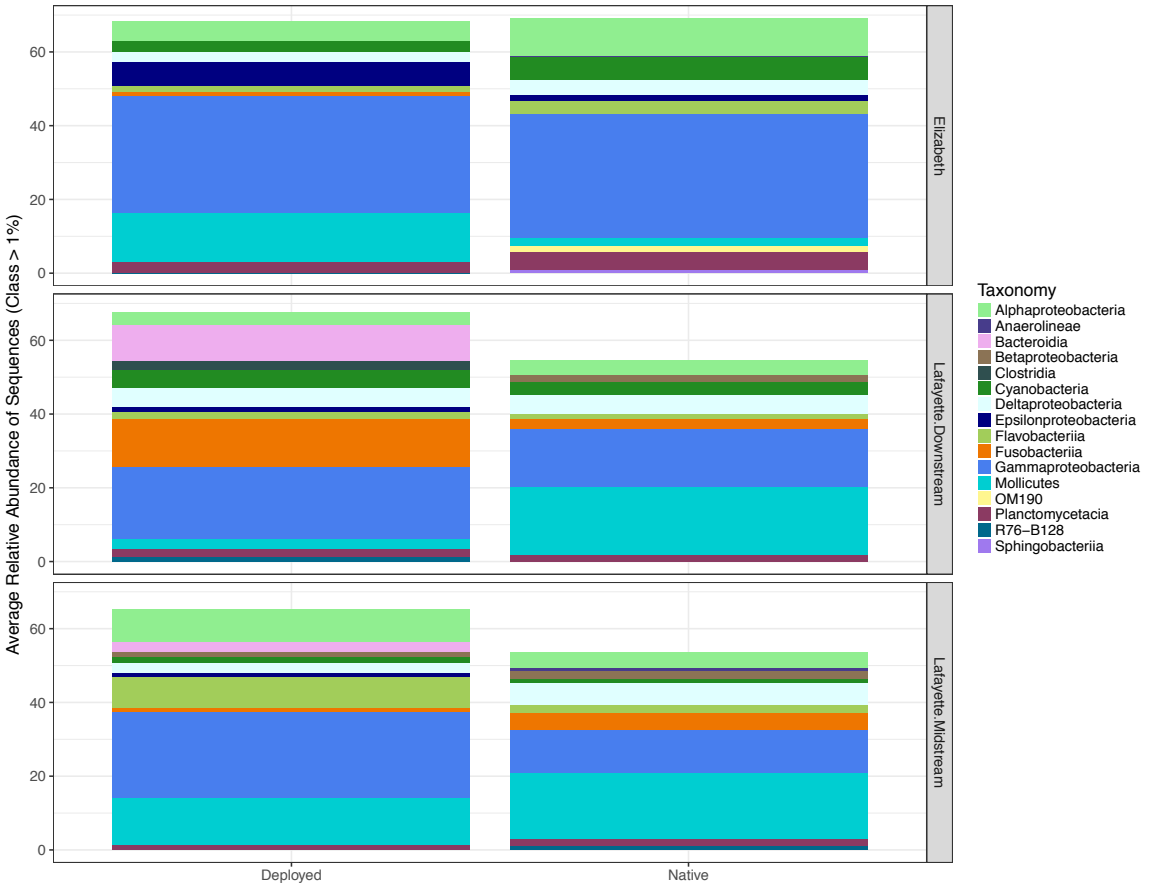

Figure 6. Average relative abundances of bacterial classes in oyster total (rDNA) gill microbiome at time point T_2 grouped by oyster type and site.

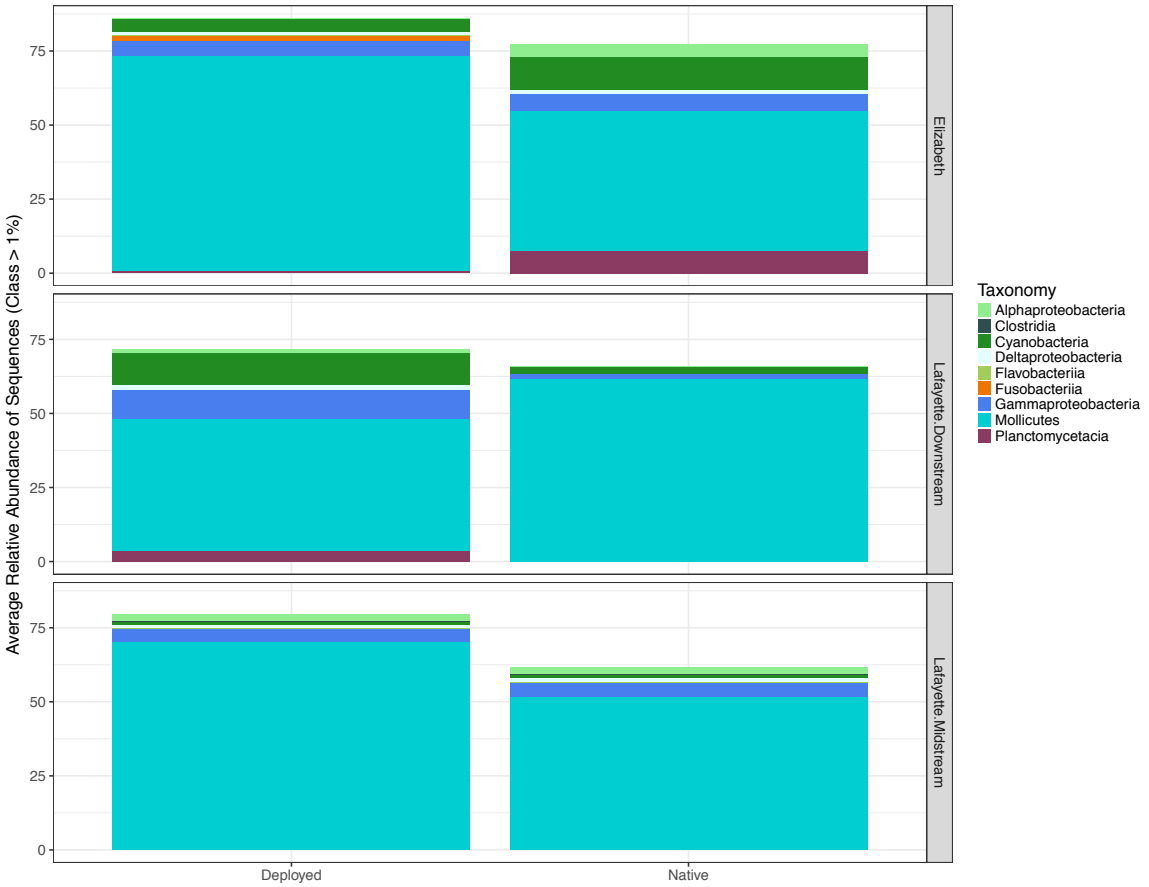

Figure 7. Average relative abundances of bacterial classes in oyster total (rDNA) gut microbiome at time point T_2 grouped by oyster type and site.

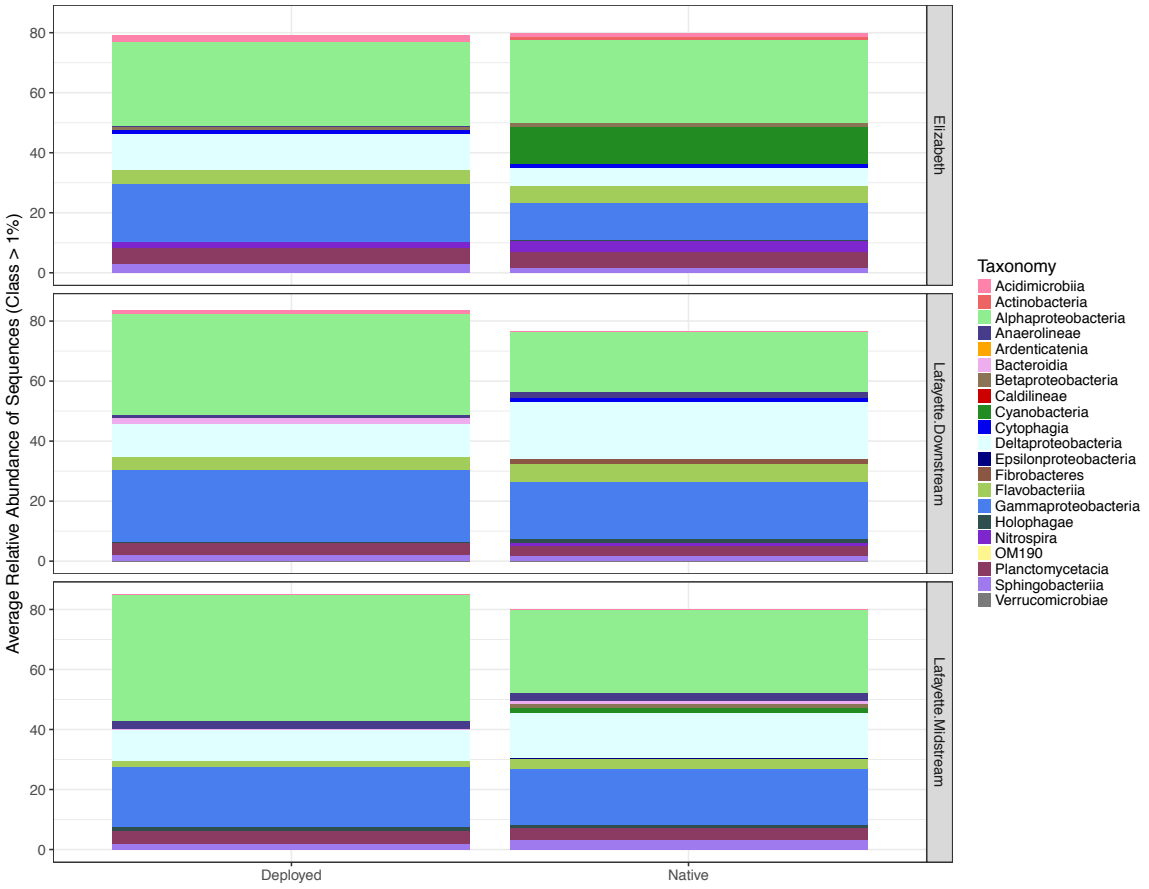

Figure 8. Average relative abundances of bacterial classes in oyster total (rDNA) gut microbiome at time point T_2 grouped by oyster type and site.

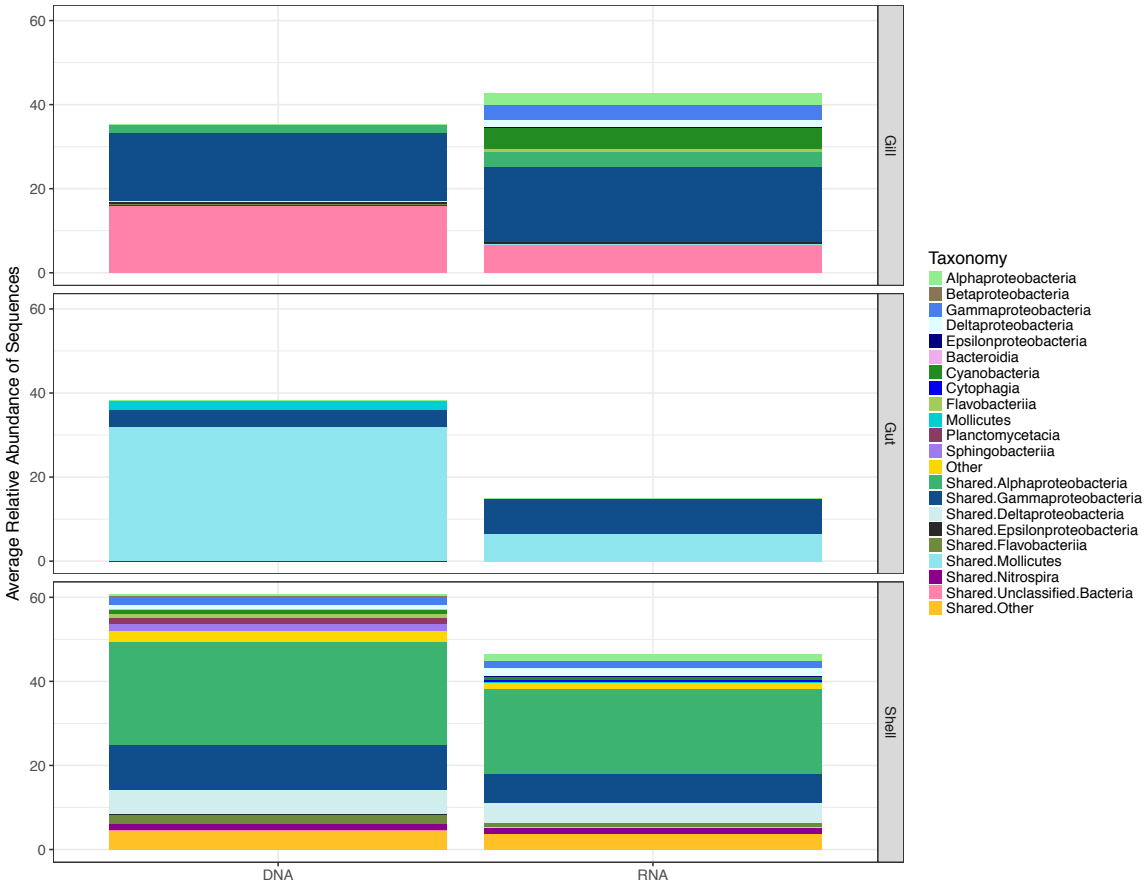

Figure 9. Average relative abundances of bacterial classes in oyster total (rDNA) and active (rRNA) core gill, gut, and shell microbiomes. "Shared" indicates that the OTUs found in that bacterial class are present in both the total and active core microbiomes for either the gill, gut, or shell.

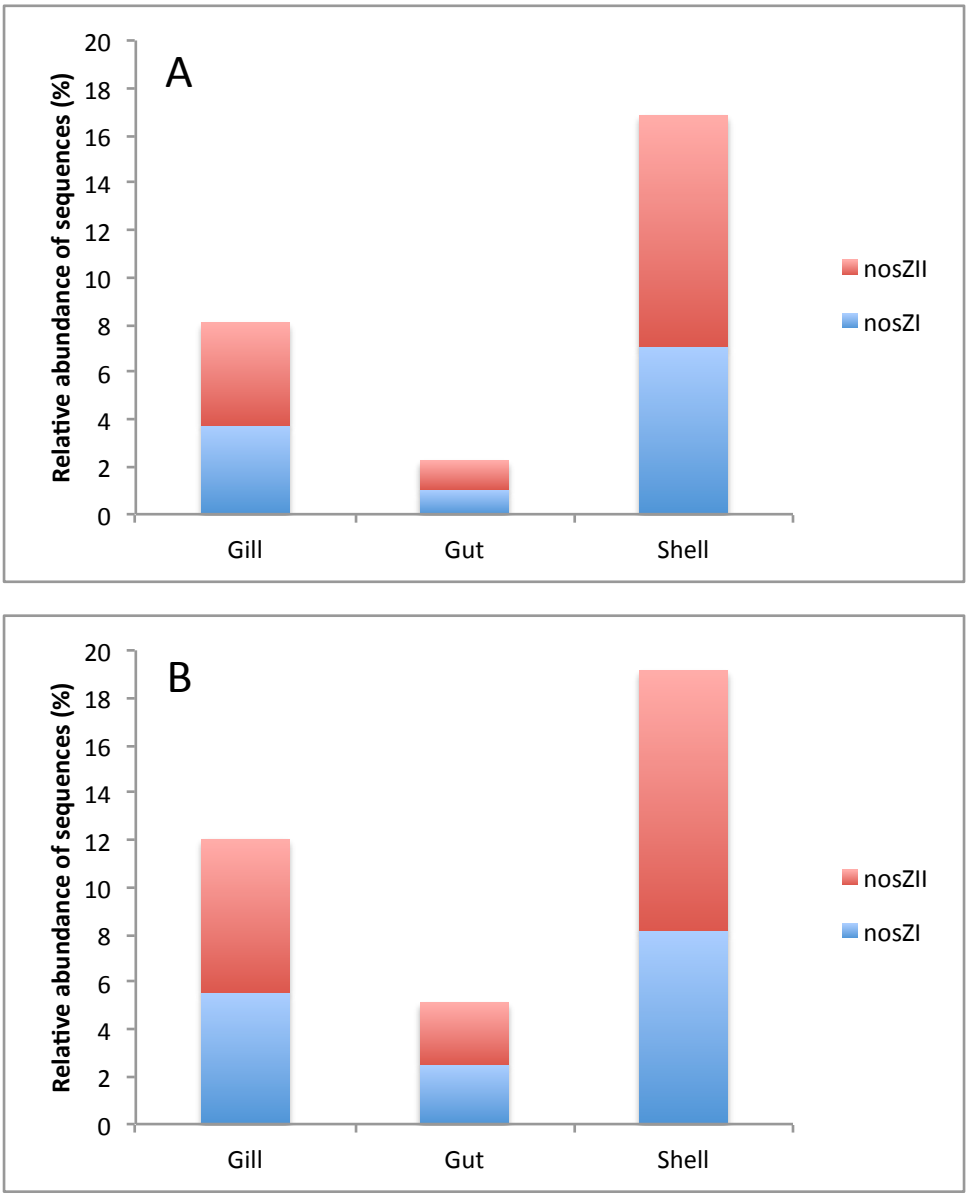

Figure 10. Comparison of mean relative abundances of *nos*ZI and *nos*ZII genes between the (A) total and (B) active oyster gill, gut, and shell microbiomes.

Figure 11. Average relative abundances of genes *nos*ZI and *nos*ZII in oyster total (rDNA) and active (rRNA) microbiomes grouped by site and oyster type.

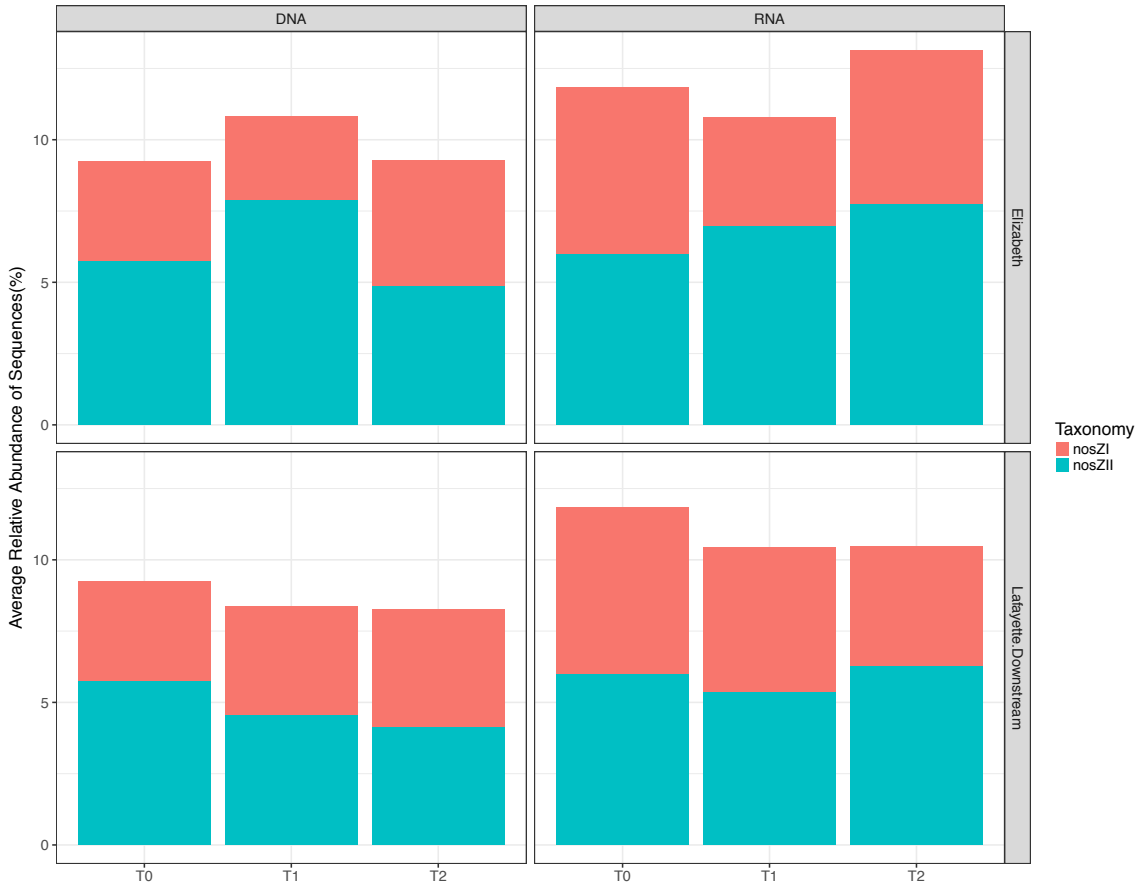

Figure 12. Average relative abundances of genes *nos*ZI and *nos*ZII in oyster total (rDNA) and active (rRNA) microbiomes a grouped by time point and site.

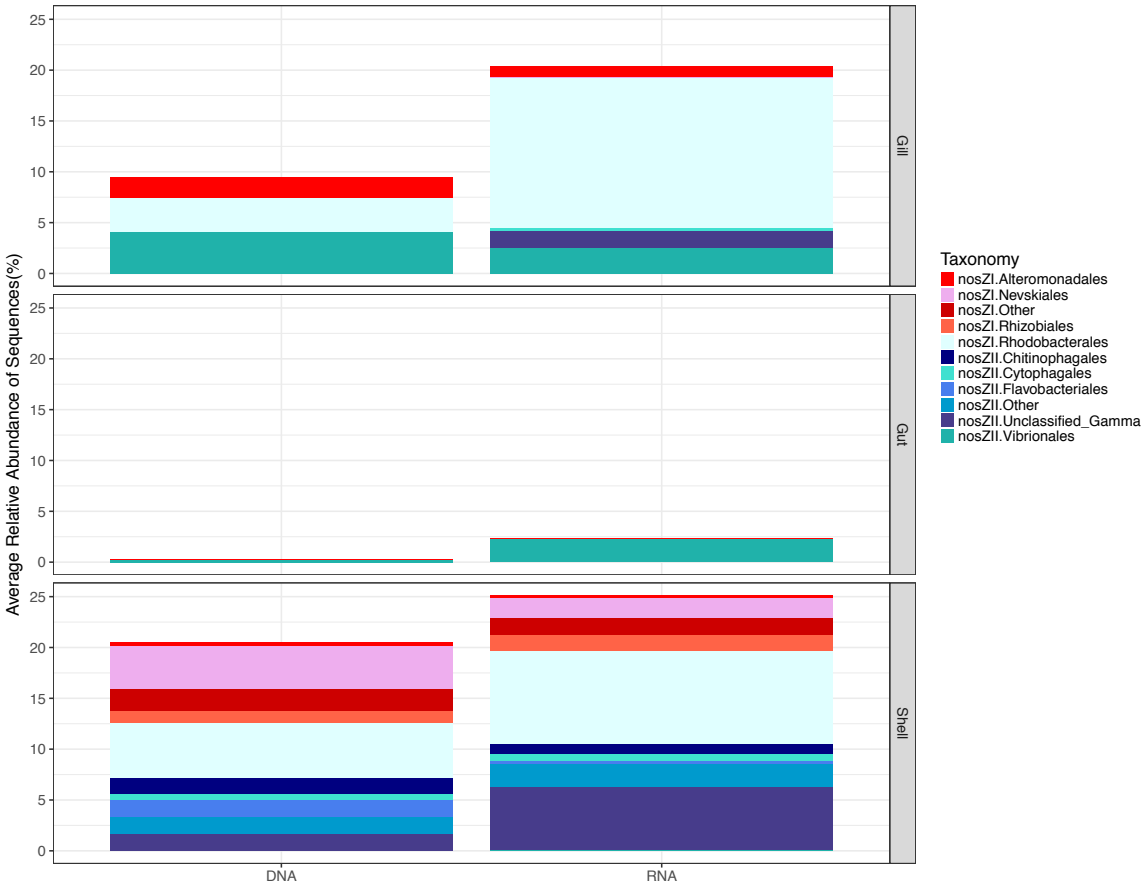

Figure 13. Average relative abundances of orders in denitrifiers carrying *nos*ZI or *nos*ZII genes in oyster total (DNA) and active (RNA) core microbiomes.

Chapter 5

16S rRNA gene-based comparison of composition and diversity of development stages in the eastern oyster (*Crassostrea virginica*) larval microbiome

ABSTRACT

An ongoing goal of the aquaculture industry is the improvement of oyster larval growth and success. One component of oyster rearing that may contribute to the health of oyster larvae is the early colonization and development of the oyster larval microbiome. The main objectives of this study were to investigate the effects on the microbiomes of larvae raised in different hatcheries and from different spawns and determine whether a core microbiome is present throughout the different larvae stages of development. Microbiome composition and structure was characterized using a 16S amplicon-based metagenomic approach on larval samples collected from four different hatcheries for during spawning events. Larval and water samples from each spawning cohort were taken at 24-hours 'D' shape (D-stage), 1-week veliger (V-stage), and 2-weeks pediveliger (PV-stage) time points. Larval microbiomes were significantly different than the hatchery seawater and were affected by hatchery and spawn, but not by developmental stage. However, there was a decrease in species richness from the initial D-stage larvae through the final PV-stage, suggesting a shift towards a more restricted microbiome as the oyster developed. Throughout all developmental stages, a core microbiome was present in the oyster larvae and comprised approximately one quarter of the larval microbiome. Some genera, such as *Alteronomonas* and *Roseobacter* identified in the larval core microbiome, include bacterial species that have shown to offer bivalve larvae some protection against pathogens. Other genera found in the larval core microbiome, such as *Citromicrobium* and *Hoeflea*, are commonly isolated from microalgal species and most likely indicate an association with oyster larval feeding. With exception of *Tenacibaculum* and *Marinobacter,* which were found to be

significantly higher in oyster larvae, the larval core microbiome was similar in composition to the hatchery water. This suggests that the larvae core is a reflection of the hatchery water microbiomes and indicates the importance of maintaining beneficial microbes in the hatchery water, with potential implications in the use of probiotics.

INTRODUCTION

Aquaculture of the eastern oyster (*Crassostrea virginica*) is a rapidly expanding and economically important industry in the Chesapeake Bay. Based on the latest Virginia survey, a reported 40.2 million aquaculture oysters were sold in 2015 and totaled $16.5 million, an increase in production of 14% from 2015 (Hudson and Murray 2017). To meet increasing demands, oyster hatcheries are continually striving to improve oyster seed and larvae health and optimize rearing conditions. The importance of microbiome on the health and growth of oyster larvae has recently received increasing attention from oyster hatcheries. Early colonization of key bacteria in the oyster larvae microbiome may provide advantages to the oyster as it transitions into an adult. Previous studies have suggested that bacterial colonization may play an important role not only in the development of a bivalve's gastrointestinal tract but may also reduce or prevent detrimental microorganisms from proliferating and causing disease by creating competition for nutrients, reducing space for settlement, or producing antimicrobials (Harris 1993, Gomez-Gil et al. 2000, Castro et al. 2002, Schulze et al. 2006, Prado et al. 2010, Kesarcodi-Watson 2012). Probiotics, for example, include beneficial bacteria that improve health or reduce disease, administered to bivalve larvae at early stages of development have shown to increase the survival of oysters, as well as inhibit pathogenic bacteria, such as *Vibrio* species *V. alginolyticus*, *V. tubiashii*, *V. anguillarum*, and *V. splendidus* (Riquelme et al. 1996, Ruiz-Ponte et al. 1999, Schulze et al. 2006, Prado et al. 2009, Prado et al. 2010).

Larval microbiomes may be established during different stages of development as larvae are exposed to different seawater and food sources provided by hatcheries. In

oyster development, ontogenesis begins with fertilization and is followed within 24 hours by a free-swimming trocophore stage. Immediately following the trocophore stage, the D-shape stage is characterized by the formation of an initial outer layer of shell composed of calcium carbonate (Kniprath 1981, His and Maurer 1988). During the transition from D-stage into the veliger or umbo stage, larvae continue to grow, incorporating aragonite and calcite into their shell (Miyazaki et al 2010), developing the umbone, and increasing the size of their digestive organs. The final phase of development, occurring approximately two weeks after the trocophore stage and before larvae settlement, is the pediveliger stage, which is characterized by a crawling foot and appearance of gill rudiments. From the initial onset of oyster larvae development through its later stages of organ and shell development, the oyster's exterior shell surface and interior tissues are continuously exposed to bacteria in the surrounding seawater. During exposure, exogenous bacteria from the hatchery environment rapidly colonize larvae oyster surfaces and tissues to become resident bacteria (Brown 1973, Kueh and Chan 1985). Factors such as temperature, salinity, nutrients, and oxygen content of seawater are all likely to influence the microbiomes of oyster larvae (Powell et al. 2013), and thus may affect larval microbiome development.

Culture-based studies that began in the 1960s primarily investigated bacterial isolates related to larval bivalve disease and survival, including species of *Vibrio* and *Pseudomonas* (Murchelano et al. 1969, Garland et al. 1993, Nicolas et al. 1996, Sainz-Hernández and Maeda-Martínez 2005). Apart from these studies, very little is known about the composition of oyster larvae microbiome. Asmani et al. (2016) is the only study to date that has examined the composition of the early oyster larvae microbiome

using non-culture based techniques. 16S rRNA gene-based metagenomic technique was used to compare the bacterial communities of 7- and 15-day-old *C. gigas* larvae from different rearing systems including a recycling aquaculture system and a flow-through system. Larval bacterial communities were found to be primarily composed of *Alpha*- and *Gammaproteobacteria*. Additionally, this study also demonstrated that the composition of oyster larvae microbiomes was highly similar regardless of treatments to the rearing systems, with most variation occurring as a function of larvae age. While Asmani et al. (2016) was the first study exploring the baseline composition of oyster larvae microbiome, all experiments were conducted at the same hatchery and used the same brood stock and algae feed, likely masking the true variation of the oyster larvae microbiome.

The variation in microbiomes is likely to arise from oyster larvae raised under different hatchery conditions, while some bacteria may be present in all oyster larvae regardless of locations and conditions. Furthermore, some of these bacteria may remain present in the oyster larvae as it transitions through different developmental stages. For example, Trabal et al. (2012) found that bacteria assigned to the genus of *Burkholderia* identified in post-larvae gastrointestinal tracts of *C. corteziensis* and *C. gigas* remained within the oysters from the post larvae stage through adulthood at different cultivation sites. The bacterial taxa that are present throughout the different development stages of the oyster larvae and different hatcheries may be considered to be part of the 'core microbiome'. Core microbiomes may be comprised of common or rare bacteria that have been hypothesized to be selectively adapted to specialized niches provided by their host (Roeselers et al. 2011, Schmitt et al. 2012, Schauer et al. 2014) and likely to be linked to

functions critical to homeostasis, development, and biological functions (McFall-Ngai et al. 2013). Thus it is essential to examine the core microbiome in larval oysters, which may have a significant role in the development and success of oyster larvae in the aquaculture industry.

To more deeply investigate the variation and complexities of the *C. virginica* larvae microbiome and examine the effects of hatchery, spawn, and development stage on the larvae microbiome, we conducted a 16S rRNA gene-based metagenomic study examining the microbiomes of *C. virginica* larvae and hatchery seawater from three different spawns at four different hatcheries over the course of three development stages. The primary objectives of this study were to (1) to compare the diversity and composition of the oyster larvae microbiomes from a variety of hatcheries and spawning events, (2) determine the changes to the larvae microbiome between the different larvae development stages, and (3) identify the set of bacteria that were shared among all larvae, defined here as the oyster larvae core microbiome, which may become a microbial indicator predicting the success of oyster hatchery practices.

MATERIALS AND METHODS

Sample Collection and Hatchery Descriptions

Live oyster larvae samples were collected from 4 different hatcheries at 3 developmental stage time points: (1) D-stage (D, 48-hours), (2) Veliger (V, 1-week), and (3) Pediveliger (PV, 2-weeks), for 3 separate, consecutive spawning events between June and August 2015. Hatcheries were selected for larval sampling based on location and participation. Hatcheries Gloucester Point (A) and Kauffman Aquaculture Center (B) are both research oyster hatcheries operated by the Virginia Institute of Marine Science Aquaculture Genetics and Breeding Technology Center (ABC) and located on the York and Locklies Creek off the Rappahanok River, respectively. Hatchery C and D are both commercial oyster hatcheries located near on the Ware River near Mobjak Bay and the Piankatank River, respectively. Water treatment at hatcheries A and B are similar with sand filtration and recirculation of water through diatomaceous earth and UV treatment. At hatchery C, larvae are raised in a flow through design in which water runs through a single pass multimedia filter system. Water at hatchery D is initially passed through different bag filters of different pore sizes, followed by sand filtration with fluidized charcoal and an additional bag filter. No antibiotics or probiotics are used to treat the water or oyster larvae at any of the facilities. At all four hatcheries, a variety of cultured algal species are grown for feeding oyster larvae. Oyster larvae at hatcheries A, B, and D are batch fed, while at hatchery C, oyster larvae are allowed to feed continuously. Several different breeding lines derived from the VIMS ABC breeding program were used at the different hatcheries during the course of the experiment. Hatchery water samples were collected at the same time as the larval samples for each of the three larval

stage time points for the first two spawning events. Dissolved inorganic nitrate (NO_3^-), ammonium (NH_4^+) and phosphate (PO_4^{3-}) were measured in hatchery water samples by filtering 25 mL of hatchery water through Whatman GF/F filters (25 mm diameter, 0.7 μm nominal pore size). Filtrate was then analyzed for nutrients using a Lachat Quick-Chem 8000 automated ion analyzer (Lachat Instruments, Milwaukee, WI, USA). An additional 300 mL of hatchery site water was filtered through a 0.22 μm pore size Millipore Sterivex filter for DNA extraction. Oyster larvae were initially washed and resuspended with 20 mL of sterile seawater before being collected on a 0.22 μm pore size Millipore Sterivex (Merck KGaA, Darmstadt, Germany) filter. Both larvae and water filters were stored at -80°C until DNA extraction. Times points for hatchery B spawn 2 were excluded from this analysis as a result of spawning failure.

DNA isolation and 16S rRNA gene amplification

DNA extractions for both oyster larvae and hatchery water samples were carried out using MoBio PowerSoil DNA isolation kit (Qiagen, Carlsbad, CA). For oyster larval samples, oyster larvae were carefully removed from the Sterivex filters, which were taken out from cartridge housing, and then resuspended in approximately 3 mL of the MoBio bead beater solution. Approximately 10,000, 4,000 and 500 oyster larvae were added to glass bead tubes for stages D-, V-, and PV-stages, respectively. For hatchery water DNA extractions, one half of the Sterivex filter from the water samples was used after carefully extruding the filter from the cartridge housing. The remaining extraction steps were conducted following the manufacturer's protocol. PCR amplification of the hypervariable V4 region of the 16S rRNA gene was conducted on the extracted DNA

using forward primer 515F and modified, barcoded reverse primer 806R (Caporaso et al. 2010), adapted for use with the Ion Torrent Personal Genome Machine (PGM). The basic manufacturer's PCR protocol was used with Taq DNA Polymerase (Invitrogen, Carlsbad, CA) to create a PCR master mix with the following modification: a 1 mM dNTP mixture was used in place of a 10 mM mixture for a final concentration of 0.02 mM dNTP. Thermal cycling conditions consisted of an initial denaturation step at 94°C for 3 min, followed by 30 cycles of 94°C for 1 min, 54°C for 1 min, 68°C for 2 min. A final elongation step of 68°C for 10 min was added to ensure complete amplification. The amplified products were gene cleaned using the UltraClean GelSpin DNA Purification Kit (Mo-Bio, Carlsbad, CA). The resulting amplicon libraries were then used as templates for sequencing with the Ion PGM platform following the manufacture's instruction (Thermo Fisher Scientific, Waltham, MA).

Sequence processing and OTU assignment

Removal of barcodes and primers from raw sequences and trimming of sequence length were conducted using the Ribosomal Database Project (RDP) pipeline initial process (Cole et al. 2014; http://rdp.cme.msu.edu) with a minimum quality score of 20, minimum length of 200 bases, and a maximum length of 500. Following initial trimming, sequences were denoised with Acacia (Bragg et al. 2012) using a minimum quality score of 25. Mothur v1.35.1 (Schloss et al. 2009) was used to further trim sequences against the SILVA v123 (Yilmaz et al., 2014) alignment template, precluster (diffs=1), and screen for chimeric sequences using the chimera.vsearch command (Rognes et al. 2016). Unknown taxon, mitochondria, chloroplast, archaea, and

eukaryotic sequences were removed from analysis using SILVA v123 reference taxonomy and the Wang classification method (Wang et al. 2007) with an 80% minimum identity. Archaea made up < 1.2% of total sequences, and were therefore excluded from further analysis. Sequences were clustered into operational taxonomic units (OTUs) based on a 97% identity using the vsearch abundance-based greedy clustering (AGC) algorithm in Mothur.

Bacterial diversity and taxonomy

Diversity metrics on OTUs including coverage, OTU numbers, Chao1, and Shannon diversity were conducted with subsampled larvae and water sequencing reads (n=5,277) in Mothur using the summary.single command. To visualize differences between hatchery water and larvae community composition, non-metric dimensional multidimensional scaling (nMDS) was performed on 4^{th} root transformed OTU counts using Bray-Curtis resemblance matrices in PRIMER v7 (Clarke et al. 2014). Classifications of larvae microbiomes and larvae core microbiomes at the taxonomic class level were based on the mean relative abundance of OTUs for each larvae stage (D, n=11; V, n=11; PV, n=8), or for each larvae stage within each hatchery using SILVA v123 reference taxonomy. Further classification of the core larval microbiome at the genus and species taxonomic levels was made using core representative sequences obtained from Mothur with the National Center for Biotechnology Information's (NCBI) Nucleotide BLAST tool.

Core microbiome

Core OTUs were analyzed using InteractiveVenn (Heberle et al. 2015) and the R packages Phyloseq (McMurdie and Holmes 2013) and Venn Diagram (Chen and Boutros 2011). Sequencing reads prior to subsampling were used to prevent reduction in coverage of samples. Shared microbiomes for each larval development stage ('larval stage core') were defined as the collection of OTUs present in at least 80% of the larvae stage being examined. OTUs shared among all larvae regardless of development stage cores were considered to be the total larval core microbiome ('larval total core'). A conservative 80% cutoff was selected for each development stage of the larvae stage or larvae total core to account for the possibility of errors associated with sampling or sequencing efforts.

Statistical analyses

Differences between Chao richness and Shannon diversity indices among the larval microbiome and water samples relating to development stage, spawn, and hatchery were tested using a one factor ANOVA with post-hoc Tukey's HSD test in R. Spearman rank correlation tests were used to determine whether Chao richness and Shannon diversity indices in larvae were correlated with hatchery water. Only samples that had both matching water and larval samples were used for this analysis (each n=18). Additional spearman rank correlation tests were conducted between nutrients measured in the hatchery water and water sample Chao richness and Shannon diversity indices. A PERMANOVAs were performed on 4^{th} root transformed Bray-Curtis resemblance matrices to test for effects of sample type of larval and water microbiomes using the one factor model sample type. Additional PERMANOVAs were conducted separately on larvae and water samples to test for the effects of development stage, hatchery, and

spawn on oyster larval microbiomes and hatchery water microbiomes using the model hatchery x spawn (hatchery) x development stage. Pairwise comparison tests between hatcheries and development stage were conducted using the pairwise function in PERMANOVA for both larval and hatchery water microbiomes. Pairwise tests were not corrected for multiple comparisons. Additional PERMDISP tests were conducted with each of the factors using Bray-Curtis resemblance matrices to determine whether multivariate dispersion also had an effect on the larval or hatchery water microbiome (i.e. whether the average group distance to the group centroid is equivalent among groups). PERMANOVAs, pairwise tests, and PERMDISP analyses were performed with PRIMER (Clarke et al. 2014). DESeq2 (Love et al. 2014) using a Wald's significance test and local fit was preformed on raw sequencing counts to test for differentially abundant OTUs among larval development stages and between larval microbiomes and water samples. Pairwise comparisons were made using the contrast option in DESeq2, and Benjamini and Hochberg's p-adjusted values correcting for FDR were used to test for significance. All tests are based on a significance of $p < 0.05$ and error bars represent ± standard error.

RESULTS

Hatchery water parameters

NO_3^-, NH_4^+, and PO_4^{3-} were measured in each of the hatchery water samples and larval stages for spawns 1 and 2 (Table 1). In general, nutrients among the hatcheries, spawns, and stages were highly variable. Concentrations of NO_3^- ranged from 0.43 μM at hatchery D from spawn 2 during stage V to 154.64 μM at hatchery B from spawn 1 during stage PV. With the exception of hatchery D water during spawn 2, the lowest of concentrations of NO_3^- within each hatchery were measured at the D-stage, ranging from 4.42 μM at hatchery C from spawn 1 to 15.51 μM at hatchery B from spawn 1. Similar to NO_3^-, concentrations of NH_4^+ were highly variable and ranged from 0.36 at hatchery A from spawn 1 during stage D to 12.56 μM at hatchery C from spawn 2 during stage PV. The lowest NH_4^+ concentrations, however, were consistently found at hatchery A, with an average concentration of 0.53 ± 0.20 μM. Levels of PO_4^{3-} ranged from 0.26 μM at hatchery A from spawn 1 during stage D to 8.55 μM at hatchery C from spawn 2 during stage PV.

Diversity comparisons among larvae and hatchery water

A total of 1,166,530 clean, trimmed bacterial 16S rRNA gene sequences were obtained from 30 oyster larval and 20 hatchery water samples. Average number of sequences was 23,331 ± 1,696 with an average coverage of 98.2 ± 0.2% (Table 2). Using subsampled sequences (n=5,277) from each sample, the larval and hatchery water samples have a range of 67 to 1,021 OTUs with an average of 338 ± 26 OTUs per

sample. Chao indices showed a decreasing trend in OTU richness as oyster larval development stages progressed, with the D-stage larval richness (881.6 ± 174.5) being higher than V-stage larvae (691.4 ± 97.5) and significantly higher than the PV-stage larvae (337.3 ± 29.7) (ANOVA: $F_{2,29} = 4.20$, p =0.02, Tukey's HSD: D-stage vs. PV-stage, p=0.02) (Fig 1). In comparison, the highest richness in the water samples occurred during the V-stage larvae (898.6 ± 0.6 OTUs) and no significant differences were detected among the different stages (ANOVA: $F_{2,17} = 0.17$, $p \geq 0.05$). Comparing equivalent larval stages, no differences in Chao richness or diversity were observed among the hatcheries (ANOVA [Chao]: $F_{3,15} = 1.19$, $p \geq 0.05$ and ANOVA [Shannon]: $F_{3,15} = 2.12$, $p \geq 0.05$) or spawns (ANOVA [Chao]: $F_{2,26} = 1.92$, $p \geq 0.05$ and ANOVA [Shannon]: $F_{2,26} = 0.37$, $p \geq 0.05$) in the larvae or hatcheries in the water samples (ANOVA [Chao]: $F_{3,11} = 3.05$, $p \geq 0.05$ and ANOVA [Shannon]: $F_{2,26} = 1.71$, $p \geq 0.05$). Due to unequal and missing samples, Chao richness and diversity could not be compared among the different spawns in the water samples. To test whether richness or diversity in larvae stage was correlated with richness or diversity in water samples, Spearman rank tests were performed on Chao and Shannon indices for each larval stage and the corresponding hatchery water sample. The rank tests showed no significant positive correlations between larvae and water microbiomes for either Chao or Shannon indices (Table 3). Additional Spearman rank tests were also conducted between Chao and Shannon indices and nutrient measurements in the water and larvae microbiomes to determine whether nutrients correlated with richness and diversity of water microbiomes (Table 4). NO_3^-, NH_4^+, and PO_4^{3-} were significantly and negatively correlated with both

richness and diversity of the water microbiomes. No significant correlations were found between nutrients and Chao or Shannon indices of the larvae microbiomes.

Microbiome composition comparisons of larvae and water

Three separate nMDS analyses were conducted with the 16S sequences (Figs 2, 3A and B). The first nMDS was performed on the combined larvae and water samples, which showed distinct differences in community composition between the total larval and hatchery water microbiomes (Fig 2). This distinction between larvae and water was found to be significant based on PERMANOVA (Table 5A). Two additional nMDS analyses were performed on larval microbiome samples-only and water microbiome samples-only to further examine the differences in the microbiomes based on hatchery site, larval developmental stage, and spawn number (Figs 3A and B). In both larvae and water microbiomes, hatchery site showed the most distinct clustering patterns among the various samples. The effect of hatchery and spawn number were determined to be significant in the larval microbiomes, while only hatchery was found to be significant in the water microbiomes (Tables 5B and C). Development stage was not found to have a significant on either the larval or water microbiomes. Subsequent pairwise comparisons of hatcheries showed that larval microbiomes from all hatcheries were significantly different from each other, while only the comparisons between hatcheries A vs. D and between C vs. D were found to be significant in the water microbiomes (Table 6). Additionally, pairwise tests showed the similarity between larvae from different hatcheries to be higher than different hatchery waters. Permutational-based pairwise comparisons of spawns at each hatchery were unable to be performed due to the low

number of spawning replicates nested within each hatchery. PERMDISP tests showed no significant effect of dispersion among the larvae or water microbiomes regarding hatchery, spawn number, or development stage (Table 7).

Taxonomic classifications of oyster larval and water sequences at > 1% mean relative abundance showed variation between hatchery site and larvae stage (Fig 4). In all larval microbiomes, *Alphaproteobacteria* and *Gammaproteobacteria* together made up the largest proportion of the community for all samples. Combined, these classes represented on average 58.2 ± 2.7% of total sequences for all larval stages and water, regardless of hatchery site. *Flavobacteriia* was also found in all samples and comprised on average 17.2 ± 2.7% of total sequences. At the class level, microbiome compositions of D-stage larvae were more similar to those from their respective hatchery water samples than PV-stage larvae microbiomes. Furthermore, the greatest variation of microbiomes among the samples was found in the PV-stage larvae. *Sphingobacteriia* was found to be a dominant class (35.2-37.5%) in the PV-stage larvae at hatchery A, but made up < 6% mean relative abundance at all other hatcheries, while *Betaproteobacteria* was a dominant class in both PV- and V-stage larvae (20.1 ± 7.4%) at hatchery B, but made up < 4% mean relative abundance at all other hatcheries. Classes *Bacilli* and *Planctoymycetacia* were uniquely dominant to PV-stage larvae at hatchery D, comprising a combined total mean relative abundance of 28.3 ± 8.5%.

Core microbiomes in larvae

The larval microbiome was compared across different developmental stages of the oyster to determine the core microbiome. A total of 4,786 OTUs were present in larval

microbiome samples (n=30). The larvae D-stage core microbiomes consisted of 51 OTUs, while the larval V-stage and PV-stage core microbiomes consisted of 62 and 17 OTUs, respectively (Figs 5 and 6). The mean relative abundance of sequences comprising each larval stage core microbiome was highest in D-stage (61.7 ± 5.1%), followed by V-stage (53.9 ± 6.7%), and PV-stage (25.3 ± 0.7%). Of the 51 and 62 core OTUs in the D- and V-stage larvae, respectively, 23 (apart from the larval core) were also common between the two stages and belonged to several families, including *Pseudoalteromonadaceae, Methylophilaceae*, *Hyphomonadaceae*, *Piscirickettsiaceae*, *Flavobacteriaceae, Rhodobacteraceae*, and *Vibrio*. Eleven core OTUs were unique to the D-stage larvae and 23 OTUs were unique to the V-stage larval core microbiomes. Family differences between the larvae D and V-stage core microbiomes were found in *Cryomorphaceae* and an unclassified *Gammaproteobacteria* in the D-stage and *Cellvibrionaceae* found in V-stage. In the larvae PV-stage core microbiome, only one OTU belonging to family *Rhodobacteraceae* was unique from other stages.

Among the larvae stage core microbiomes, 16 OTUs were shared across all stages and constituted the larvae total core microbiome (Fig 6 and Table 8A). Families *Altermonadaceae*, *Flavobacteriaceae*, *Erythrobacteraceae*, and *Rhodobacteraceae* were the dominant families in the larvae total core microbiome and represented on average, about 25-30% of the total larval microbiome, regardless of developmental stage. Among the hatcheries, the dominant families making up the larvae total core microbiomes ranged between 24-38% (Table 8B) and fluctuated on average ± 12% between the spawns within each hatchery (Data not shown). Two other minor families, *Oleiphilaceae* and *Phyllobacteriaceae*, were also part of the total larval core microbiome, but made up less

than <1% of the total microbiome. Significant differences in the abundance of the larval stage core OTUs were only detected between stages D and PV (Table 9). One OTU assigned to the genus *Labrenzia* was significantly more abundant in the PV stage larvae, while 3 OTUs from phylum *Bacteroidetes,* 2 OTUs, assigned to the genus *Flavobacterium* and one to an unclassified genus, and 1 OTU from phylum *Proteobacteria*, genus *Hyphomonas*, were significantly more abundant in the D-stage larvae.

The larvae total core microbiomes were compared to their respective hatchery water samples. All 16 larvae core OTUs were also found in the hatchery water (Table 10). Among these core OTUs, only 3 were considered to be significantly different between the larvae and the water samples. Otu00096 identified as *Marinobacter hydrocarbonoclasticus* and OTU00010 identified as *Tenacibaculum sp*. were found to be significantly higher in the oyster larvae core, while OTU00025 identified as *Citromicrobium bathyomarinum* was found to be significantly higher in the hatchery water.

DISCUSSION

Effects of Hatchery, Spawn, and Development Stage on Larval Microbiomes

Hatcheries and the spawning events within each hatchery had a significant effect on the composition of the oyster larval microbiomes, while the developmental stage of the oyster did not (Fig 3A and Tables 5B). Between hatcheries and spawns, hatcheries explained higher variability and showed a greater separation among the microbiomes. The same significant effect of hatchery and distinctive clustering between hatcheries was also shown in the water microbiomes, providing evidence that hatchery conditions affecting its water may also impact the oyster larval microbiome (Fig 3B and Table 5C). Furthermore, in all larval microbiomes and among some of the hatchery water microbiomes, hatcheries were found to be significantly different between each other (Table 6). Variations among the hatchery operations in this study included differences in location, water filtration methods, and feeding methods. While the individual operational conditions were not examined in this study, the combined effect of these different operations likely resulted in the uniqueness of the different hatchery water and larval microbiomes.

Despite the similar distinctive clustering patterns of larval and water microbiomes in relation to hatchery, oyster larval microbiomes were also unique from the hatchery water (Figs 2, 4, and Table 5). Asmani et al. (2016) found a similar distinction between *C. gigas* larval microbiomes and seawater microbiomes when examining larvae raised under different oyster rearing systems, including a flow-through and recycling system. This suggests that the oyster microbiomes are not merely reflections of the surrounding hatchery seawater, but are selectively colonized by distinct bacterial taxa. Selection of

bacteria by oysters at the hatcheries is further evidenced by the lack of correlation between richness and diversity of the oyster larvae microbiomes and their corresponding water microbiomes (Table 3). Water microbiome richness was found to be significantly and negatively correlated with nutrients NO_3^-, NH_4^+, and PO_4^{3-}, while no correlation was found in the oyster larvae microbiomes (Table 4). This suggests the hatchery conditions, such as nutrients that affect the water microbiomes, are not having the same impact on the larvae microbiomes.

Another distinction between the larvae and water microbiome was the significant effect of spawn on the larvae microbiome only (Table 5B and C). In this study, three unique spawning cohorts from different breeding lines were selected from each hatchery over a period of 3 consecutive months, with the first spawn occurring in late spring/early summer and the final spawn occurring in late summer. Genetic differences between oysters used for spawning or seasonality factors associated with the spawns may all contribute to variation in the oyster larval microbiomes. Oyster genotypes have been shown to play a role in shaping gill bacterial communities, particularly among rare taxa (Wegner et al. 2013), while environmental conditions such as temperature and substrate availability, which exhibit clear seasonal trends have been shown to strongly influence bacterial communities (Shiah and Ducklow 1994, Schultz et al. 2003). Temperature of the hatchery water was not measured during this study; however, it is unlikely that seasonal effects alone contributed to the variability in the oyster larval microbiomes, as spawn did not similarly affect the water microbiomes. This may suggest that oyster genetics exert some influence on the early development of the larvae microbiome.

The lack of significant effect and low explanation of variability of the development stage on the larval microbiome (Table 5B) may hint at the idea that the initial, early colonization of the oyster larval microbiome establishes a set of resident, core bacteria that remains with the oyster, and is unaffected by larval stage development. Furthermore, the similarity between the larval microbiomes at each of the hatcheries is higher than that of the water microbiomes, indicating a more uniform structure of the larval microbiome across the different hatcheries.

Composition and Diversity of Larval Development Stage Microbiomes

The structure of the larval microbiome development stages was examined more deeply by identifying the compositional members of the larval microbiomes for each stage of development at the different hatcheries. Among all the larval and water microbiomes, *Alpha*- and *Gammaproteobacteria* were the two most dominant bacterial classes based on mean relative abundances of sequences (Fig 4). This is consistent with previous studies that have shown these two classes to be abundant in marine environments, hatcheries, and oysters (Giovannoni and Rappe 2000, Schulze et al. 2006, King et al. 2012, Trabal Fernández et al. 2014, Asmani et al. 2016). *Flavobacteriia* was also present in all of the samples, but showed a great amount of variation among hatcheries and between larval stages. *Flavobacteriia* has been found to be an abundant class in intake seawater from an oyster hatchery (Powell et al. 2013) and in algae cultures used to feed bivalve larvae (Nicolas et al. 2004).

Of the three larval stages, the PV-stage larval microbiomes showed the overall greatest variation compared to their corresponding hatchery water samples. As oyster

larvae begin to develop a more complex digestive tract, gill tissues, and shell structures, they may be more selective for specific bacterial taxa associated with food during feeding or encourage colonization of a wider range of bacterial taxa. For example, Pacific oysters have been shown to exhibit low consumption of microalgae during D-stage to early V-stage larvae, followed by a dramatic increase from umbonate to PV-stage (Rico-Villa et al. 2009). This feeding pattern may be a result from the incomplete development of the digestive tract during early larvae, including a narrow oesophagus and reduced gut volume (Gallager 1988). The increased ability in feeding and gut volume in older oyster larvae may partly explain the increased compositional variation.

Despite the greater variation in microbiome composition among the PV-stage larvae, total OTU richness of the PV-stage microbiomes were lower than the V-stage larvae, and significantly lower than D-stage larvae (Fig 1). Chao richness indices for PV-stage larvae in this study (337.3 $\pm$ 29.7) were similar to those found in different post larvae *Crassostrea* oysters from Trabal Fernández et al. (2014). This decrease in richness, however, did not correspond to a large decrease in overall microbiome diversity; microbiome diversity remained somewhat stable over the three stages. This suggests that the total number of OTUs may be reduced in each oyster as the oyster reaches a later stage of development, but the OTUs present may become more evenly distributed. Early D-stage larvae may be more likely to be rapidly colonized by several bacterial taxa from the surrounding water column, while later PV-stage larvae may be better able to select for or against bacterial colonization. Alternatively, the bacteria themselves that have a competitive advantage may begin to outcompete and replace other bacteria by the PV-stage. Several bacteria species are known to colonize surfaces and

produce polymers, inhibitory compounds, and antimicrobials that prevent competitors from succeeding (Bruhn et al. 2005, Rao et al. 2005, Xavier and Foster 2007). Neither water sample richness and diversity were positively correlated with the richness and diversity changes in the larvae microbiome, providing evidence that the bacteria associated with the oysters may be independently affecting these changes (Table 3). In fact, by stage PV, both richness and diversity were negatively correlated with richness and diversity in the hatchery water samples.

Larval Core Microbiome and Its Implication

Among the 4,786 OTUs present in the larval microbiomes, only 16 OTUs were considered to be part of the core oyster larval microbiome as they were shared by at least 80% of the oyster larvae at each stage of development (Fig 5). Despite the low number of OTUs, the core microbiome still represented between 25.3-32.0% of the mean relative abundance of sequences in the larval microbiome. This suggests that the larval core microbiome is primarily comprised of a few highly abundant taxa as opposed to rare species. Broken down by developmental stage, shared OTUs were much higher among the D- and V-stage larvae with 51 (61.7 ± 5.1%) and 62 (59.3 ± 6.7%) shared OTUs, respectively. In comparison, PV-stage larvae shared 17 OTUs (25.3% ± 4.8%), and only 1 unique OTU that was not part of the core microbiome. This reduction in the core OTUs from D- and V-stage larvae to PV-stage larvae similarly corresponds to a decrease in microbiome OTU richness at the PV-stage (Fig 1) as well as a much greater variation among microbiome composition between hatcheries (Fig 4). As stated above, oysters may be able to better select for or against colonization by different bacteria at the later

stages of development, which may result in a greater number of individual differences between oysters and a reduction in the number of core OTUs. Furthermore, individual food selection among the more highly developed PV-larvae may be more discriminating than that of D-stage larvae, reducing the number of shared OTUs and increasing the taxonomic variation observed among the PV-stage larval microbiome.

Of the 16 OTUs that made up the larval core microbiomes, the majority (10 OTUs) belonged to family *Rhodobacteraceae* from the class *Alphaproteobacteria* and comprised between 19.67-24.71% of the core microbiome sequences by larvae stage (Fig 6 and Table 8). Rhodobacter bacteria are rapid primary surface colonizers (Dang et al. 2008) and have been shown to be abundant in phytoplankton cultures used in bivalve larvae feed (Nicolas et al. 2004), and thus may explain the dominance of *Rhodobacteraceae* as a dominant family in early core larval microbiomes. The water microbiomes also exhibited correspondingly similar high abundances of *Rhodobacteraceae* relating to the same larval core OTUs, supporting the idea that the dominance of *Rhodobacter* in the oyster larvae is a result of the surrounding water. Some *Rhodobacteraceae* bacteria, specifically *Phaeobacter* [*Roseobacter*] *gallaciensis,* have been shown to benefit mollusc larvae (Ruiz-Ponte et al. 1999) and provide protection against pathogens (Kesarcodi-Watson et al. 2012), while others have been shown to contribute to diseases like Juvenile oyster disease (Boettcher et al. 2000). The second and third most abundant families (1.17-5.91% and 0.72-4.02) shared by the larvae were *Flavobacteriaceae* from class *Flavobacteriia* (1 OTU) and *Alteromonadaceae* (2 OTUs) from class *Gammaproteobacteria*. OTU #00010 from family *Flavobacteriaceae* most closely identified with genus *Tenacibaculum*, which has been identified in juvenile and

adult oysters (Fernandez-Piquer et al. 2012, Lee et al. 2009; Trabal Fernández et al. 2014) as well as in other marine animals and macroalgae (Suzuki et al. 2001, Heindl et al. 2008, Wang et al. 2008). Additionally, this OTU was found to be significantly higher in the oyster larvae than the water (Table 10), suggesting that some type of association between the bacterial taxa and the oyster may exist, such as adaptation of the *Tenacibaculum* to the oyster larvae environment or selective uptake by the oyster larvae. Of the two OTUs (OTU #00015) from family *Alteromonadaceae*, one closely identified with *Alteromonas macleodii. A. macleodii* has been isolated from microalgal cultures in an aquaculture hatchery (Schulze et al. 2006) and found in larval cultures of flat oysters (Farto et al. 2006) (Table 8). In mollusc larvae, *A. macleodii* has been demonstrated to offer some protection against oyster larvae pathogens *V. coralliilyticus* and *V. pectenicida* (Kesarcodi-Watson et al. 2012). OTUs #00025, #00040, #00059 identified as *Citromicrobium*, *Hoeflea,* and an unidentified *Gamma* proteobacterium from families *Erythrobacteraceae*, *Phyllobacteriaceae,* and *Oleiphilaceae* respectively, comprised the remaining oyster larval total core microbiome. Both *Citromicrobium* and *Hoeflea* have been isolated from microalgal cultures (Le Chevanton et al. 2013), with no known associations with oyster larvae or adult oysters. While still part of the core microbiome by definition, these bacteria may be an important component of the oyster larvae diet rather than permanent resident bacteria. *Citromicrobium* in particular, was found to be significantly higher in the hatchery water than in the oyster (Table 10), providing support that these bacteria may be reflective of a microalgal food source. Family *Oleiphilaceae* has also not been previously associated with oysters. Bacteria from this family are thought to be obligate hydrocarbonoclastic bacteria and have been isolated from

sediments, biofilms, and microbial mats (Golyshin et al. 2002). Interestingly, *Marinobacter hydrocarbinoclasticus* (OTU #00096) from family *Alteromonadaceae*, another hydrocarbon-degrading bacterium, was also present in the oyster core microbiome (Table 8). While low in abundance, this OTU was also found to be significantly higher in the larval core than in the surrounding water (Table 10). Further investigation into hatchery operations may be useful to determine whether the presence of these bacteria in the oyster larval core microbiome is indicative of exposure of oyster larvae to hydrocarbons in the hatchery environment. Overall, the presence of 16 core OTUs in healthy larvae provides the first insight of developing microbial indicator to evaluate and predict the success of larvae rearing practices at hatcheries.

CONCLUSIONS

Oyster larvae showed a wide range of variation in their microbiomes primarily due to the hatchery in which they were raised and factors associated with spawning events. These significant effects of hatchery and spawn on the larval microbiome may have implications in the selection of hatchery operation and rearing methods. In our study, hatcheries varied according to filtration, feeding methods, and location. Isolation and testing of each of these different methods on larvae microbiome is necessary to identify which specific hatchery practices have the most impact the oyster larval microbiome.

While development stage was not determined to have a significant effect, there were a few distinct differences between the larval stages of development including a significant decrease in species richness between the early and late stages of oyster development and greater variability in class composition than corresponding D-stage larval and water microbiomes. Together, these changes suggest a shift towards a more selective larval microbiome as the oyster develops. The selective stage of the oyster larvae as it transitions from D-stage to PV-stage may be a critical time period to ensure the oyster larvae are exposed to beneficial bacteria, such as those used in probiotics, that may be incorporated into the microbiome.

A quarter of the larvae microbiomes were composed of the same 16 core OTUs found at all stages of development and present at all of the hatcheries. The core primarily consisted of high abundances of OTUs from family *Rhodobacteraceae, Flavobacteriaceae*, and *Alteromonadaceae*. These same core OTUs were similarly found in the corresponding water microbiomes, with the exception of OTUs identified as genus

Tenacibaculum and *Marinobacter*, which were found to be significantly higher in abundance in the oyster larvae. The similarities between the larval core and water microbiomes suggest that the majority of the oyster larval core microbiome is a reflection of the hatchery water it is raised in. Further investigation is warranted to determine whether these same core OTUs persist in larvae as they transition to juveniles and are placed in the environment.

Overall, this is the first study to examine the variation and diversity in the larval microbiomes from the earliest D-stage through PV-stage at several different hatcheries and from different spawns. Investigation of changes that occur to the oyster larval microbiome as it develops as well as identification of the larval core provides an important first step in unraveling the complexity associated with the oyster larval microbiome and may provide clues to the health or success of oyster larvae and aid the development diagnostic tools to monitor hatchery practices.

ACKNOWLEDGEMENTS

I thank Stan Allen and the Virginia Institute of Marine Science Aquatic Genetics and Breeding Technology Center for providing several of the oyster larvae samples used in this study and Raegan Bostic for assistance with sample processing. Funding was provided by Virginia Sea Development Grant. This work was performed in part using computing facilities at the College of William and Mary, which were provided by contributions from the National Science Foundation, the Commonwealth of Virginia Equipment Trust Fund and the Office of Naval Research.

REFERENCES

Asmani, K, Petton, B, Le Grand, J, Mounier, J, Robert, R, and Nicolas, J-L (2016) Establishment of microbiota in larval culture of Pacific oyster, *Crassostrea Gigas*. *Aquaculture* **464**: 434–44. doi: 10.1016/j.aquaculture.2016.07.020.

Boettcher, KJ, Barber, BJ, and Singer, JT (2000) Additional evidence that juvenile oyster disease is caused by a member of the *Roseobacter* group and colonization of nonaffected animals by *Stappia stellulata*-like strains. *Environ Microbiol* **66**(9): 3924-30. 10.1128/AEM.66.9.3924-3930.2000.

Bragg, L, Stong, G, Imelfort, M, Hugenholtz, P, and Tyson, GW (2012) Fast, accurate error-correction of amplicon pyrosequences using Acacia. *Nat Methods* **9**(5); 425-26.

Brown, C (1973) The effects of some selected bacteria on embryos and larvae of the American oyster, *Crassostrea virginica*. *J Invertebr Pathol* **21**: 215-23.

Bruhn, JB, Nielsen, KF, Hjelm, M, Hansen, M, Bresciania, J, Schulz, S, and Gram, L (2005) Ecology, inhibitory activitym and morphogenesis of a marine antagonistic bacteium belonging to the *Roseobacter* clade. *Environ Microbiol* **71**(11): 7263-70. doi: 10.1128/AEM.71.11.7263-7270.2005.

Castro, D, Pujalte, MJ, Garay, E, and Borrego, JJ (2002) Vibrios isolated from the cultured manila clam (*Ruditapes Phillippinarum*): numerical taxonomy and antibacterial activities. J Appl Microbiol **93**: 438-447.

Chen, H, and Boutros, PC (2011) VennDiagram: a package for the generation of highly-customizable venn and euler diagrams in R. *BMC Bioinformatics* **12**(1): 35. doi:10.1186/1471-2105-12-35.

Clarke, KR, Gorley, RN, Somerfield, PJ and Warwick, RM (2014) Change in marine communities: an approach to statistical analysis and interpretation, 3rd edition. PRIMER-E, Plymouth, 260 pp.

Cole, JR, Wang, Q, Fish, JA, Chai, B, McGarrell, DM, Sun, Y, Brown, CT, Porras-Alfaro, A, Kuske, CR, and Tiedje, JT (2014) Ribosomal database project: data and tools for high throughput rRNA analysis. *Nucleic Acids Res* **42** : D633–42. doi:10.1093/nar/gkt1244.

Dang, H, Li, T, Chen, M and Huang, G (2008) Cross-ocean distribution of *Rhodobacterales* bacteria as primary surface colonizers in temperate coastal marine waters. *Appl Environ Microbiol* **74**(1): 52–60. doi:10.1128/AEM.01400-07.

Farto, R, Guisande, JA, Armada, SP, Prado, S, Nieto, TP (2006) An improved and rapid biochemical identification of indigenous aerobic culturable bacteria associated with Galician oyster production. *J Shellfish Res* **25**(3): 1059-65. doi: 10.2983/0730-8000(2006)25[1059:AIARBI]2.0.CO;2.

Fernandez-Piquer, J, Bowman, JP, Ross, T, and Tamplin, ML (2012) Molecular analysis of the bacterial communities in the live Pacific oyster (*Crassostrea gigas*) and the influence of postharvest temperature on its structure. *J Appl Microbiol* **112**(6): 1134–43. doi: 0.1111/j.1365-2672.2012.05287.x.

Gallager, SM (1988) Visual observations of particle manipulation during feeding in larvae of bivalve mollusc. *B Mar Sci* **43**(3): 344-65.

Garland, CD, Nash, GV, Summer, CE, and McMeekin, TA (1983) Bacterial pathogens of oyster larvae (*Crassostrea gigas*) in a Tasmanian hatchery. *Mar Freshwater Res* **34**: 483-87. doi: 10.1071/MF9830483.

Giovannoni, S, and Rappe, M (2000) Evolution, diversity, and molecular ecology of marine prokaryotes. In DL Kirchman (Ed.), *Microbial Ecology of the Oceans* (pp. 47-84). Chichester: Wiley-Liss.

Goyshin, PN, Chernikova, TN, Abraham, W-R, Lünsdorf, H, Timmis, KN, Yakimov, MM (2002) *Oleiphilaceae* fam nov., to include *Oleiphilus messinensis* gen. nov., sp. nov., a novel bacterium that obligately utilizes hydrocarbons. *Int J Syst Evol Micr* **52**: 901-11. doi: 10.1099/ijs.0.01890-0.

Gomez-Gil, B, Roque, A, and Turnball, JF (2000) The use and selection of probiotic bacteria for use in the culture of larval aquatic organisms. *Aquaculture* **191**: 259-270.

Heberle, H, Meirelles, GV, da Silva, FR, Telles, GP, and Minghim, R (2015) InteractiVenn: a web-based tool for the analysis of sets through venn diagrams. *BMC Bioinformatics* **16**(1): 169. doi:10.1186/s12859-015-0611-3.

Heindl, H, Wiese, J, and Imhoff, JF (2008) Tenacibaculum adriaticum sp. nov., from a bryozoan in the Adriatic Sea. *Int J Syst Evol Micr* **58**: 542-47. doi: 10.1099/ijs.0.65383-0.

His, E, and Maurer, D (1988) Shell growth and gross biochemical composition of oyster larvae (*Crassostrea gigas*) in the field. *Aquaculture* **69**: 185-94.

Hudson, K, and Murray, TJ (2017) Virginia shellfish aquaculture situation and outlook report: Results of the 2016 Virginia Shellfish Aquaculture Crop Reporting Survey May 2017 (VIMS Resource Report No. 2017-7).

Kesarcodi-Watson, A, Miner, P, Nicolas, J-L, and Robert, R (2012) Protective effect of four potential probiotics against pathogen-challenge of the larvae of three bivalves:

Pacific oyster (*Crassostrea gigas*), flat oyster (*Ostrea edulis*) and scallop (*Pecten maximus*). *Aquaculture* **344–349**: 29–34. doi:10.1016/j.aquaculture.2012.02.029.

King, GM, Judd, C, Kuske, CR, and Smith, C (2012) Analysis of stomach and gut microbiomes of the eastern oyster (*Crassostrea virginica*) from coastal Louisiana, USA. *PLoS One* **7**(12): e51475. doi: 10.1371/journal.pone.0051475.

Kniprath, E (1981) Ontogeny of the molluscan shell field: a review. *Zool scr* **10**(1): 61-79. doi: 10.1111/j.1463-6409.1981.tb00485.x.

Kueh, CS, and Chan, KY (1985) Bacteria in bivalve shellfish with special reference to the oyster. J Appli Bacteriol **59**(1): 41-47. doi: 10.1111/j.1365-2672.1985.tb01773.x.

Le Chevanton, M, Garnier, M, Bougaran, G, Schreiber, N, Lukomska, E, Bérard, J-B, Fouilland, E, Bernard, O, and Cadoret, J-P (2013) Screening and selection of growth-promoting bacteria for *Dunaliella* cultures. *Algal Res*. doi: 10.1016/j.algal.2013.05.003.

Lee, YS, Baik, KS, Park, SY, Kim, EM, Lee, D-H, Kahng, H-Y, Jeon, CO, and Jung, JS (2009) *Tenacibaculum crassostrea* sp. nov., isolated from the Pacific oyster, *Crassostrea gigas*. *Int J Syst Evol Micr* **59**: 1609-14. 10.1099/ijs.0.006866-0.

Love, MI, Huber, W, and Anders, S (2014) Moderated estimation of fold change and dispersion for RNA-seq data with DESeq2. *Genome Biol* **15**: 550. doi: 0.1186/s13059-014-0550-8.

McFall-Ngai, M, Hadfield, MG, Bosch, TCG, Carey, HV, Domazet-Lošo, T, Douglas, AE, Duilier, N, et al. (2013) Animals in a bacterial world, a new imperative for the life sciences. *Proc Natl Acad Sci* USA **110**: 3229–36. doi: 10.1073/pnas.1218525110.

McMurdie, PJ, and Holmes, S (2013) Phyloseq: an R package for reproducible interactive analysis and graphics of microbiome census data. *PLoS ONE* **8**(4): e61217. doi:10.1371/journal.pone.0061217.

Miyazaki, Y, Nishida, T, Aoki, H, and Samata, T (2010) Expression of genes responsible for biomineralization of *Pinctada fucata* during development. *Comp Biochem Phys B* **155**: 241-48. 10.1016/j.cbpb.2009.11.009.

Murchelano, RA, and Bishop, JL (1969) Bacteriological study of laboratory-reared juvenile American oysters (*Crassostrea virgnica*). *J Invertebr Pathol* **14**(3): 321-27. doi: 10.1016/0022-2011(69)90158-X.

Nicolas, JL, Corre, S, Gauthier, G, Robert, R, Ansquer, D (1996) Bacterial problems associated with scallop *Pecten maximus* larval culture. *Dis Aquat Org* **27**: 67-76. doi: 0.3354/dao027067.

Nicolas, JL, Corre, S and Cochard, JC (2004) Bacterial population association with phytoplankton cultured in a bivalve hatchery. *Microb Ecol* **48**(3): 400–13. doi:10.1007/s00248-003-2031-6.

Powell, SM, Chapman, CC, Bermudes, M, and Tamplin, ML (2013) Dynamics of seawater bacterial communities in a shellfish hatchery. *Microb Ecol* **66**(2): 245–56. 10.1007/s00248-013-0183-6.

Prado, S, Montes, J, Romalde, JL, and Barja, JL (2009) Inhibitory activity of *Phaeobacter* strains against aquaculture of pathogenic bacteria. *Int Microbiol* **12**(2): 107-14. 10.2436/20.1501.01.87.

Prado, S, Romalde, JL, Barja, JL (2010) Review of probiotics for use in bivalve hatcheries. *Vet Microbiol* **145**(3-4): 187-97. doi: 10.1016/j.vetmic.2010.08.021.

Rao, D, Webb, JS, and Kjelleberg, S (2005) Competitive interaction in mixed-species biofilms containing the marine bacterium *Pseudoalteromonas tunicata*. *Appl Enivron Microb* **71**(4): 1729-36. doi: 10.1128/AEM.71.4.1729-1736.2005.

Rico-Villa, B, and Pouvreau, RR (2009) Influence of food density and temperature on ingestion, growth, and settlement of Pacific oyster larvae, Crassostrea gigas. (2009) *Aquaculture* **287**: 395-401. doi: 10.1016/j.aquaculture.2008.10.054.

Riquelme, C, Toranzo AE, Barja, JL, Vergara, N, and Araya, R (1996) Association of Aeromonas hydophila and Vibrio alginolyticus with larval mortalities of Scallop (*Argopecten purpuratus*). *Invertebr Pathol* **67**(3): 213-18. doi: 10.1006/jipa.1996.0035.

Roeselers, G, Mittge, EK, Stephens, WZ, Parichy, DM, Cavanaugh, CM, Guillemin, K, and Rawls, JF (2011) Evidence for a core gut microbiota in the zebrafish. *ISME J* **5**: 1595–1608. doi: 10.1038/ismej.2011.38.

Rognes, T, Flouri, T, Nichols, B, Quince, C, and Mahé, F (2016) VSEARCH: a versatile open source tool for metagenomics. *PeerJ* **4**: e2584. doi:10.7717/peerj.2584.

Ruiz-Ponte, C, Samain, JF, Sánchez, JL, and Nicolas, JL (1999) The benefit of *Roseabacter* species on the survival of scallop larvae. *Mar Biotechnol* **1**: 52-99. doi: 10.1007/PL00011751.

Sainz-Hernández, JC, and Maeda-Martinez, AN (2005) Sources of Vibrio bacteria in mollusc hatcheries and control methods: a case study. *Aquac Res* **36**: 1611-18. doi: 10.1111/j.1365-2109.2005.01386.x.

Schauer, C, Thompson, C, and Brune, A (2014) Pyrotag sequencing of the gut micobiota of the cockroach *Shelfordella lateralis* reveals a highly dynamic core but only

limited effects of diet on community structure. *PLoS One* **9**(1): e85861.

Schloss, PD, Westcott, SL, Ryabin, T, Hall, JR, Hartmann, M, Hollister, EB, Lesniewski, RA, et al. (2009) Introducing Mothur: open-source, platform-independent, community-supported software for describing and comparing microbial communities. *Appl Environ Micob* **75**(23): 7537–41. doi:10.1128/AEM.01541-09.

Schmitt, S, Tsai, P, Bell, J, Fromont, J, Ilan, M, Lindquist, N, Perez, T, Rodrigo, A, Schupp, P, Vacelet, J, Webster, N, Hentschel, U, and Taylor, MW (2012) Assessing the complex sponge microbiota: core, variable and species-specific bacterial communities in marine sponges. *ISME J* **6**: 564–576. doi: 10.1038/ismej.2011.116.

Schultz, GE, White, ED, and Ducklow, HW (2003) Bacterioplankton dynamics in the York River estuary: primary influence of temperature and freshwater inputs. *Aquat Microb Ecol* **30**: 135-48. doi: 10.3354/ame030135.

Schulze, AD, Alabi, AO, Tattersall-Sheldrake, AR, and Miller, KM (2006) Bacterial diversity in a marine hatchery: balance between pathogenic and potentially probiotic bacterial strains.

Aquaculture **256**(1–4): 50–73. doi:10.1016/j.aquaculture.2006.02.008.

Shiah, F-K, and Ducklow, HW (1994) Temperature and substrate regulation of bacterial abundance, production and specific growth rate in Chesapeake Bay, USA. *Mar Ecol Prog Ser* **103**: 297-308. doi: 10.3354/meps104297.

Suzuki, M, Nakagawa, Y, Harayama, S, and Yamamoto, S (2001) Phylogenetic analysis and taxonomic study of marine *Cytophaga*-like bactria: proposal for *Tenacibaculum* gen. nov. with *Tenacibaculum maritimum* comb. nov. and *Tenacibaculum ovolyticum* comb. nov., and description of *Tenacibaculum mesophilum* sp. nov. and

Tenacibaculum amyloticum sp. nov. *Int J Syst Evol Micr* **51**: 1639-52.

Trabal, N, Mazón-Suástegui, JM, Vázquez-Juárez, R, Ascencio-Valle, F, Morales-Bojórquez, E, and Romero, J (2012) Molecular analysis of bacterial microbiota associated with oysters (*Crassostrea gigas* and *Crassostrea cortieziensis*) in different growth phases at two cultivation sites. *Microb Ecol* **64**: 555-69. doi: 10.1007/s00248-012-0039-5.

Trabal Fernández, N, Mazón-Suástegui, JM, Vázquez-Juárez, R, Ascencio-Valle, F, and Romero, J (2014) Changes in the composition and diversity of the bacterial microbiota associated with oysters (*Crassostrea corteziensis*, *Crassostrea gigas* and *Crassostrea sikamea*) during commercial production. *FEMS Microbiol Ecol* **88**: 69–83. doi: 10.1111/1574-6941.12270

Wang, J-T, Chou, Y-J, Chou, J-H, Chen, CA, and Chen, W-M (2008) *Tenacibaculum aiptasiae* sp. nov., isolated from a sea anemone Aiptasia pulchella. *Int J Syst Evol Micr* **58**: 761-66. doi: 10.1099/ijs.0.65437-0.

Wang, Qi, Garrity, GM, Tiedje, JM, and Cole, JR (2007) Naive bayesian classifier for rapid assignment of rRNA sequences into the new bacterial taxonomy. *Appl Environ Micob* **73**(16): 5261–67. doi:10.1128/AEM.00062-07.

Wegner, KM, Volkenborn, N, Peter, H, and Eiler, A (2013) Disturbance induced decoupling between host genetics and composition of the associated microbiome. *BMC Microbiol* **13**(1) doi: 10.1186/1471-2180-13-252.

Xavier, JB, and Foster, KR (2007) Cooperation and conflict in microbial biofilms. *Proc Natl Acad Sci* USA **104**(3): 876-81. doi: 10.1073/pnas.0607651104.

Yilmaz, P, Parfrey, LW, Yarza, P, Gerken, J, Ludwig, W, Pruesse, E, Quast, C, Schweer,

T, and Glo, FO (2014) The SILVA “and all-species living tree project (LTP)” taxonomic frameworks. *Nucleic Acids Res* **42**(November 2013): D643–48. doi:10.1093/nar/gkt1209.

TABLES

Table 1. Nutrient parameters of the water collected from each hatchery corresponding to different spawning events and larval stages. Missing data points from sample collection are indicated by "*NA*"

Hatchery	Spawn	Stage	NO_3^- (μM)	NH_4^+ (μM)	PO_4^{3-} (μM)
A	1				
		D	5.43	0.36	1.16
		V	4.04	0.55	0.26
		PV	5.46	0.57	0.29
A	2				
		D	9.71	0.89	0.76
		V	20.75	0.48	1.14
		PV	11.90	0.31	0.72
B	1				
		D	15.51	0.68	0.32
		V	36.28	0.53	0.55
		PV	154.64	10.29	3.42
C	1				
		D	4.42	1.22	0.78
		V	12.59	2.02	1.96
		PV	17.11	7.74	3.06
C	2				
		D	*NA*	*NA*	*NA*
		V	48.18	2.70	6.10
		PV	63.58	12.56	8.55
D	1				
		D	14.52	11.71	0.72
		V	15.32	4.73	0.76
		PV	16.51	5.08	1.61
D	2				
		D	19.90	1.06	0.93
		V	0.43	0.69	0.18
		PV	0.45	2.21	0.29

Table 2. Summary statistics of 16S rRNA gene amplicon sequencing for oyster larval and hatchery water microbiomes.

Hatchery	Spawn	Stage	Sample	Sequence Total	coverage	coverage*	OTUs*	Chao*	Shannon*	Sample	Sequence Total	coverage	coverage*	OTUs*	Chao*	Shannon*
A	1	D	Oyster	28,015	1.00	1.00	110	133.10	2.97	Water	9,697	0.98	0.97	256	649.12	2.94
A	1	V	Oyster	24,789	0.99	0.99	183	268.20	2.67	Water	34,065	0.98	0.95	447	1071.64	3.67
A	1	PV	Oyster	*NA*	*NA*	*NA*	*NA*	*NA*	*NA*	Water	12,746	0.96	0.95	474	1079.23	3.75
A	2	D	Oyster	7,127	0.94	0.93	587	1249.88	4.33	Water	28,882	0.98	0.95	435	1185.96	2.96
A	2	V	Oyster	11,516	0.98	0.96	331	793.58	3.34	Water	23,657	0.97	0.89	1021	1927.27	5.14
A	2	PV	Oyster	9,289	0.99	0.99	131	266.14	2.66	Water	32,481	0.97	0.91	801	1638.86	4.65
A	3	D	Oyster	28,048	0.97	0.95	478	1040.31	4.05	Water	*NA*	*NA*	*NA*	*NA*	*NA*	*NA*
A	3	V	Oyster	26,816	0.97	0.95	465	1272.07	4.19	Water	*NA*	*NA*	*NA*	*NA*	*NA*	*NA*
A	3	PV	Oyster	38,591	0.99	0.98	175	302.73	2.35	Water	*NA*	*NA*	*NA*	*NA*	*NA*	*NA*
B	1	D	Oyster	11,910	0.98	0.97	244	498.60	3.26	Water	6,980	0.98	0.98	170	434.06	2.77
B	1	V	Oyster	11,704	0.99	0.98	235	377.80	3.73	Water	19,049	0.99	0.99	110	171.88	2.30
B	1	PV	Oyster	19,978	0.99	0.99	186	267.06	3.77	Water	17,847	1.00	0.99	67	134.36	0.66
B	2	D	Oyster	*NA*	*NA*	*NA*	*NA*	*NA*	*NA*	*NA*	*NA*	*NA*	*NA*	*NA*	*NA*	*NA*
B	2	V	Oyster	*NA*	*NA*	*NA*	*NA*	*NA*	*NA*	*NA*	*NA*	*NA*	*NA*	*NA*	*NA*	*NA*
B	2	PV	Oyster	*NA*	*NA*	*NA*	*NA*	*NA*	*NA*	*NA*	*NA*	*NA*	*NA*	*NA*	*NA*	*NA*
B	3	D	Oyster	25,148	0.99	0.97	258	516.43	3.39	Water	*NA*	*NA*	*NA*	*NA*	*NA*	*NA*
B	3	V	Oyster	46,299	0.99	0.96	366	711.29	3.58	Water	*NA*	*NA*	*NA*	*NA*	*NA*	*NA*
B	3	PV	Oyster	36,317	0.99	0.98	266	516.18	3.20	Water	*NA*	*NA*	*NA*	*NA*	*NA*	*NA*
C	1	D	Oyster	33,582	0.99	0.98	254	410.16	3.13	Water	58,062	0.99	0.98	168	405.67	2.20
C	1	V	Oyster	34,745	0.99	0.98	221	451.66	1.95	Water	16,907	0.98	0.96	372	859.58	4.17
C	1	PV	Oyster	9,554	0.99	0.99	237	294.00	3.85	Water	15,006	0.99	0.98	213	489.12	2.28
C	2	D	Oyster	25,628	0.98	0.96	334	768.32	3.18	Water	*NA*	*NA*	*NA*	*NA*	*NA*	*NA*
C	2	V	Oyster	24,032	1.00	0.99	270	341.19	3.72	Water	27,709	0.99	0.98	189	363.42	3.13
C	2	PV	Oyster	22,298	0.99	0.99	172	392.07	2.81	Water	32,552	0.99	0.98	164	305.79	1.83
C	3	D	Oyster	34,262	0.99	0.97	311	688.23	3.77	Water	*NA*	*NA*	*NA*	*NA*	*NA*	*NA*
C	3	V	Oyster	19,532	0.98	0.96	420	854.41	4.09	Water	*NA*	*NA*	*NA*	*NA*	*NA*	*NA*
C	3	PV	Oyster	*NA*	*NA*	*NA*	*NA*	*NA*	*NA*	Water	*NA*	*NA*	*NA*	*NA*	*NA*	*NA*
D	1	D	Oyster	16,170	0.97	0.95	450	1022.76	3.97	Water	34,506	0.97	0.95	477	1155.60	4.36
D	1	V	Oyster	10,639	0.97	0.95	585	913.76	4.54	Water	56,390	0.99	0.97	244	645.54	2.88
D	1	PV	Oyster	*NA*	*NA*	*NA*	*NA*	*NA*	*NA*	Water	21,604	0.99	0.98	171	318.96	2.76
D	2	D	Oyster	14,097	0.97	0.94	643	1066.63	4.82	Water	15,065	0.96	0.95	461	1126.79	4.22
D	2	V	Oyster	11,670	0.98	0.97	349	550.25	3.52	Water	28,880	0.97	0.96	350	1250.93	3.21
D	2	PV	Oyster	5,277	0.99	0.99	222	305.15	4.23	Water	30,590	0.98	0.96	297	1004.78	2.97
D	3	D	Oyster	9,273	0.92	0.90	788	2303.41	4.48	Water	*NA*	*NA*	*NA*	*NA*	*NA*	*NA*
D	3	V	Oyster	26,617	0.98	0.95	439	1071.50	2.46	Water	*NA*	*NA*	*NA*	*NA*	*NA*	*NA*
D	3	PV	Oyster	20,572	1.00	0.99	313	355.09	4.16	Water	*NA*	*NA*	*NA*	*NA*	*NA*	*NA*

* Based on subsampled sequences (n=5277)

Table 3. Spearman rank correlations of Chao richness and Shannon diversity between oyster larval development stages and corresponding hatchery water.

Significance is denoted in bold ($p<0.05$).

	Chao		Shannon	
	ρ (rho)	p-value	ρ (rho)	p-value
Total	0.35	0.16	-0.09	0.74
D-stage	0.77	0.07	0.65	0.15
V-stage	0.32	0.48	**-0.85**	**0.01**
PV-stage	-0.30	0.62	-0.1	-0.87

Table 4. Spearman rank correlations between hatchery water nutrients and Chao richness and Shannon diversity in oyster larvae and hatchery water microbiomes. Significance is denoted in bold ($p<0.05$).

	Oyster Larvae				Hatchery Water			
	Chao		Shannon		Chao		Shannon	
Nutrient	ρ (rho)	p-value	ρ (rho)	p-value	ρ (rho)	p-value	ρ (rho)	p-value
NO_3	0.04	0.87	0.12	0.53	-0.52	**0.02**	-0.29	0.29
NH_4	0.09	0.72	0.38	0.11	-0.47	**0.04**	-0.44	0.05
PO_4	-0.12	0.62	-0.10	0.80	-0.49	**0.03**	-0.36	0.12

Table 5. PERMANOVA results showing the effects of sample type, hatchery, spawning event, and development stage on larval and hatchery water microbiomes. (A) Comparisons were made between larval and hatchery water microbiomes using a one factor model design for sample type. (B-C) Separate comparisons were made between hatcheries, spawning events, and development stages using the nested model design hatchery x development stage (spawning event) for (B) larval microbiomes and (C) hatchery water microbiomes. PERMANOVAs were conducted using Bray-Curtis resemblance matrices. Significance is denoted in bold ($p<0.05$).

PERMANOVA Sample Type — Hatchery Water vs. Larvae

A	Source	Degrees of Freedom	Mean Squares	Pseudo-F	Estimate Variation (Sq. root)	p-value
Sample Type		1	10982	3.3229	17.753	0.001

PERMANOVA Hatchery x Hatchery (Spawn) x Development Stage — Larvae

B	Source	Degrees of Freedom	Mean Squares	Pseudo-F	Estimate Variation (Sq. root)	p-value
Hatchery		3	6136.4	2.7499	23.812	**0.001**
Development Stage		2	3176.8	1.4236	10.064	0.065
Spawn (Hatchery)		7	3558	1.5944	22.712	**0.001**
Hatchery x Development Stage		6	2587.8	1.1597	12.278	0.122

PERMANOVA Hatchery x Hatchery (Spawn) x Development Stage — Hatchery Water

C	Source	Degrees of Freedom	Mean Squares	Pseudo-F	Estimate Variation (Sq. root)	p-value
Hatchery		3	7798.6	3.4615	34.603	**0.006**
Development Stage		2	2877.9	1.2774	10.321	0.281
Spawn (Hatchery)		3	3873.7	1.7194	24.653	0.073
Hatchery x Development Stage		6	2531.0	1.1234	13.270	0.338

Table 6. Permutational-based pairwise comparisons of differences between hatcheries in oyster larval and hatchery water microbiomes. Significance is denoted in bold ($p<0.05$)

Pairwise test	Larvae			Water		
Hatchery	Average Similarity (%)	t	p-value	Average Similarity (%)	t	p-value
A,B	23.951	1.546	**0.038**	8.5135	1.546	0.094
A,C	20.452	1.5603	**0.016**	10.870	1.5603	0.058
A,D	17.794	1.6533	**0.015**	13.645	1.6533	**0.034**
B,C	21.756	1.7355	**0.031**	17.428	1.7355	0.288
B,D	17.606	1.8183	**0.015**	10.559	1.8183	0.055
C,D	17.604	1.6371	**0.017**	15.493	1.6371	**0.036**

Table 7. Dispersion effect of hatchery, development stage, and spawn on oyster larval and hatchery water microbiomes. Dispersion effects were determined using the PERMDISP test and are based on Bray-Curtis resemblance matrices. Significance is denoted in bold ($p<0.05$)

PERMDISP	Larvae			Hatchery Water		
Factor	df	F-statistic	p-value	df	F-statistic	p-value
Hatchery	3	3.3932	0.086	3	4.317	0.159
Development Stage	2	3.0644	0.128	2	1.8758	0.247
Spawn	2	1.9041	0.228	1	0.1901	0.752

Table 8. Relative abundances and taxonomic classifications of larval core OTUs.

Relative abundances of larval core OTUs are grouped by development stage and by hatchery**.** Errors represent ± SE.

A

OTU	Taxon Family	Nearest BLAST result	E-value	Mean Relative Abundance (%)		
				D.stage	V.stage	PV.stage
Otu00015	*Alteromonadaceae*	*Alteromonas macleodii*	1E-127	4.02 ± 1.42	1.04 ± 0.46	0.72 ± 0.29
Otu00096		*Marinobacter hydrocarbonoclasticus*	3E-128			
Otu00025	*Erythrobacteraceae*	*Citromicrobium bathyomarinum*	3E-128	1.49 ± 0.40	1.62 ± 0.82	0.83 ± 0.37
Otu00010	*Flavobacteriaceae*	*Tenacibaculum sp.*	3E-128	1.17 ± 0.49	5.91 ± 4.10	3.37 ± 2.50
Otu00059	*Oleiphilaceae*	*Gamma proteobacterium*	3E-128	0.50 ± 0.18	0.23 ± 0.12	0.14 ± 0.07
Otu00040	*Phyllobacteriaceae*	*Hoflea sp.*	3E-128	0.13 ± 0.04	0.48 ± 0.15	0.52 ± 0.19
Otu00001	*Rhodobacteraceae*	*Roseobacter sp.*	5E-126	24.71 ± 2.93	22.71 ± 5.01	19.67 ± 2.93
Otu00002		*Donghicoloa ebumeus*	5E-126			
Otu00003		*Nautella sp.*	5E-126			
Otu00007		*Rhodovulum iodosum*	3E-128			
Otu00012		*Sulfitobacter sp.*	3E-128			
Otu00023		*Ponticoccus sp.*	3E-124			
Otu00030		*Rhodobacteraceae bacterium*	1E-122			
Otu00051		*Paracoccus marcusii*	2E-126			
Otu00058		*Labrenzia aggregata*	3E-128			
Otu00067		*Donghicola tyrosinivorans*	5E-126			

B

OTU	Taxon Family	Nearest BLAST result	E-value	Mean Relative Abundance (%)			
				A	B	C	D
Otu00015	*Alteromonadaceae*	*Alteromonas macleodii*	1E-127	3.81 ± 1.98	2.26 ± 0.79	1.01 ± 0.82	1.17 ± 0.27
Otu00096		*Marinobacter hydrocarbonoclasticus*	3E-128				
Otu00025	*Erythrobacteraceae*	*Citromicrobium bathyomarinum*	3E-128	0.95 ± 0.32	1.14 ± 0.50	2.10 ± 1.17	1.37 ± 0.48
Otu00010	*Flavobacteriaceae*	*Tenacibaculum sp.*	3E-128	8.71 ± 5.75	1.94 ± 0.71	2.84 ± 2.56	0.49 ± 0.32
Otu00059	*Oleiphilaceae*	*Gamma proteobacterium*	3E-128	0.42 ± 0.15	0.03 ± 0.02	0.36 ± 0.24	0.36 ± 0.16
Otu00040	*Phyllobacteriaceae*	*Hoflea sp.*	3E-128	0.31 ± 0.17	0.18 ± 0.05	0.41 ± 0.17	0.38 ± 0.19
Otu00001	*Rhodobacteraceae*	*Roseobacter sp.*	5E-126	24.80 ± 3.56	20.77 ± 2.95	18.13 ± 3.25	28.15 ± 6.44
Otu00002		*Donghicoloa ebumeus*	5E-126				
Otu00003		*Nautella sp.*	5E-126				
Otu00007		*Rhodovulum iodosum*	3E-128				
Otu00012		*Sulfitobacter sp.*	3E-128				
Otu00023		*Ponticoccus sp.*	3E-124				
Otu00030		*Rhodobacteraceae bacterium*	1E-122				
Otu00051		*Paracoccus marcusii*	2E-126				
Otu00058		*Labrenzia aggregata*	3E-128				
Otu00067		*Donghicola tyrosinivorans*	5E-126				

Table 9. Differentially abundant OTUs between larval D- and PV-stage microbiomes. OTUs identified from DESeq2 using Benjamini Hochberg's p-adjusted values correcting for FDR. Only OTUs that were found to be significant ($p<0.5$) are listed.

OTU	Phylum	Class	Order	Family	Genus	Closest NCBI blast match	E value	Accession Nos.
Otu00004	*Bacteroidetes*	*Flavobacteriia*	*Flavobacteriales*	*Flavobacteriaceae*	*Flavobacterium*	*Flavobacterium ahnfeltiae*	3.00E-128	KC247359.1
Otu00032	*Proteobacteria*	*Alphaproteobacteria*	*Caulobacterales*	*Hyphomonadaceae*	*Hyphomonas*	*Hyphomonas jannaschiana*	5.00E-126	KT581517.1
Otu00033	*Bacteroidetes*	*Flavobacteriia*	*Flavobacteriales*	*Flavobacteriaceae*	*Flavobacterium*	Flavobacteriium sp.	3.00E-128	KM875710.1
Otu00056	*Bacteroidetes*	*Flavobacteriia*	*Flavobacteriales*	*Flavobacteriaceae*	*NA*	*Sabulilitoribacter multivorans*	3.00E-128	NR_133850.1
Otu00058	*Proteobacteria*	*Alphaproteobacteria*	*Rhodobacterales*	*Rhodobacteraceae*	*Labrenzia*	*Labrenzia aggregata*	3.00E-128	CP019630.1

Table 10. Differentially abundant OTUs between oyster larval microbiomes and their respective hatchery water microbiomes. OTUs identified from DESeq2 using Benjamini Hochberg's p-adjusted values correcting for FDR. P-values are only given for significant OTUs ($p<0.05$). Mean relative abundances indicated in bold indicate whether the OTU was significantly higher in the larval or in the hatchery water microbiome.

OTU	Nearest BLAST result	Mean Relative Abundance (%)		p-adjusted value
		Larvae	Water	
Otu00015	*Alteromonas macleodii*	7.05 ± 1.33	1.34 ± 0.75	
Otu00096	***Marinobacter hydrocarbonoclasticus***	**0.34 ± 0.10**	0.14 ± 0.13	**0.0046**
Otu00025	***Citromicrobium bathyomarinum***	2.03 ± 0.54	**3.86 ± 1.49**	**0.0009**
Otu00010	***Tenacibaculum sp.***	**5.41 ± 2.78**	0.33 ± 0.21	**0.0004**
Otu00059	*Gamma proteobacterium*	0.40 ± 0.13	0.33 ± 0.02	
Otu00040	*Hoflea sp.*	0.47 ± 0.11	0.61 ± 0.40	
Otu00001	*Roseobacter sp.*	7.05 ± 1.33	11.10 ± 5.12	
Otu00002	*Donghicoloa ebumeus*	5.53 ± 1.70	3.72 ± 1.57	
Otu00003	*Nautella sp.*	3.97 ± 0.98	3.86 ± 1.49	
Otu00007	*Rhodovulum iodosum*	1.92 ± 0.46	1.62 ± 0.99	
Otu00012	*Sulfitobacter sp.*	0.53 ± 0.18	0.42 ± 0.22	
Otu00023	*Ponticoccus sp.*	0.83 ± 0.35	0.87 ± 0.58	
Otu00030	*Rhodobacteraceae bacterium*	0.75 ± 0.38	0.45 ± 0.23	
Otu00051	*Paracoccus marcusii*	0.42 ± 0.18	0.43 ± 0.22	
Otu00058	*Labrenzia aggregata*	0.66 ± 0.32	0.15 ± 0.08	
Otu00067	*Donghicola tyrosinivorans*	0.51 ± 0.23	0.54 ± 0.02	

FIGURE

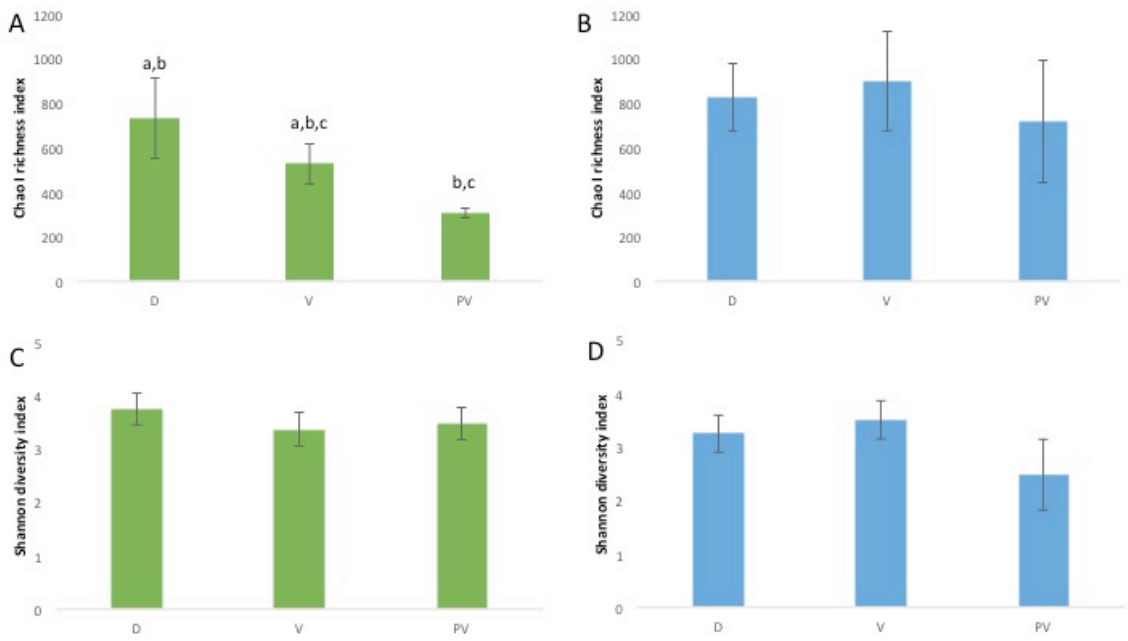

Figure 1. Chao richness and Shannon Diversity in oyster larval and hatchery water microbiomes. Mean Chao richness in (A) oyster larvae (B) and hatchery water and mean Shannon diversity in (C) oyster larvae and (D) hatchery water for larval stages D-, V-, and PV. Significance differences between larvae stages are denoted with different letters ($p<0.5$). Error bars represent ± SE.

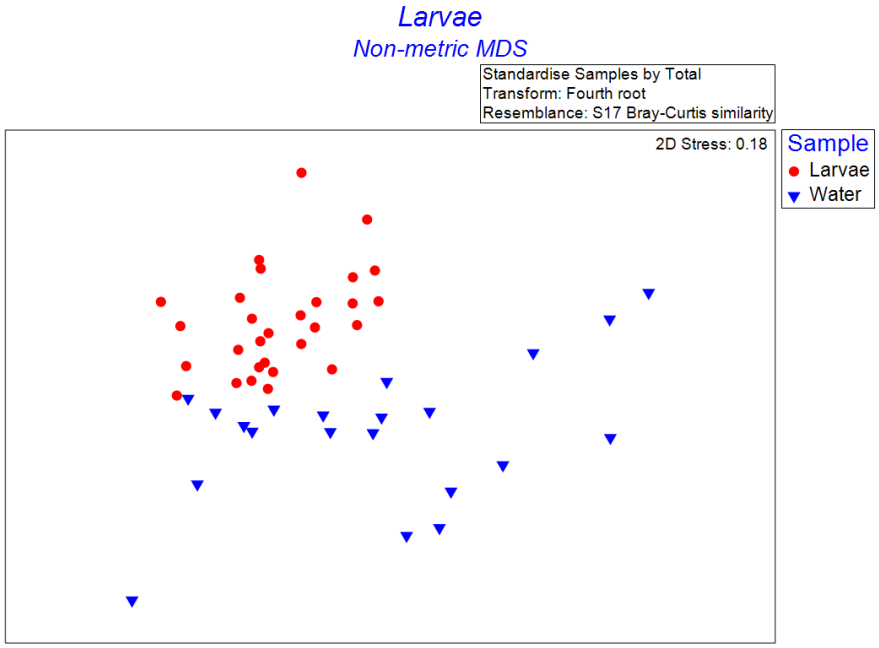

Figure 2. Non-metric multidimensional scaling (nMDS) plot based on a Bray-Curtis resemblance matrix depicting β-diversity between larval and water microbiomes

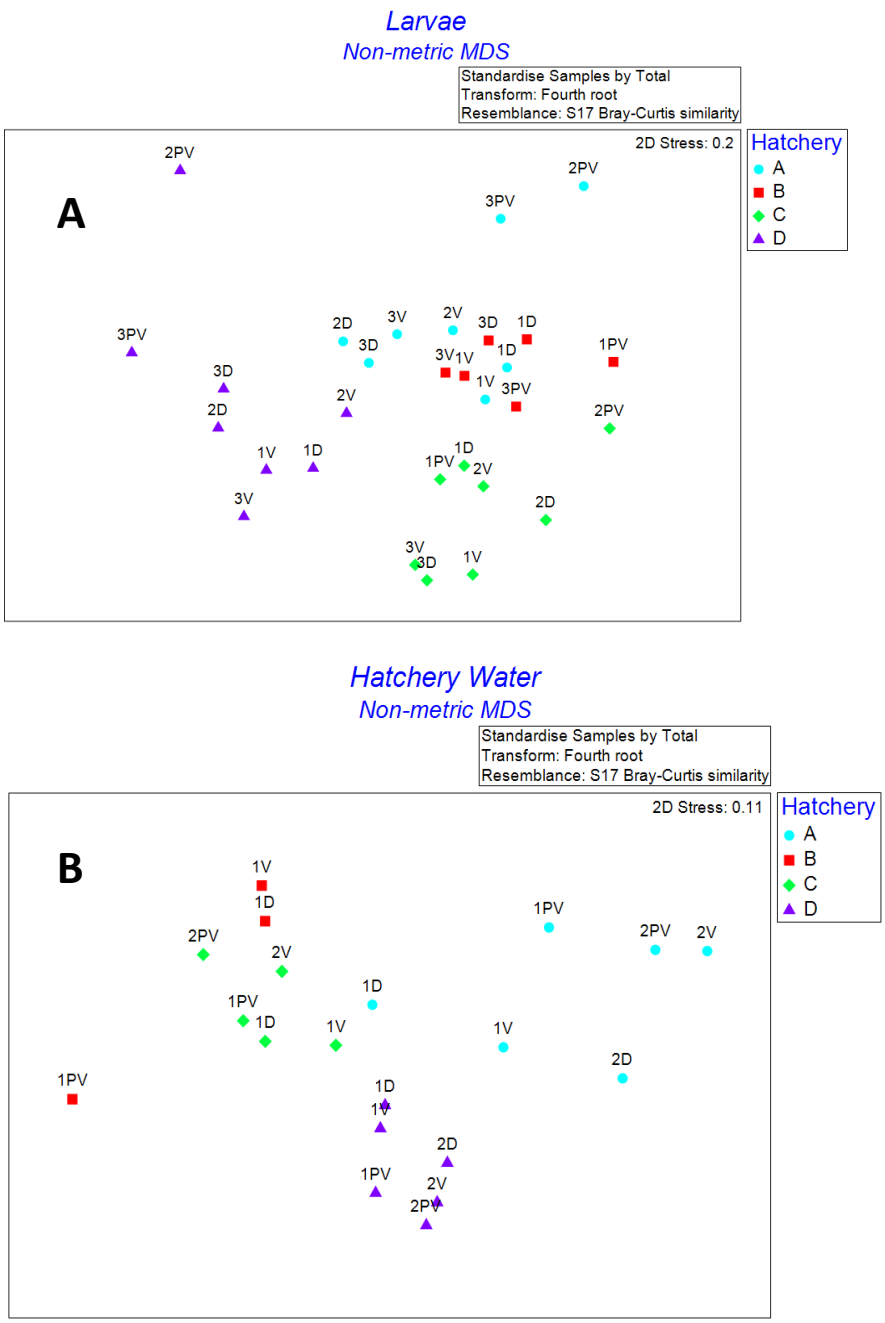

Figure 3. Non-metric multidimensional scaling (nMDS) plot based on Bray-Curtis resemblance matrices depicting β-diversity among different hatcheries, spawning events, and development stages in (A) oyster larval and (B) hatchery water microbiomes. Numbers 1-3 indicate spawning event and D-, V-, and PV- represent different larvae stages.

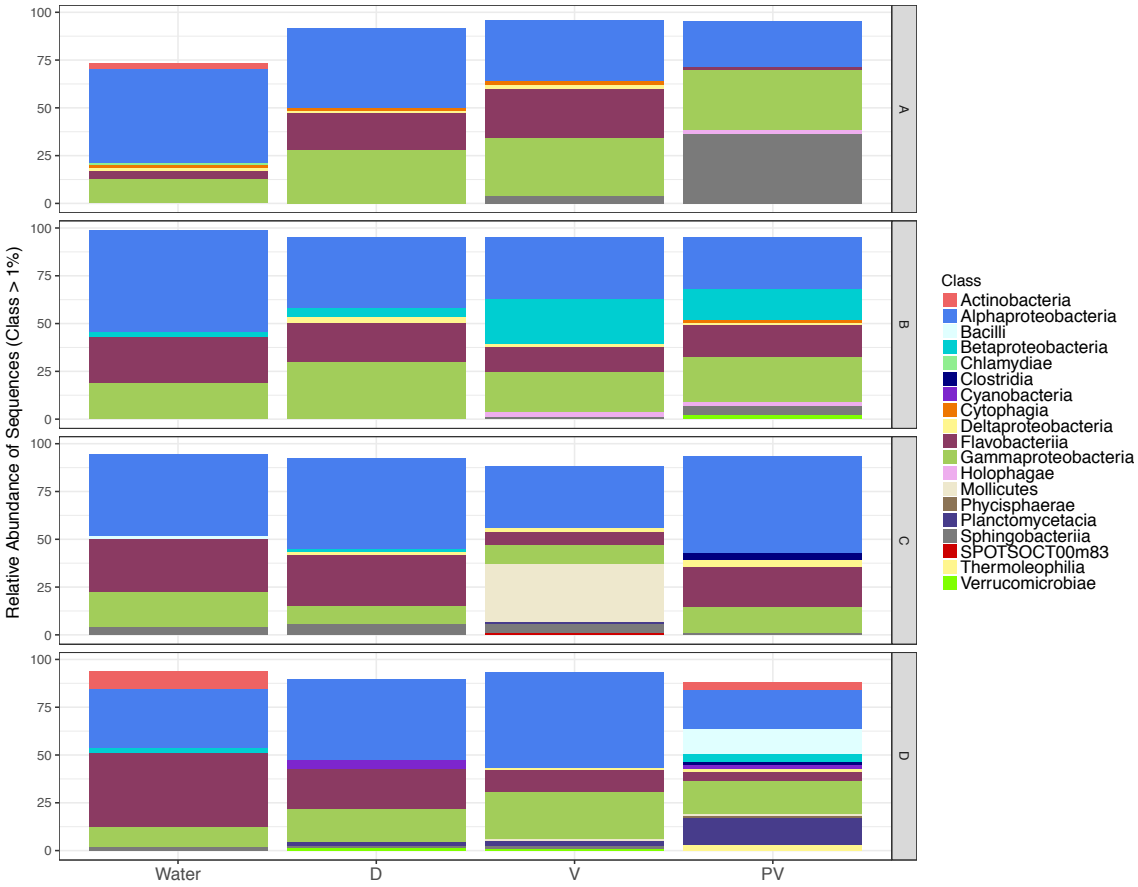

Figure 4. Mean relative abundances of bacterial classes grouped by water and larval development stage microbiomes for each hatchery. Only classes with > 1% relative abundance are shown.

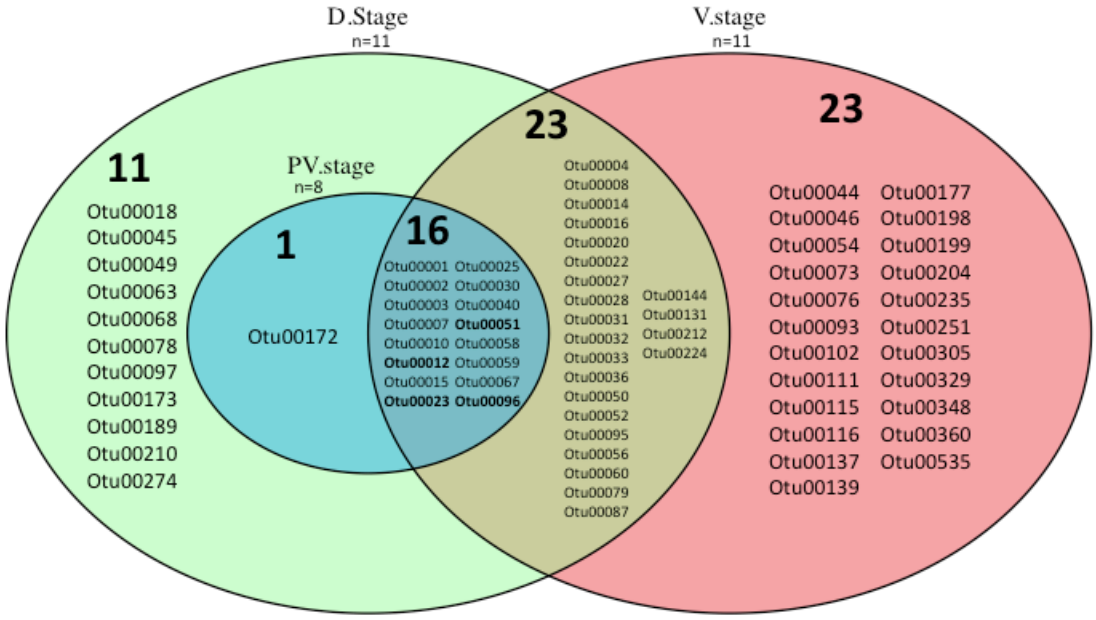

Figure 5. Shared OTUs within larval stage (larval stage core) and shared OTUs among all larval stages (larval total core).

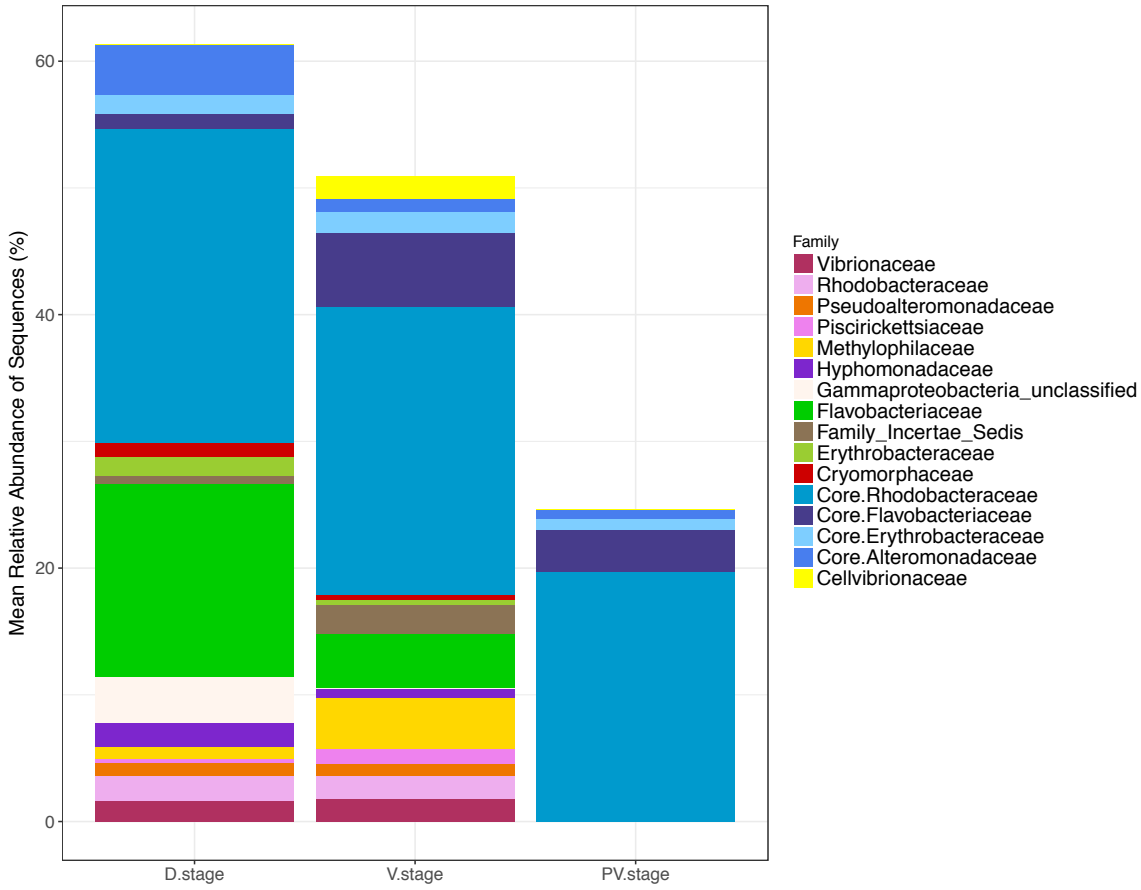

Figure 6. Mean relative abundances of bacterial families in the larval stage core microbiomes and the relative abundance of the larval total core microbiome. Larvae total core microbiome identified as "Core".

Chapter 6

Conclusions

CONCLUSIONS

This dissertation provided an in depth characterization of the eastern oyster *Crassostrea virginica* microbiomes and its associated denitrifiers. Furthermore, core oyster gill, gut, and shell microbiomes were identified and oyster denitrifiers were connected to potential oyster denitrification and denitrification activity in the environment. Microbiomes and associated denitrifiers of oysters were investigated using a combined 16S targeted metagenome and metabolic inference approach. Denitrification activity was linked to community structure using methods such as qPCR of *nos*Z genes and IPT with experimental flow-through designs. The combined approaches and methods used in these studies allowed for a greater understanding of the oyster microbiome and its contribution to the marine nitrogen cycle.

In Chapter 2, the microbiomes of the oyster digestive gland, shell, and reef sediment were examined and a customized gene database in conjunction with a metabolic inference bioinformatic program to identify oyster denitrifiers was developed. Shell and oyster microbiomes were found to have higher abundances of denitrifiers carrying the *nos*ZI gene, which corresponded to higher denitrification rates than those measured in the reef sediments. The metabolic inference for gene prediction was validated with qCPR of the *nos*ZI gene.

The effects of seasonality on the oyster microbiomes and associated denitrifiers were explored and the presence of core microbiomes was investigated in Chapter 3. Season had a significant effect on the oyster gill, gut and shell microbiomes, but not on the reef sediment microbiome. In all microbiomes, however, a core set of microbes was found in relation to season. The gut and gill core had a low number of OTUs, but made

up a large percentage of the total microbiome, suggesting an important connection to oyster health or physiology. In contrast, the shell and sediment microbiomes had a large number of core OTUs, with each OTU making up a small percentage of the total microbiome suggesting a more widespread and diverse role of the shell microbiome in the environment. Denitrifier abundance in the shell and sediment core microbiomes was stable and relatively consistent reflecting a constant pool of potential denitrifiers, while most denitrifier identified in the gill and gut were transient in nature and likely reflected a connection to food particle ingestion. Further evidence of shell denitrifier stability and gill and gut denitrifier variability was evidenced in denitrification rates. Oysters had significantly higher denitrification rates than shells or sediments, but were highly variable. In comparison, sediment and shell denitrification had lower rates but were relatively constant. Niche differentiation of *nos*ZI and *nos*ZII genes was also demonstrated between the different microbiomes indicating distinct communities of bacteria are performing denitrification in the oyster gill, gut, shell, and sediment microbiomes.

Temporal and spatial environmental changes on oyster microbiomes and associated denitrifiers in addition to the existence of a core microbiome were investigated by conducting oyster deployment experiments in the Chapter 4. Both site and time had a significant effect on the gill, gut, and shell microbiomes with temporal effects having a greater effect on the gut microbiome and spatial effects having a greater effect on the gill and shell microbiome. Despite these environmental changes, core microbiomes were found in all three parts of oysters indicating evidence of stability and a strong association with oyster health or ecosystem function. Differences between the total core and active

core microbiomes were primarily due to differences in relative abundances of dominant taxa, with some exceptions. In the gill core microbiome, the active microbiome contained a greater number of members than the total microbiome suggesting an increased contribution of rare bacteria to the gill core microbiome, while the gut core microbiome showed a decrease in active members indicating most activity in the oyster gut is highly variable and may be linked to factors such as site, food selection, season, or genetic lineage. Relative abundances of denitrifiers fluctuated among the gill and gut microbiomes and exhibited low relative abundances in their respective core microbiomes, suggesting that most denitrifiers in the gut and gill microbiome are transient. In comparison, denitrifier relative abundances remained relatively consistent in the shell microbiome regardless of site or time point, reflecting the quick recovery of potential denitrification function the shell microbiome following disturbance.

The microbiomes of oyster larvae were examined in Chapter 5 for the presence of a core larvae microbiome in relation to developmental stages D-, V-, and PV- and among different hatcheries. Larvae microbiomes were significantly affected by hatchery and spawning events, but not by development stage. However, richness of larvae microbiomes decreased as oysters developed from D- to PV-stage, indicating the overall structure of the microbiome is affected by larvae development. Throughout all three larvae development stages, a core microbiome was present regardless of hatchery or spawning event, suggesting a possible link to larvae health and development. While the overall larvae microbiome was distinct from the hatchery water, the core members of the larvae were also present in the hatchery water suggesting the importance of hatchery water in the development of the oyster core.

Investigation of the oyster microbiome, oyster core microbiome, and associated denitrifiers provides an important step in unraveling the complex dynamics of the oyster microbiome and its role in oyster health and functional role in denitrification. Identification of the core microbiome and core denitrifiers found in these studies is critical in understanding the effect of disturbances on the oyster and denitrification potential in the environment. Furthermore, the results of these studies advance our knowledge of the oyster microbiome and may help shape future research efforts in linking members of the oyster microbiome to incidences of disease and identifying factors to maximize nutrient removal mediate by oysters and mitigate coastal eutrophication.

Appendix I

Perkinsus marinus infection in oyster microbiomes

Quantitative PCR method for detection of *Perkinsus marinus* in extracted oyster tissue DNA

The detection and quantification of *P. marinus* was conducted by targeting the species specific ITS region of the rRNA gene unit in DNA samples extracted from oyster gut (n=16) and gill tissue (n=16) in Chapter 3 using TaqMan quantitative PCR (qPCR) assays developed for oyster DNA by Gauthier et al. 2006. DNA concentrations were quantified using a Qubit 3.0 Fluorometer (Thermo Scientific, Waltham, MA). *P. marinus* qPCR assays were performed in MicroAmp Fast 96-well reaction plates (Applied Biosystems, Foster City, CA) using a 10 µL reaction volume with the following final concentrations: 1X TaqMan Fast Advanced Master Mix (Thermo Scientific, Waltham, MA), 0.2 mg/mL bovine serum albumin (BSA), 0.9 µM combined (PMAR) forward and reverse primers targeting the internal transcribed spacer ITS region in *P. marinus*, and 0.25 µM TaqMan (PMAR) probe. Thermal cycling was conducted on a 7500 Fast Real-Time PCR system (Applied Biosystems, Foster City, CA). Cycling condition consisted of an initial denaturation step at 95°C for 20 s, followed by 40 cycles of 95°C for 3 s and 60°C for 30 s. Each assay included a negative control and a *P. marinus* dilution series to serve as a positive control and for creating standard curves. Final results were normalized to copy numbers of *P. marinus* rDNA /1 ng DNA.

Table 1. *P. marinus* qPCR results for extracted oyster gut and gill DNA. Gill and gut samples described in Chapter 3.

Sample Name	*P. marinus* copy number/ng of DNA
Gill.June.1	3.E+01
Gill.June.2	5.E+01
Gill.June.3	9.E+02
Gill.Aug.1	4.E+01
Gill.Aug.2	1.E+02
Gill.Aug.3	1.E+01
Gill.Aug.S2	1.E+02
Gill.Aug.S3	2.E+02
Gill.Oct.1	3.E+02
Gill.Oct.2	1.E+06
Gill.Oct.3	4.E+02
Gill.Oct.4	3.E+02
Gill.Oct.S1	5.E+02
Gill.Oct.S2	2.E+03
Gill.Oct.S3	3.E+02
Gill.Oct.S4	6.E+02
Gut.June.1	2.E+02
Gut.June.2	6.E+03
Gut.June.3	3.E+03
Gut.Aug.1	2.E+03
Gut.Aug.2	6.E+03
Gut.Aug.3	1.E+03
Gut.Aug.S2	2.E+03
Gut.Aug.S3	2.E+01
Gut.Oct.1	1.E+03
Gut.Oct.2	1.E+06
Gut.Oct.3	2.E+03
Gut.Oct.4	1.E+01
Gut.Oct.S1	1.E+03
Gut.Oct.S2	2.E+04
Gut.Oct.S3	3.E+02
Gut.Oct.S4	1.E+03

Table 2. Spearman rank correlations between gene copy numbers of *P. marinus* determined by qPCR and relative abundances OTUs identified in the oyster gill and gut core microbiomes. Gill and gut core microbiomes described in Chapter 3. Significance is denoted in bold ($p<0.0.5$)

Microbiome	OTU	Genus	Rho
Gill	Otu00002	Unclassified Bacteria	-0.06
	Otu00004	*Vibrio*	0.17
	Otu00006	*Neptuniibacter*	-0.33
	Otu00012	*Alteromonas*	-0.15
	Otu00015	*Pseudoalteromonas*	0.28
Gut	Otu00001	*Mycoplasma*	**0.59**
	Otu00003	*Mycoplasma*	**-0.50**
	Otu00004	*Vibrio*	**-0.43**
	Otu00005	*Mycoplasma*	0.14
	Otu00011	*Unclassified Rhodobacteraceae*	**-0.57**

Appendix II

N_2O production by oyster microbiomes

Table 1. N_2O flux measurements of oysters, shells, and reef sediments. Flow through experiments were conducted on live oysters (Oyster), oysters with biofilms removed (Oyster.Scr), empty paired oyster shells (Shell), and reef sediments (Sed). Details of experiments are described in Chapter 3.

Sample Name	N_2O $\mu mol\ N_2O\text{-}N\ m^{-2}\ hr^{-1}$
Sed.June.1	0.80
Sed.June.2	3.71
Sed.June.3	1.91
Sed.August.1	0.09
Sed.August.2	0.57
Sed.August.3	0.13
Sed.October.1	0.13
Sed.October.2	0.15
Sed.October.3	0.14
Shell.June.1	0.82
Shell.June.2	1.72
Shell.June.3	3.81
Shell.August.1	2.70
Shell.August.2	0.48
Shell.August.3	1.81
Shell.October.1	0.30
Shell.October.2	0.18
Shell.October.3	0.32
Shell.October.4	0.61
Oyster.June.1	2.03
Oyster.June.2	4.06
Oyster.June.3	5.10
Oyster.August.1	3.03
Oyster.August.2	1.65
Oyster.August.3	2.17
Oyster.October.1	1.92
Oyster.October.2	5.52
Oyster.October.3	0.91
Oyster.October.4	1.91
Oyster.Scr.August.2	1.94
Oyster.Scr.August.3	1.64
Oyster.Scr.October.1	0.39
Oyster.Scr.October.2	0.63
Oyster.Scr.October.3	0.36
Oyster.Scr.October.4	0.21

VITA

ANN M. ARFKEN

Born in Carmel, IN, USA. Graduated from Carmel High School, Carmel, IN. Earned a B.S. in Zoology from Miami University, Oxford, OH in 2001. Earned a J.D. from Wake Forest University School of Law, Winston-Salem, NC in 2006. Became a licensed member of the North Carolina Bar in 2006. Earned an M.S. in Marine Biology from University of North Carolina at Wilmington in 2011 under Dr. Bongkeun Song. Entered into the Ph.D. program at the Virginia Institute of Marine Science, College of William and Mary in 2013 as a student of Dr. Bongkeun Song.